

**Functional genomic and molecular analyses of transcripts related to
glycerol synthesis and trafficking in rainbow smelt (*Osmerus mordax*)**

using cold temperature-induced models of glycerol production

by

© Jennifer R. Hall

A thesis submitted to the
School of Graduate Studies
in partial fulfillment of the
requirements for the degree of

Doctor of Philosophy

Department of Biology/School of Graduate Studies/Faculty of Science

Memorial University of Newfoundland

January 2016

St. John's

Newfoundland and Labrador

ABSTRACT

The rainbow smelt (*Osmerus mordax*) is an anadromous teleost that produces type II antifreeze protein (AFP) and accumulates modest urea and high glycerol levels in plasma and tissues as adaptive cryoprotectant mechanisms in sub-zero temperatures. It is known that glyceroneogenesis occurs in liver via a branch in glycolysis and gluconeogenesis and is activated by low temperature; however, the precise mechanisms of glycerol synthesis and trafficking in smelt remain to be elucidated. The objective of this thesis was to provide further insight using functional genomic techniques [e.g. suppression subtractive hybridization (SSH) cDNA library construction, microarray analyses] and molecular analyses [e.g. cloning, quantitative reverse transcription - polymerase chain reaction (QPCR)].

Novel molecular mechanisms related to glyceroneogenesis were deciphered by comparing the transcript expression profiles of glycerol (cold temperature) and non-glycerol (warm temperature) accumulating hepatocytes (Chapter 2) and livers from intact smelt (Chapter 3). Briefly, glycerol synthesis can be initiated from both amino acids and carbohydrate; however carbohydrate appears to be the preferred source when it is readily available. In glycerol accumulating hepatocytes, levels of the hepatic glucose transporter (GLUT2) plummeted and transcript levels of a suite of genes (PEPCK, MDH2, AAT2, GDH and AQP9) associated with the mobilization of amino acids to fuel glycerol synthesis were all transiently higher. In contrast, in glycerol accumulating livers from intact smelt, glycerol synthesis was primarily fuelled by glycogen degradation with higher PGM and PFK (glycolysis) transcript levels. Whether initiated from amino acids or carbohydrate, there were common metabolic underpinnings. Increased PDK2 (an

inhibitor of PDH) transcript levels would direct pyruvate derived from amino acids and / or DHAP derived from G6P to glycerol as opposed to oxidation via the citric acid cycle. Robust LIPL (triglyceride catabolism) transcript levels would provide free fatty acids that could be oxidized to fuel ATP synthesis. Increased cGPDH (glyceroneogenesis) transcript levels were not required for increased glycerol production, suggesting that regulation is more likely by post-translational modification. Finally, levels of a transcript potentially encoding glycerol-3-phosphatase, an enzyme not yet characterized in any vertebrate species, were transiently higher. These comparisons also led to the novel discoveries that increased G6Pase (glucose synthesis) and increased GS (glutamine synthesis) transcript levels were part of the low temperature response in smelt. Glucose may provide increased colligative protection against freezing; whereas glutamine could serve to store nitrogen released from amino acid catabolism in a non-toxic form and / or be used to synthesize urea via purine synthesis-uricolysis.

Novel key aspects of cryoprotectant osmolyte (glycerol and urea) trafficking were elucidated by cloning and characterizing three aquaglyceroporin (GLP)-encoding genes from smelt at the gene and cDNA levels in Chapter 4. GLPs are integral membrane proteins that facilitate passive movement of water, glycerol and urea across cellular membranes. The highlight was the discovery that AQP10ba transcript levels always increase in posterior kidney only at low temperature. This AQP10b gene paralogue may have evolved to aid in the reabsorption of urea from the proximal tubule.

This research has contributed significantly to a general understanding of the cold adaptation response in smelt, and more specifically to the development of a working scenario for the mechanisms involved in glycerol synthesis and trafficking in this species.

ACKNOWLEDGEMENTS

I would like to thank my co-supervisors Dr. William Driedzic and Dr. Matthew Rise for their continuous support, encouragement, and intellectual input throughout this thesis. It was a tough road to get permission to do this thesis on a part-time basis and I am forever grateful for you never doubting my ability to do so. I would like to thank Dr. Ross McGowan (supervisory committee) for his constructive comments. I would like to acknowledge Dr. K. Vanya Ewart, National Research Council, Institute for Marine Biosciences, who was a long-time collaborator on the smelt project. In my early days at the Ocean Sciences Centre (OSC), I trained in Dr. Ewart's laboratory in Halifax where I was taught some new molecular techniques which I have used throughout my career as a research assistant and doctoral candidate. It was an honour to collaborate with my colleagues at Memorial University. Kathy Clow (Driedzic laboratory) helped with animal husbandry and sampling, and performed the hepatocyte isolations and biochemical assays. Connie Short (Driedzic laboratory/OSC) played an extensive role in animal husbandry and sampling, performed the temperature step-down experiment and biochemical assays, and provided training in statistical analyses and figure preparation. Jason Robinson (Driedzic laboratory) performed the glycerol assays in the seasonal study. Dr. Elizabeth Perry [Genomics and Proteomics Facility, Core Research Equipment and Instrument Training (CREAIT) Network] provided training on the 3730xl DNA Analyzer for SSH cDNA library sequencing; Lidan Tao and Brettney Pilgrim performed many sequencing reactions thereafter. Members of the OSC field services unit (Robert O'Donnell, Philip Sargent) collected the smelt. Ken Langdon (CREAIT Network) provided computer support. OSC administrative staff (Winnie Sparkes, Delores Wheeler,

JoAnn Greening and Marsha Roche) and laboratory services staff (James Devereaux, Danny Au, Damian Whitten, Chris Canning and Jerry Ennis) provided a smorgasbord of assistance. This thesis was done on a part-time basis and the OSC facility custodians (Randy Cahill, Michael Carrigan, Robert Cadigan, Harry Young, Wayne Morrissey, Jim Hopkins and especially Wayne Morris) looked out for me on the countless evenings and weekends that I spent at the OSC. Finally, on a personal level, I would like to thank my family (Barbara, Gerald and Dr. Allison Hall), close friends (Nicole and Philip Strong, Dawn Squires and Holly Cooper), fellow research assistants at the OSC – a.k.a. the lunch guy and girls (Gordon Nash, Connie Short, Kathy Clow, Candice Way, Margaret Shears, Jeanette Wells and the late Madonna King) for their support, and Cathy Driedzic for her kindness and fantastic meals during the years I've worked with Bill.

This work was supported by the Canadian Institutes of Health Research through the Regional Partnership Program (WRD, KVE) matched by the Newfoundland and Labrador Department of Innovation, Trade and Rural Development (WRD), Genome Canada and Genome BC [as part of the consortium for Genomic Research on All Salmonids Project (cGRASP)], the Research and Development Corporation of Newfoundland and Labrador, and by a Natural Sciences and Engineering Research Council of Canada Discovery Grant (WRD). WRD holds the Canada Research Chair (Tier 1) in Marine Bioscience and MLR holds the Canada Research Chair (Tier 2) in Marine Biotechnology.

TABLE OF CONTENTS

Abstract.....	ii
Acknowledgements.....	iv
Table of Contents.....	vi
List of Tables.....	xiii
List of Figures.....	xiv
List of Supplemental Files.....	xvi
List of Abbreviations.....	xviii
Co-authorship statement.....	xxii
Chapter 1: Introduction.....	1
1.1 Teleost fishes and temperature.....	1
1.2 Functional genomic approaches to study the transcriptomes of teleost fishes in response to changes in temperature.....	4
1.3 Freeze resistance in rainbow smelt.....	8
1.4 Glycerol synthesis in smelt.....	9
1.5 Functional genomic approaches to study glycerol synthesis in smelt liver.....	13
1.6 Models of glycerol synthesis in smelt.....	16
1.7 Thesis objectives: glycerol synthesis in smelt.....	16
1.8 Glycerol and urea trafficking in smelt.....	19
1.9 Thesis objectives: glycerol and urea trafficking in smelt.....	20
1.10 References.....	22

Chapter 2: Identification and validation of differentially expressed transcripts in a hepatocyte model of cold-induced glycerol production in rainbow smelt (<i>Osmerus mordax</i>).....	34
2.1 Abstract.....	35
2.2 Introduction.....	36
2.3 Materials and Methods.....	40
2.3.1 Animals.....	40
2.3.2 Hepatocyte isolation and glycerol determination.....	41
2.3.3 RNA preparation.....	41
2.3.4 SSH cDNA library construction.....	42
2.3.5 DNA sequencing, sequence assembly and gene identification.....	43
2.3.6 Microarray hybridization.....	45
2.3.7 Microarray image analysis.....	48
2.3.8 cDNA cloning [aquaglyceroporin 9 (AQP9), facilitated glucose transporter 2 (GLUT2), mitochondrial glycerol-3-phosphate dehydrogenase (mGPDH)].....	50
2.3.9 Sequence analysis of full-length cDNA clones.....	53
2.3.10 Quantitative reverse transcription - polymerase chain reaction (QPCR).....	53
2.3.11 Statistical analysis.....	56
2.4 Results.....	58
2.4.1 Glycerol production by hepatocytes incubated at cold or warm temperature.....	58
2.4.2 Reciprocal SSH cDNA library characterization.....	58
2.4.3 Microarray analyses of transcript levels in hepatocytes.....	62
2.4.4 AQP9 and GLUT2 cDNA cloning and classification.....	64

2.4.5 mGPDH cDNA cloning and characterization.....	65
2.4.6 QPCR analysis of transcripts whose products are potentially related to freeze resistance.....	76
2.4.6.1 Transcripts whose products are involved in carbohydrate metabolism.....	79
2.4.6.2 Transcripts whose products are involved in amino acid metabolism.....	85
2.4.6.3 Transcripts whose products are involved in lipid metabolism.....	86
2.4.6.4 Transcripts whose products are involved in glycerol metabolism and diffusion.....	87
2.4.6.5 Transcript encoding a phosphatase-like protein.....	87
2.4.6.6 Transcript encoding an antifreeze protein.....	88
2.5 Discussion.....	89
2.5.1 Smelt hepatocyte model of cold-induced glycerol production.....	89
2.5.2 SSH and microarray studies.....	89
2.5.3 Smelt hepatocyte transcriptome response to cold in comparison to whole animal studies.....	91
2.5.4 QPCR studies suggest key regulatory genes.....	91
2.5.4.1 Transcripts whose products are involved in carbohydrate metabolism.....	92
2.5.4.2 Transcripts whose products are involved in amino acid metabolism.....	96
2.5.4.3 Transcripts whose products are involved in lipid metabolism.....	97
2.5.4.4 Transcripts whose products are involved in glycerol metabolism and diffusion.....	98
2.5.4.5 Transcript encoding a phosphatase-like protein.....	101
2.5.4.6 Transcript encoding an antifreeze protein.....	102
2.5.5 Perspectives and Significance.....	102
2.6 References.....	104

Chapter 3: Expression analysis of glycerol synthesis-related liver transcripts in rainbow smelt (*Osmerus mordax*) exposed to a controlled decrease in temperature.....112

3.1 Abstract.....113

3.2 Introduction.....114

3.3 Materials and Methods.....118

3.3.1 Animals..... 118

3.3.2 Temperature step-down experiment..... 118

3.3.3 Tissue sampling..... 119

3.3.4 Biochemical Analyses..... 120

3.3.5 RNA preparation and QPCR..... 120

3.3.6 Statistical analysis..... 121

3.4 Results.....122

3.4.1 Biochemical analyses..... 122

3.4.2 QPCR analysis of glycerol synthesis-related liver transcript levels..... 122

3.4.2.1 Temporal-related changes..... 122

3.4.2.2 Temperature-induced changes..... 129

3.5 Discussion.....131

3.5.1 Temperature step-down (*in vivo*) model of glycerol production..... 131

3.5.2 The branch point pathway to glycerol..... 132

3.5.3 Lipid metabolism..... 137

3.5.4 Glycogen and glucose metabolism..... 138

3.5.5 Amino acid metabolism..... 140

3.5.6 Insights from *in vivo* compared to *in vitro* transcript expression levels..... 141

3.5.7 Conclusions.....	142
3.6 References.....	144
Chapter 4: Cloning and characterization of aquaglyceroporin genes from rainbow smelt (<i>Osmerus mordax</i>) and transcript expression in response to cold temperature.....	151
4.1 Abstract.....	152
4.2 Introduction.....	153
4.3 Materials and Methods.....	160
4.3.1 Study overview and animals.....	160
4.3.2 RNA preparation and cDNA synthesis.....	162
4.3.3 cDNA cloning.....	163
4.3.4 Phylogenetic and structural analysis of predicted smelt AQP10b-like protein sequences.....	166
4.3.5 Isolation of genomic and promoter sequences of smelt GLP- encoding genes.....	167
4.3.6 Analysis of smelt GLP promoter sequences.....	170
4.3.7 QPCR analysis of GLP transcript levels.....	170
4.3.8 Plasma glycerol and urea.....	174
4.3.9 Statistical analysis.....	174
4.4 Results.....	176
4.4.1 AQP10ba and AQP10bb cDNA and predicted protein sequences.....	176
4.4.2 AQP10ba, AQP10bb and AQP9b gene sequences.....	179
4.4.3 AQP10ba, AQP10bb and AQP9b promoter sequences.....	184
4.4.4 Biochemical analysis of plasma glycerol and urea levels, and QPCR analysis of kidney AQP10ba and AQP10bb transcript levels.....	185

4.4.4.1 Temperature decrease challenge.....	185
4.4.4.2 Seasonal study.....	190
4.4.5 Tissue distribution of AQP10ba, AQP10bb and AQP9b transcripts in cold- and warm-acclimated smelt.....	193
4.4.5.1 Transcript levels of AQP10ba, AQP10bb and AQP9b across tissues.....	193
4.4.5.2 Transcript levels of AQP10ba, AQP10bb and AQP9b in specific tissues.....	194
4.5 Discussion.....	201
4.5.1 Sequence analysis.....	201
4.5.1.2 Smelt GLP gene and promoter sequences.....	201
4.5.1.2 Smelt AQP10b gene duplicates.....	203
4.5.2 Tissue distribution.....	204
4.5.3 General impact of cold temperature on GLP transcript expression and glycerol transport.....	205
4.5.4 Plasma urea and kidney AQP10ba transcript levels in response to cold temperature.....	207
4.5.5 Conclusions.....	210
4.6 References.....	212
Chapter 5: Summary.....	223
5.1 Summary of thesis findings.....	223
5.1.1 Glycerol synthesis.....	223
5.1.1.1 Hepatocyte model of cold temperature-induced glycerol synthesis.....	223
5.1.1.2 Whole animal temperature “step-down” model of cold temperature-induced glycerol synthesis.....	227
5.1.1.3 Insights from <i>in vivo</i> compared to <i>in vitro</i> transcript levels in liver.....	229
5.1.2 Glycerol trafficking.....	233
5.1.2.1 Smelt GLP gene and promoter sequences.....	234

5.1.2.2 Smelt AQP10b gene duplicates.....	235
5.1.2.3 Transcript tissue expression profiles.....	236
5.1.2.4 Impact of cold temperature on glycerol and urea levels in plasma and on GLP transcript levels in smelt tissues.....	236
5.1.3 Cold adaptation in smelt compared with other teleosts.....	240
5.2 Perspectives and significance.....	242
5.3 Future directions.....	244
5.4 References.....	249

LIST OF TABLES

Table 2.1 Sequences of oligonucleotides used in cDNA cloning.....	51
Table 2.2 Primers used in QPCR studies.....	54
Table 2.3 Summary of SSH, microarray and QPCR results for genes subjected to QPCR.....	63
Table 4.1 Sequences of oligonucleotides used in cDNA cloning.....	164
Table 4.2 Sequences of oligonucleotides used in gene cloning.....	168
Table 4.3 Primers used in QPCR studies.....	171
Table 4.4 Smelt GLP cDNA, predicted protein and gene characteristics.....	178

LIST OF FIGURES

Figure 1.1 Metabolic pathways.....	11
Figure 2.1 Glycerol levels (cell pellet and incubation medium) for hepatocytes isolated from the 9 fish that were used in SSH cDNA library construction and microarray analyses.....	59
Figure 2.2 Phylogenetic analysis of smelt (A) AQP9 and (B) GLUT2 predicted protein sequences.....	66
Figure 2.3 Phylogenetic analysis of smelt mGPDH predicted protein sequences.....	71
Figure 2.4 Amino acid alignment of mGPDH from human, rat, frog and smelt.....	73
Figure 2.5. Tissue distribution of smelt mGPDH transcripts.....	77
Figure 2.6 QPCR analyses of a subset of transcripts identified as differentially expressed in cold compared to warm cells by either SSH, microarray analysis (or both) or selected by the authors because of their theoretical relationship to glycerol management.....	80
Figure 2.7 A schematic representation of glycerol synthesis pathway-related transcript levels in glycerol accumulating cultured smelt hepatocytes.....	93
Figure 3.1 (A) plasma glycerol ($\mu\text{mol/ml}$) (B) plasma glucose ($\mu\text{mol/ml}$) and (C) liver glycogen ($\mu\text{mol/g}$) in smelt held at high or low temperature.....	123
Figure 3.2 QPCR analyses of glycerol metabolism-related liver transcripts in smelt held at high or low temperature.....	125
Figure 3.3 A schematic representation of glycerol synthesis pathway-related transcript levels in liver of glycerol accumulating smelt.....	133
Figure 4.1 Alignment of protein sequences for piscine AQP10b orthologues.....	156
Figure 4.2 Phylogenetic analysis of full-length smelt GLP predicted protein sequences.....	180
Figure 4.3 A schematic representation of the structure of smelt GLP-encoding genes.....	182
Figure 4.4 A schematic comparison of selected putative transcription factor binding motifs in the smelt AQP10ba, AQP10bb and AQP9b proximal (1 kb) promoter sequences.....	186

Figure 4.5 (A) plasma glycerol (mM) (B) plasma urea (mM) (C) kidney AQP10ba transcript levels and (D) kidney AQP10bb transcript levels in smelt held at high or low temperature.....	188
Figure 4.6 A seasonal (November 2008 to May 2009) analysis of (A) ambient water temperature (B) plasma glycerol (mM) (C) plasma urea (mM) (D) kidney AQP10ba transcript levels and (E) kidney AQP10bb transcript levels in smelt held at high or ambient seawater temperature.....	191
Figure 4.7 QPCR analysis of transcript levels of (A) AQP10ba (B) AQP10bb and (C) AQP9b in various tissues from smelt held at high or low temperature.....	195
Figure 4.8 Transcript levels of AQP10ba, AQP10bb and AQP9b in various smelt tissues.....	197
Figure 5.1 Proposed model for urea reabsorption from the proximal tubule of the smelt nephron.....	238

LIST OF SUPPLEMENTAL FILES (AVAILABLE ON CD)

Supplemental Table S2.1 Complete list of contigs and singletons in the forward (enriched for transcripts expressed at higher levels in cold compared to warm cells at 72 h) hepatocyte SSH library with associated accession numbers, statistics and annotations.

Supplemental Table S2.2 Complete list of contigs and singletons in the reverse (enriched for transcripts expressed at higher levels in warm compared to cold cells at 72 h) hepatocyte SSH library with associated accession numbers, statistics and annotations.

Supplemental Table S2.3 Microarray-identified reproducibly informative genes in cold compared to warm cells at 24 h with associated accession numbers, statistics, annotations and mean fold change values.

Supplemental Table S2.4 Microarray-identified reproducibly informative genes in cold compared to warm cells at 48 h with associated accession numbers, statistics, annotations and mean fold change values.

Supplemental Table S2.5 Microarray-identified reproducibly informative genes in cold compared to warm cells at 72 h with associated accession numbers, statistics, annotations and mean fold change values.

Supplemental Table S2.6 Summary of microarray-identified reproducibly informative genes in cold compared to warm cells at 24 h, 48 h and 72 h with associated accession numbers, statistics and mean fold change values.

Supplemental Table S4.1A Forty-five putative transcription factor recognition sites in the promoter region of AQP10ba identified using a MATCH (vertebrate non-redundant MFP group of matrices) search of the TRANSFAC database.

Supplemental Table S4.1B Eighty-eight putative transcription factor recognition sites in the promoter region of AQP10bb identified using a MATCH (vertebrate non-redundant MFP group of matrices) search of the TRANSFAC database.

Supplemental Table S4.1C Fifty-two putative transcription factor recognition sites in the promoter region of AQP9b identified using a MATCH (vertebrate non-redundant MFP group of matrices) search of the TRANSFAC database.

Supplemental Table S4.1D Three hundred and six putative transcription factor recognition sites in the promoter region of AQP10ba identified using a MATCH (vertebrate non-redundant MSUM group of matrices) search of the TRANSFAC database.

Supplemental Table S4.1E Seven hundred and forty-six putative transcription factor recognition sites in the promoter region of AQP10bb identified using a MATCH (vertebrate non-redundant MSUM group of matrices) search of the TRANSFAC database.

Supplemental Table S4.1F Four hundred and twenty-eight putative transcription factor recognition sites in the promoter region of AQP9b identified using a MATCH (vertebrate non-redundant MSUM group of matrices) search of the TRANSFAC database.

Supplemental Figure S4.1 The gene sequence for (A) AQP10ba, (B) AQP10bb, and (C) AQP9b.

Supplemental Figure S4.2 Nucleotide sequences of the 5' flanking regions of the (A) AQP10ba, (B) AQP10bb and (C) AQP9b genes and the location of selected putative transcription factor binding motifs.

LIST OF ABBREVIATIONS

2-PG	2-phosphoglycolate
6PGDH	6-phosphogluconate dehydrogenase
°C	Celsius (degrees)
aa	amino acid
AAT2	alanine aminotransferase 2
AAV	adeno-associated virus
ACSL4	acyl-CoA synthetase 4
AFGP	antifreeze glycoprotein
AFP	antifreeze protein
ALD	aldolase
ANOVA	analysis of variance
AP-1	activator protein-1
AQP	aquaporin
ar/R	aromatic residue/arginine
AspAT	aspartate aminotransferase
ATP	adenosine triphosphate
BCLN	Background Corrected Lowess Normalized
BLAST	Basic Local Alignment Search Tool
bp	base pair
BP	biological process
BPI	bactericidal/permeability-increasing protein
¹³ C	carbon-13
C	cysteine
cAMP	cyclic adenosine monophosphate
CC	cellular component
CDD	Conserved Domains Database
cDNA	complementary deoxyribonucleic acid
CDS	coding sequence
C/EBP	CCAAT/enhancer-binding protein
cGPDH	cytosolic glycerol-3-phosphate dehydrogenase
cGRASP	consortium for Genomics Research on All Salmonids Project
CIRBP	cold inducible RNA binding protein
CO ₂	carbon dioxide
CoA	coenzyme A
CREAIT	Core Research Equipment and Instrument Training
CREB1	cAMP responsive element binding protein 1
CRISPR	Clustered Regularly Interspaced Short Palindromic Repeats
C _T	threshold cycle
Cy	cyanine
D	aspartic acid
dbEST	expressed sequence tag database of GenBank
dCTP	deoxycytidine triphosphate
DHAP	dihydroxyacetone phosphate
DNA	deoxyribonucleic acid

dNTP	2'-deoxyribonucleoside triphosphate
DTT	dithiothreitol
E-value	Expect-value
EST	expressed sequence tag
ETF	electron-transferring flavoprotein
F	phenylalanine
FAD	flavin adenine dinucleotide
FADH ₂	flavin adenine dinucleotide, reduced
FAM	fluorescein
FATP	fatty acid transporter
g	gram
G3P	glycerol-3-phosphate
G3Pase	glycerol-3-phosphatase
G6P	glucose-6-phosphate
G6Pase	glucose-6-phosphatase
GaP	Genomics and Proteomics Facility
GAPDH	glyceraldehyde-3-phosphate dehydrogenase
GDH	glutamate dehydrogenase
GEO	Gene Expression Omnibus
GFP	green fluorescent protein
GLP	aquaglyceroporin
GLUT	glucose transporter
GO	gene ontology
GR	glucocorticoid receptor
GS	glutamine synthetase
h	hour
H	histidine
HMGB1	high mobility group b1
HNF	hepatic nuclear factor
HSD	honest significant difference
HSI	hepatic somatic index
IRE	insulin response element
K	thousand
kb	kilobase
kDa	kilodalton
l	litre
L	leucine
LB	Luria broth
LBP	lipopolysaccharide binding protein
LIPL	lipoprotein lipase
LNA	locked nucleic acid
LPS	lipopolysaccharide
MDH2	mitochondrial malate dehydrogenase 2
MEGA	Molecular Evolutionary Genetics Analysis
MF	molecular function
MFN	minimize false negatives

MFP	minimize false positives
µg	microgram
mg	milligram
MGB	minor groove binder
MGBNFQ	minor groove binder – non-fluorescent quencher
mGPDH	mitochondrial glycerol-3-phosphate dehydrogenase
MIAME	Minimum Information About a Microarray Experiment
µl	microlitre
ml	millilitre
µM	micromolar
mM	millimolar
mRNA	messenger ribonucleic acid
MSF	multiple sequence alignment file
MSUM	minimize false positives and minimize false negatives
mya	million years ago
n	number
NADH	nicotinamide adenine dinucleotide, reduced
NADPH	nicotinamide adenine dinucleotide phosphate, reduced
NCBI	National Center for Biotechnology Information
NEFA	non-esterified fatty acid
NF	nuclear factor
ng	nanogram
NJ	Neighbour-Joining
nM	nanomolar
NMR	nuclear magnetic resonance
NPA	Asn-Pro-Ala
nr	non-redundant
nt	nucleotide
ORF	open reading frame
OSC	Ocean Sciences Centre
P	proline
PCR	polymerase chain reaction
PDH	pyruvate dehydrogenase
PDK2	pyruvate dehydrogenase kinase 2
PEPCK	phosphoenolpyruvate carboxykinase
PFK	phosphofructokinase
PGE	precise genome-editing
PGM	phosphoglucomutase
PLA ₂	phospholipase A ₂
PMT	photomultiplier tube
PVC	polyvinyl chloride
QPCR	quantitative reverse transcription - polymerase chain reaction
R	arginine
RAQ	relative absolute quantity
RBC	red blood cell
RLM-RACE	RNA ligase-mediated rapid amplification of 5' and 3' cDNA ends

RNA	ribonucleic acid
RNAi	ribonucleic acid interference
RNA-Seq	ribonucleic acid sequencing
RQ	relative quantity
RT-PCR	reverse transcription - polymerase chain reaction
S	subunit
SDS	sodium dodecyl sulfate
SE	standard error
shRNA	small hairpin ribonucleic acid
siRNA	small interfering ribonucleic acid
SLC27A6	solute carrier family 27 member 6
SSC	saline sodium citrate
SSH	suppression subtractive hybridization
TAG	triacylglycerol
TALDO1	transaldolase 1
TCA	trichloroacetic acid
TEF-1	transcription enhancer factor-1
TIFF	tagged image file format
TIM	triose phosphate isomerase
TMAO	trimethylamine oxide
TMD	transmembrane domain
TRANSFAC	transcription factor database
U	unit
UNG	uracil N-glycosylase
UTR	untranslated region
UV	ultraviolet
V	valine
Y	tyrosine
WGD	whole genome duplication

CO-AUTHORSHIP STATEMENT

Chapter 2:

Hall JR, Clow KA, Rise ML, Driedzic WR. Identification and validation of differentially expressed transcripts in a hepatocyte model of cold-induced glycerol production in rainbow smelt (*Osmerus mordax*). *Am J Physiol Regul Integr Comp Physiol* 301: R995-R1010, 2011.

Author contributions:

J.R.H., M.L.R. and W.R.D. conception and design of research.

K.A.C. performed hepatocyte isolations and glycerol measurements.

J.R.H. performed all remaining experiments.

J.R.H. analyzed data.

J.R.H. interpreted results of experiments.

J.R.H. prepared figures.

J.R.H. drafted manuscript.

J.R.H., M.L.R. and W.R.D. edited and revised manuscript.

J.R.H., K.A.C., M.L.R. and W.R.D. approved final version of manuscript.

Chapter 3:

Hall JR, Short CE, Rise ML, Driedzic WR. Expression analysis of glycerol synthesis-related liver transcripts in rainbow smelt (*Osmerus mordax*) exposed to a controlled decrease in temperature. *Physiol Biochem Zool* 85: 74-84, 2012.

Author contributions:

J.R.H., M.L.R. and W.R.D. conception and design of research.

C.E.S. performed the temperature step-down experiment and the biochemical analyses.

J.R.H. performed all remaining experiments.

J.R.H. analyzed data.

J.R.H. interpreted results of experiments.

J.R.H. prepared figures.

J.R.H. drafted manuscript.

J.R.H., M.L.R. and W.R.D. edited and revised manuscript.

J.R.H., C.E.S., M.L.R. and W.R.D. approved final version of manuscript.

Chapter 4:

Hall JR, Clow KA, Rise ML, Driedzic WR. Cloning and characterization of aquaglyceroporin genes from rainbow smelt (*Osmerus mordax*) and transcript expression in response to cold temperature. *Comp Biochem Physiol B Biochem Mol Biol* 187: 39-54, 2015.

Author contributions:

J.R.H., M.L.R. and W.R.D. conception and design of research.

K.A.C. performed urea measurements and glycerol measurements.

C.E.S. performed the temperature step-down experiment and glycerol measurements.

J.L. Robinson performed glycerol measurements.

J.R.H. performed all remaining experiments.

J.R.H. analyzed data.

J.R.H. interpreted results of experiments.

J.R.H. prepared figures.

J.R.H. drafted manuscript.

J.R.H., M.L.R. and W.R.D. edited and revised manuscript.

J.R.H., K.A.C., M.L.R. and W.R.D. approved final version of manuscript.

CHAPTER 1: INTRODUCTION

1.1 TELEOST FISHES AND TEMPERATURE

There are approximately 27,000 living teleostean species that inhabit a vast range of freshwater and marine environments, from 41°C hot springs [e.g. desert pupfish (*Cyprinodon macularius*)] to -1.9°C polar oceans (e.g. Notothenioids) (31). A fish-specific whole genome duplication (WGD) event at the root of the crown clade of Teleostei ~350 mya was critical for this expansion (3).

Teleosts are ectothermic which means that their body temperature is generally that of the ambient water. A given teleostean species has a thermal tolerance range in which it is able to cope with natural (e.g. daily and seasonal) fluctuations in water temperature within its habitat. Outside of this thermal temperature range, health and survival are threatened. Thermal tolerance range is variable; eurythermal fishes can survive a broad range of temperature fluctuations, while stenothermal fishes cannot (44).

The behavioural, physiological and biochemical responses and adaptations of teleosts to temperature (high and low) have been studied exhaustively. These studies have generally focused on responses and adaptations that allow fishes to survive temperature shock (i.e. when a fish has been acclimated to a specific water temperature or range of temperatures and is subsequently exposed to a rapid increase or decrease in temperature), that allow eurythermal fishes to survive wide temperature extremes and that allow marine fishes living in temperate and polar regions to survive at low and/or sub-zero temperatures.

The cold shock responses of teleosts are generally grouped into three categories. Primary responses include neuroendocrine, catecholamine and corticosteroid responses.

Secondary responses include metabolic and haematological responses, cellular responses such as expression of heat shock proteins, and osmoregulatory and immunological changes. Tertiary responses include changes in growth and development rates, disease resistance, and behavioural modifications such as changes in microhabitat use, abundance and distribution, feeding, predation, migration and spawning behaviours (15).

Eurythermal fishes have many strategies that allow them to survive temperature extremes. These can include polyploidy [e.g. common carp (*Cyprinus carpio*) (37)], different rates of protein synthesis at different temperatures [e.g. common carp (67)], the presence of isozymes that catalyze the same reaction more efficiently at different temperatures [e.g. acetylcholinesterase from rainbow trout (*Oncorhynchus mykiss*) (4), cytosolic malate dehydrogenase from longjaw mudsucker (*Gillichthys mirabilis*) (41)], and changes in the ratio of saturated and unsaturated fatty acids in cell membranes [e.g. rainbow trout (30)] to name a few.

Marine teleosts that inhabit temperate and polar waters must employ freeze prevention strategies to avoid death in the winter months, when water temperatures can reach sub-zero levels. The freezing point of teleost blood is typically about -0.8°C (12); however in these regions, water temperature can decrease to -1.9°C and these waters are frequently ice covered (19). Teleost freeze prevention strategies may include behavioural strategies such as migration further off shore to deeper, warmer waters where freezing will not occur (i.e. freeze avoidance) (59). Cunners (*Tautoglabrus adspersus*) avoid contact with ice by aggregating in rock crevices on the ocean bottom, enter a state of dormancy in which activity and feeding cease (27) and downregulate their metabolism (10). Teleost freeze prevention strategies may also include biochemical adaptations such

as the synthesis of macromolecular antifreeze proteins (AFPs) (22, 59), and/or the accumulation of osmolytes such as ions (Na^+ , Cl^-), and small organic solutes such as trimethylamine oxide (TMAO), urea (52) and glycerol (50) that lower their freezing point to that of their environment (i.e. freeze resistance).

AFPs lower the freezing point non-colligatively by binding to ice crystals and preventing their growth (68). In fish, this is a common method of freeze resistance, with five structurally defined types having been identified [reviewed in (26)]. Antifreeze glycoproteins (AFGPs) are composed of multiple Ala-Ala-Thr repeats with a disaccharide linked to each Thr residue (1), and are found in Arctic cod (*Boreogadus saida*) and Antarctic notothenioid fishes (6, 48). Type I AFPs are alanine-rich, amphiphilic α helices with a repeating pattern of Thr residues (1) and are widely distributed, being found in winter flounder (*Pseudopleuronectes americanus*) (20), shorthorn sculpin (*Myoxocephalus scorpius*) (32), Atlantic snailfish (*Liparis atlanticus*) (21), dusky snailfish (*Liparis gibbus*) (21) and cunner (33). Type II AFPs are more complex globular proteins homologous to C-type lectins (1) and are found in sea raven (*Hermitripteris americanus*) (47), Atlantic herring (*Clupea harengus harengus*) (43) and rainbow smelt (*Osmerus mordax*) (1). Type III AFPs have a globular fold with one flattened surface required for ice binding (1) and are found in northern and Antarctic eel pouts (39). Type IV AFP is composed of an antiparallel helix bundle homologous to an apolipoprotein (1) and has only been found in longhorn sculpin (*Myoxocephalus octodecimspinosis*) (11).

Osmolyte accumulation lowers the freezing point colligatively by increasing osmotic pressure. Osmolyte accumulation at high levels is not a common method of

freeze resistance in fish. However, high glycerol level has been reported in rainbow smelt, in smelt from Alaska (*O. mordax dentex*) and Japan (*Hypomesus pretiosus japonica*), and in two species of greenling (*Hexagrammos octogrammus* and *H. stelleri*) (50).

1.2 FUNCTIONAL GENOMIC APPROACHES TO STUDY THE TRANSCRIPTOMES OF TELEOST FISHES IN RESPONSE TO CHANGES IN TEMPERATURE

The aforementioned information highlights some of the responses and adaptations of teleost fishes to temperature changes at the behavioural, physiological and biochemical levels. However, deciphering the molecular mechanisms governing the responses and adaptations of teleost fishes to temperature changes remains paramount. Previously, molecular studies were limited to single or few genes and proteins; however, in the last decade (i.e. just prior to and concurrent with the research conducted herein), the advent of functional genomic tools and techniques has allowed genome-wide analyses of the transcriptome response of several teleosts to changes in temperature [reviewed in (44)]. These techniques include the generation and characterization (sequencing) of suppression subtractive hybridization (SSH) cDNA libraries (13) and microarray analyses. Expression levels of differentially expressed transcripts identified in functional genomic analyses can then be validated using quantitative reverse transcription - polymerase chain reaction (QPCR).

Subtractive hybridization allows the comparison of two populations of mRNA by obtaining clones of genes that are expressed in one population but not the other. Briefly, double-stranded cDNA is synthesized for each mRNA population (e.g. fish held at low

and high temperature). The cDNA that contains the differentially expressed transcripts is referred to as the tester and the reference cDNA as the driver. The tester and driver cDNAs are digested with *RsaI* to generate blunt ends. The tester cDNA is subdivided into two portions and a different adaptor [e.g. adaptor 1 or adaptor 2R; PCR-Select cDNA Subtraction Kit (Clontech, Mountain View, CA)] is ligated to the 5' end; the driver cDNA has no adaptors. These adaptors have both identical and unique PCR primer annealing sites. Two hybridizations are performed. In the first hybridization, each tester cDNA (with either adaptor 1 or adaptor 2R ligated to the 5' end) is combined with excess driver in separate reactions, heat denatured and allowed to anneal. Following hybridization, differentially expressed sequences, with adaptor 1 ligated to the 5' end in one reaction and adaptor 2R ligated to the 5' end in the other, are the only single-stranded cDNA sequences that remain. In the second hybridization, the two primary hybridization samples are combined without denaturing (in the presence of fresh denatured driver). The remaining equalized and subtracted tester cDNAs reassociate to form double-stranded tester molecules with different adaptors (i.e. 1 or 2R) at the 5' end. The ends are then filled in by DNA polymerase to generate double-stranded differentially expressed tester sequences whose 5' and 3' ends have identical annealing sites for the PCR primer in the primary PCR reaction and different annealing sites for the nested PCR primers in the secondary PCR reaction. Only these equalized, differentially expressed sequences with two different adaptors are amplified by PCR. Reciprocal libraries are constructed [i.e. mRNA from fish at low temperature would be the tester in the forward SSH library (enriched for transcripts expressed at higher levels in cold than warm fish) and the driver in the reverse SSH library (enriched for transcripts expressed at higher levels in warm

than cold fish). The warm fish would be the tester in the reverse SSH library and the driver in the forward SSH library]. Differentially expressed cDNAs are subcloned, sequenced and identified by BLAST searches against nucleotide and/or protein sequences deposited in NCBI databases.

There are many types of microarray platforms including spotted arrays, inkjet printed arrays, photolithography constructed arrays and others. There are also different types of chemistries available for hybridization including fluorescent (e.g. cyanine) and biotin. For the research conducted herein, the microarray platform was the consortium for Genomic Research on All Salmonids Project (cGRASP) 16K cDNA salmonid cDNA array (65), which is a spotted array; the hybridization chemistry was cyanine (Cy3 and Cy5) fluorophores. Briefly, in this thesis, the mRNA from each population (e.g. cold and warm hepatocytes) is reverse-transcribed using an oligo d(T) primer with a unique 5-prime sequence overhang that is complementary to a primer labelled with a specific three dimensional fluorescent dye (e.g. Cy5 for the cold hepatocytes and Cy3 for the warm hepatocytes). The cDNAs for each mRNA population are combined and hybridized to the array. Unbound cDNA is washed away and the Cy3 and Cy5 fluorescent molecules are hybridized to the bound cDNA on the microarray. Fluorescent images of hybridized arrays are then acquired using a microarray scanner.

More specifically, in addition to the research conducted herein, functional genomic studies have been performed to study the molecular responses to cold temperature in eurythermal fishes such as common carp (24), killifish (*Austrofundulus limnaeus*) (49), zebrafish (*Danio rerio*) (34, 45) and gilthead seabream (*Sparus aurata*) (46), and the stenothermal Antarctic toothfish (*Dissostichus mawsoni*) (7). These studies

have provided valuable insight into the transcriptional responses, Gene Ontology (GO) functional groups and potential regulators associated with cold temperature at both the individual species and global levels. At the global level, a comparison of cold-responsive transcripts in zebrafish and in common carp identified 38 transcripts that were in common between the two species, including cold inducible RNA binding protein (CIRBP) and high mobility group b1 (HMGB1) (34). Interestingly, HMGB1 was identified as a putative global regulator of transcription in response to temperature in killifish (49). Cold-responsive transcripts in common between zebrafish and common carp are involved in oxidative phosphorylation, in protein folding and degradation, and in RNA processing and translation, which comprise the set of evolutionarily conserved cold-responsive mechanisms in the teleost (34).

The aforementioned functional genomic studies were performed on eurythermal fishes that are not subjected to sub-zero temperatures in their natural habitats, and on an Antarctic notothenioid fish that survives sub-zero temperatures by the synthesis of AFGPs. The species of interest for the research conducted herein is the rainbow smelt (*Osmerus mordax*, Mitchill, 1814). Compared to these fishes, as described below, the rainbow smelt has a different thermal history and a unique biochemical adaptation (high glycerol level) to avoid freezing in sub-zero temperatures. The overall goal of this thesis was to apply functional genomic and molecular tools and techniques to elucidate the molecular underpinnings of the adaptations and responses (with a particular focus on glycerol synthesis and trafficking) of the rainbow smelt to cold temperature, while perhaps contributing to a global understanding of the molecular mechanisms governing cold adaptation in teleosts.

1.3 FREEZE RESISTANCE IN RAINBOW SMELT

The rainbow smelt (hereafter referred to as smelt) is a small (less than 20 cm in length) anadromous teleost that inhabits the waters along the North American Atlantic coastline. Smelt often overwinter in ice-covered inshore seawaters where water temperatures can reach as low as -1.8°C before freezing (58). As stated previously, the freezing point of teleost blood is typically about -0.8°C (12); however, smelt are quite active under the ice and feed on a high protein diet consisting of mysid shrimp, amphipods and polychaetes (53).

As stated previously, freeze resistance in smelt is accomplished via the synthesis of type II AFP and the accumulation of osmolytes in plasma and tissues. These osmolytes include ions, TMAO and urea at modest levels (52), and glycerol at levels 1000-fold greater than at summer temperatures (50). Smelt type II AFP is a member of the C-type (i.e. it requires Ca^{2+} to be bound before it can bind to its substrate) lectin superfamily. It shares the Gln-Pro-Asp (galactose-binding) motif of galactose-binding C-type lectins; however, in type II AFPs this is the ice-binding site. Unlike other C-type lectins and type II AFPs, in smelt type II AFP this protein core is protease resistant. Smelt type II AFP is unique among fish AFPs in that it forms an intermolecular dimer composed of two separate subunits, and it has an N-linked oligosaccharide located on Asn18 that is not present in other known fish AFPs (1). Glycerol is a three carbon polyol which forms the backbone of triglycerides and phospholipids. Glycerol also serves as a chemical chaperone (23).

In smelt from Newfoundland, maintained in aquaria, the initiation of type II AFP production is photoperiod dependent and occurs in early fall when water temperatures are

~11°C (38, 40). However, high glycerol production is low temperature dependent. Smelt held at high (8-10°C) temperature maintain low (~0.3 mM) glycerol level; in fish following ambient seawater temperatures, glycerol level follows a seasonal pattern. Glycerol level begins to slowly increase in plasma in November, when water temperature decreases to ~5°C, with levels reaching in excess of 200 mM by February when water temperatures (-1°C) are at their lowest (38, 57). Smelt urea level also follows a seasonal pattern similar to glycerol although levels in plasma increased from 3 mM to only 9 mM at peak plasma glycerol concentration (63). Winter levels of type II AFP and glycerol can provide a freezing point depression of about 0.3°C and 0.5°C, respectively (38).

1.4 GLYCEROL SYNTHESIS IN SMELT

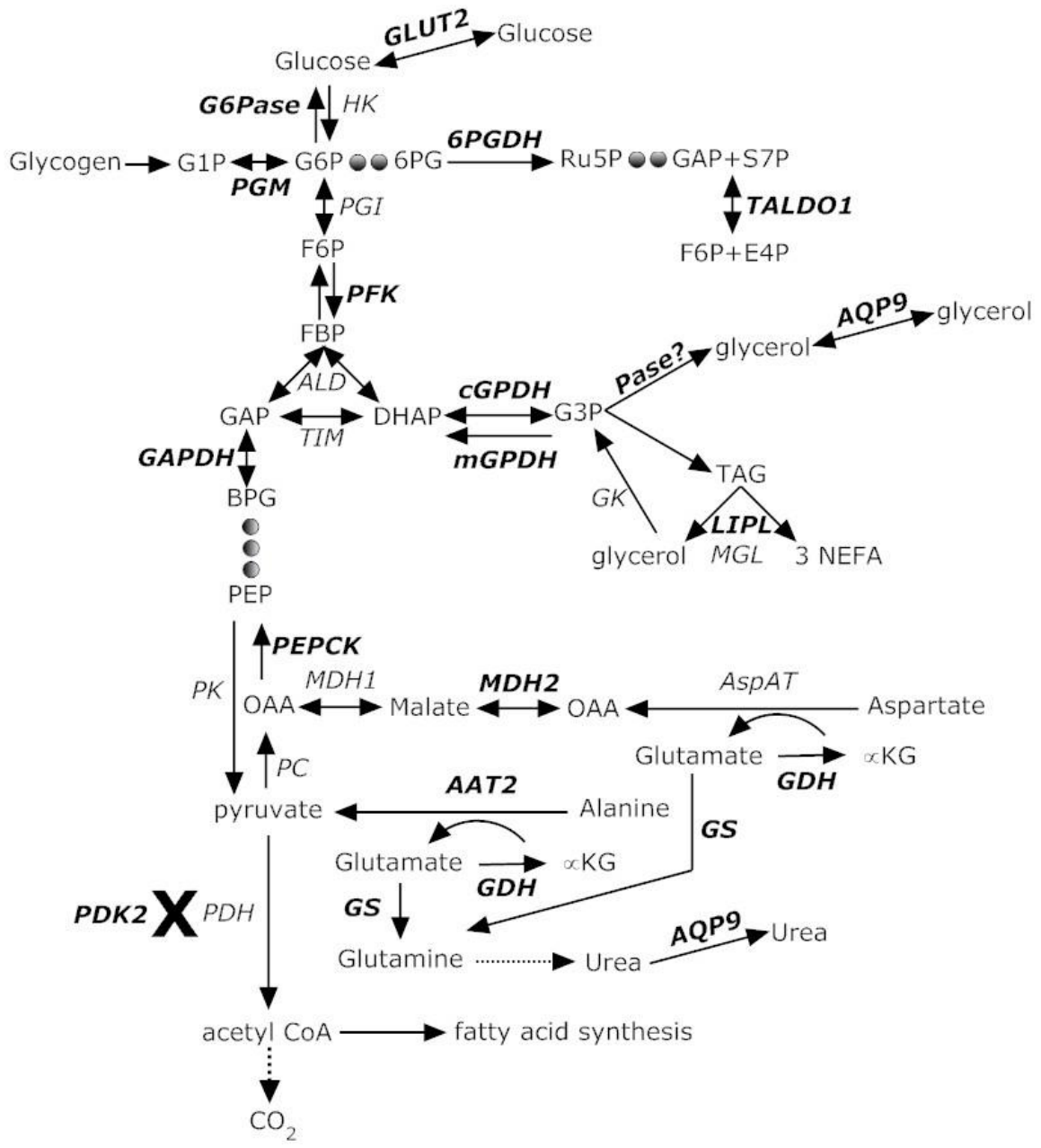
In smelt, glycerol is lost across the skin and gills at a rate of about 10% per day in the winter months (51) and must therefore be constantly synthesized to maintain the level required for its role in freeze prevention. Synthesis primarily occurs in liver (38, 40, 57) and is derived from both glycolytic and gluconeogenic sources as evidenced by nuclear magnetic resonance (NMR) studies (66) in which winter smelt injected with ¹³C glucose or ¹³C alanine produced glycerol with intact incorporation of the neighbouring ¹³C labeled atoms. During the fall-to-winter transition, glycerol accumulation is primarily fuelled through the mobilization of glycogen reserves; however, in order to sustain the carbon demand for glycerol production, smelt must feed constantly (17, 63). Since their diet is protein rich, as carbohydrate reserves become limiting, amino acids become increasingly important in supporting glycerol production. When glycerol synthesis is fuelled by the deamination of amino acids, the resultant ammonia can be detoxified by

the production of urea, which serves the dual function of conserving nitrogen in a non-toxic form and increasing osmotic pressure.

The proposed pathway for glycerol synthesis (glyceroneogenesis) (Fig. 1.1) from carbohydrate and amino acids is via a branch point in glycolysis and gluconeogenesis, respectively, in which dihydroxyacetone phosphate (DHAP) is converted to glycerol-3-phosphate (G3P) by cytosolic glycerol-3-phosphate dehydrogenase (cGPDH). There are two pathways in which G3P can be converted to glycerol. G3P can be dephosphorylated to glycerol directly by an unidentified glycerol-3-phosphatase (G3Pase) (14, 16, 18). Alternatively, G3P could theoretically be incorporated into triglyceride which can be thereafter broken down into glycerol and three free fatty acids. Recent studies suggest that it is G3Pase and not lipid recycling that is the primary pathway for glycerol accumulation in smelt (14). The resultant glycerol can enter the plasma via aquaglyceroporins (GLPs) or be phosphorylated back to G3P by glycerol kinase and subsequently directed to glucose synthesis or oxidation to CO₂, depending on the metabolic needs of the cell.

Analyses of transcript and enzyme activity levels of selected genes in smelt liver have provided substantial evidence to support this proposed pathway for glycerol synthesis. For the glycolytic branch, in cultured hepatocytes, glycerol synthesis was fuelled by glycogen stores in the absence of exogenous substrate and was associated with an increase in the activity of total glycogen phosphorylase and glycogen phosphorylase *a*, the active form of the enzyme (9). In fish living at low temperature, phosphofructokinase (PFK) and aldolase (ALD) activity levels were significantly higher in smelt compared to the non-glycerol accumulating capelin (*Mallotus villosus*) (62). In smelt following ambient seawater temperatures, ALD transcript levels were about 25-fold significantly

Figure 1.1. Metabolic pathways. The proposed pathway for glycerol synthesis in smelt liver is via a branch point in glycolysis and gluconeogenesis. Genes encoding proteins involved in the conversion of L-amino acids to glyceroneogenic precursors, triglyceride metabolism and the non-glyceroneogenic fates of G6P (glucose synthesis or pentose phosphate pathway) are also included. Gene name abbreviations are in italics and those whose transcripts were analyzed by QPCR are in bold italics, and are defined as follows: **GLUT2**, glucose transporter 2; **PGM**, phosphoglucomutase; **G6Pase**, glucose-6-phosphatase; **6PGDH**, 6-phosphogluconate dehydrogenase; **TALDO1**, transaldolase; HK, hexokinase; PGI, phosphoglucoisomerase; **PFK**, phosphofructokinase; ALD, aldolase; TIM, triose isomerase; **GAPDH**, glyceraldehyde-3-phosphate dehydrogenase; PK, pyruvate kinase; PDH, pyruvate dehydrogenase; **PDK2**, pyruvate dehydrogenase kinase; PC, pyruvate carboxylase; **PEPCK**, phosphoenolpyruvate carboxykinase; **MDH2**, mitochondrial malate dehydrogenase; MDH1, cytosolic malate dehydrogenase; AspAT, aspartate aminotransferase; **AAT2**, alanine aminotransferase; **GS**, glutamine synthetase; **GDH**, glutamate dehydrogenase; **LIPL**, lipoprotein lipase; MGL, monoacylglycerol lipase; **cGPDH**, cytosolic glycerol-3-phosphate dehydrogenase; **mGPDH**, mitochondrial glycerol-3-phosphate dehydrogenase; GK, glycerol kinase; **AQP9**, aquaglyceroporin 9. Metabolite abbreviations are as follows: G1P, glucose-1-phosphate; G6P, glucose-6-phosphate; F6P, fructose-6-phosphate; FBP, fructose-1,6-bisphosphate; GAP, glyceraldehyde-3-phosphate; DHAP, dihydroxyacetone phosphate; BPG, 1,3-bisphosphoglycerate; PEP, phosphoenolpyruvate; OAA, oxaloacetate; α KG, alpha-ketoglutarate; 6PG, 6-phosphogluconate; Ru5P, ribulose-5-phosphate; S7P, sedoheptulose-7-phosphate; E4P, erythrose-4-phosphate; G3P, glycerol-3-phosphate; TAG, triglyceride; NEFA, non-esterified free fatty acid. Dots represent pathway intermediates that are not shown.



higher at peak glycerol level in February than in October (55).

For the gluconeogenic branch, in fish living at low temperature, aspartate aminotransferase (AspAT), alanine aminotransferase (AAT), and glutamate dehydrogenase (GDH) activity levels were all significantly higher in smelt compared to the non-glycerol accumulating Atlantic tomcod (*Microgadus tomcod*) and smooth flounder (*Liopsetta putmani*) (18). AspAT, AAT and phosphoenolpyruvate carboxykinase (PEPCK) activity levels were all significantly higher in smelt compared to capelin (62). In smelt following ambient seawater temperatures, AspAT, AAT and PEPCK activity (38) and PEPCK transcript (40) levels increased during the seasonal transition from October through to March. GDH transcript levels increased from October through to January (55).

For glyceroneogenesis, in fish living at low temperature, cGPDH and G3Pase activity levels were significantly higher in smelt compared to Atlantic tomcod and smooth flounder (18), and cGPDH activity levels were significantly higher in smelt compared to capelin (62). In smelt following ambient seawater temperatures, cGPDH transcript (40, 55, 57) and activity (16, 38) levels, and G3Pase activity (14) levels increased in association with decreases in water temperature and elevated glycerol accumulation.

1.5 FUNCTIONAL GENOMIC APPROACHES TO STUDY GLYCEROL SYNTHESIS IN SMELT LIVER

Although the aforementioned studies have provided invaluable information on glycerol synthesis in smelt liver, such specific analyses may hinder the identification of novel key regulatory genes. Therefore, complementary functional genomic approaches

(microarray analyses, SSH cDNA library construction) were undertaken to study glycerol synthesis in smelt liver.

Complementary analyses were performed when this research was initiated, since there were limited genomic resources available for smelt as it is a non-model species. There was no smelt microarray platform; however, there was a cGRASP 16K salmonid cDNA array available to which the average percentage binding of smelt liver targets was 30% (65). There were potential limitations to this inter-specific microarray approach. First, important genes in cold adaptation in smelt may not hybridize to the array due to sequence differences between the two species. Second, smelt are diploid and have less than half the amount of genomic DNA of the pseudotetraploid salmonids (56, 65). Third, smelt and salmon represent different scales of cold adaptation in that salmon do not produce type II AFP (25) or accumulate glycerol (57) so important genes in these processes may not even be present on the microarray. Fourth, there was limited nucleotide sequence data available for smelt. Therefore, designing QPCR primers to analyze transcript levels of differentially expressed genes identified in microarray analyses would require cloning of orthologous cDNA sequences from smelt; however, efforts were underway to develop genomic library and expressed sequence tag (EST) resources for smelt (64). The construction of SSH cDNA libraries would potentially identify transcripts missed in the microarray analyses. Furthermore, the cDNA sequences generated would be from smelt facilitating QPCR primer design. However, this was prior to the advent of Next Generation Sequencing, so characterization of SSH cDNA libraries was relatively expensive.

In the first functional genomic analyses of the low temperature response in smelt, the gene expression profiles of pooled RNA from livers of non-glycerol accumulating smelt collected in October (fall smelt) and of pooled RNA from livers of smelt at peak glycerol production in January/February (winter smelt) were compared by SSH and microarray analyses and levels of selected transcripts were measured by QPCR (54, 55). SSH analyses, enriched for transcripts differentially expressed between winter and fall smelt, generated 441 ESTs (54). Microarray analyses identified 83 transcripts (69 upregulated, 14 downregulated) that were reproducibly greater than two-fold differentially expressed in winter compared to fall smelt (55). Some of these informative transcripts, such as fructose 1,6-bisphosphate aldolase B (ALD) and glutamate dehydrogenase (GDH), were related to maintenance of glycerol production, and to other aspects of long-term cold adaptation.

A potential limitation of these studies (54, 55) is that genes involved in the proposed pathway for glycerol production are also part of glycolysis, gluconeogenesis and/or triglyceride metabolism. Therefore, expression of these genes could be quite variable between fish due to factors unrelated to glycerol production i.e. differences in metabolic rate, activity level and nutritional status. This could be particularly relevant when fish are sampled four months apart. Furthermore, with this experimental design, differentially expressed transcripts are potentially related to maintenance of glycerol production. Their role and that of other potentially informative transcripts in the initiation and/or early stages of glycerol synthesis are also of interest.

1.6 MODELS OF GLYCEROL SYNTHESIS IN SMELT

To assess temperature-specific control mechanisms and identify potentially informative transcripts in the initiation and early stages of glycerol synthesis in smelt, an *in vitro* hepatocyte model (9) and an *in vivo* whole-animal temperature step-down model (17) of glycerol synthesis were designed. These models were based on the premise that, in smelt, glycerol production is low temperature dependent. Smelt held at high (8-10°C) temperature maintain low glycerol level throughout a seasonal cycle (38, 57); however, rapid glycerol production may be triggered artificially with a sharp decrease in temperature even in winter months (16).

In the *in vitro* model, hepatocytes were isolated from liver of smelt that had been held at 8°C. If the hepatocytes were incubated at 8°C they did not produce glycerol; however, if they were incubated at 0.4°C there was a linear increase in glycerol production for at least 72 h. At 72 h, glycerol level in the cold incubated cells was 16-fold significantly higher than pre-incubation level (9). In the *in vivo* model, smelt that had been held at 8°C were subjected to a gradual controlled decrease in water temperature from 8°C to -1°C over a 19-day period and were then maintained at -1°C. Plasma glycerol levels increased from 5 mM to levels in excess of 300 mM at day 42 of the study (17).

1.7 THESIS OBJECTIVES: GLYCEROL SYNTHESIS IN SMELT

The aim of the first two studies (i.e. Chapters 2 and 3) conducted in this thesis was to identify potentially informative transcripts in the initiation and early stages of glycerol synthesis by (1) artificially generating populations of glycerol and non-glycerol accumulating smelt livers using the aforementioned low temperature-induced models of

glycerol synthesis, and by (2) comparing their transcriptomes using functional genomic analyses and QPCR. I hypothesize that the identification of these transcripts will help elucidate the molecular underpinnings of glycerol synthesis in smelt liver. As glycerol synthesis is but one of a multitude of biological processes that will change in response to cold temperature, I hypothesize that this research will also provide insight into additional molecular mechanisms and pathways underlying the cold temperature adaptations and responses in smelt liver.

Briefly, in Chapter 2 of this thesis, the hepatocyte model of glycerol synthesis, in conjunction with functional genomic analyses (the construction of SSH cDNA libraries and microarray analyses) and QPCR, was used to identify potentially informative transcripts in the initiation of glycerol synthesis in smelt. A liver from one individual fish that had been held at 8°C and not accumulating glycerol was perfused, thereby generating a population of about 300 million hepatocytes. Reference or “pre-incubation” samples were taken and the remaining cells were then split into individual vials containing 5 million cells and incubated at either a non-glycerol (8°C) or glycerol (0.4°C) accumulating temperature, over a 72 hour time course. Individual vials of cells were harvested from both temperatures at identical incubation times for RNA isolation (functional genomics studies and QPCR), viability assays and glycerol measurements. This was then repeated for more individual fish to increase the sample number. At a given time point, two RNA pools (one consisting of RNA extracted from cells incubated at warm temperature and one consisting of RNA extracted from cells incubated at cold temperature) were then generated for SSH cDNA library construction and microarray analyses. The advantage of this experimental design is that an identical population of

hepatocytes with the only experimental variability being incubation temperature can be compared. Furthermore, since the time course was repeatedly performed using hepatocytes isolated from one individual fish, expression of genes shown by SSH and/or microarray analyses to potentially be temperature-responsive can be measured by QPCR for each individual at both temperatures, over time, and in relation to baseline (pre-incubation) levels.

Genes shown to be differentially expressed in hepatocytes incubated at cold (glycerol accumulating) compared to warm (non-glycerol accumulating) incubation temperatures by SSH analysis at the 72h incubation time and by microarray analyses using the cGRASP 16K (salmonid) cDNA array (65) at the 24, 48 and 72 h incubation times are reported herein. These gene lists reflect changes in gene expression in hepatocytes incubated at two different temperatures over time, including, but not limited to, changes in gene expression that result in higher glycerol levels as part of the cold adaptation response. For QPCR, the focus was on genes involved in the metabolism of glycerol sources, namely glycolytic (glycogen, glucose), gluconeogenic (amino acids) and lipid. Levels of AFP_{II} were also measured, due to its previously described role in freeze prevention.

Briefly, in Chapter 3 of this thesis, the whole animal temperature “step-down” model of cold temperature-induced glycerol production was used to determine if the transcript expression profiles of the same 21 glycerol synthesis pathway-related genes that had been measured *in vitro* in Chapter 2 were also cold temperature-responsive *in vivo*, where livers are exposed to a physiological extracellular environment. Smelt were either held at 8°C (warm smelt) or subjected to a controlled decrease (from 8°C to ~ 0°C)

in water temperature and then held at low temperature (cold smelt). Smelt from both groups were sampled at the end of the temperature decrease and after the cold smelt had been held at 0 to -0.5°C for approximately one month. Levels of plasma glycerol and glucose, as well as liver glycogen were measured using biochemical assays, and liver transcript levels of the aforementioned genes were measured by QPCR. Since transcript levels were assessed after the controlled decrease in water temperature and approximately one month later, an indication of their importance in both the early stages of glycerol synthesis and in the longer term maintenance of glycerol levels was elucidated.

1.8 GLYCEROL AND UREA TRAFFICKING IN SMELT

As stated previously, smelt accumulate high glycerol and modest urea levels in plasma and tissues as an adaptive cryoprotectant mechanism in sub-zero temperatures. However, the precise mechanisms underlying the movement of these osmolytes across cellular membranes remain to be elucidated. Glycerol uptake studies in perfused heart and red blood cells (RBCs) indicate that glycerol uptake is by passive diffusion in heart but by facilitated transport in RBCs at high glycerol concentrations (8).

Aquaglyceroporins (GLPs), a subgroup of the aquaporin (AQP) superfamily of integral membrane channel proteins, could be responsible for the facilitated component of glycerol (and possibly urea) trafficking in cold-acclimated smelt.

AQPs facilitate passive yet rapid permeation of water molecules across cellular membranes (2, 35). Thirteen AQP subfamilies (AQP0-12) have been identified in mammals (35). The AQP multigene family has been further subdivided into four grades: the classical water-selective subgroup (AQP0, -1, and -4), the water and urea transporter (AQP8), the unorthodox subgroup (AQP11b and -12) and the GLP subgroup (AQP3, -7,

-9, and -10) (60). GLPs are permeable to glycerol, urea, and ammonia in addition to water (2, 42).

GLPs have been identified in numerous fish species [reviewed in (5)]. For example, AQP3 and AQP10 transcripts are expressed in Atlantic salmon (*Salmo salar*) kidney and are elevated with transfer from freshwater to seawater (61). AQP7 and AQP9 transcripts are expressed in zebrafish intestine and liver, respectively (29, 60). In fasted rodents, glycerol is released from adipocytes via AQP7 and enters liver via AQP9 where it is an important substrate for hepatic gluconeogenesis (36). The tissue distribution of AQP7 and AQP9 in fish suggests that they could play a similar role as in mammals.

1.9 THESIS OBJECTIVES: GLYCEROL AND UREA TRAFFICKING IN SMELT

The aim of the third study (i.e. Chapter 4) conducted in this thesis was to (1) clone GLP-encoding genes (AQP9 and AQP10) from smelt and (2) assess their transcript expression profiles in tissues from glycerol and non-glycerol accumulating smelt. AQP9 was selected as it is expressed in fish liver (29), the site of glycerol synthesis in smelt. AQP10 was chosen as it is expressed in extrahepatic tissues (61) and smelt ESTs for AQP10 were available (64). I hypothesize that AQP9 transcript levels will be higher in liver from glycerol compared to non-glycerol accumulating smelt to facilitate glycerol efflux. I hypothesize that AQP10 transcript levels will be higher in extrahepatic tissues from glycerol compared to non-glycerol accumulating smelt to facilitate glycerol uptake.

Briefly, in Chapter 4 of this thesis, three GLP-encoding genes [two AQP10b-like genes (AQP10ba and AQP10bb) and an AQP9b-like gene] from smelt were cloned and characterized. Full-length cDNA sequences for the two AQP10b-like genes were also cloned; the full-length cDNA sequence for AQP9b was cloned in Chapter 2. Glycerol and

urea levels in plasma were measured using biochemical assays, and AQP10b transcript levels in posterior kidney were measured using QPCR in two studies. In the first, smelt were subjected to the whole animal temperature “step-down” model of cold temperature-induced glycerol production (28). In the second, smelt were either held at ~8°C (warm smelt) or allowed to follow ambient seawater temperature (ambient smelt) throughout a season (encompassing the glycerol production and termination phases) (57). In a third study, transcript levels of the two AQP10b-like and the AQP9b-like genes were measured using QPCR in ten tissues from both warm- and cold-acclimated smelt. As the AQP10ba-like gene had a different gene structure from AQP10bb and AQP9b, and AQP10ba transcripts displayed distinct tissue-specific expression and cold-responsiveness, the promoter regions of the three GLP-encoding genes were isolated and screened for the presence of putative transcription factor recognition sites that could influence regulation of gene expression. The studies conducted herein are the first reports in which GLP gene / promoter structure and transcript expression levels have been assessed in a glycerol accumulating fish.

1.10 REFERENCES

1. **Achenbach JC, Ewart KV.** Structural and functional characterization of a C-type lectin-like antifreeze protein from rainbow smelt (*Osmerus mordax*). *Eur J Biochem* 269: 1219-1226, 2002.
2. **Agre P, King LS, Yasui M, Guggino WB, Ottersen OP, Fujiyoshi Y, Engel A, Nielsen S.** Aquaporin water channels - from atomic structure to clinical medicine. *J Physiol* 542: 3-16, 2002.
3. **Amores A, Force A, Yan YL, Joly L, Amemiya C, Fritz A, Ho RK, Langeland J, Prince V, Wang YL, Westerfield M, Ekker M, Postlethwait JH.** Zebrafish hox clusters and vertebrate genome evolution. *Science* 282: 1711-1714, 1998.
4. **Baldwin J, Hochachka PW.** Functional significance of isoenzymes in thermal acclimatization. Acetylcholinesterase from trout brain. *Biochem J* 116: 883-887, 1970.
5. **Cerdà J, Finn RN.** Piscine aquaporins: an overview of recent advances. *J Exp Zool A Ecol Genet Physiol* 313: 623-650, 2010.
6. **Chen L, DeVries AL, Cheng CH.** Convergent evolution of antifreeze glycoproteins in Antarctic notothenioid fish and Arctic cod. *Proc Natl Acad Sci USA* 94: 3817-3822, 1997.

7. **Chen Z, Cheng CH, Zhang J, Cao L, Chen L, Zhou L, Jin Y, Ye H, Deng C, Dai Z, Xu Q, Hu P, Sun S, Shen Y, Chen L.** Transcriptomic and genomic evolution under constant cold in Antarctic notothenioid fish. *Proc Natl Acad Sci U S A* 105: 12944-12949, 2008.
8. **Clow KA, Driedzic WR.** Glycerol uptake is by passive diffusion in the heart but by facilitated transport in RBCs at high glycerol levels in cold acclimated rainbow smelt (*Osmerus mordax*). *Am J Physiol Regul Integr Comp Physiol* 302: R1012-R1021, 2012.
9. **Clow KA, Ewart KV, Driedzic WR.** Low temperature directly activates the initial glycerol antifreeze response in isolated rainbow smelt (*Osmerus mordax*) liver cells. *Am J Physiol Regul Integr Comp Physiol* 295: R961-R970, 2008.
10. **Costa IASF, Driedzic WR, Gamperl AK.** Metabolic and cardiac responses of cunner (*Tautoglabrus adspersus*) to seasonal and acute changes in temperature. *Physiol Biochem Zool* 186: 233–244, 2013.
11. **Deng G, Andrews DW, Laursen RA.** Amino acid sequence of a new type of antifreeze protein, from the longhorn sculpin *Myoxocephalus octodecimspinosus*. *FEBS Lett* 402: 17-20, 1997.
12. **DeVries AL.** Biological antifreeze agents in coldwater fishes. *Comp Biochem Physiol* 73A: 627-640, 1982.

13. **Diatchenko L, Lau YFC, Campbell AP, Chenchik A, Moqadam F, Huang B, Lukyanov S, Lukyanov K, Gurskaya N, Sverdlov ED, Siebert PD.** Suppression subtractive hybridization: A method for generating differentially regulated or tissue-specific cDNA probes and libraries. *Proc Natl Acad Sci USA* 93: 6025-6030, 1996.
14. **Ditlecadet D, Driedzic WR.** Glycerol-3-phosphatase and not lipid recycling is the primary pathway in the accumulation of high concentrations of glycerol in rainbow smelt (*Osmerus mordax*). *Am J Physiol Regul Integr Comp Physiol* 304: R304-R312, 2013.
15. **Donaldson MR, Cooke SJ, Patterson DA, MacDonald, JS.** Cold shock and fish. *J Fish Biol* 73: 1491-1530, 2008.
16. **Driedzic WR, Clow KA, Short CE, Ewart KV.** Glycerol production in rainbow smelt (*Osmerus mordax*) may be triggered by low temperature alone and is associated with the activation of glycerol-3-phosphate dehydrogenase and glycerol-3-phosphatase. *J Exp Biol* 209: 1016-1023, 2006.
17. **Driedzic WR, Short CE.** Relationship between food availability, glycerol and glycogen levels in low-temperature challenged rainbow smelt *Osmerus mordax*. *J Exp Biol* 210: 2866-2872, 2007.

18. **Driedzic WR, West JL, Sephton DH, Raymond JA.** Enzyme activity levels associated with the production of glycerol as an antifreeze in liver of rainbow smelt (*Osmerus mordax*). *Fish Physiol Biochem* 18: 125-134, 1998.
19. **Duman JG, de Vries AL.** The effects of temperature and photoperiod on antifreeze production in cold water fishes. *J Exp Zool* 190: 89-98, 1974.
20. **Duman JG, de Vries AL.** Isolation, characterization, and physical properties of protein antifreezes from the winter flounder, *Pseudopleuronectes americanus*. *Comp Biochem Physiol B* 54: 375–380, 1976.
21. **Evans RP, Fletcher GL.** Isolation and characterization of type I antifreeze proteins from Atlantic snailfish (*Liparis atlanticus*) and dusky snailfish (*Liparis gibbus*). *Biochim Biophys Acta* 1547: 235–244, 2001.
22. **Ewart KV, Lin Q, Hew CL.** Structure, function and evolution of antifreeze proteins. *Cell Mol Life Sci* 55: 271-283, 1999.
23. **Gong H, Croft K, Driedzic WR, Ewart, KV.** Chemical chaperoning action of glycerol on the antifreeze protein of rainbow smelt. *J Thermal Biology* 36: 78-83, 2011.

24. **Gracey AY, Fraser EJ, Li W, Fang Y, Taylor RR, Rogers J, Brass A, Cossins AR.** Coping with cold: An integrative, multitissue analysis of the transcriptome of a poikilothermic vertebrate. *Proc Natl Acad Sci U S A* 101: 16970-16975, 2004.
25. **Graham LA, Lougheed SC, Ewart KV, Davies PL.** Lateral transfer of a lectin-like antifreeze protein gene in fishes. *PLoS One* 3: e2616, 2008.
26. **Graham LA, Hobbs RS, Fletcher GL, Davies PL.** Helical antifreeze proteins have independently evolved in fishes on four occasions. *PLoS One* 8: e81285, 2013.
27. **Green M, Farwell JM.** Winter habits of the cunner, *Tautoglabrus adspersus* (Walbaum 1792), in Newfoundland. *Can J Zool* 49: 1497–1499, 1971.
28. **Hall JR, Short CE, Rise ML, Driedzic WR.** Expression analysis of glycerol synthesis-related liver transcripts in rainbow smelt (*Osmerus mordax*) exposed to a controlled decrease in temperature. *Physiol Biochem Zool* 85: 74-84, 2012.
29. **Hamdi M, Sanchez MA, Beene LC, Liu Q, Landfear SM, Rosen BP, Liu Z.** Arsenic transport by zebrafish aquaglyceroporins. *BMC Mol Biol* 10: 104, 2009.
30. **Hazel JR.** Influence of thermal acclimation on membrane lipid composition of rainbow trout liver. *Am J Physiol* 236: R91-R101, 1979.

31. **Helfman GS, Collette BB, Facey DE, Bowen BW.** *The diversity of fishes: biology, evolution and ecology*, 2nd edn. Hoboken, NJ: Wiley-Blackwell, 2009.
32. **Hew CL, Fletcher GL, Ananthanarayanan VS.** Antifreeze proteins from the shorthorn sculpin, *Myoxocephalus scorpius*: isolation and characterization. *Can J Biochem* 58: 377–383, 1980.
33. **Hobbs RS, Shears MA, Graham LA, Davies PL, Fletcher GL.** Isolation and characterization of type I antifreeze proteins from cunner, *Tautoglabrus adspersus*, order Perciformes. *FEBS J* 278: 3699–3710, 2011.
34. **Hu P, Liu M, Zhang D, Wang J, Niu H, Liu Y, Wu Z, Han B, Zhai W, Shen Y, Chen L.** Global identification of the genetic networks and cis-regulatory elements of the cold response in zebrafish. *Nucleic Acids Res* 43: 9198-9213, 2015.
35. **King LS, Kozono D, Agre P.** From structure to disease: the evolving tale of aquaporin biology. *Nat Rev Mol Cell Biol* 5: 687-698, 2004.
36. **Kuriyama H, Shimomura I, Kishida K, Kondo H, Furuyama N, Nishizawa H, Maeda N, Matsuda M, Nagaretani H, Kihara S, Nakamura T, Tochino Y, Funahashi T, Matsuzawa Y.** Coordinated regulation of fat-specific and liver specific glycerol channels, aquaporin adipose and aquaporin 9. *Diabetes* 51: 2915-2921, 2002.

37. **Larhammar D, Risinger C.** Molecular genetic aspects of tetraploidy in the common carp *Cyprinus carpio*. *Mol Phylogenet Evol* 3: 59-68, 1994.
38. **Lewis JM, Ewart KV, Driedzic WR.** Freeze resistance in rainbow smelt (*Osmerus mordax*): seasonal pattern of glycerol and antifreeze protein levels and liver enzyme activity associated with glycerol production. *Physiol Biochem Zool* 77: 415-422, 2004.
39. **Li XM, Trinh KY, Hew CL, Buettner B, Baenziger J, Davies PL.** Structure of an antifreeze polypeptide and its precursor from the ocean pout, *Macrozoarces americanus*. *J Biol Chem* 260: 12904–12909, 1985.
40. **Liebscher RS, Richards RC, Lewis JM, Short CE, Muise DM, Driedzic WR, Ewart KV.** Seasonal freeze resistance of rainbow smelt (*Osmerus mordax*) is generated by differential expression of glycerol-3-phosphate dehydrogenase, phosphoenolpyruvate carboxykinase, and antifreeze protein genes. *Physiol Biochem Zool* 79: 411-423, 2006.
41. **Lin JJ, Somero GN.** Temperature-dependent changes in expression of thermostable and thermolabile isozymes of cytosolic malate dehydrogenase in the eurythermal goby fish *Gillichthys mirabilis*. *Physiol Zool* 68: 114-128, 1995.
42. **Litman T, Søgaard R, Zeuthen T.** Ammonia and urea permeability of mammalian aquaporins. In: *Handb Exp Pharmacol*, edited by Beitz E. Berlin: Springer, 2009, p. 327-358.

43. **Liu Y, Li Z, Lin Q, Kosinski J, Seetharaman J, Bujnicki JM, Sivaraman J, Hew CL.** Structure and evolutionary origin of Ca²⁺-dependent herring type II antifreeze protein. *PLoS ONE* 2: e548, 2007.
44. **Logan CA, Buckley BA.** Transcriptomic responses to environmental temperature in eurythermal and stenothermal fishes. *J Exp Biol* 218: 1915-1924, 2015.
45. **Long Y, Song G, Yan J, He X, Li Q, Cui Z.** Transcriptomic characterization of cold acclimation in larval zebrafish. *BMC Genomics* 14: 612, 2013.
46. **Mininni AN, Milan M, Ferrareso S, Petochi T, Di Marco P, Marino G, Livi S, Romualdi C, Bargelloni L, Patarnello T.** Liver transcriptome analysis in gilthead sea bream upon exposure to low temperature. *BMC Genomics* 15: 765, 2014.
47. **Ng NF, Trinh KY, Hew CL.** Structure of an antifreeze polypeptide precursor from the sea raven, *Hemitripterus americanus*. *J Biol Chem* 261: 15690–15695, 1986.
48. **Petricorena ZL, Somero GN.** Biochemical adaptations of notothenioid fishes: comparisons between cold temperate South American and New Zealand species and Antarctic species. *Comp Biochem Physiol A Mol Integr Physiol* 147: 799-807, 2007.

49. **Podrabsky JE, Somero GN.** Changes in gene expression associated with acclimation to constant temperatures and fluctuating daily temperatures in an annual killifish *Austrofundulus limnaeus*. *J Exp Biol* 207: 2237-2254, 2004.
50. **Raymond JA.** Glycerol is a colligative antifreeze in some northern fishes. *J Exp Zool* 262: 347-352, 1992.
51. **Raymond JA.** Glycerol and water balance in a near-isosmotic teleost, winter-acclimated smelt. *Can J Zool* 71: 1849-1854, 1993.
52. **Raymond JA.** Seasonal variations of trimethylamine oxide and urea in the blood of a cold-adapted marine teleost, the rainbow smelt. *Fish Physiol Biochem* 13: 13-22, 1994.
53. **Raymond JA.** Glycerol synthesis in the rainbow smelt *Osmerus mordax*. *J Exp Biol* 198: 2569-2573, 1995.
54. **Richards RC, Achenbach JC, Short CE, Kimball J, Reith ME, Driedzic WR, Ewart KV.** Seasonal expressed sequence tags of rainbow smelt (*Osmerus mordax*) revealed by subtractive hybridization and the identification of two genes up-regulated during winter. *Gene* 424: 56-62, 2008.

55. **Richards RC, Short CE, Driedzic WR, Ewart KV.** Seasonal changes in hepatic gene expression reveal modulation of multiple processes in rainbow smelt (*Osmerus mordax*). *Mar Biotechnol* 12: 650-663, 2010.
56. **Rise ML, von Schalburg KR, Brown GD, Mawer MA, Devlin RH, Kuipers N, Busby M, Beetz-Sargent M, Alberto R, Gibbs AR, Hunt P, Shukin R, Zeznik JA, Nelson C, Jones SR, Smailus DE, Jones SJ, Schein JE, Marra MA, Butterfield YS, Stott JM, Ng SH, Davidson WS, Koop BF.** Development and application of a salmonid EST database and cDNA microarray: data mining and interspecific hybridization characteristics. *Genome Res* 14: 478-490, 2004.
57. **Robinson J, Hall JR, Charman M, Ewart KV, Driedzic WR.** Molecular analysis, tissue profiles and seasonal patterns of cytosolic and mitochondrial GPDH in freeze resistant rainbow smelt (*Osmerus mordax*). *Physiol Biochem Zool* 84: 363-376, 2011.
58. **Scott WB, Scott MG.** Atlantic fishes of Canada. *Can Bull Fish Aquat Sci* 219: 761, 1988.
59. **Storey KB, Storey JM.** Freeze tolerance in animals. *Physiol Rev* 68: 27-84, 1988.

60. **Tingaud-Sequeira A, Calusinska M, Finn RN, Chauvigné F, Lozano J, Cerdà J.** The zebrafish genome encodes the largest vertebrate repertoire of functional aquaporins with dual paralogy and substrate specificities similar to mammals. *BMC Evol Biol* 10: 38, 2010.
61. **Tipsmark CK, Sørensen KJ, Madsen SS.** Aquaporin expression dynamics in osmoregulatory tissues of Atlantic salmon during smoltification and seawater acclimation. *J Exp Biol* 213: 368-379, 2010.
62. **Treberg JR, Lewis JM, Driedzic WR.** Comparison of liver enzymes in osmerid fishes: key differences between a glycerol accumulating species, rainbow smelt (*Osmerus mordax*), and a species that does not accumulate glycerol, capelin (*Mallotus villosus*). *Comp Biochem Physiol A Mol Integr Physiol* 132: 433-438, 2002.
63. **Treberg JR, Wilson CE, Richards RC, Ewart KV, Driedzic WR.** The freeze-avoidance response of smelt *Osmerus mordax*: initiation and subsequent suppression of glycerol, trimethylamine oxide and urea accumulation. *J Exp Biol* 205: 1419-1427, 2002.
64. **von Schalburg KR, Leong J, Cooper GA, Robb A, Beetz-Sargent MR, Lieph R, Holt RA, Moore R, Ewart KV, Driedzic WR, ten Hallers BF, Zhu B, de Jong PJ, Davidson WS, Koop BF.** Rainbow smelt (*Osmerus mordax*) genomic library and EST resources. *Mar Biotechnol (NY)* 10: 487-491, 2008.

65. **von Schalburg KR, Rise ML, Cooper GA, Brown GD, Gibbs AR, Nelson CC, Davidson WS, Koop BF.** Fish and chips: various methodologies demonstrate utility of a 16,006-gene salmonid microarray. *BMC Genomics* 6: 126-144, 2005.
66. **Walter JA, Ewart KV, Short CE, Burton IW, Driedzic WR.** Accelerated hepatic glycerol synthesis in rainbow smelt (*Osmerus mordax*) is fuelled directly by glucose and alanine: a ^1H and ^{13}C nuclear magnetic resonance study. *J Exp Zool A* 305: 480-488, 2006.
67. **Watt PW, Marshall PA, Heap SP, Loughna PT, Goldspink G.** Protein synthesis in tissues of fed and starved carp, acclimated to different temperatures. *Fish Physiol Biochem* 4: 165-173, 1988.
68. **Yeh Y, Feeney RE.** Antifreeze Proteins: Structures and Mechanisms of Function. *Chem Rev* 96: 601-618, 1996.

CHAPTER 2

Identification and validation of differentially expressed transcripts in a hepatocyte model of cold-induced glycerol production in rainbow smelt (*Osmerus mordax*)

Preface

The research described in Chapter 2, with the exception of the mGPDH cloning and characterization, was published in *The American Journal of Physiology - Regulatory, Integrative and Comparative Physiology*:

Hall JR, Clow KA, Rise ML, Driedzic WR. Identification and validation of differentially expressed transcripts in a hepatocyte model of cold-induced glycerol production in rainbow smelt (*Osmerus mordax*). *Am J Physiol Regul Integr Comp Physiol* 301: R995-R1010, 2011.

The mGPDH research was published separately in *Physiological and Biochemical Zoology* to supplement independent research conducted by my co-authors. **Only my research is described herein:**

Robinson J, **Hall JR**, Charman M, Ewart KV, Driedzic WR. Molecular analysis, tissue profiles and seasonal patterns of cytosolic and mitochondrial GPDH in freeze resistant rainbow smelt (*Osmerus mordax*). *Physiol Biochem Zool* 84: 363-376, 2011.

2.1 ABSTRACT

Rainbow smelt (*Osmerus mordax*) avoid freezing by producing antifreeze protein (AFP) and accumulating glycerol. Glyceroneogenesis occurs in liver via a branch in glycolysis and gluconeogenesis and is activated by low temperature. Hepatocytes were isolated from the livers of fish acclimated to 8°C. Cells were incubated at warm (8°C; non-glycerol accumulating) or cold (0.4°C; glycerol accumulating) temperature over a 72 h time course. Reciprocal SSH libraries enriched for cold-responsive transcripts were constructed at 72 h. Microarray analyses using a 16K salmonid cDNA array were performed at 24, 48 and 72 h. Expression of type II AFP and 21 carbohydrate, amino acid or lipid metabolism-related transcripts were validated using QPCR. Type II AFP transcript levels were not significantly influenced by temperature. In cold cells, transcript levels of G6Pase (glucose synthesis) were transiently higher. Increased glycerol production was not associated with increased PFK or cGPDH transcript levels. Levels of transcripts (PEPCK, MDH2, AAT2, GDH and AQP9) associated with mobilization of amino acids to fuel glycerol accumulation were all transiently higher, suggesting a common regulatory mechanism. In cold compared to warm cells, PDK2 (an inhibitor of PDH) transcript levels were 20-fold higher. Potent inhibition of PDH would direct pyruvate and oxaloacetate derived from amino acids to glycerol, as opposed to oxidation via the citric acid cycle. Levels of a transcript potentially encoding glycerol-3-phosphatase, an enzyme not yet characterized in any vertebrate species, were higher following cold incubation. Finally, this study also presents the novel finding of increased GS transcript levels in response to low temperature.

2.2 INTRODUCTION

Rainbow smelt (*Osmerus mordax*, Mitchill, 1814), hereafter referred to as smelt, is a small (less than 20 cm) anadromous teleost that often overwinters in ice-covered inshore seawaters (34) where water temperatures can reach as low as -1.8°C before freezing. The freezing point of teleost blood is typically about -0.8°C ; however, smelt are quite active under the ice and feed on a high protein invertebrate diet (28). Freeze resistance is accomplished non-colligatively via type II antifreeze protein (AFP) and colligatively via the accumulation of osmolytes, especially glycerol (11). High glycerol level is not a common method of freeze prevention in fish and has only been reported in smelt from Alaska (*O. mordax dentex*) and Japan (*Hypomesus pretiosus japonica*) and two greenlings (*Hexagrammos octogrammus* and *H. stelleri*) (27).

Plasma glycerol levels in smelt maintained in aquaria, with flow-through water at ambient temperature, follow a seasonal pattern and can reach values of 230 mM in February (when water temperatures are at their lowest) compared with 0.3 mM in mid-October. Glycerol begins to accumulate when water temperature decreases to about 5°C (19). Synthesis primarily occurs in the liver (19, 20, 32) directly from both glycolytic and gluconeogenic sources as evidenced by nuclear magnetic resonance studies (44) in which winter smelt injected with ^{13}C glucose or ^{13}C alanine produced glycerol with intact incorporation of the neighbouring ^{13}C labeled atoms. The proposed pathway for glycerol synthesis (glyceroneogenesis) (Fig. 1.1) from these sources is via a branch point in these pathways in which dihydroxyacetone phosphate (DHAP) is converted to glycerol-3-phosphate (G3P) by cytosolic glycerol-3-phosphate dehydrogenase (cGPDH). There is substantial evidence that cGPDH plays a critical role in the early stages of glycerol

accumulation (10, 19). Subsequently, the G3P may be dephosphorylated to glycerol directly by an unidentified phosphatase (10). Alternatively, G3P may theoretically be incorporated into triglyceride which can be thereafter broken down into glycerol and free fatty acids. Regardless, the resultant glycerol can enter the plasma via aquaglyceroporins or be phosphorylated back to G3P by glycerol kinase and subsequently directed to glucose synthesis or oxidation to CO₂, depending on the metabolic needs of the cell.

Having identified sources of glycerol, confirmation of the proposed pathways to glycerol synthesis and identification of additional key regulatory genes is paramount. Functional genomic techniques such as the generation and characterization (sequencing) of suppression subtractive hybridization (SSH) cDNA libraries and microarray analysis are useful for identifying differentially expressed transcripts between experimental and control groups. Expression levels of selected transcripts can then be validated using quantitative reverse transcription - polymerase chain reaction (QPCR).

Richards et al. (30, 31) compared the expression profiles of pooled RNA from livers of smelt collected in October (fall smelt) with pooled RNA from livers of smelt at peak glycerol production in January/February (winter smelt). SSH analyses, enriched for transcripts differentially expressed between winter and fall smelt, generated 441 expressed sequence tags (ESTs). Microarray analyses identified 83 transcripts (69 upregulated, 14 downregulated) that were reproducibly greater than two-fold differentially expressed in winter compared to fall smelt. Some of these informative transcripts, such as fructose 1,6-bisphosphate aldolase B (ALD) and glutamate dehydrogenase (GDH), were related to maintenance of glycerol production.

The goal of the current study was to identify changes in transcript expression in the initiation and/or early stages of cold adaptation and more specifically glycerol production. The problem was approached by using an *in vitro* hepatocyte model of cold-induced glycerol production. Clow et al. (7) showed that when hepatocytes isolated from the livers of smelt held at 8°C (non-glycerol accumulating) are incubated at 8°C they do not produce glycerol; if the hepatocytes are incubated at 0.4°C there is a linear increase in glycerol production for at least 72 h.

In the current study, hepatocytes were isolated from the liver of a smelt that had been held for 1 to 2 months at 8°C. A pre-incubation sample was taken and the remaining cells were incubated at high or low temperature for various lengths of time. As a point of departure, RNA isolated from the individual warm or cold incubated hepatocyte preparations was pooled and compared by SSH and microarray analyses. This was undertaken to provide an overview of potential changes in transcript expression induced by a decrease in temperature alone. Thereafter, detailed QPCR analyses were conducted on individual hepatocyte RNA preparations to convey information on biological variability. A subset of transcripts identified by SSH and/or microarray analysis or selected by the authors as being potentially important in glycerol management (full-length cDNAs for three of these genes were cloned and characterized) were analyzed. More specifically, the focus was on transcripts involved in the metabolism of potential glycerol sources, namely carbohydrate, amino acid and lipid. Transcript levels of type II AFP were also measured, due to its previously described role in freeze prevention. These studies identified two genes [pyruvate dehydrogenase kinase (PDK2) and glutamine

synthetase (GS)] that were not previously associated with the low temperature response in smelt, as being important in the early stages of this response.

2.3 MATERIALS AND METHODS

2.3.1 Animals

For hepatocyte isolations, smelt were collected by seine netting from Mount Arlington Heights, Placentia Bay, Newfoundland in late October 2007 and transported to the Ocean Sciences Centre, Memorial University of Newfoundland. The fish were held in a 3000 L indoor free-flowing seawater tank maintained at 8°C to 10°C and followed a natural photoperiod with fluorescent lights set by an outdoor photocell. Fish were fed a diet of chopped herring twice a week to satiation. Hepatocyte isolations were performed for male fish only from Nov. 27th to Dec. 17th, 2007.

For the mitochondrial glycerol-3-phosphate dehydrogenase (mGPDH) transcript tissue distribution analysis, smelt were collected in late October 2009 and maintained as above. On March 5, 2010 two fish were sampled. One fish had been held at warm temperature (warm-acclimated). A second fish was sampled from a population that had been subjected to a controlled temperature decrease from 8°C to 5 °C on February 12, to 3°C on February 15, to 1°C on February 22, and held at 1°C until sampled (cold-acclimated). Blood was drawn via the caudal vessel using heparinized syringes, placed in a 1.5 ml nuclease-free microcentrifuge tube and centrifuged at 10,000 x g for 10 min at 4°C. Plasma was removed and red blood cells (RBCs) were snap frozen in liquid nitrogen and stored at -80°C. Fish were killed by a sharp blow to the head. The tissues were removed quickly, snap frozen and stored at -80°C.

Experiments were carried out in accordance with Animal Utilization Protocols issued by Memorial University of Newfoundland's Animal Care Committee.

2.3.2 Hepatocyte isolation and glycerol determination

Hepatocyte isolations and glycerol measurements were performed as described by Clow et al. (7). However, in the current study, hepatocyte preparations from different fish were not pooled prior to incubation. Individual smelt liver perfusions yielded approximately 300 million cells. Initial or “pre-incubation” samples were collected in duplicate for RNA isolation and glycerol determination; the remaining cell suspension was divided into vials (6×10^6 cells per vial) containing 2 ml of incubation medium and incubated at either 0.4°C (cold incubation) or 8°C (warm incubation) for up to 72 h. Duplicate vials from each temperature were sampled at 24, 48 and 72 h incubation times for RNA isolation and at 72 h for cell viability (trypan blue exclusion) and glycerol determination. Any preparations showing less than 90% viability were excluded. Glycerol content in the medium and pellet were summed and expressed per g cell (i.e. per gram wet weight of isolated hepatocytes).

2.3.3 RNA preparation

For RNA isolation from cultured hepatocytes, cells were immediately resuspended by gentle pipetting, transferred to a 1.5 ml microcentrifuge tube and centrifuged at $1000 \times g$ for 10 min at 4°C. The supernatant was discarded and the cell pellet was homogenized in 400 μ l of TRIzol Reagent (Invitrogen, Burlington, ON) using a motorized Kontes RNase-Free Pellet Pestle Grinder (Kimble Chase, Vineland, NJ). Duplicate vials were combined and topped up to approximately 1 ml with 200 μ l of TRIzol (Invitrogen). The samples were stored at -80°C for a maximum of two weeks before completion of the total RNA isolation. For RNA isolation from frozen tissues (cDNA cloning and mGPDH transcript tissue distribution analysis), total RNA was

extracted using TRIzol Reagent (Invitrogen). RNA integrity was verified by 1% agarose gel electrophoresis and purity was assessed by A260/280 (cut-off ratio > 2) and A260/230 (cut-off ratio > 1.8) NanoDrop UV spectrophotometry.

For cDNA cloning, 1 µg of total RNA was treated with 1U of Amplification Grade DNase I (Invitrogen) with the manufacturer's buffer (1X final concentration), prior to reverse transcription. For RNA ligase-mediated rapid amplification of 5' and 3' cDNA ends (RLM-RACE), poly(A)⁺ RNA was isolated from total RNA using the Oligotex mRNA Mini Kit (QIAGEN, Mississauga, ON). For QPCR (mGPDH transcript tissue distribution analysis), 10 µg of total RNA was treated with 4 U TURBO DNase (TURBO DNA-free Kit, Ambion, Austin TX). For SSH cDNA library construction, microarray analysis and QPCR (hepatocytes), individual total RNA samples were treated with 6.8 Kunitz units DNaseI (RNase-Free DNase Set, QIAGEN) with the manufacturer's buffer (1X final concentration) at room temperature for 10 min and column-purified using the RNeasy MinElute Cleanup Kit (QIAGEN). For SSH cDNA library construction, poly(A)⁺ RNA (mRNA) was isolated from DNaseI-treated, column-purified total RNA pools using the MicroPoly(A) Purist Small Scale mRNA Purification Kit (Ambion). In all protocols involving commercial kits cited here and elsewhere in this study, the manufacturers' instructions were followed.

2.3.4 SSH cDNA library construction

Cells from the 72 h time point only were used for SSH cDNA library construction. DNaseI-treated, column-purified total RNA [20 µg per fish (i.e. this amount is a sub-sample of the total amount of RNA available for that fish so that RNA from individual fish samples could be archived for QPCR studies)] isolated from the

hepatocytes of 9 fish with high levels of glycerol production at 0.4°C were used to generate 2 mRNA pools: a cold pool and a warm pool. To summarize, the cold pool contained cells incubated at 0.4°C for 72 h which exhibited increases in glycerol levels at 72 h compared to pre-incubation levels, and the warm pool contained cells from the same individual fish but incubated at 8°C and thus not exhibiting glycerol production. The cold cells were the tester in the forward SSH library (enriched for transcripts expressed at higher levels in cold than warm cells at 72 h) and the driver in the reverse SSH library (enriched for transcripts expressed at higher levels in warm than cold cells at 72 h). The warm cells were the tester in the reverse SSH library and the driver in the forward SSH library.

The SSH cDNA libraries (8) were constructed using the PCR-Select cDNA Subtraction Kit (Clontech, Mountain View, CA). The hybridizations were performed in a hybridization oven, with the first hybridization run at 68°C for ~ 8 h and the second hybridization run at 68°C for ~ 16 h. The PCR amplified libraries were purified using the MinElute PCR Purification Kit (QIAGEN), and subcloned into pGEM-T-Easy (Promega, Madison, WI). Transformations were performed using MAX Efficiency DH5 α chemically competent cells (Invitrogen). Prior to sequencing, initial evaluation of library insert size and complexity was made by visual comparison of clone restriction fragments with a DNA size marker [1 kb plus ladder (Invitrogen)] using 1.0% agarose gel electrophoresis.

2.3.5 DNA sequencing, sequence assembly and gene identification

For the initial clones used in library evaluation, plasmid DNA was isolated using the QIAprep Spin Miniprep Kit (QIAGEN). For higher throughput sequencing, individual

bacterial clones were grown in LB/ampicillin in 96-well plate format and the plasmid DNA was purified using a plate-based modification of the alkaline lysis protocol. DNA was amplified from approximately 100 ng of plasmid DNA using the BigDye Terminator v3.1 Cycle Sequencing Kit (Applied Biosystems, Foster City, CA) and the unincorporated BigDye terminators were removed using the BigDye XTerminator Purification Kit (Applied Biosystems). The purified sequencing reactions were processed by capillary electrophoresis using the 3730xl DNA Analyzer (Applied Biosystems).

Vector and SSH library adaptor sequences were trimmed and contiguous (contig) consensus sequences and individual sequence reads (singletons) were assembled using ContigExpress, Vector NTI Advance 10 (Invitrogen). Gene identifications were made by a BLASTx 2.2.20 search of the non-redundant (nr) protein sequence database of NCBI. For any BLASTx queries with an Expect (E) value $\geq 10^{-5}$, or no significant BLASTx hits, a BLASTn 2.2.20 search of the non-human, non-mouse EST database (est_others) component of NCBI's EST nucleotide sequence database was then performed. SSH cDNA libraries are 3' biased and often contain sequences entirely within the 3' untranslated regions (UTRs) which would not be identifiable by a BLASTx search. A large number of smelt EST resources were submitted to GenBank by von Schalburg et al. (43) making this a useful database for potentially identifying unclassified sequences after the initial BLASTx search. If a clone overlapping with the SSH-identified sequence (100% identity at the nucleotide level over the aligned region) was present in dbEST, a second BLASTx search was performed using the contig of the two aligned ESTs.

For all SSH library assembled sequences (contigs and singletons) with significant BLASTx hits (E-value $\leq 10^{-5}$), or at the discretion of the authors for nine assembled

sequences with higher E-values (e.g. high similarity short alignments against N terminal residues of BLASTx hits with 5'UTR or C terminal residues of BLASTx hits with 3'UTR), complete gene ontology (GO) annotations including GO term/GO description for the biological process (BP), molecular function (MF) and cellular component (CC) GO categories, were obtained from the Protein Knowledgebase UniProtKB/Swiss-Prot (www.uniprot.org) [Supplemental Table S2.1 (forward SSH library) and Supplemental Table S2.2 (reverse SSH library)]. GO annotations were based upon the putative human orthologue [unless another species is indicated (e.g. for type II AFP, GO annotations are for *O. mordax*)] of the best BLASTx hit. All gene identifications, including percent identities (% ID) over an aligned region (align) and E-value, and GO annotations (including the SwissProt accession number for the putative human orthologue) for genes present in the forward SSH library were made between April 3 and May 19, 2009. The exception to this was Contig 42 which was identified by a BLASTn 2.2.20 search of the non-redundant nucleotide (nr/nt) sequence database of NCBI in January, 2010. All gene identifications and GO annotations for genes present in the reverse SSH library were made between May 29 and June 10, 2009.

2.3.6 Microarray hybridization

Microarray experiments were designed to comply with the Minimum Information About a Microarray Experiment (MIAME) guidelines (4). The microarray data discussed in this publication have been deposited in NCBI's Gene Expression Omnibus (GEO) (12) and are accessible through GEO series accession number GSE23516 (<http://www.ncbi.nlm.nih.gov/geo/query/acc.cgi?acc=GSE23516>).

Microarray analyses were performed using the consortium for Genomics Research on All Salmonids Project (cGRASP) 16K salmonid cDNA array (42) (batch number

IB008, slides 055-066). von Schalburg et al. (42), reported that the average percentage binding of smelt liver targets to the 16K chip was 30%. Due to the known performance of smelt targets on salmonid cDNA probes, a green fluorescent protein (GFP) spike was included in the hybridization to aid in gridding the microarray; GFP features are located in the corners of each sub-grid on the cGRASP 16K microarray. A GFP100 expression clone was kindly provided by Dr. Ben Koop of cGRASP. A 280 bp GFP cDNA fragment was amplified from this plasmid using primers GFP-F (5'-GAAACATTCTTGGACACAATTTGG-3') and GFP-R (5'-GCAGCTGTTACAAACTCAAGAAGG-3') and DyNAzyme EXT DNA polymerase (MJ Research, Waltham, MA). Briefly, 50 µl reactions were prepared containing 100 ng of plasmid DNA, DyNAzyme EXT DNA polymerase (1 U), the manufacturer's Optimized DyNAzyme EXT Buffer (1X final concentration), 0.2 mM dNTPs and 0.2 µM each of forward and of reverse primer. PCR cycling conditions consisted of 40 cycles of (94°C for 30 sec, 55°C for 30 sec and 72°C for 30 sec). The amplicon was electrophoretically separated on a 2% agarose gel and extracted using the QIAquick Gel Extraction Kit (QIAGEN). Fifty nanograms of purified PCR product was labeled with Cy5-dCTP (PerkinElmer, Waltham, MA) using the Random Primed DNA Labeling Kit (Roche Applied Science, Laval, QC). The labeling reaction was purified using the QIAquick PCR Purification Kit (QIAGEN) and yielded a DNA concentration of 5 ng/µl with Cy5 at 0.7 pmol/µl.

Total RNA pools from the same fish used in SSH cDNA library construction were used for microarray analysis. Briefly, 6 separate pools (i.e. warm and cold RNA at the 24, 48 and 72 h incubation times) were prepared by combining 2 µg of DNaseI-treated and

column-purified total RNA isolated from each of the applicable hepatocyte samples from the nine individual fish and then adding DNase-free, RNase-free ultraPURE distilled water (Invitrogen) to a final concentration of 1 µg/µl. Two micrograms of each pool was then used to prepare the microarray targets. Comparisons were made for the cold versus warm pools at the 24, 48 and 72 h time points. For each time point, technical quadruplicate slides including two dye-swaps were run per comparison.

Microarray targets were synthesized using the 3DNA Array 900 Expression Array Detection Kit for Microarrays (Cy3 and Cy5) (Genisphere, Hatfield, PA) and SuperScript II (Invitrogen). Briefly, 2 µg of the total RNA pool was reverse transcribed for 2.5 h at 42°C using 200 U of SuperScript II and the manufacturer's 5X SuperScript II buffer and oligo d(T) primers with unique 5-prime sequence overhangs for the Cy3 or Cy5 Capture Reagent Anchors (Genisphere).

Stock solutions [10% SDS and 20X SSC (Ambion)] used in microarray slide preparation and/or post-hybridization washes were diluted to working concentrations using DNase-free, RNase-free ultraPURE distilled water (Invitrogen). Microarray preparation and post-hybridization washes and centrifugations were performed in 50 ml conical tubes (BD Biosciences, Mississauga, ON). Microarrays were prepared for hybridization by washing at room temperature for 2 X 5 min in 0.1% SDS and 5 X 1 min in DNase-free, RNase-free ultraPURE distilled water (Invitrogen), immersing for 3 min in 95°C DNase-free, RNase-free ultraPURE distilled water (Invitrogen) and drying by centrifugation at 1000 rpm for 5 min at room temperature, in loosely-capped 50 ml tubes.

The smelt hepatocyte cDNAs (cold and warm for a given incubation time, each containing an anchor for one of the Cy dye labeled Capture Reagents, e.g. cold

hepatocyte 24 h pool with Cy5 anchor and warm hepatocyte 24 h pool with Cy3 anchor) were pooled and hybridized with 3 μ l of the Cy5 labeled GFP spike and 2 μ l of LNA dT blocker to the array in 2X formamide-based buffer (25% formamide, 4X SSC, 0.5% SDS, 2X Denhardt's solution) (Genisphere). Microarray hybridizations were performed in the dark under Hybri-slips hybridization covers (Sigma-Aldrich) in slide hybridization chambers (Corning Life Sciences, Lowell, MA) placed in a 48°C water bath for 16 h.

Hybri-slips were floated off at 48°C in (2X SSC, 0.2% SDS) for 5 min, and the arrays were washed with gentle agitation, in the dark and at room temperature in (2X SSC, 0.2% SDS) for 1 X 15 min, in 2X SSC for 1 X 15 min, and in 0.2X SSC for 1 X 15 min, and dried by centrifugation at room temperature at 1000 rpm for 5 min. The Cy3 and Cy5 three dimensional fluorescent molecules (3DNA Capture Reagent, Genisphere) were hybridized to the bound cDNA on the microarray in 2X formamide-based buffer (Genisphere) for 4 h at 48°C and then washed and dried as previously described.

2.3.7 Microarray image analysis

Fluorescent images of hybridized arrays were acquired immediately at 10 μ m resolution using a ScanArray G_X PLUS microarray scanner (PerkinElmer) and ScanArray Express software (PerkinElmer). The Cy3 and Cy5 cyanine fluorophores were excited at 543 nm and 633 nm, respectively. The laser power was set at 90% and the photomultiplier tube (PMT) settings were 79 (Cy3) and 75 (Cy5) for all of the microarrays in this study.

For each microarray, fluorescent intensity data were extracted from TIFF images using ImaGene 7.5 software (BioDiscovery, El Segundo, CA). Briefly, microarray elements were gridded manually and then spot sizes were adjusted automatically. Spatial

effects were manually flagged and then fluorescent intensity measurements were made. ImaGene files were imported into GeneSpring GX 7.3.1 (Agilent Technologies, Mississauga, ON). Data transformation (background correction and setting background corrected values less than 0.01 to 0.01) and per spot and per chip intensity dependent (Lowess) normalization were performed to generate background corrected lowess normalized (BCLN) data. These data were then analyzed to generate informative gene lists for each microarray slide. Two separate lists (transcripts expressed at levels greater than two-fold higher in cold than warm cells and transcripts expressed at levels greater than two-fold higher in warm than cold cells) were compiled for each of the four slides (technical quadruplicate slides including two dye-swaps) at each time point.

To identify the reproducibly informative transcripts for each time point and temperature comparison, the four informative gene lists were compared in GeneSpring using Venn diagrams. The final gene lists were then thresholded using MS Excel. Briefly, fluorescent threshold levels for determining if genes were present were calculated by analyzing raw (i.e. not transformed or normalized) median signal levels from *Arabidopsis thaliana* control spots present on the 16K chip (6 *Arabidopsis thaliana* cDNAs X 16 replicates) for each channel (Cy5, Cy3) in each array. BCLN signal strength was considered above threshold (i.e. the transcript was deemed “present”) if it was greater than or equal to the average *Arabidopsis thaliana* raw signal plus two standard deviations in the dominant channel (i.e. the channel with the highest signal in a given comparison). Therefore, genes were considered to be reproducibly informative if they passed threshold and their transcripts were greater than two-fold differentially expressed (in the same

direction) between cold and warm cells in all four technical replicate slides (including two dye-swaps) of a given comparison.

For reproducibly informative microarray features, gene identifications were made by using the corresponding GenBank dbEST accession number to search the non-redundant protein (nr) protein sequence database of NCBI (BLASTx). If no identification could be made by a BLASTx search, a search of the non-redundant nucleotide sequence database of NCBI (BLASTn) was performed. BLAST statistics were collected from October to December 2009 and reflect the status of these sequence databases at that time. Complete GO functional annotations were collected as per genes identified in the SSH cDNA libraries.

2.3.8 cDNA cloning [aquaglyceroporin 9 (AQP9), facilitated glucose transporter 2 (GLUT2), mitochondrial glycerol-3-phosphate dehydrogenase (mGPDH)]

Full-length cDNAs for smelt AQP9 and mGPDH were cloned using reverse transcription – polymerase chain reaction (RT-PCR) and RLM-RACE. Partial cDNAs for GLUT2 were available in dbEST (EL545782, EL545783, EL544453, EL544454 and EL536783), and RACE was performed to obtain the remaining sequence. The sequences of all primers used in cDNA cloning and their applications are presented in Table 2.1.

Partial cDNA clones for AQP9 and mGPDH were amplified using RT-PCR. Degenerate primers were designed based upon consensus sequences from conserved areas of aligned vertebrate cDNAs. DNaseI-treated liver total RNA (1 µg) was reverse-transcribed in a 20 µl reaction using an oligo-dT primer [500 ng (Invitrogen); AQP9] or random primers [250 ng (Invitrogen); mGPDH] and M-MLV reverse transcriptase [200 U (Invitrogen)] with the manufacturer's first strand buffer (1X final concentration) and DTT

Table 2.1. Sequences of oligonucleotides used in cDNA cloning.

cDNA	Nucleotide sequence (5'-3')*	Direction**	Application	Position of 5'-end in cDNA
AQP9	TCTGG K GGYCACATCAACCCAGC	F	RT-PCR	281
AQP9	CCCCAKCCNGCCANNGCAGTGAA	R	RT-PCR	744
AQP9	AGGTCTCGRGCNGGGTTC	R	RT-PCR (semi-nested)	708
AQP9	GTTGAGGACTGAGAGGTGTGGC	R	5' RACE	526
AQP9	TAGCATTTGGCCAGTAACTGAC	R	5' RACE (nested)	476
AQP9	GTCAGTTACTGGGCCAAATGCTA	F	3' RACE	454
AQP9	GCCACACCTCTCAGTCCTCAAC	F	3' RACE (nested)	505
GLUT2	CTTCAGACGATGTAAACTCTTGCG	R	5' RACE	743
GLUT2	TGCGTATGTAGAGGTACCGAGG	R	5' RACE (nested)	699
GLUT2	CAGTCCCTGCTACTACCTCTATG	F	3' RACE	646
GLUT2	CCTCGGTACCTCTACATACGCA	F	3' RACE (nested)	678
mGPDH	CYTGCCCTGGGAGAAGATGAC	F	RT-PCR	1148
mGPDH	CCGCTGTC G CTGACGTTGAC	R	RT-PCR	1401
mGPDH	GGTTCCTGCAGATGGACTGCGT	R	5' RACE	1376
mGPDH	CGTATTCCACTCCACGCTGCCA	R	5' RACE (nested)	1323
mGPDH	GACATCAACTTCATCCTGACGGA	F	3' RACE	1229
mGPDH	GGCAGCGTGGAGTGGAATACG	F	3' RACE (nested)	1303

*-Nucleotides highlighted in bold differ from the actual cDNA sequence.

-Degenerate base symbols: K=T+G; Y=C+T; N=A+C+G+T; R = A+G

**F is forward and R is reverse direction.

(10 mM final concentration) at 37°C for 50 min. PCR amplification was performed using DyNAzyme EXT DNA polymerase (MJ Research) and 100 ng of cDNA (corresponding to 100 ng of input total RNA). PCR core reaction component concentrations were as described for GFP cDNA cloning. Touchdown PCR was used with 40 cycles of [94°C for 30 sec, 65°C decreasing by 0.5°C per cycle (to 45.5°C at cycle 40) for 30 sec and 72°C for 1 min]. For AQP9, one-fiftieth of the first PCR reaction was used as template in a semi-nested PCR reaction (same forward primer, nested reverse primer) with the same conditions as the initial PCR. PCR products were electrophoretically separated on 1% agarose gels (alongside 1 kb plus ladder, Invitrogen), excised and purified using the QIAquick Gel Extraction Kit (QIAGEN). They were then subcloned into pGEM-T Easy (Promega, Madison, WI), and transformations were performed using Subcloning Efficiency DH5 α chemically competent cells (Invitrogen). Triplicate clones were sequenced on both strands at the McMaster Institute for Molecular Biology and Biotechnology (MOBIX) (McMaster University, ON).

The 5' and 3' ends of the three partial cDNAs were cloned using a commercial kit for RLM-RACE [GeneRacer Kit (Invitrogen)] using either DNaseI-treated total RNA (1 μ g; mGPDH) or poly(A)⁺ RNA (250 ng; AQP9, GLUT2) from liver. PCR amplification was performed using DyNAzyme EXT DNA polymerase (MJ Research), with core reaction component concentrations as described for GFP cDNA cloning. PCR cycling conditions were 40 cycles of [94°C for 30 sec, 70°C decreasing by 0.3°C per cycle (to 58.3°C at cycle 40) for 30 sec and 72°C for 2 min].

2.3.9 Sequence analysis of full-length cDNA clones

Sequence data was compiled and analyzed using Vector NTI (Vector NTI Advance 10, Invitrogen). Multiple sequence alignments were performed using AlignX (Vector NTI Advance 10, Invitrogen) which uses the ClustalW algorithm (38). Molecular phylogenetic analyses were used to compare the deduced amino acid sequences of smelt AQP9, GLUT2 and mGPDH with corresponding proteins from other vertebrates. Protein alignments were imported in MSF format into MEGA version 4.0.2 (37). Phylogenetic trees were constructed using the Neighbour-Joining (NJ) method (33) with Poisson correction. Bootstrap analysis was performed with 1000 replicates.

2.3.10 Quantitative reverse transcription - polymerase chain reaction (QPCR)

mRNA levels of genes identified as differentially expressed between cold and warm cells by SSH and/or microarray analyses or selected by the authors [mGPDH, AQP9, phosphoenolpyruvate carboxykinase (PEPCK) and phosphofructokinase (PFK)], with a conceptual link to glycerol production, and type II AFP were quantified by QPCR using SYBR Green I dye chemistry (with the exception of AQP9, which used TaqMan probe-based chemistry) with normalization to 18S ribosomal RNA using a commercially available TaqMan assay and the 7300 Real Time PCR system (Applied Biosystems).

The 22 genes chosen for QPCR analysis and the sequences of their QPCR primer pairs are presented in Table 2.2. These primers were quality tested to ensure that a single product was amplified (dissociation curve analysis) and that there was no primer-dimer or template contamination present in the no-template control. Amplicons were electrophoretically separated on 2% agarose gels and compared with a 1 kb plus ladder (Invitrogen) to ensure the correct size fragment was being amplified. Finally,

Table 2.2. Primers used in QPCR studies.

Gene name	Primer name	Nucleotide sequence (5'-3')*	Efficiency (%)**	Amplicon size (bp)
Glucose transporter type 2	GLUT2-f	GGTGTTCCTCCAGCCTGTCTA	86	129
	GLUT2-r	CATCCCTCCTAAGCCAATCA		
Phosphoglucosmutase	PGM-f	TTGCTGCGCTGAAGGAGAT	93	137
	PGM-r	ATTCATGGCTGAGTTGGCG		
Glucose-6-phosphatase	G6Pase -f	TACACCACCCTCTTCCTGCT	103	107
	G6Pase -r	CACCACTTCTGGGCTCTCTC		
6-Phosphogluconate dehydrogenase	6PGDH -f	TGCATCATCCGCAGTGTGTT	90	107
	6PGDH -r	TCCTGTACGGCATTGCTGAAG		
Transaldolase	TALDO1-f	GGCTGTGGAAAAGCTCTCAG	100	100
	TALDO1-r	GCCATTTTTTACATTCAGCA		
Phosphofruktokinase	PFK-f	CATTGACAACGACTTCTGCGG	86	140
	PFK-r	GCCTTCCCATGACTTCCAAAA		
Glyceraldehyde-3-phosphate dehydrogenase	GAPDH-f	GACTGTCCGTCTGGAGAAGC	90	137
	GAPDH-r	GGGTGTCACCGTTGAAGTCT		
Pyruvate dehydrogenase kinase 2	PDK2-f	TGAGCTGGATTTGACGGAGGT	105	121
	PDK2-r	GGTGGCTCTCATGGCATTCTT		
Phosphoenolpyruvate carboxykinase	PEPCK-f	TGGCCGAACACATGCTGAT	86	101
	PEPCK-r	GGCCAGGTTAGTTTTCCACA		
Mitochondrial malate dehydrogenase	MDH2-f	AGCCTTTGAGGAGAAGCTGGT	99	114
	MDH2-r	ACAGAGGCTGAGTCAAACCCA		
Alanine aminotransferase 2	AAT2-f	GGCATTGAGTGCATACGACA	103	100
	AAT2-r	TAGCTCCGGTGGAGAGGTAG		
Glutamine synthetase	GS-f	ATACGCAGTGACCGAAGCTC	102	108
	GS-r	GTGGTGAGATGCAGTCCAGA		
Glutamate dehydrogenase	GDH-f	GCGTGACCGTGTCTACTTT	98	116
	GDH-r	CTCCTGGACAGACATCAGCA		
Lipoprotein lipase	LIPL -f	CGGATTGGCTCTTGGACTACA	94	113
	LIPL -r	TGCGATGGTCTTTGGTTGG		
Solute carrier family 27 (fatty acid transporter), member 6	SLC27A6-f	ACTCGGATGCTCTGTGGCTTT	99	102
	SLC27A6-r	TCTGCGCCAACAACAAGAGTC		
Acyl-CoA synthetase 4	ACSL4-f	CAGCCTCAATCAAAGTCAA	91	161
	ACSL4-r	CCCTCCGTACATCCTCTCAA		
Phospholipase A ₂	PLA ₂ -f	CGACATAGGCATCCCATCCAT	99	102
	PLA ₂ -r	TCCTGGAAGTGGTCGTCACAA		
Cytosolic glycerol-3-phosphate dehydrogenase	cGPDH-f	GAGGCGTTCGCTAAAACAGGA	104	102
	cGPDH-r	ATGGTGGACTTCTGATGCCGT		
Mitochondrial glycerol-3-phosphate dehydrogenase	mGPDH-f	TGGCCAAGATGGCACAATGT	97	101
	mGPDH-r	CATGGCATAACAACACCTCGCT		
Aquaglyceroporin 9	AQP9-f	CCCATCAAGAAGTCCCAGTCT	Not calculated	120
	AQP9-r	CTGACAGAAGTCCACCCGTGTA		
	AQP9-f (probe)	6-FAM-CTGTACTATGATGCTCTCATGGT-MGBNFQ-3'		
Uncharacterized phosphatase	Phosphatase-f	CTCTCACCTAAGCGGTCCAC	103	108
	Phosphatase-r	GCACCTGGAACAACCTGTTT		
Type II antifreeze protein	AFPII-f	CAATGGTCGCTGTTTCCTTT	92	105
	AFPII-r	TCAAGGCTGTGTATGGATGC		

*6-FAM = 6-carboxyfluorescein; MGBNFQ = Minor groove binder/Non-fluorescent quencher

**See Methods for information on the standard curves used to determine amplification efficiency.

amplification efficiencies (26) were calculated and were required to be between 85% and 110%. Briefly, amplification efficiencies were calculated for separate pools of warm and cold cells from the 72 h time point. cDNA from four fish with the highest rates of glycerol production at 0.4°C were used to generate the two pools. A 5-point 1:5 dilution series starting with cDNA (corresponding to 10 ng of input total RNA) was analyzed for both the warm and cold pools. The reported efficiencies are an average of the two values. This dilution series was also performed for the 18S ribosomal RNA TaqMan assay to ensure that 18S RNA levels were consistent between the cold and warm pools and hence that it was an acceptable normalizer.

First-strand cDNA was synthesized from 1 µg of DNaseI-treated, column-purified total RNA using M-MLV reverse transcriptase (Invitrogen) as described in the cDNA cloning section, with the exception that random primers [250 ng (Invitrogen)] were used instead of oligo-dT primer. PCR amplification of the target genes, with the exception of AQP9, was performed in a 25 µl reaction using 1X Power SYBR Green PCR Master Mix (Applied Biosystems), 50 nM each of each forward and reverse primer and typically cDNA corresponding to 10 ng of input total RNA. Input cDNA was increased (corresponding to 25 ng of input total RNA) for six of the genes [phosphoglucomutase (PGM), glucose-6-phosphatase (G6Pase), mGPDH, acyl-CoA synthetase 4 (ACSL4), PEPCCK and PFK] due to higher fluorescence threshold cycle (C_T) values, and decreased (corresponding to 0.4 ng of input total RNA) for one gene (type II AFP) due to lower C_T values observed during the primer quality tests. For AQP9, PCR amplification was performed in a 25 µl reaction using 1X TaqMan Universal PCR Master Mix, with AmpErase UNG (Applied Biosystems), 900 nM each of forward and reverse primer, 250

nM TaqMan probe and cDNA corresponding to 25 ng of input total RNA. Expression levels of the target genes were normalized to 18S ribosomal RNA, using the Eukaryotic 18S rRNA Endogenous Control (VIC / MGB Probe, Primer Limited) (Applied Biosystems). PCR amplification of 18S was performed in a separate 25 µl reaction using 1X TaqMan Universal PCR Master Mix, with AmpErase UNG (Applied Biosystems), 1X probe/primer mix and cDNA corresponding to 0.4 ng of input total RNA. The real-time analysis program consisted of 1 cycle of 50°C for 2 min, 1 cycle of 95°C for 10 min and 40 cycles of (95°C for 15 sec and 60°C for 1 min) with fluorescence detection at the end of each 60°C step. On each plate, for every sample, the target gene and endogenous control were tested in duplicate (25). The C_T values were determined using the 7300 PCR Detection System SDS Software Relative Quantification Study Application (Version 1.2.3) (Applied Biosystems) using automated threshold and walking baseline. The relative quantity (RQ) of each transcript was determined with this software using the $2^{-\Delta\Delta C_T}$ relative quantification method and assuming 100% amplification efficiencies (21). For each target gene, the individual with the lowest normalized transcript expression level was set as the calibrator sample (assigned an RQ value = 1). Transcript expression levels are presented as mean \pm standard error (SE) RQ relative to the calibrator.

2.3.11 Statistical analysis

For glycerol measurements, a two-tailed *t*-test was used to assess if there were any significant differences in glycerol levels in cold compared to warm cells at 72 h, and in cold and warm cells at 72 h compared to pre-incubation levels. For QPCR analyses, a two-tailed *t*-test was used to assess if there were any significant differences in transcript levels between cold and warm cells at a given incubation time. A one-way ANOVA

followed by Tukey's HSD post-hoc test was used to assess if there were any significant differences in transcript levels within an incubation temperature over the 72 h time course. In all cases, $p < 0.05$ was considered to be statistically significant. All data are expressed as mean \pm SE.

For microarray studies, the same cold and warm RNA pools were compared at the 24, 48 and 72 h incubation times. For each time point, technical quadruplicate slides (including two dye-swaps) were run. Data are expressed as mean \pm SE and represent technical and not biological variability.

2.4 RESULTS

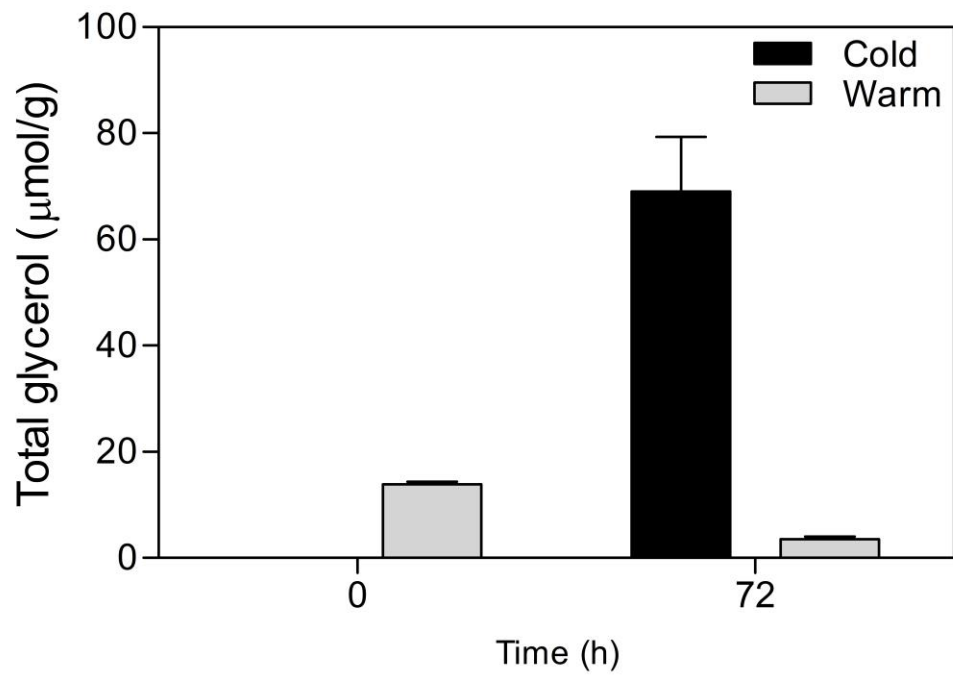
2.4.1 Glycerol production by hepatocytes incubated at cold or warm temperature

Glycerol levels in hepatocyte preparations were measured prior to and following 72 h incubation at 0.4°C or 8°C. For SSH cDNA library construction and microarray analyses, 9 fish that exhibited the highest rates of glycerol production at 0.4°C were selected from a total of 14 preparations. The 9 fish chosen for further experimentation had 8- to 29- fold higher glycerol levels in hepatocytes incubated at 0.4°C compared to 8°C for 72 h. For these fish, average glycerol levels for hepatocytes incubated at 0.4°C were $69.1 \pm 10.3 \mu\text{mol/g}$ and at 8°C were $3.6 \pm 0.5 \mu\text{mol/g}$ (Fig. 2.1).

2.4.2 Reciprocal SSH cDNA library characterization

RNA was pooled from 9 cell preparations incubated at 0.4°C or 8°C for 72 h. Five hundred and eighty-one ESTs from the forward SSH library (enriched for transcripts that were expressed at higher levels in cold than warm cells at 72 h) and 179 ESTs from the reverse SSH library (enriched for transcripts that were expressed at higher levels in warm than cold cells at 72 h) were generated. Both the forward and reverse SSH libraries contained some ESTs that were immature (i.e. incompletely spliced) transcripts (e.g. type II AFP) and therefore contained both intronic and exonic sequences. All individual EST sequences have been deposited in GenBank dbEST under accession numbers GR556841 to GR557421 for the forward SSH library and GR557422 to GR557600 for the reverse SSH library. For each SSH library, individual ESTs were assembled, identified and functionally annotated. Complete lists of assembled sequences (contigs and singletons), along with their contributing GenBank accession number(s), BLAST identification

Figure 2.1. Glycerol levels (cell pellet and incubation medium) for hepatocytes isolated from the 9 fish that were used in SSH cDNA library construction and microarray analyses. Fish were at 8°C prior to the liver perfusion. Time = 0 h represents pre-incubation glycerol levels prior to the cells being split into warm (8°C) and cold (0.4°C) groups and incubated for 72 h. Glycerol levels are expressed as μmol per gram cell and all values were significantly different from each other where $p < 0.05$ was considered to be statistically significant.



statistics and functional annotations (GO terms, descriptions and types) for the putative human orthologues (i.e. best human BLASTx hits) are presented in Supplemental Table S2.1 for the forward SSH library and Supplemental Table S2.2 for the reverse SSH library.

The 581 ESTs from the forward SSH library were assembled into 74 contigs and 298 singletons, or 372 non-redundant ESTs (# contigs + # singletons). Percentage redundancy [$1 - (\# \text{ non-redundant ESTs} / \text{total \# ESTs}) * 100$] for this library was 36%. The deepest three contigs (i.e. having the highest numbers of contributing sequences) in the forward SSH library were type II AFP (33 ESTs), 28S ribosomal RNA (19 ESTs) and PDK2 (14 ESTs). A second contig (8 ESTs), as well as 3 singletons, were also identified as type II AFP. Two additional contigs (each with 3 ESTs) and a singleton were also identified as PDK2. Other highly represented sequences in the forward SSH library were apolipoprotein C (1 contig of 12 ESTs), transferrin (3 contigs of 9, 5 and 4 ESTs and 1 singleton), transcription factor CP2-like protein 1 (4 contigs of 6, 4, 3 and 2 ESTs) and complement C3 (4 contigs of 6, 4, 2 and 2 ESTs and 4 singletons).

The 179 ESTs from the reverse SSH library were assembled into 20 contigs and 129 singletons, or 149 non-redundant ESTs. Percentage redundancy was 17%. The three deepest contigs in the reverse SSH library were cathelicidin-1 like (7 ESTs), transferrin (4 ESTs) and type II AFP (3 ESTs); both transferrin and type II AFP were also present in the forward SSH library. Other highly represented sequences in the reverse SSH library were cytochrome P450, family 51, subfamily A, polypeptide 1 (1 contig of 3 ESTs), heme-binding protein 2 (2 contigs each of 2 ESTs), heparan-alpha-glucosaminide N-acetyltransferase (1 contig of 2 ESTs and 3 singletons), tissue inhibitor of

metalloproteinase 2 (1 contig of 2 ESTs and 1 singleton) and cellular nucleic acid-binding protein (1 contig of 2 ESTs and 1 singleton).

Seventeen transcripts that were enriched in either the forward or reverse SSH library and had a theoretical association with the glycerol production pathway or non-colligative freeze prevention (type II AFP) were selected for QPCR analysis (Table 2.3). One of these, PDK2, was highly represented in the forward SSH library and type II AFP was present in both libraries.

2.4.3 Microarray analyses of transcript levels in hepatocytes

Microarray analyses were used to compare transcript levels in cold and warm RNA pools. Lists were created of microarray-identified reproducibly informative genes that were greater than 2-fold differentially expressed (in the same direction) in hepatocytes incubated at 0.4°C compared to 8°C at 24 h (Supplemental Table S2.3), 48 h (Supplemental Table S2.4) and 72 h (Supplemental Table S2.5). GO functional annotations reported in these tables are those associated with the putative human orthologue of the gene name of microarray features (salmonid ESTs) with significant BLAST hits. A summary of all reproducibly informative transcripts (25 higher expressed in cold cells, 87 higher expressed in warm cells) for the 24 h, 48 h and 72 h time points is presented in Supplemental Table S2.6.

Microarray-identified transcripts that were reproducibly expressed at greater than two-fold higher levels in cold than warm cells included transcription factor HES and 8 transcripts that were also found in the forward SSH library: catalase, cytochrome P450 1A1, DNA-binding protein inhibitor (ID) isoforms, electron transfer flavoprotein subunit

Table 2.3. Summary of SSH, microarray and QPCR results for genes subjected to QPCR.

Gene Name	SSH ¹		Microarray mean (SE) fold change ²			QPCR mean fold change ³		
	72 h		24 h	48 h	72 h	24 h	48 h	72 h
GLUT2	F					1.66	1.97	1.06
PGM	F					2.58	1.62	1.34
G6Pase	F					1.43	1.32	1.37
6PGDH					3.92 (0.52) CA061100	4.45	10.85	15.52
			6.68 (2.54) CA064428	5.99 (1.97) CA064428				
TALDO1	R				2.47 (0.25) CA063027	2.47	5.29	5.55
PFK ⁴						2.04	3.01	2.94
GAPDH	F					1.11	1.01	1.04
PDK2	F					2.39	15.83	20.35
PEPCK ⁴						1.09	1.37	1.19
MDH2	F					1.09	1.42	1.74
AAT2	F					2.47	2.56	2.19
GS	F		6.23 (1.49) CA041659	5.66 (1.44) CA041659	2.56	4.59	5.11	
		2.33 (0.06) CB514092	4.41 (0.69) CB514092	4.16 (0.80) CB514092				
GDH	F					1.20	1.00	1.26
LIPL	F					1.45	4.43	4.78
SLC27A6	F					1.53	2.09	2.56
ACSL4	F					4.86	2.95	1.33
PLA ₂	F					1.50	2.98	2.69
cGPDH	F					1.28	1.20	1.17
mGPDH ⁴						23.53	19.95	4.39
AQP9 ⁴						1.37	1.49	1.38
phosphatase	F					4.74	8.32	19.82
type II AFP	F	R				1.07	1.16	1.80

¹ “F” (white shading) indicates that the transcript was present in the forward SSH library (i.e. enriched for transcripts expressed at higher levels in cold than warm cells). “R” (grey shading) indicates that the transcript was present in the reverse SSH library (i.e. enriched for transcripts expressed at higher levels in warm than cold cells).

² Microarray features were considered to be reproducibly informative if they were 2-fold or greater differentially expressed (in the same direction) in all 4 thresholded technical replicate microarrays (including 2 dye-swaps) at that given time point. As replicate microarray analyses were performed comparing the same sample pools, standard error (SE) for microarray data reflects technical rather than biological variability. Microarray feature EST accession number is listed. For genes with multiple accession numbers, multiple ESTs with significant BLASTx hits against that gene name are present on the array. White shading indicates that the transcript was expressed at higher levels in cold than warm cells at that given time point. Grey shading indicates that the transcript was expressed at higher levels in warm than cold cells at that given time point.

³ QPCR analyses were performed on 9 individual samples at a given incubation temperature and time. QPCR data (Fig. 2.6) conveys biological variability information since individuals (i.e. biological replicates) were incorporated into the QPCR experimental design. White shading indicates the ratio is for cold compared to warm cells at that given time point. Grey shading indicates the ratio is for warm compared to cold cells at that given time point. Values highlighted in bold were **significantly** different ($p < 0.05$).

⁴ These genes were not identified in SSH or microarray analyses but were selected for QPCR analyses due to their conceptual link to glycerol synthesis.

beta, formimidoyltransferase-cyclodeaminase, glutamine synthetase, hemoglobin subunit alpha and tripartite motif-containing protein 16.

Microarray-identified transcripts that were reproducibly expressed at greater than two-fold higher levels in warm than cold cells included 6-phosphogluconate dehydrogenase (6PGDH), mitochondrial coproporphyrinogen III oxidase, cytochrome P450 7A1, erythrocyte band 7 integral membrane protein, ferritin and metallothionein A, and ten transcripts that were also found in the reverse SSH library: 3-hydroxy-3-methylglutaryl-coenzyme A reductase, BPI (bactericidal/permeability-increasing protein)/ LBP (LPS binding protein), catechol-O-methyltransferase domain-containing protein 1, C-type lectin domain family 4 member E, diamine acetyl transferase 1, fibroleukin precursor, glutathione peroxidase, multidrug resistance-associated protein 4, transaldolase 1 (TALDO1) and vitelline membrane outer layer protein 1.

6PGDH, TALDO1, and GS were selected for QPCR analysis as these transcripts showed a 2-fold or greater differential expression by microarray analysis and had a theoretical relationship to glycerol production.

2.4.4 AQP9 and GLUT2 cDNA cloning and classification

cDNA cloning and phylogenetic analyses were performed to classify AQP9 and GLUT2 and to obtain nucleotide sequences for QPCR primer design. Full-length cDNA sequences were deposited in GenBank under accession numbers DQ533629 (AQP9) and FJ797642 (GLUT2). AQP9 is a 1047 bp cDNA that contains a 55 bp 5'UTR, an 867 bp open reading frame (ORF) and a 125 bp 3'UTR; it encodes a 288 aa protein which has a predicted molecular mass of 30.7 kDa and an isoelectric point of 5.74. GLUT2 is a 1913 bp cDNA that contains a 14 bp 5'UTR, a 1515 bp ORF and a 384 bp 3'UTR; it encodes a

504 aa protein which has a predicted molecular mass of 55.1 kDa and an isoelectric point of 7.16.

At least ten water channel proteins (aquaporins) responsible for the water permeability of biological membranes have been identified in mammals. Of these, four (AQP3, AQP7, AQP9 and AQP10) are selectively permeated by both water and glycerol (aquaglyceroporins) (1). At least thirteen GLUTs have been reported in mammals. The Class I sodium-independent GLUTs are comprised of GLUTs 1-4 (16). Phylogenetic analyses with putative orthologous proteins from other vertebrates were performed for both the aquaglyceroporin (Fig. 2.2A) and GLUT (Fig. 2.2B) deduced amino acid sequences to ensure correct classification. According to these analyses, smelt AQP9 and GLUT2 cluster with the appropriate protein sequences for other vertebrates. This supports categorizing the aquaglyceroporin cloned herein as a type 9 member of the aquaporin family of transmembrane channel proteins and the GLUT as a type 2 member of the Class I sodium-independent GLUTs.

2.4.5 mGPDH cDNA cloning and characterization

A full-length cDNA for smelt mGPDH was cloned using a combination of RT-PCR and RLM-RACE and the sequence deposited in GenBank (accession no. FJ797643). mGPDH is a 2790 bp cDNA that contains a 109 bp 5'UTR, a 2193 bp ORF and a 488 bp 3'UTR. It encodes a 730 aa protein which has a predicted molecular mass of 81.1 kDa and isoelectric point of 6.24.

A BLASTx 2.2.20 search of the non-redundant (nr) protein sequence database of NCBI was performed to compare the relatedness of smelt mGPDH to protein sequences from other species. At the amino acid level, smelt mGPDH had the highest sequence

Figure 2.2A. Phylogenetic analysis of smelt AQP9 predicted protein sequences. A phylogenetic tree of protein sequences from smelt AQP9 and aquaglyceroporins from other vertebrates. GenBank protein accession numbers are as follows: AQP3 human (AAH13566), AQP3 mouse (BAB03270), AQP3 rat (P47862), AQP3 frog (CAA10517), AQP3 eel (CAC85286), AQP3 zebrafish (AAH44188), AQP seabream (AAR13054), AQP7 human (NP_001161), AQP7 mouse (BAA24537), AQP7 rat (P56403), AQP9 human (O43315), AQP9 mouse (BAB03271), AQP9 rat (AAC36020), AQP9 chimp (XP_523087), AQP9 chicken (XP_413787), AQP9 (XP_544701) dog, **AQP9 rainbow smelt (ABG24574)**, AQP10 human (BAB91223). The tree was constructed as described in the materials and methods section. The scale bar represents the number of substitutions per amino acid site. All bootstrap values are shown, however only values ≥ 90 are considered trustworthy.

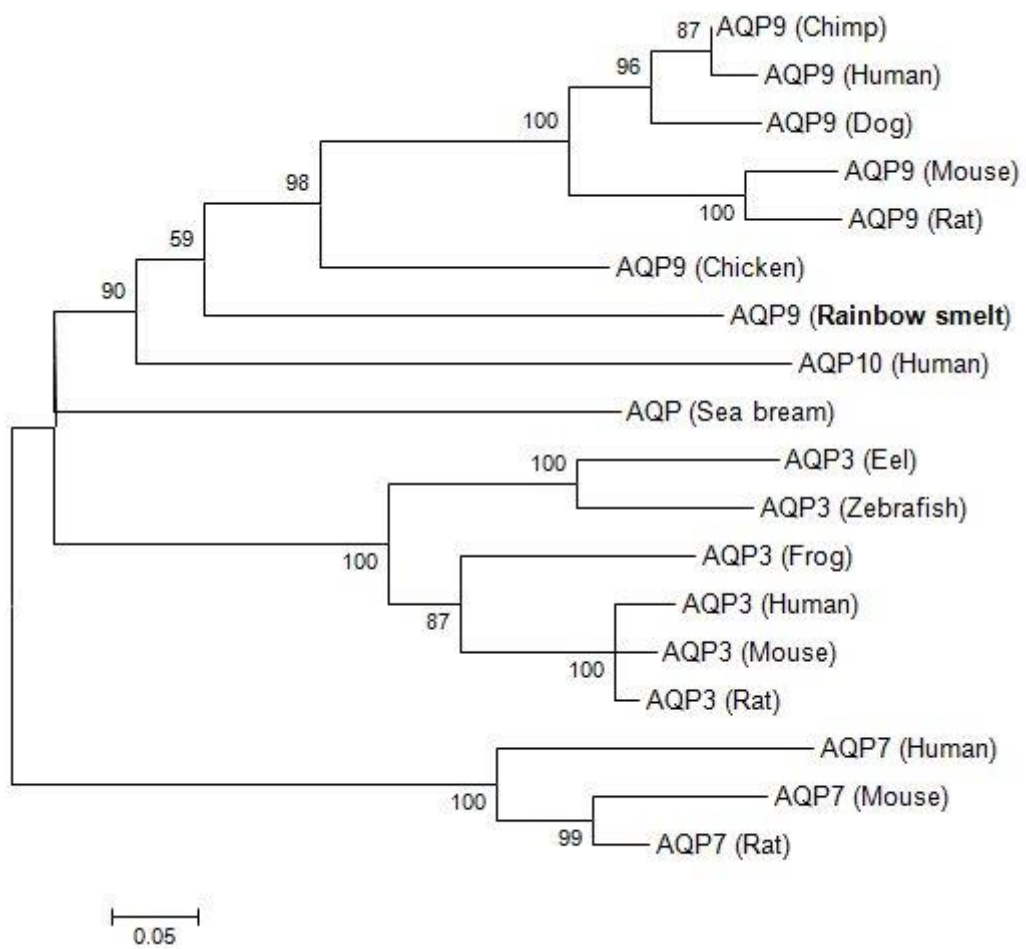
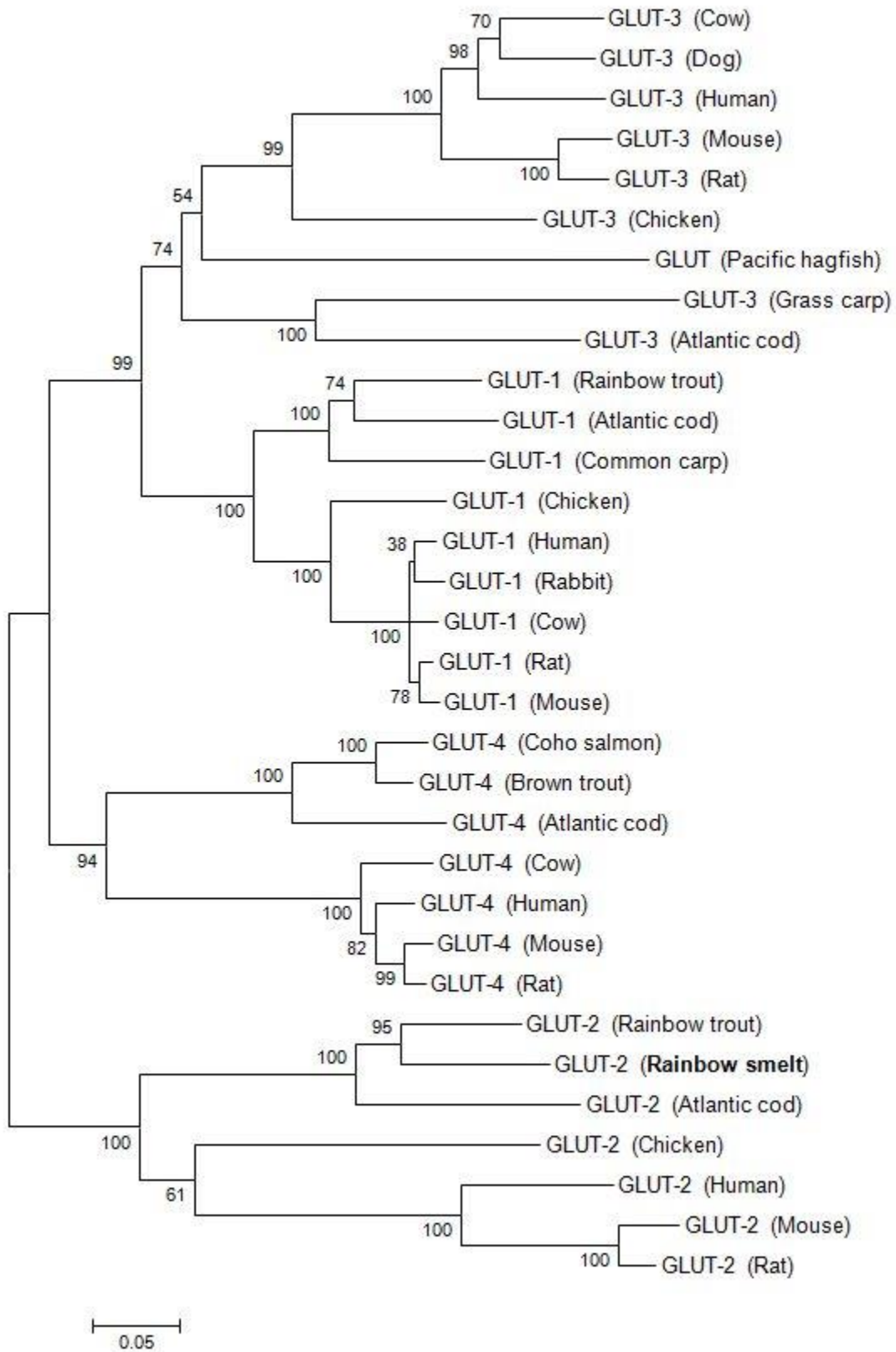


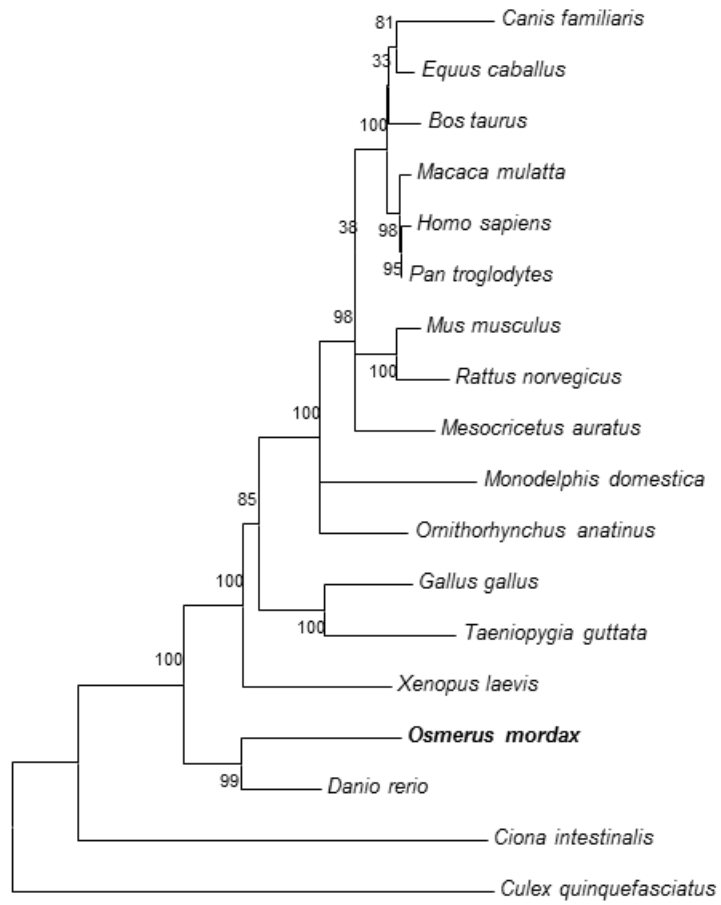
Figure 2.2B. Phylogenetic analysis of smelt GLUT2 predicted protein sequences. A phylogenetic tree of protein sequences from smelt GLUT2 and GLUTs 1-4 from other vertebrates. GenBank protein accession numbers are as follows: GLUT1 common carp (AAF75683), GLUT1 rainbow trout (AAF75681), GLUT1 Atlantic cod (AAS17880), GLUT1 chicken (AAB02037), GLUT1 human (AAA52571), GLUT1 rabbit (P13355), GLUT1 cow (P27674), GLUT1 rat (P11167), GLUT1 mouse (AAA37752), GLUT2 chicken (Q90592), GLUT2 rainbow trout (AAK09377), GLUT2 human (AAA59514), GLUT2 mouse (P14246), GLUT2 rat (P12336), GLUT2 Atlantic cod (AAV63984), **GLUT2 rainbow smelt (ACO34844)**, GLUT3 cow (AAK70222), GLUT3 dog (P47842), GLUT3 human (AAB61083), GLUT3 mouse (AAH34122), GLUT3 rat (Q07647), GLUT3 chicken (AAA48662), GLUT3 grass carp (AAP03065), GLUT3 Atlantic cod (AAT67456), GLUT4 cow (Q27994), GLUT4 human (AAA59189), GLUT4 mouse (P14142), GLUT4 rat (P19357), GLUT4 coho salmon (AAM22227), GLUT4 brown trout (AAG12191), GLUT4 Atlantic cod (AAZ15731), Pacific hagfish (AAL27090). The tree was constructed as described in the materials and methods section. The scale bar represents the number of substitutions per amino acid site. All bootstrap values are shown, however only values ≥ 90 are considered trustworthy.



identity with that of zebrafish (*Danio rerio*). The zebrafish protein was truncated (536 aa); however, there was 86% identity over that alignment length. Amino acid identities ranged from 72% [dog (*Canis familiaris*)] to 79% [frog (*Xenopus laevis*)] for other vertebrates, to 64% and 57%, for the vase tunicate (*Ciona intestinalis*) and mosquito (*Culex quinquefasciatus*), respectively. A multiple alignment of 18 mGPDH protein sequences (16 vertebrates, 2 invertebrates), identified by BLASTx analysis, was performed and a phylogenetic tree was constructed (Fig. 2.3). Smelt mGPDH clusters with that of zebrafish and frog and concurs with percentage amino acid identities.

mGPDH proteins are characterized by the presence of several structural motifs. They contain a mitochondrial leader peptide, an FAD-binding domain, a glycerol-3-phosphate binding domain and a region near the carboxyl terminus that contains a pair of sequences homologous to EF-hand Ca^{2+} -binding domains, the second of which has features consistent with high Ca^{2+} affinity. EF-hands are around 29 amino acids in length and form a helix-loop-helix structure in which the Ca^{2+} ion is coordinated by oxygen atoms from six amino acids in the loop. They typically occur in groups of two or four, with pairings of high and low affinity Ca^{2+} -binding domains being commonplace (5, 18, 23). An alignment of the amino acid sequences of mGPDH from smelt, human, rat and frog showing these structural features is presented in Fig. 2.4. Amino acid sequences pertaining to the mitochondrial leader peptide, the FAD-binding domain and the glycerol 3-phosphate binding domain were described previously (5, 18, 23). The two EF-hand Ca^{2+} -binding domains, with their 8 Ca^{2+} -binding residues, were identified using the Conserved Domains Database (CDD) (www.ncbi.nlm.nih.gov/Structure/cdd/cdd.shtml).

Figure 2.3. Phylogenetic analysis of smelt mGPDH predicted protein sequences. A phylogenetic tree of protein sequences for mGPDH from a variety of species. GenBank protein accession numbers are as follows: African clawed frog (*Xenopus laevis*): AAH73694. chimpanzee (*Pan troglodytes*): XP_001142893. chicken (*Gallus gallus*): XP_422168. cow (*Bos taurus*): AAI48086. dog (*Canis familiaris*): XP_848389. golden hamster (*Mesocricetus auratus*): CAO79918. gray short-tailed opossum (*Monodelphis domestica*): XP_001365971. horse (*Equus caballus*): XP_001490923. house mouse (*Mus musculus*): AAH21359. human (*Homo sapiens*): AAB60403. platypus (*Ornithorhynchus anatinus*): XP_001509091. rainbow smelt (*Osmerus mordax*): ACO34845. rat (*Rattus norvegicus*): AAB60443. rhesus macaque (*Macaca mulatta*): XP_001086947. southern house mosquito (*Culex quinquefasciatus*): XP_001845276. vase tunicate (*Ciona intestinalis*): XP_002123583. zebra finch (*Taeniopygia guttata*): XP_002187076. zebrafish (*Danio rerio*): AAI65374. The tree was constructed as described in the materials and methods section. The scale bar represents the number of substitutions per amino acid site. All bootstrap values are shown, however only values ≥ 90 are considered trustworthy.



0.02

Figure 2.4. Amino acid alignment of mGPDH from human, rat, frog and smelt. GenBank protein accession numbers are as follows: human (AAB60403), rat (AAB60443), frog (AAH73694) and smelt (ACO34845). Amino acids are represented by the single letter code. Dashes are inserted where gaps are present in the amino acid sequences. Asterisks indicate residues that are identical among all four sequences shown, whereas colons indicate residues that are similar. Residues highlighted with bold italic characters form the mitochondrial leader peptide, those highlighted with a black background form the FAD-binding domain, those highlighted with bold underlined characters form the glycerol-3-phosphate binding domain and those highlighted with a grey background form the two EF-hands, with their 8 calcium-binding residues highlighted by bold characters with a white background.

Human	FLYYEMGYKSRSEQLTDRSEISLLPSDIDRYKKRFHKFDADQKGFITIVDVQRVLESINV	657
Rat	FLYYEMGYKSRTEQLTDSSTEISLLPPDIDRYKKRFHMFDEDEKGFITIVDVQRVLESINV	657
Frog	FLYYEMGYKSRSEQLTDRSEINLSPSDVDRYTKRFHKFDKDKKGFITILDVQHVLENINV	655
Smelt	FLYHEMGYRSRSEQITKTSEITLDAQEVARYQKRFHKFDKECKGFITTVDVQRVLKNINV	660
	::***:***:*. :*. * . :. ** **** ** : ***** :***:***:***	
Human	QMDENTLHEILNEVDLNKNGQVELNEFLQLMSAIQKGRVSGSRLAILMKTAEENLDRRVP	717
Rat	QMDEDTLHEILCEVDLNKNGQVELHEFLQLMSAVHTGRVSGSRLAILMKTAEENLDRRVP	717
Frog	HMDANNLHEILNEVDLNKNGQVELNEFLQLMSAIQKGFVSSSRLAILMKSAAENLEQREP	715
Smelt	QIDENALHEILNEVDLNKNGQVEIDEFLQLMSAVKKGQVSDSRLALLLKSAAESLDRAP	720
	::* : ***** *****:*****:.* **.*:*.***.*: * *	
Human	IPVDRSCGGL	727
Rat	IPVDRSCGGL	727
Frog	IPVHRSGGV	725
Smelt	VSVDRSGGV	730
	:.*.** **:	

The mGPDH protein from zebrafish was not included in this alignment as it is truncated and therefore does not contain the EF-hand calcium binding domains.

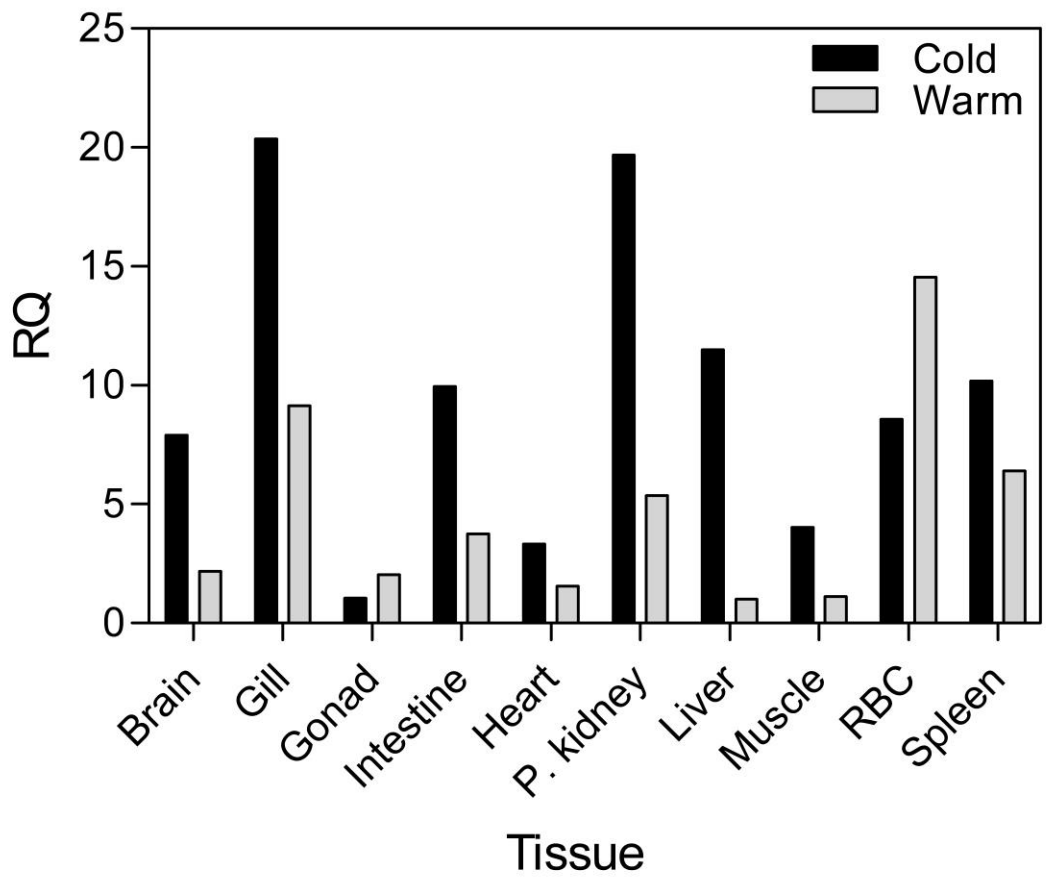
mGPDH transcript levels from tissues of one warm- and one cold-adapted smelt were analyzed by QPCR (Fig. 2.5). The calibrator sample (sample with the lowest normalized expression level) was warm-acclimated smelt liver. mGPDH is ubiquitously expressed in both warm- and cold-acclimated smelt. Transcript levels were highest in RBCs, gill, spleen and posterior kidney in the warm smelt and in gill, posterior kidney, liver and spleen in the cold smelt. With the exception of RBCs and gonad, mGPDH transcript levels were higher in the cold than the warm smelt. However, these results are based on the comparison of two fish and should be viewed with caution.

2.4.6 QPCR analysis of transcripts whose products are potentially related to freeze resistance

SSH and microarray analyses showed that cold temperature affected transcript levels of genes involved in various biological processes (e.g. oxidation reduction, iron homeostasis, immune response, transcription) in cultured smelt hepatocytes. The QPCR studies conducted herein, however, were specifically focused on transcripts encoding proteins that are potentially involved in the non-colligative (type II AFP) and colligative (glycerol accumulation) freeze prevention strategies. Type II AFP and 21 transcripts involved in the metabolism of 3 sources of glycerol [glycolytic (glycogen, glucose), gluconeogenic (amino acids) and lipid (triglyceride, phospholipid)] were analyzed. A schematic outlining the metabolic functions of their encoded proteins (18 glycerol-related) is presented in Fig. 1.1. Transcripts subjected to QPCR but not shown in Fig. 1.1 are solute carrier family 27 member 6 (SLC27A6) [a fatty acid transporter (FATP),

Figure 2.5. Tissue distribution of smelt mGPDH transcripts. mGPDH transcript levels were measured in various tissues from one warm- and one cold-acclimated smelt by QPCR. Gene expression data are presented as mean RQ (relative quantity) values for mGPDH expression normalized to 18S ribosomal RNA and are calibrated to the sample with the lowest normalized expression (warm liver; assigned a value = 1). P. kidney, posterior kidney; RBC, red blood cell. As transcript levels were measured in only a single fish for each condition, only a qualitative analysis is possible.

mGPDH



mainly of long-chain fatty acids], ACSL4 [activates long-chain (C12–20) NEFAs by adding Coenzyme A so they can be incorporated into triglyceride] and phospholipase A₂ (PLA₂) (catalyzes the hydrolysis of the sn-2 position of membrane glycerophospholipids).

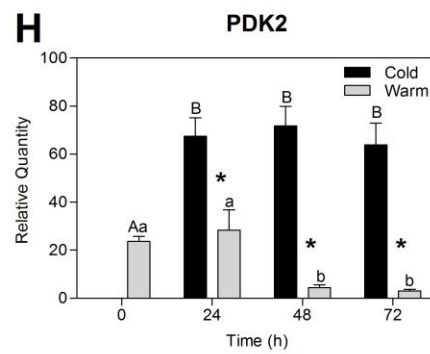
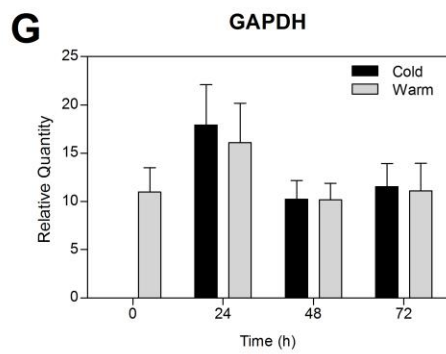
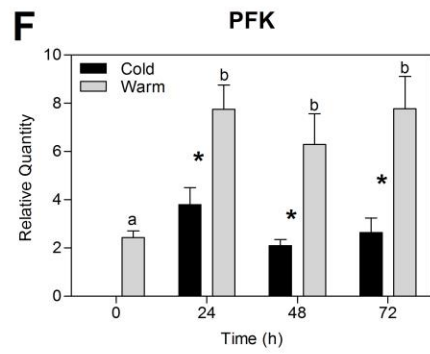
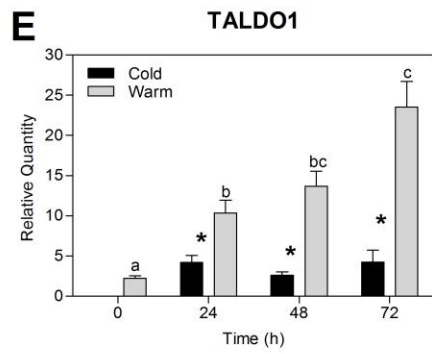
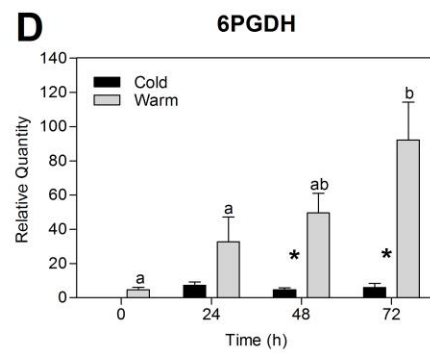
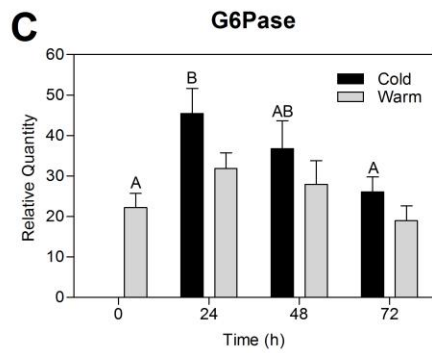
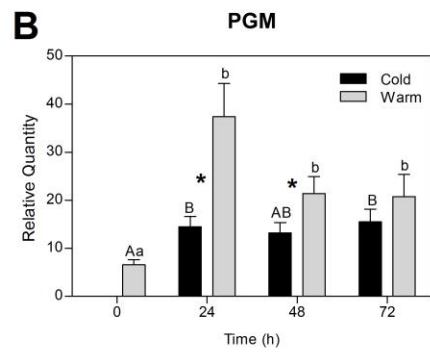
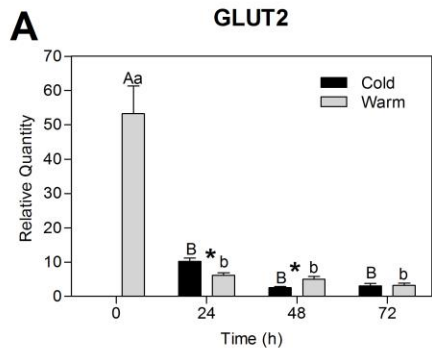
Table 2.3 links the results of the functional genomic (SSH and microarray) and QPCR studies. Of the 22 transcripts subjected to QPCR, 16 were present in the forward SSH library and 1 (TALDO1) in the reverse SSH library. Of these 17 SSH-identified transcripts, 2 were also reproducibly informative in the microarray analysis: GS (greater than two-fold higher expressed in cold cells) and TALDO1 (greater than two-fold higher expressed in warm cells). 6PGDH was identified by microarray analysis alone as greater than two-fold higher expressed in warm cells. The smelt cDNA for 6PGDH has been cloned (GenBank accession number ACO09011) and QPCR primers were based upon this sequence. The following 4 additional transcripts were studied by QPCR because of their potential involvement in glycerol management: mGPDH (FJ797643), AQP9 (DQ533629), PEPCK (DQ230919), and PFK (EL544745).

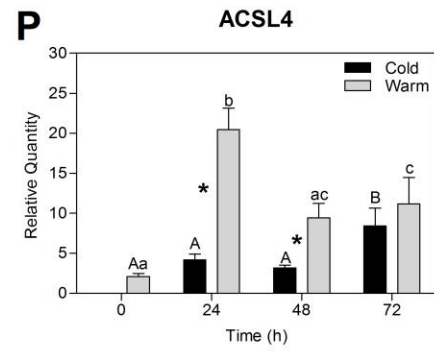
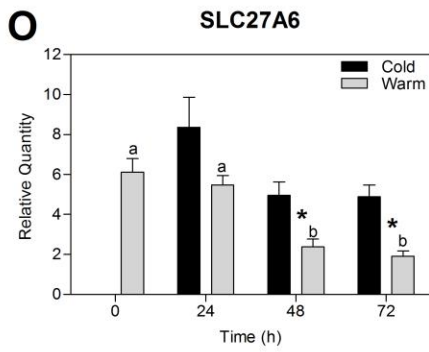
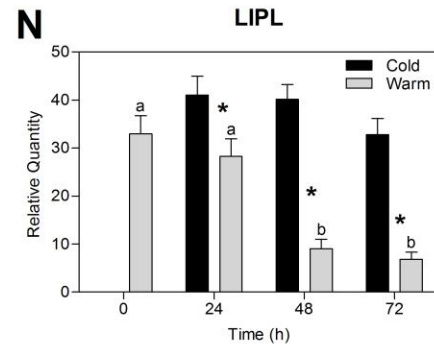
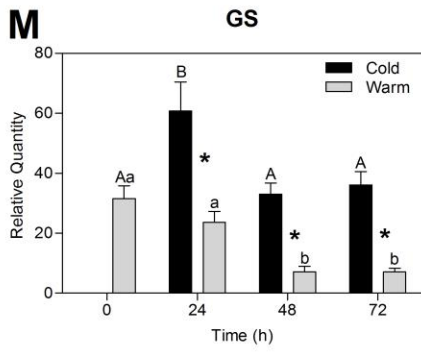
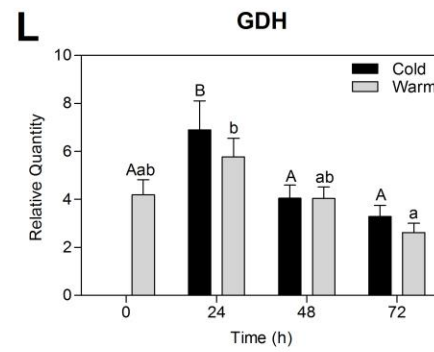
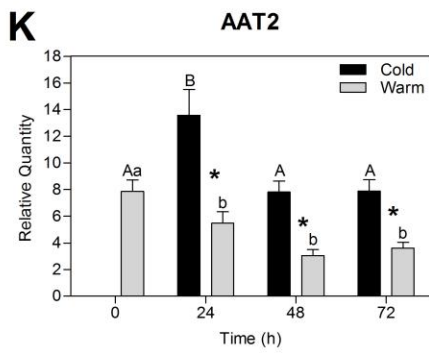
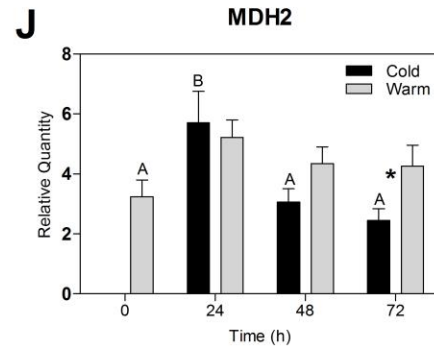
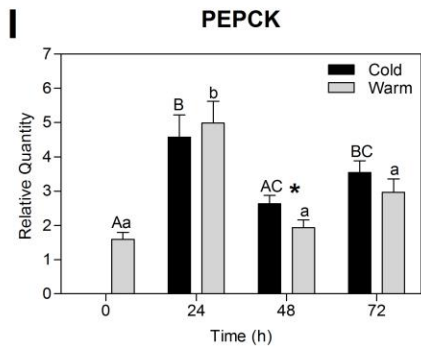
QPCR was performed on individual fish hepatocyte samples so that biological variability could be assessed. Cells collected prior to incubation (to establish reference transcript levels), as well as both cold and warm cells harvested at the 24, 48 and 72 h incubation times were analyzed. Normalized expression levels of each transcript are presented in Fig. 2.6 (A-V).

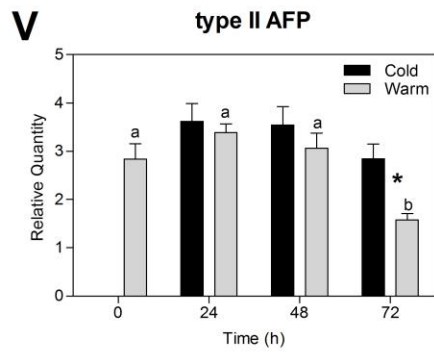
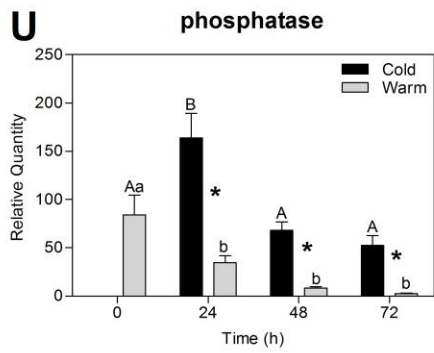
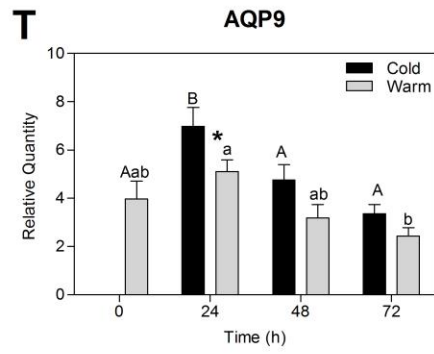
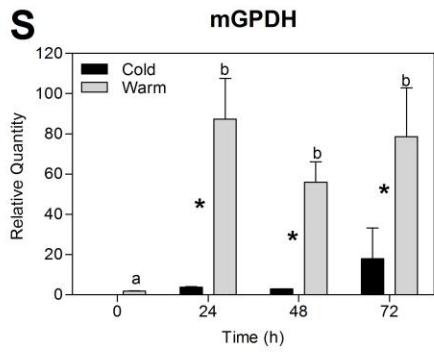
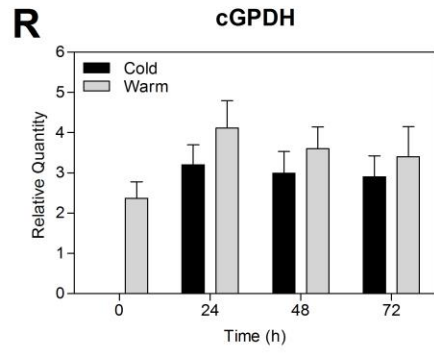
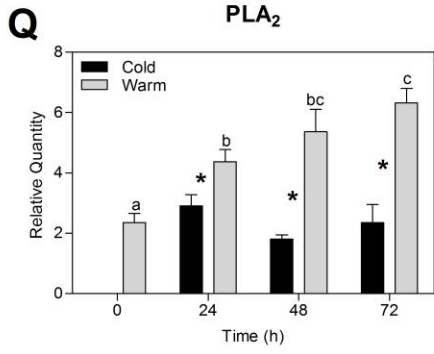
2.4.6.1 Transcripts whose products are involved in carbohydrate metabolism

For the glucose transport relevant gene (GLUT2), in both cold and warm cells, levels were significantly lower at 24 h (5- and 8.5- fold, respectively), 48 h (21- and 11- fold, respectively) and 72 h (17- and 16-fold, respectively) than pre-incubation. Levels in

Figure 2.6. QPCR analyses of a subset of transcripts identified as differentially expressed in cold compared to warm cells by either SSH, microarray analysis (or both) or selected by the authors because of their theoretical relationship to glycerol management. QPCR studies were specifically focused on non-colligative (type II AFP) and colligative (glycerol accumulation) freeze prevention strategies. Transcript levels are presented as mean \pm SE relative quantity (RQ) values (i.e. values for the gene of interest were normalized to 18S ribosomal RNA) and were calibrated to the individual with the lowest normalized transcript levels of that given gene. Identical letters (upper case for the cold cells and lower case for the warm cells) indicate that there were no significant differences in transcript levels throughout the incubation time. Asterisks denote significant differences in transcript levels between cold and warm cells at a given incubation time. In all cases, $n=9$ and $p < 0.05$ was considered to be statistically significant.







cold cells were 1.7-fold significantly higher at 24 h and 2-fold significantly lower at 48 h than warm cells (Fig. 2.6A).

For the glycogen metabolism relevant gene (PGM), in cold cells, levels were significantly higher at 24 h (2.2-fold) and 72 h (2.4-fold) than pre-incubation. In warm cells, levels were significantly higher at 24 h (5.7-fold), 48 h (3.2-fold) and 72 h (3.2-fold) than pre-incubation. Levels in cold cells were significantly lower at 24 h (2.6-fold) and 48 h (1.6-fold) than warm cells (Fig. 2.6B).

For the glucose synthesis relevant gene (G6Pase), in cold cells, levels were significantly higher at 24 h (2-fold) than pre-incubation. In warm cells, levels were not significantly different at any time point than pre-incubation. There were no significant differences in levels in cold compared to warm cells at any time point (Fig. 2.6C).

Two pentose phosphate shunt relevant genes were subjected to QPCR: 6PGDH and TALDO1. In cold cells, 6PGDH levels were not significantly different at any time point than pre-incubation. In warm cells, 6PGDH levels were significantly higher at 72 h (20-fold) than pre-incubation. Levels for 6PGDH in cold cells were significantly lower at 48 h (11-fold) and 72 h (16-fold) than warm cells (Fig. 2.6D). In cold cells, TALDO1 levels were not significantly different at any time point than pre-incubation. In warm cells, TALDO1 levels were significantly higher at 24 h (4.7-fold), 48 h (6.2-fold) and 72 h (10.6-fold) than pre-incubation. Levels for TALDO1 in cold cells were significantly lower at 24 h (2.5-fold), 48 h (5-fold) and 72 h (5.5-fold) than warm cells (Fig. 2.6E).

For the glycolysis relevant gene (PFK), in cold cells, levels were not significantly different at any time point than pre-incubation. In warm cells, levels were approximately 3-fold significantly higher than pre-incubation at all three time points. Levels in cold cells

were 2-fold significantly lower at 24 h and 3-fold significantly lower at 48 h and at 72 h than warm cells (Fig. 2.6F).

Two glycolysis and gluconeogenesis relevant genes were subjected to QPCR: glyceraldehyde-3-phosphate dehydrogenase (GAPDH) and PDK2. GAPDH levels in cold and warm cells were not significantly different at any time point than pre-incubation or in cold compared to warm cells at any time point (Fig. 2.6G). In cold cells, PDK2 levels were approximately 3-fold higher than pre-incubation at all three time points. In warm cells, PDK2 levels were significantly lower at 48 h (5.2-fold) and 72 h (7.5-fold) than pre-incubation. Levels for PDK2 in cold cells were significantly higher at 24 h (2.4-fold), 48 h (16-fold) and 72 h (20-fold) than warm cells (Fig. 2.6H).

2.4.6.2 Transcripts whose products are involved in amino acid metabolism

For the gluconeogenesis relevant gene (PEPCK), in cold cells, levels were significantly higher at 24 h (2.9-fold) and 72 h (2.2-fold) than pre-incubation. In warm cells, levels were significantly higher at 24 h (3.2-fold) than pre-incubation. Levels in cold cells were significantly higher at 48 h (1.4-fold) than warm cells (Fig. 2.6I).

Four genes related to amino acid metabolism were subjected to QPCR: mitochondrial malate dehydrogenase (MDH2), alanine aminotransferase (AAT2), GDH and GS. In cold cells, MDH2 levels were significantly higher at 24 h (1.8-fold) than pre-incubation. In warm cells, MDH2 levels were not significantly different at any time point than pre-incubation. Levels for MDH2 in cold cells were significantly lower at 72 h (1.7-fold) than warm cells (Fig. 2.6J). In cold cells, AAT2 levels were significantly higher at 24 h (1.7-fold) than pre-incubation. In warm cells, AAT2 levels were significantly lower at 24 h (1.4-fold), 48 h (2.6-fold) and 72 h (2.2-fold) than pre-incubation. Levels for

AAT2 in cold cells were significantly higher at 24 h (2.5-fold), 48 h (2.6-fold) and 72 h (2.2-fold) than warm cells (Fig. 2.6K). In cold cells, GDH levels were significantly higher at 24 h (1.6-fold) than pre-incubation. In warm cells, GDH levels were not significantly different at any time point than pre-incubation. There were no significant differences in GDH levels between cold and warm cells at any time point (Fig. 2.6L). In cold cells, GS levels were significantly higher at 24 h (1.9-fold) than pre-incubation. In warm cells, GS levels were 4.4-fold significantly lower at 48 h and 72 h than pre-incubation. Levels for GS in cold cells were significantly higher at 24 h (2.6-fold), 48 h (4.6-fold) and 72 h (5.1-fold) than warm cells (Fig. 2.6M).

2.4.6.3 Transcripts whose products are involved in lipid metabolism

Four genes related to lipid metabolism were subjected to QPCR: lipoprotein lipase (LIPL), SLC27A6, ACSL4 and PLA₂. In cold cells, LIPL levels were not significantly different at any time point than pre-incubation. In warm cells, LIPL levels were significantly lower at 48 h (3.6-fold) and 72 h (4.8-fold) than pre-incubation. Levels for LIPL in cold cells were significantly higher at 24 h (1.5-fold), 48 h (4.4-fold) and 72 h (4.8-fold) than warm cells (Fig. 2.6N). In cold cells, SLC27A6 levels were not significantly different at any time point than pre-incubation. In warm cells, SLC27A6 levels were significantly lower at 48 h (2.6-fold) and 72 h (3.2-fold) than pre-incubation. Levels for SLC27A6 in cold cells were significantly higher at 48 h (2.1-fold) and 72 h (2.6-fold) than warm cells (Fig. 2.6O). In cold cells, ACSL4 levels were significantly higher at 72 h (4-fold) than pre-incubation. In warm cells, ACSL4 levels were significantly higher at 24 h (10-fold) and 72 h (5.3-fold) than pre-incubation. Levels for ACSL4 in cold cells were significantly lower at 24 h (4.9-fold) and 48 h (3-fold) than

warm cells (Fig. 2.6P). In cold cells, PLA₂ levels were not significantly different at any time point than pre-incubation. In warm cells, PLA₂ levels were significantly higher at 24 h (1.9-fold), 48 h (2.3-fold) and 72 h (2.7-fold) than pre-incubation. Levels for PLA₂ in cold cells were significantly lower at 24 h (1.5-fold), 48 h (3-fold) and 72 h (2.7-fold) than warm cells (Fig. 2.6Q).

2.4.6.4 Transcripts whose products are involved in glycerol metabolism and diffusion

Two genes related to glyceroneogenesis were subjected to QPCR: cGPDH and mGPDH. There were no significant differences in cGPDH levels in cold and warm cells at any time point compared to pre-incubation or in cold compared to warm cells at any time point (Fig. 2.6R). In cold cells, mGPDH levels were not significantly different at any time point than pre-incubation. In warm cells, mGPDH levels were significantly higher at 24 h (50-fold), 48 h (32-fold) and 72 h (46-fold) than pre-incubation. Levels for mGPDH in cold cells were significantly lower at 24 h (24-fold), 48 h (20-fold) and 72 h (4.4-fold) than warm cells (Fig. 2.6S).

For the glycerol diffusion-related gene (AQP9), in cold cells, AQP9 levels were significantly higher at 24 h (1.8-fold) than pre-incubation. In warm cells, AQP9 levels were not significantly different at any time point than pre-incubation. Levels for AQP9 in cold cells were significantly higher at 24 h (1.4-fold) than warm cells (Fig. 2.6T).

2.4.6.5 Transcript encoding a phosphatase-like protein

For the phosphatase-like gene, in cold cells, levels were significantly higher at 24 h (2-fold) than pre-incubation. In warm cells, levels were significantly lower at 24 h (2.4-fold), 48 h (10-fold) and 72 h (32-fold) than pre-incubation. Levels in cold cells were

significantly higher at 24 h (4.7-fold), 48 h (8.3-fold) and 72 h (20-fold) than warm cells (Fig. 2.6U).

2.4.6.6 Transcript encoding an antifreeze protein

For the non-colligative antifreeze gene (type II AFP), in cold cells, levels were not significantly different at any time point than pre-incubation. In warm cells, there was a significant decrease in levels at 72 h (1.8-fold) compared to pre-incubation. Levels in cold cells were significantly higher at 72 h (1.8-fold) than warm cells (Fig. 2.6V).

2.5 DISCUSSION

2.5.1 Smelt hepatocyte model of cold-induced glycerol production

This model was successful in generating two populations of hepatocytes [non-glycerol accumulating (warm temperature incubation) and glycerol accumulating (cold temperature incubation)] prepared from fish maintained at non-glycerol producing temperature. Transcriptomes of these cells were compared using functional genomic techniques (SSH cDNA library construction and microarray hybridization) and QPCR. The hepatocytes faced the challenge of moving from an *in vivo* to an *in vitro* environment. All cells were incubated in minimal medium [(in mM) 176 NaCl, 5.4 KCl, 0.81 MgSO₄, 0.44 KH₂PO₄, 0.35 Na₂HPO₄, 5 NaHCO₃, 10 HEPES, and 1 EGTA, adjusted to pH 7.63] that contained 5 mM glucose as the only nutritional supplement and were thus deprived of exogenous sources of other normal metabolic fuels (e.g. amino acids and lipids) and hormonal input. As such, metabolic reorganization was generally anticipated; however, cold cells also faced the challenge of a substantial decrease in temperature and therefore additional changes in the transcriptome were anticipated.

2.5.2 SSH and microarray studies

The experimental design compared cold and warm hepatocyte RNA pools generated by pooling RNA extracted from the same 9 individual fish. The SSH and microarray studies were complementary; smelt transcripts not represented by orthologous sequences on available salmonid microarrays could potentially be identified using the SSH approach. By combining these functional genomic techniques, transcripts were identified that were differentially expressed between cold and warm cells. GO functional annotations were collected for these genes; a subset with functional annotations

suggesting involvement in the antifreeze response were then selected for QPCR. In the QPCR studies, transcript levels of the selected genes were compared in hepatocytes isolated from 9 individual fish to convey detailed information on biological variability.

Reciprocal SSH libraries enriched for cold-responsive hepatocyte transcripts were constructed at the 72 h incubation time point. The most abundant transcript in the forward SSH library was type II AFP that encodes a protein important in non-colligative freeze prevention. PDK2 was the third largest contig in the forward SSH library. This was a novel and unexpected finding and, as discussed below, this transcript is considered to be critical in regulating glycerol production.

Microarray analyses were conducted at the 24, 48 and 72 h time points using the cGRASP 16K salmonid cDNA array (42). These time points were chosen to monitor gene expression throughout the linear phase of glycerol production (7). The comparison of RNA pools was considered acceptable since only qualitative changes were being probed with this approach. Since these microarray analyses were inter-specific (i.e. labeled smelt targets hybridized to salmonid cDNA probes), there were potential limitations to this study. Firstly, since only 30% of smelt transcripts bind to the salmonid microarray (42), important transcripts in cold adaptation in smelt may not hybridize to orthologous sequences on the array due to species-specific sequence differences. Furthermore, salmon and smelt vary in their cold adaptation response in that salmon do not produce type II AFP (14) or accumulate glycerol (32); therefore, important transcripts in these processes may not be represented on the microarray.

2.5.3 Smelt hepatocyte transcriptome response to cold in comparison to whole animal studies

In earlier studies, transcripts differentially expressed in livers directly sampled from smelt in fall and winter were assessed (30, 31). The current work reveals transcripts that are activated within hours of exposure to low temperature in contrast to long term acclimatization. Transcripts identified at higher levels at cold temperature in the *in vitro* and *in vivo* studies by SSH libraries and/or microarray analysis included 4-hydroxyphenyl pyruvate dioxygenase, cytochrome P450, dolichyl-diphosphooligosaccharide-protein glycosyltransferase, hemopexin, nucleoside diphosphate kinase, tryptophan 2,3-dioxygenase, 14-kDa apolipoprotein, adenosylhomocysteinase, betaine-homocysteine methyltransferase, ALD, GDH, and type II AFP. The identification of these transcripts by both the *in vitro* and *in vivo* experimental approaches provides strong support for their importance during both the immediate temperature transition from warm to cold, and for sustained maintenance of altered metabolic pathways. In addition to these transcripts, this hepatocyte model was successful in identifying novel upregulated transcripts in response to an immediate low temperature. As discussed below, these transcripts include PDK2 which may play a key regulatory role in glyceroneogenesis, a transcript potentially encoding glycerol-3-phosphatase which is a yet-to-be characterized enzyme in any vertebrate species, and G6Pase and GS which suggest increased glucose and glutamine synthesis, respectively.

2.5.4 QPCR studies suggest key regulatory genes

The QPCR studies conducted herein were focused on transcripts that encode type II AFP or proteins potentially involved in glycerol accumulation, freeze prevention

strategies that are important for the survival of smelt in sub-zero temperatures. Since QPCR studies measure changes in gene expression at the transcript level, these changes do not necessarily translate through to metabolic flux, per se. Therefore, statements regarding metabolic rate must be interpreted with caution although the end product of an altered metabolism (i.e. glycerol production) is unequivocal. A schematic representation of glycerol synthesis pathway-related transcript levels in glycerol accumulating cultured smelt hepatocytes measured herein is provided in Fig. 2.7.

2.5.4.1 Transcripts whose products are involved in carbohydrate metabolism

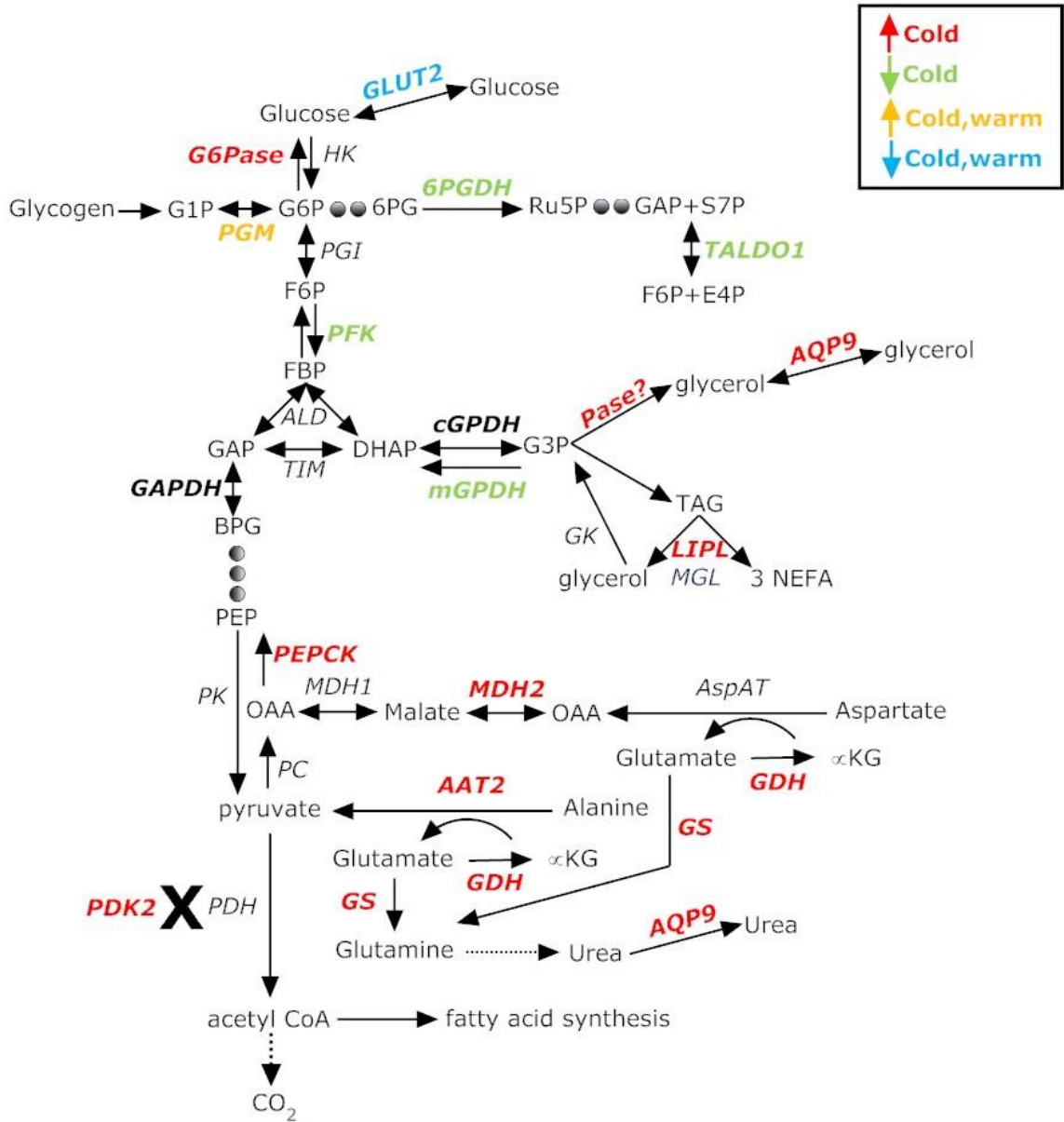
In both warm and cold cells, there were significant decreases, likely related to cell culture, in GLUT2 transcript levels at all three incubation times compared to pre-incubation. Decreased GLUT2 transcript levels may have impaired glucose transport out of and into the cells, even in the presence of the exogenous glucose supplement. When glucose levels are low, liver glycogen stores are catabolized by the glycogen phosphorylase complex to generate glucose-1-phosphate, which is then converted to glucose-6-phosphate (G6P) by PGM (Fig. 2.7). PGM transcript levels were higher in cells incubated at both cold and warm temperatures compared to pre-incubation. This response would be consistent with glycogen degradation as has been previously shown for cells incubated in the absence of glucose (7).

Cells incubated at cold temperature, at least transiently, had significantly higher levels of the glucose synthesis transcript G6Pase than pre-incubation and marginally higher ($p=0.08$) levels than warm cells at 24 h, which could result in increased glucose levels. Smelt subjected to a controlled decrease in water temperature exhibited a small but significant increase in liver glucose as temperature reached 0°C (10). Considered

Figure 2.7. A schematic representation of glycerol synthesis pathway-related transcript levels in glycerol accumulating cultured smelt hepatocytes. The proposed pathway for glycerol synthesis in smelt liver is via a branch point in glycolysis and gluconeogenesis. Genes encoding proteins involved in the conversion of L-amino acids to glyceroneogenic precursors, triglyceride metabolism and the non-glyceroneogenic fates of G6P (glucose synthesis or pentose phosphate pathway) are also included. Gene name abbreviations are in italics and those whose transcripts were analyzed by QPCR are in bold italics.

Transcripts expressed at higher levels in cold cells compared to pre-incubation or in cold compared to warm cells are coloured red; those expressed at lower levels in cold compared to warm cells are coloured green; those not significantly differentially expressed in cold cells compared to pre-incubation or in cold compared to warm cells are shown in black; PFK which was expressed at higher levels in cold cells compared to pre-incubation but at lower levels in cold compared to warm cells is coloured orange; GLUT2 which was expressed at lower levels in both cold and warm cells compared to pre-incubation is coloured blue. Gene name abbreviations are: **GLUT2**, glucose transporter 2; **PGM**, phosphoglucomutase; **G6Pase**, glucose-6-phosphatase; **6PGDH**, 6-phosphogluconate dehydrogenase; **TALDO1**, transaldolase; HK, hexokinase; PGI, phosphoglucoisomerase; **PFK**, phosphofructokinase; ALD, aldolase; TIM, triose isomerase; **GAPDH**, glyceraldehyde-3-phosphate dehydrogenase; PK, pyruvate kinase; PDH, pyruvate dehydrogenase; **PDK2**, pyruvate dehydrogenase kinase; PC, pyruvate carboxylase; **PEPCK**, phosphoenolpyruvate carboxykinase; **MDH2**, mitochondrial malate dehydrogenase; MDH1, cytosolic malate dehydrogenase; AspAT, aspartate aminotransferase; **AAT2**, alanine aminotransferase; **GS**, glutamine synthetase; **GDH**,

glutamate dehydrogenase; **LIPL**, lipoprotein lipase; **MGL**, monoacylglycerol lipase; **cGPDH**, cytosolic glycerol-3-phosphate dehydrogenase; **mGPDH**, mitochondrial glycerol-3-phosphate dehydrogenase; **GK**, glycerol kinase; **AQP9**, aquaglyceroporin 9. Metabolite abbreviations are: **G1P**, glucose-1-phosphate; **G6P**, glucose-6-phosphate; **F6P**, fructose-6-phosphate; **FBP**, fructose-1,6-bisphosphate; **GAP**, glyceraldehyde-3-phosphate; **DHAP**, dihydroxyacetone phosphate; **BPG**, 1,3-bisphosphoglycerate; **PEP**, phosphoenolpyruvate; **OAA**, oxaloacetate; α **KG**, alpha-ketoglutarate; **6PG**, 6-phosphogluconate; **Ru5P**, ribulose-5-phosphate; **S7P**, sedoheptulose-7-phosphate; **E4P**, erythrose-4-phosphate; **G3P**, glycerol-3-phosphate; **TAG**, triglyceride; **NEFA**, non-esterified free fatty acid. Dots represent pathway intermediates that are not shown.



together, these data suggest that increases in glucose in association with elevated G6Pase transcript levels may be a component of the cold temperature defense mechanism in smelt, just as increases in glucose in association with elevated G6Pase enzyme activity are part of the defense strategy in freeze-tolerant frogs (9, 41).

In cold cells, there were no significant differences in levels of pentose phosphate shunt transcripts (6PGDH, TALDO1) at any time point compared to pre-incubation. Levels of these transcripts were significantly lower in cold than warm cells suggesting a lower requirement for the products of the pentose phosphate shunt (e.g. NADPH, 5-carbon carbohydrates, etc.) at low temperature.

In cold cells, transcript levels of PFK, a key regulatory enzyme in glycolysis, were significantly lower in cold than warm cells at all three incubation times and in cold cells did not change during incubation. This finding reveals that increased expression of PFK is not a requirement for the initial increase in glycerol production.

Perhaps the most novel and compelling finding relates to PDK2, an inhibitor of PDH. PDK2 transcript levels were significantly higher in cold than warm cells at all three incubation times (20-fold higher at 72 h) and about 3-fold significantly higher at all three incubation times than pre-incubation. An inhibition of PDH would serve to inhibit the lower portion of glycolysis and thereby channel any glucose-derived DHAP towards glycerol. In addition, PDH inhibition would serve to channel any pyruvate produced from amino acids towards glyceroneogenesis.

2.5.4.2 Transcripts whose products are involved in amino acid metabolism

Studies with labeled amino acids have demonstrated that alanine and glutamate

can serve as precursors for glycerol (29, 44) in smelt living at cold temperatures. Activities of AAT2 and aspartate aminotransferase increase over the fall-winter transition in smelt liver (19), as do PEPCK transcript (20) and activity (19) levels. In cold cells, transcript levels of PEPCK, MDH2, AAT2, GDH and GS were significantly higher at 24 h compared to pre-incubation. Furthermore, in cold compared to warm cells, AAT2 and GS transcript levels were significantly higher at all time points. Higher levels of gluconeogenic transcripts are consistent with the provision of amino acid-derived metabolites for glyceroneogenesis. The immediate response of the *in vitro* cell preparation is therefore similar to the longer term response of whole smelt during the fall winter transition when water temperatures decline. The critical and novel aspect of this data set is that an entire suite of associated genes follows the same pattern, suggestive of a common control mechanism (e.g. transcription factor, microRNA).

The potential importance of glutamine synthesis in the cold response of smelt liver has not previously been recognized. Increased glutamine levels play a role in cold tolerance in other species as increased levels of this amino acid were observed in crustaceans (15), insects (13) and worms (35) upon cold exposure. Anchordoguy et al. (2) suggested that amino acids that contain positively charged amine groups in their side chain (e.g. glutamine) minimize membrane disruption by interacting directly with negatively charged phospholipids. Glutamine levels have yet-to-be measured in cold challenged smelt tissues.

2.5.4.3 *Transcripts whose products are involved in lipid metabolism*

There were no significant differences in levels of lipid metabolism-related transcripts in cold cells compared to pre-incubation except ACSL4 which was 4-fold

significantly higher at 72 h. This increase may reflect the role that ACSL4 plays in blocking apoptosis by lowering the cellular level of free arachidonic acid (36).

LIPL transcript levels were significantly higher at all time points in cold compared to warm cells. As LIPL catalyzes the rate limiting step in the hydrolysis of triglyceride to generate non-esterified fatty acids and 2-monoacylglycerol, maintaining high levels of this transcript may be important in glycerol management and/or in supplying fatty acids as a metabolic fuel. This finding, coupled with the observation of lower levels of pentose phosphate shunt transcripts (provide NADPH for triglyceride synthesis) at all time points in cold compared to warm cells, implies that triglyceride breakdown is higher than synthesis with low temperature and thus triglyceride could at least be a transient source of glycerol.

2.5.4.4 Transcripts whose products are involved in glycerol metabolism and diffusion

In smelt, cGPDH is deemed to play an important role in glyceroneogenesis. cGPDH enzyme activities are much higher in smelt liver than in non-glycerol accumulating fish [e.g. capelin (*Mallotus villosus*) and Atlantic salmon (*Salmo salar*)] (32, 40). At the whole animal level, there are significant increases in cGPDH transcript levels (20, 32) and activities (10, 19) associated with sharp increases in plasma glycerol. However, in the current study, in cold cells, there were no significant differences in cGPDH transcript levels at any time point compared to pre-incubation or compared to warm cells throughout the incubation. An explanation for the difference between the isolated cell experiments conducted herein and the *in vivo* studies is that there are two mechanisms for the control of metabolic flux through GPDH. Over a time course of weeks, shown by whole animal studies, there is an increase in gene expression leading to

an increase in enzyme activity. Over the shorter term GPDH enzyme activity could be regulated post-translationally. Clow et al. (7) showed 1.4-fold significantly higher cGPDH activities in cold than warm smelt hepatocytes. The specific activity of rabbit cGPDH increases upon complex formation with ALD (3). Smelt ALD transcript levels increase sharply with the onset of glycerol production (31). Post-translational interactions of ALD with cGPDH could account for the increase in smelt cGPDH activity. Regardless of how cGPDH may be controlled post-translationally, the important new insight is that increased transcript levels were not essential for the initial low temperature-induced increase in glycerol production by smelt hepatocytes.

mGPDH is an irreversible bi-substrate enzyme located on the outer face of the inner mitochondrial membrane (17). mGPDH reduces FAD to FADH₂ within the matrix, thus yielding reducing equivalents for ATP production via the glycerol-3-phosphate shuttle (Fig. 2.7). The cloning and characterization of the smelt mGPDH cDNA, the analysis of the tissue distribution of mGPDH transcripts and the measurement of mGPDH transcript levels in cold and warm hepatocytes described herein, and studies performed by my co-authors [seasonal pattern of mGPDH transcript levels and enzyme activities (32)] are the first analyses of this gene in glycerol metabolism. Smelt mGPDH contains all the structural motifs characteristic of mGPDH sequences from rat, mouse and human (5, 18, 23). The ubiquitous tissue distribution is also consistent with that reported in rat (24) and mouse (18). Although a decrease in mGPDH levels during glycerol synthesis could result in decreased rates of conversion of G3P to DHAP and thus favor the conversion of G3P to glycerol, there were no significant differences in mGPDH transcript levels at any time point in cold cells compared to pre-incubation. This is consistent with liver mGPDH

transcript levels analysed throughout a seasonal study (encompassing the glycerol production and termination phases) in which no significant variation was noted at any specific time point throughout the season. However, the seasonal study indicated that in liver, mGPDH transcript levels tended to be higher and enzyme activities were significantly higher during glycerol decline than other phases. As such, when glycerol is no longer required for freeze prevention, mGPDH may be important in channeling it, via 3-carbon intermediates, into the gluconeogenic pathway for rebuilding liver glycogen pools (32). In cultured hepatocytes, mGPDH transcript levels were significantly lower in cold than warm cells at all three incubation times. The mGPDH transcript expression pattern in cold and warm cells is consistent with that of PFK. Higher PFK transcript levels in warm cells would suggest increased flux through glycolysis and in the generation of cytosolic NADH. As such, higher mGPDH transcript levels in warm cells may be associated an increased need for the transport of reducing equivalents across the mitochondrial membrane via the glycerol-3-phosphate shuttle.

AQP9 is a water channel protein permeated by both water and glycerol and is highly expressed in mammalian liver (6). In fasted mammals, glycerol formed from the breakdown of triglyceride in adipose tissue is released into the blood via AQP7 and enters the liver via AQP9. In the opposite direction, AQP9 provides an exit route for urea (6). In cold cells, compared to pre-incubation, AQP9 transcript levels responded similarly to that of transcripts encoding amino acid catabolism-related proteins (e.g. AAT2, GDH). The deamination of amino acids generates the toxic byproduct ammonia which is detoxified by the production of urea. Urea levels in livers of smelt following a seasonal cycle of seawater temperatures show a profile similar to glycerol (39). In cold cells, the

increase in AQP9 transcript levels at 24 h compared to pre-incubation may reflect its role in the release of urea generated from the synthesis of gluconeogenic precursors for glycerol production.

2.5.4.5 Transcript encoding a phosphatase-like protein

A phosphatase-like transcript in the forward SSH library had top BLASTx hits against phosphoglycolate phosphatase and pyridoxal (pyridoxine, vitamin B6) phosphatase. Although its function has yet-to-be characterized in smelt, there are three potential roles for this phosphatase in glycerol production. Foremost, G3P must be dephosphorylated to generate glycerol and this uncharacterized phosphatase might catalyze this reaction. Driedzic et al. (10) reported that glycerol accumulation in smelt plasma was associated with changes in metabolites in liver leading to increases in the mass action ratio across the reaction catalyzed by glycerol-3-phosphatase. However, the sequence of the phosphatase that catalyzes this reaction had yet-to-be identified in smelt. Secondly, this phosphatase could take 2-phosphoglycolate (2-PG) as a substrate. 2-PG acts as an inhibitor of human triose phosphate isomerase (TIM) (22) and could also regulate smelt TIM activity. Thirdly, pyridoxal phosphate is a coenzyme derived from vitamin B₆ utilized by aminotransferases such as AAT2. This phosphatase could indirectly regulate transamination of glyceroneogenic amino acids. In cold cells, transcript levels of this phosphatase were significantly higher than pre-incubation at 24 h, and were significantly higher than warm cells at all three incubation times. Regardless of its function, its transcript expression profile suggests it plays an important role in cold adaptation.

2.5.4.6 Transcript encoding an antifreeze protein

In the SSH studies, type II AFP was the most abundant transcript in the forward library and was also present in the reverse library. QPCR studies showed that in cold cells, type II AFP transcript levels were not significantly different than pre-incubation at all three incubation times. However, they were significantly higher (1.8-fold) in cold than warm cells at 72 h. Type II AFP transcripts were present at high levels in cold and warm cells as evidenced by lower C_T values (~12) compared to the other target genes in the QPCR analyses (~25). Although type II AFP transcript levels were only 1.8-fold higher in cold than warm cells at 72 h, since this transcript was present such high levels this small difference could account for its abundance in the forward library. Although SSH libraries enrich for transcripts that are differentially expressed in the tester and driver mRNA samples, the subtracted sample may still contain cDNAs corresponding to transcripts common to both. The high abundance of type II AFP transcripts in both cold and warm cells likely explains its presence in the reverse library. Constant type II AFP transcript levels in cold cells at all three incubation times compared to pre-incubation can be explained by evidence of its upregulation based upon winter photoperiod and not temperature-related cues (19). Since hepatocytes were isolated from the livers of warm smelt from between late November to mid December, the increase in type II AFP transcript levels had most likely already occurred.

2.5.5 Perspectives and significance

Liver was isolated from smelt living at a high enough temperature that glycerol was not accumulating. Hepatocytes were prepared and incubated at cold (glycerol accumulating) and warm temperatures. SSH and microarray analyses were used to

identify, and QPCR analyses to validate, transcripts differentially expressed between cold and warm cells. QPCR studies focused on transcripts potentially involved in the type II AFP or glycerol accumulation antifreeze strategies. These analyses confirmed at the cellular level that increases in type II AFP transcript levels were not significantly influenced by temperature. Similarly, increased glycerol production by isolated hepatocytes was not associated with increased transcript levels of PFK or cGPDH. Regulation of cGPDH, a key locus in glycerol synthesis, is more likely by post-translational modification over a short time course of hours. In contrast, a number of transcripts (MDH2, AAT2, GDH, PEPCK, and AQP9) associated with mobilization of amino acids to fuel glycerol accumulation were all transiently higher during the early stage of the temperature transition. The similarity in the expression pattern of this suite of genes suggests a common regulatory mechanism (e.g. transcription factor, microRNA). Unexpected in this area of metabolism were the potential roles of GS in the synthesis of glutamine and AQP9 in the release of urea. A further novel and important finding was the 20-fold higher transcript levels of PDK2, an inhibitor of PDH, in cold compared to warm cells. Potent inhibition of PDH would serve to direct pyruvate and oxaloacetate derived from amino acids to glycerol as opposed to oxidation via the citric acid cycle. This study also revealed higher transcript levels, in cold cells, of a phosphatase that is potentially glycerol-3-phosphatase, an enzyme that has yet-to-be characterized in any vertebrate species.

2.6 REFERENCES

1. **Agre P, King LS, Yasui M, Guggino WB, Ottersen OP, Fujiyoshi Y, Engel A, Nielsen S.** Aquaporin water channels--from atomic structure to clinical medicine. *J Physiol* 542: 3-16, 2002.
2. **Anchordoguy T, Carpenter JF, Loomis SH, Crowe JH.** Mechanisms of interaction of amino acids with phospholipid bilayers during freezing. *Biochim Biophys Acta* 946: 299-306, 1988.
3. **Batke J, Asbóth G, Lakatos S, Schmitt B, Cohen R.** Substrate-induced dissociation of glycerol-3-phosphate dehydrogenase and its complex formation with fructose biphosphate aldolase. *Eur J Biochem* 107: 389-394, 1980.
4. **Brazma A, Hingamp P, Quackenbush J, Sherlock G, Spellman P, Stoeckert C, Aach J, Ansorge W, Ball CA, Causton HC, Gaasterland T, Glenisson P, Holstege FC, Kim IF, Markowitz V, Matese JC, Parkinson H, Robinson A, Sarkans U, Schulze-Kremer S, Stewart J, Taylor R, Vilo J, Vingron M.** Minimum information about a microarray experiment (MIAME)-toward standards for microarray data. *Nat Genet* 29: 365-371, 2001.

5. **Brown LJ, MacDonald MJ, Lehn DA, Moran SM.** Sequence of rat mitochondrial glycerol-3-phosphate dehydrogenase cDNA. Evidence for EF-hand calcium-binding domains. *J Biol Chem* 269: 14363-14366, 1994.

6. **Carbrey JM, Gorelick-Feldman DA, Kozono D, Praetorius J, Nielsen S, Agre P.** Aquaglyceroporin AQP9: solute permeation and metabolic control of expression in liver. *Proc Natl Acad Sci U S A* 100: 2945-2950, 2003.

7. **Clow KA, Ewart KV, Driedzic WR.** Low temperature directly activates the initial glycerol antifreeze response in isolated rainbow smelt (*Osmerus mordax*) liver cells. *Am J Physiol Regul Integr Comp Physiol* 295: R961-R970, 2008.

8. **Diatchenko L, Lau YFC, Campbell AP, Chenchik A, Moqadam F, Huang B, Lukyanov S, Lukyanov K, Gurskaya N, Sverdlov ED, Siebert PD.** Suppression subtractive hybridization: A method for generating differentially regulated or tissue-specific cDNA probes and libraries. *Proc Natl Acad Sci USA* 93: 6025-6030, 1996.

9. **Dziewulska-Szwajkowska D, Lozincka-Gabska M, Dzugaj A.** *Rana esculenta* L. liver Fru-P2ase and G-6-Pase activity and Fru-2,6-P2 concentration after acclimation at 5 and 25°C. *Comp Biochem Physiol A* 118A: 745-751, 1997.

10. **Driedzic WR, Clow KA, Short CE, Ewart KV.** Glycerol production in rainbow smelt (*Osmerus mordax*) may be triggered by low temperature alone and is associated with the activation of glycerol-3-phosphate dehydrogenase and glycerol-3-phosphatase. *J Exp Biol* 209: 1016-1023, 2006.
11. **Driedzic WR, Ewart KV.** Control of glycerol production by rainbow smelt (*Osmerus mordax*) to provide freeze resistance and allow foraging at low winter temperatures. *Comp Biochem Physiol B* 139: 347-357, 2004.
12. **Edgar R, Domrachev M, Lash AE.** Gene Expression Omnibus: NCBI gene expression and hybridization array data repository. *Nucleic Acids Res* 30: 207-210, 2002.
13. **Fields PG, Fleurat-Lessard F, Lavenseau L, Febvay G, Peypelut L, Bonnot G.** The effect of cold acclimation and deacclimation on cold tolerance, trehalose and free amino acid levels in *Sitophilus granarius* and *Cryptolestes ferrugineus* (Coleoptera). *J Insect Physiol* 44: 955-965, 1998.
14. **Graham LA, Loughheed SC, Ewart KV, Davies PL.** Lateral transfer of a lectin-like antifreeze protein gene in fishes. *PLoS One* 3:e2616, 2008.
15. **Issartel J, Renault D, Voituron Y, Bouchereau A, Vernon P, Hervant F.** Metabolic responses to cold in subterranean crustaceans. *J Exp Biol* 208: 2923-2929, 2005.

16. **Joost HG, Thorens B.** The extended GLUT-family of sugar/polyol transport facilitators: nomenclature, sequence characteristics, and potential function of its novel members (review). *Mol Membr Biol* 18: 247-256, 2001.
17. **Klingenberg M.** Localization of the glycerol-phosphate dehydrogenase in the outer phase of the mitochondrial inner membrane. *Eur J Biochem* 13: 247-252, 1970.
18. **Koza RA, Kozak UC, Brown LJ, Leiter EH, MacDonald MJ, Kozak LP.** Sequence and tissue-dependent RNA expression of mouse FAD-linked glycerol-3 phosphate dehydrogenase. *Arch Biochem Biophys* 336: 97-104, 1996.
19. **Lewis JM, Ewart KV, Driedzic WR.** Freeze resistance in rainbow smelt (*Osmerus mordax*): seasonal pattern of glycerol and antifreeze protein levels and liver enzyme activity associated with glycerol production. *Physiol Biochem Zool* 77: 415-422, 2004.
20. **Liebscher RS, Richards RC, Lewis JM, Short CE, Muise DM, Driedzic WR, Ewart KV.** Seasonal freeze resistance of rainbow smelt (*Osmerus mordax*) is generated by differential expression of glycerol-3-phosphate dehydrogenase, phosphoenolpyruvate carboxykinase, and antifreeze protein genes. *Physiol Biochem Zool* 79: 411-423, 2006.
21. **Livak KJ, Schmittgen TD.** Analysis of relative gene expression data using real-time quantitative PCR and the $2^{-\Delta\Delta CT}$ method. *Methods* 25: 402-408, 2001.

22. **Mande SC, Mainfroid V, Kalk KH, Goraj K, Martial JA, Hol WG.** Crystal structure of recombinant human triosephosphate isomerase at 2.8 Å resolution. Triosephosphate isomerase-related human genetic disorders and comparison with the trypanosomal enzyme. *Protein Sci* 3: 810-821, 1994.
23. **Matsutani A, Takeuchi Y, Ishihara H, Kuwano S, Oka Y.** Molecular cloning of human mitochondrial glycerophosphate dehydrogenase gene: genomic structure, chromosomal localization, and existence of a pseudogene. *Biochem Biophys Res Commun* 223: 481-486, 1996.
24. **Müller S, Seitz HJ.** Cloning of a cDNA for the FAD-linked glycerol-3-phosphate dehydrogenase from rat liver and its regulation by thyroid hormones. *Proc Natl Acad Sci USA* 91: 10581-10585, 1994.
25. **Nolan T, Hands RE, Bustin SA.** Quantification of mRNA using real-time RT-PCR. *Nat Protoc* 1: 1559-1582, 2006.
26. **Pfaffl MW.** A new mathematical model for relative quantification in real-time RT-PCR. *Nucleic Acids Res* 29: e45, 2001.
27. **Raymond JA.** Glycerol is a colligative antifreeze in some northern fishes. *J Exp Zool* 262: 347-352, 1992.

28. **Raymond JA.** Glycerol synthesis in the rainbow smelt *Osmerus mordax*. *J Exp Biol* 198: 2569-2573, 1995.
29. **Raymond JA, Driedzic WR.** Amino acids are a source of glycerol in cold acclimatized rainbow smelt. *Comp Biochem Phys* 118B: 387-393, 1997.
30. **Richards RC, Achenbach JC, Short CE, Kimball J, Reith ME, Driedzic WR, Ewart KV.** Seasonal expressed sequence tags of rainbow smelt (*Osmerus mordax*) revealed by subtractive hybridization and the identification of two genes up-regulated during winter. *Gene* 424: 56-62, 2008.
31. **Richards RC, Short CE, Driedzic WR, Ewart KV.** Seasonal changes in hepatic gene expression reveal modulation of multiple processes in rainbow smelt (*Osmerus mordax*). *Mar Biotechnol* 12: 650-663, 2010.
32. **Robinson J, Hall JR, Charman M, Ewart KV, Driedzic WR.** Molecular analysis, tissue profiles and seasonal patterns of cytosolic and mitochondrial GPDH in freeze resistant rainbow smelt (*Osmerus mordax*). *Physiol Biochem Zool* 84: 363-376, 2011.
33. **Saitou N, Nei M.** The neighbor-joining method: a new method for reconstructing phylogenetic trees. *Mol Biol Evol* 4: 406-425, 1987.

34. **Scott WB, Scott MG.** Atlantic fishes of Canada. *Can Bull Fish Aquat Sci* 219: 761, 1988.
35. **Slotsbo S, Maraldo K, Malmendal A, Nielsen NC, Holmstrup M.** Freeze tolerance and accumulation of cryoprotectants in the enchytraeid *Enchytraeus albidus* (Oligochaeta) from Greenland and Europe. *Cryobiology* 57: 286-291, 2008.
36. **Sung YK, Hwang SY, Park MK, Bae HI, Kim WH, Kim JC, Kim M.** Fatty acid CoA ligase 4 is overexpressed in human hepatocellular carcinoma. *Cancer Sci* 94: 421-424, 2003.
37. **Tamura K, Dudley J, Nei M, Kumar S.** MEGA4: Molecular Evolutionary Genetics Analysis (MEGA) software version 4.0. *Mol Biol Evol* 24: 1596-1599, 2007.
38. **Thompson JD, Higgins DG, Gibson TJ.** CLUSTAL W: improving the sensitivity of progressive multiple sequence alignment through sequence weighting, position-specific gap penalties and weight matrix choice. *Nucleic Acids Res* 22: 4673-4680, 1994.
39. **Treberg JR, Wilson CE, Richards RC, Ewart KV, Driedzic WR.** The freeze-avoidance response of smelt *Osmerus mordax*: initiation and subsequent suppression of glycerol, trimethylamine oxide and urea accumulation. *J Exp Biol* 205: 1419-1427, 2002.

40. **Treberg JR, Lewis JM, Driedzic WR.** Comparison of liver enzymes in osmerid fishes: key differences between a glycerol accumulating species, rainbow smelt (*Osmerus mordax*), and a species that does not accumulate glycerol, capelin (*Mallotus villosus*). *Comp Biochem Physiol A Mol Integr Physiol* 132: 433-438, 2002.
41. **Voituron Y, Joly P, Eugène M, Barré H.** Freezing tolerance of the European water frogs: the good, the bad, and the ugly. *Am J Physiol Regul Integr Comp Physiol* 288: R1563-R1570, 2005.
42. **von Schalburg KR, Rise ML, Cooper GA, Brown GD, Gibbs AR, Nelson CC, Davidson WS, Koop BF.** Fish and chips: various methodologies demonstrate utility of a 16,006-gene salmonid microarray. *BMC Genomics* 6: 126-144, 2005.
43. **von Schalburg KR, Leong J, Cooper GA, Robb A, Beetz-Sargent MR, Lieph R, Holt RA, Moore R, Ewart KV, Driedzic WR, ten Hallers BF, Zhu B, de Jong PJ, Davidson WS, Koop BF.** Rainbow smelt (*Osmerus mordax*) genomic library and EST resources. *Mar Biotechnol (NY)* 10: 487-491, 2008.
44. **Walter JA, Ewart KV, Short CE, Burton IW, Driedzic WR.** Accelerated hepatic glycerol synthesis in rainbow smelt (*Osmerus mordax*) is fuelled directly by glucose and alanine: a ¹H and ¹³C nuclear magnetic resonance study. *J Exp Zool A* 305: 480-488, 2006.

CHAPTER 3

Expression analysis of glycerol synthesis-related liver transcripts in rainbow smelt (*Osmerus mordax*) exposed to a controlled decrease in temperature

Preface

The research described in Chapter 3 was published in *Physiological and Biochemical Zoology*:

Hall JR, Short CE, Rise ML, Driedzic WR. Expression analysis of glycerol synthesis-related liver transcripts in rainbow smelt (*Osmerus mordax*) exposed to a controlled decrease in temperature. *Physiol Biochem Zool* 85: 74-84, 2012.

3.1 ABSTRACT

Rainbow smelt (*Osmerus mordax*) accumulate high glycerol levels to avoid freezing at sub-zero temperatures. Glyceroneogenesis is activated by low temperature and occurs in liver via a branch in glycolysis and gluconeogenesis. In the current study, carbohydrate and liver transcript levels of 21 genes potentially associated with glycerol production were assessed during a controlled warm to cold transition. Smelt were held at 8°C (warm smelt; non-glycerol accumulating) or subjected to a controlled decrease in water temperature from 8°C to 0°C (cold smelt; glycerol accumulating) and sampled at the end of the temperature decrease and one month later. In cold compared to warm smelt, liver glycogen levels were lower; PGM transcript levels were higher. Plasma glycerol levels were higher and in cold smelt increased over time; in cold smelt liver, PFK and PDK2 transcript levels increased over time. These findings imply that glycerol production is being fuelled by glycogen degradation, and inhibition of pyruvate oxidation serves to channel metabolic flux towards glycerol as opposed to complete glycolysis. In cold compared to warm smelt, plasma glucose and liver G6Pase transcript levels were higher. In cold compared to warm smelt liver, LIPL transcript levels were higher suggesting enhanced lipid breakdown to fuel energy metabolism. In cold compared to warm smelt liver, GS transcript levels were higher, perhaps to store nitrogen for biosynthesis (e.g. nucleotides and amino acids) in spring.

3.2 INTRODUCTION

Rainbow smelt (*Osmerus mordax*, Mitchill, 1814), hereafter referred to as smelt, is an anadromous teleost that survives winter water temperatures that can reach as low as -1.8°C before freezing. One mechanism that smelt use to avoid freezing is to accumulate high levels of glycerol (24). Glycerol prevents freezing colligatively by increasing osmotic pressure and also serves as a chemical chaperone (11). High glycerol production is low temperature dependent. For example, in smelt from Newfoundland maintained in aquaria throughout a seasonal study (encompassing the glycerol production and termination phases), fish held at high (8°C) temperature do not accumulate glycerol; however, in fish following ambient seawater temperatures, glycerol begins to slowly increase in plasma in November, when water temperature decreases to $3\text{--}5^{\circ}\text{C}$, with levels reaching in excess of 200 mM by February/March when water temperatures (-1°C) are at their lowest (20, 29). In smelt, glycerol is lost across the skin and gills at a rate of about 10% per day in the winter months (4, 25) and must therefore be constantly synthesized to maintain the levels required for its role in freeze prevention. In cold adapted smelt, glycerol production occurs primarily in liver (20, 21) and is fuelled by dietary carbohydrate and protein (6, 26, 27, 37). In smelt held at high (8°C) temperature, rapid glycerol production may be triggered artificially with a sharp decrease in water temperature even in winter months and under these conditions is supported initially by liver glycogen (5, 6). The induction of glycerol production through an imposed decrease in water temperature is a useful model in which to assess temperature-specific control mechanisms.

A number of liver transcript levels [cytosolic glycerol-3-phosphate dehydrogenase (cGPDH), fructose 1,6-bisphosphate aldolase B (ALD), phosphoenolpyruvate carboxykinase (PEPCK)] and enzyme activity levels [cGPDH, PEPCK, alanine aminotransferase (AAT)] increase in association with the seasonal glycerol increase (20, 21, 28, 29). These transcripts and enzymes are all related to carbohydrate and amino acid metabolism. Gene expression has also been assessed in an isolated cell model (14, i.e. Chapter 2) that has revealed increased transcript levels including a suite of genes associated with amino acid metabolism, a phosphatase and pyruvate dehydrogenase kinase (PDK2). The current study complements the above experimental approaches. Smelt were subjected to a rapid decrease in water temperature to assess if increases in transcript levels of specific genes occur *in vivo* as a direct consequence of reduced temperature. Transcripts (described below) were selected based on findings with the isolated cell preparation (14, i.e. Chapter 2).

The proposed pathway for glycerol synthesis (glyceroneogenesis) from glycogen/glucose or amino acids is via a branch point in glycolysis and gluconeogenesis in which dihydroxyacetone phosphate (DHAP) is converted to glycerol-3-phosphate (G3P) by cGPDH. G3P may then be dephosphorylated to glycerol directly via a phosphatase not yet characterized in any vertebrate species (5) or be incorporated into triglyceride which can thereafter be hydrolyzed to glycerol and free fatty acids. Glycerol generated in liver could enter the plasma via an aquaglyceroporin (AQP), most likely a mammalian-like AQP9. A detailed schematic of this proposed pathway was presented previously (Fig. 1.1).

Transcript levels of a number of genes associated with this area of metabolism were assessed in isolated smelt hepatocytes subjected to a decrease in temperature (14, i.e. Chapter 2). These included cGPDH, mitochondrial glycerol-3-phosphate dehydrogenase (mGPDH), a phosphatase that is potentially glycerol-3-phosphatase, AQP9, lipoprotein lipase (LIPL), acyl-CoA synthetase 4 (ACSL4), solute carrier family 27 member 6 (SLC27A6) and phospholipase A₂ (PLA₂). As glycogen/glucose are established precursors of glycerol, a number of carbohydrate metabolism related transcripts were also studied. These included phosphoglucomutase (PGM, necessary for glycogen breakdown), the glucose synthesis transcript glucose-6-phosphatase (G6Pase), the hepatic glucose transporter (GLUT2), the pentose phosphate shunt transcripts 6-phosphogluconate dehydrogenase (6PGDH) and transaldolase (TALDO1), the glycolytic transcript phosphofructokinase (PFK), the glycolytic/gluconeogenic transcript glyceraldehyde dehydrogenase (GAPDH) and the pyruvate dehydrogenase (PDH) inhibitor, PDK2. In isolated cells, PDK2 was highly upregulated within hours in response to a cold challenge. Transcript levels of genes associated with glyceroneogenesis from amino acids were also measured. These included AAT2, glutamate dehydrogenase (GDH), mitochondrial malate dehydrogenase (MDH2), PEPCK and glutamine synthetase (GS). This suite of genes was identified as being cold upregulated in isolated smelt hepatocytes (14, i.e. Chapter 2).

In the current study, levels of plasma glycerol and glucose, liver glycogen, and liver transcripts of the same 21 glycerol synthesis pathway-related genes that had been previously studied *in vitro* (14, i.e. Chapter 2) were assessed using the whole animal temperature “step-down” model of cold-induced glycerol production (6). Smelt were

either held at 8°C (warm smelt) or subjected to a controlled decrease (from 8°C to ~ 0°C) in water temperature and then held at low temperature (cold smelt). Smelt from both groups were sampled at the end of the temperature decrease and after the cold smelt had been held at 0 to -0.5°C for approximately one month. The current study determines if the expression profiles of these transcripts hold true *in vivo*, where livers are exposed to a physiological extracellular environment. Also, since transcript levels were measured after the controlled decrease in water temperature and approximately one month later, an indication of their importance in both the early stages of glycerol synthesis and in the longer term maintenance of glycerol levels is elucidated.

3.3 MATERIALS AND METHODS

3.3.1 Animals

Smelt were collected by seine netting from Mount Arlington Heights, Placentia Bay, Newfoundland in late October 2006. They were transported to the Ocean Sciences Centre, Memorial University of Newfoundland where they were held in a 3000 L indoor free-flowing seawater tank maintained at 8°C to 11°C (primary heated holding tank). In both the holding and experimental tanks, flow-through seawater was run through a polyvinyl chloride (PVC) pipe containing BioBalls (Pentair Aquatic Eco-Systems, Vancouver, BC) to remove excess gas prior to entering the tank. Sweetwater air diffusers (Pentair Aquatic Eco-Systems) were placed in the tank to gradually diffuse air into the seawater. Dissolved oxygen levels were measured daily using the OxyGuard Handy Polaris (Pentair Aquatic Eco-Systems) and were maintained at approximately 100%. All smelt were subjected to a natural photoperiod with fluorescent lights set by an outdoor photocell, and were fed a diet of chopped herring twice a week to satiation. Experiments were carried out in accordance with an Animal Utilization Protocol (09-03-WD) issued by Memorial University of Newfoundland's Animal Care Committee.

3.3.2 Temperature step-down experiment

On January 3, 2007, smelt (a mixture of males and females) were removed from the primary tank and were divided into two heated (7°C -8°C) (warm smelt) and two to-be-cooled (cold smelt) 350 l indoor free-flowing seawater experimental tanks. In the cold tanks, the water temperature was gradually decreased from 8°C to 0°C (to 5°C on January 12; to 3°C on January 15; to 1°C on January 17; and to 0°C on January 22) and held at between 0°C to -0.5°C for the duration of the experiment. Smelt were sampled from each

temperature on Jan. 25, 2007 [warm (females n=5, males n=3); cold (females n=5, males n=3)] and on Feb. 22, 2007 [warm (females n=5, males n=3); cold (females n=4, males n=3)] between 9 am and 12 noon.

3.3.3 Tissue sampling

Body mass and length were measured and condition factor $[(\text{body mass} / \text{length}^3) \times 100]$ was calculated. There were no significant differences in body mass and length amongst the various populations. Overall mass and length [mean \pm standard error (SE)] were 76 ± 3.4 g and 21 ± 0.3 cm, respectively. Smelt maintained at warm temperature had a significantly higher condition factor in February (0.92 ± 0.04) compared to the other groups that ranged from 0.75 to 0.79. Thus, other than smelt maintained at warm temperature and sampled in February being somewhat heavier relative to body length, the holding condition had no impact on these basic morphometrics.

Blood was drawn via the caudal vessel and centrifuged at $10,000 \times g$ for 10 min at 4°C . The plasma was collected, snap-frozen in liquid nitrogen and stored at -80°C until biochemical analyses were performed. Fish were killed by a sharp blow to the head, the livers were removed quickly and weighed, and hepatic somatic index (HSI) $[(\text{liver mass} / \text{body mass}) \times 100]$ was calculated. There were no significant differences amongst the populations in HSI that had an overall value (mean \pm SE) of $2.02 \pm .09$. For glycogen analysis, a sub-sample of the liver was snap-frozen in liquid nitrogen and stored at -80°C . For total RNA isolation, a sub-sample of the liver was immediately homogenized in TRIzol Reagent (Invitrogen, Burlington, ON) using a motorized Kontes RNase-Free Pellet Pestle Grinder (Kimble Chase, Vineland, NJ) and was stored at -80°C for a maximum of two weeks before completion of the RNA extraction.

3.3.4 Biochemical analyses

Plasma glycerol and glucose, and liver glycogen were measured as previously described (3, 6).

3.3.5 RNA preparation and QPCR

Total RNA was extracted using TRIzol Reagent (Invitrogen) with the manufacturer's instructions. RNA integrity was verified by 1% agarose gel electrophoresis and purity was assessed by A260/280 (cut-off ratio > 2) and A260/230 (cut-off ratio > 1.8) UV NanoDrop spectrophotometry. TRIzol extracted total RNA (45 µg) was then treated with 6.8 Kunitz units DNaseI (RNase-Free DNase Set, QIAGEN, Mississauga, ON) at room temperature for 10 min and column-purified using the RNeasy MinElute Cleanup Kit (QIAGEN) with the manufacturer's instructions. cDNA was synthesized from DNaseI-treated, column-purified total RNA (1 µg) in a 20 µl reaction using random primers (250 ng) (Invitrogen) and M-MLV reverse transcriptase (200 U) (Invitrogen) with the manufacturer's first strand buffer (1X final concentration) and DTT (10 mM final concentration) at 37°C for 50 min.

Transcript levels of 21 glycerol synthesis pathway-related genes were quantified by QPCR as described previously (14, i.e. Chapter 2). Typically, cDNA (corresponding to 10 ng of input total RNA) was used as template in the QPCR reactions. Input cDNA was increased (corresponding to 25 ng of input total RNA) for seven of the target genes (GLUT2, PGM, PFK, PEPCK, ACSL4, mGPDH and AQP9) due to higher fluorescence threshold cycle (C_T) values observed during the primer quality tests, and decreased (corresponding to 0.4 ng of input total RNA) for the endogenous control (18S ribosomal

RNA) due to lower C_T values. With these amounts of input cDNA, C_T values ranged from 20 to 30 for the target genes and were ~16 for the endogenous control.

3.3.6 Statistical analysis

Data were analyzed with non-parametric statistics as there were some cases where values did not exhibit homogeneity of variance, even after log transformation. The Mann-Whitney test was used to assess if there were any biologically relevant significant differences in parameters in the cold or warm smelt in February compared to January (i.e. a temporal response) and in the cold compared to warm smelt at both sampling dates (i.e. a temperature response). This simple analysis was selected to provide a focus on the biologically relevant comparisons of time and temperature. In all cases, $p < 0.05$ was considered to be statistically significant. All data are expressed as mean \pm SE.

3.4 RESULTS

3.4.1 Biochemical analyses

Plasma glycerol levels, in smelt held at cold temperature, were 3.3-fold significantly higher in February compared to January (Fig. 3.1A). Plasma glycerol, plasma glucose or liver glycogen did not significantly change between the January and February sampling dates for any of the other comparisons at a given temperature (Fig. 3.1A, 3.1B, 3.1C).

Plasma glycerol and glucose were significantly higher in cold compared to warm smelt at both sampling time points. The largest change was at the February sampling date where plasma glycerol at $234 \pm 33 \mu\text{mol/ml}$ was 20-fold higher in cold compared to warm smelt. Liver glycogen was 2.3-fold significantly lower in cold compared to warm smelt at the January time point and tended to be lower (4.4-fold, $p = 0.13$) in cold compared to warm smelt at the February time point.

These data show that the controlled decrease in water temperature led to the start of glycerol accumulation that continued over the next month and was fuelled in part by glycogen reserves. The balance of the study assesses if the response is associated with increased transcript levels of genes related to the metabolic pathways leading to glycerol.

3.4.2 QPCR analysis of glycerol synthesis-related liver transcript levels

3.4.2.1 Temporal-related changes

In smelt held at high temperature, there were only two transcripts [6PGDH (2.3-fold; Fig. 3.2D) and PFK (2.4-fold; Fig. 3.2F)] with significant increases in levels in February compared to January. In smelt held at low temperature, there were four transcripts with significant increases in levels in February compared to January [PFK

Figure 3.1. (A) plasma glycerol ($\mu\text{mol/ml}$) (B) plasma glucose ($\mu\text{mol/ml}$) and (C) liver glycogen ($\mu\text{mol/g}$) in smelt held at high or low temperature. Smelt were either held at 8°C [warm smelt; January ($n=8$) and February ($n=8$)] or subjected to a controlled temperature decrease from 8°C to 0°C [cold smelt; January ($n=8$)] and then held at 0°C to -0.5°C for approximately one month [cold smelt; February ($n=7$)]. Values are presented as mean \pm SE. Different letters indicate a significant difference in levels between the sampling time points for a given temperature. Asterisks denote significant differences in levels between cold and warm smelt at that sampling time point. In all cases, $p < 0.05$ was considered to be statistically significant.

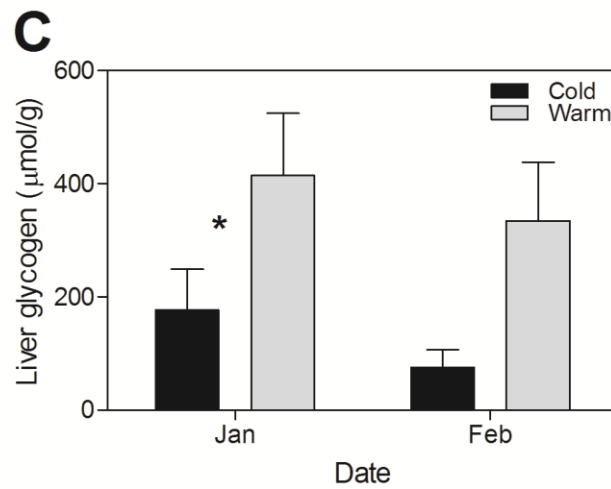
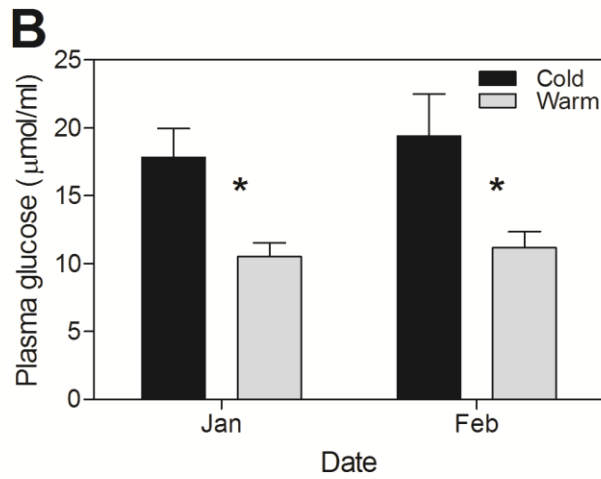
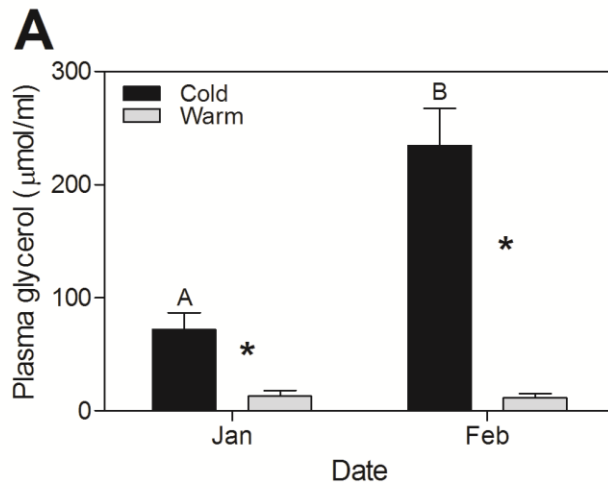
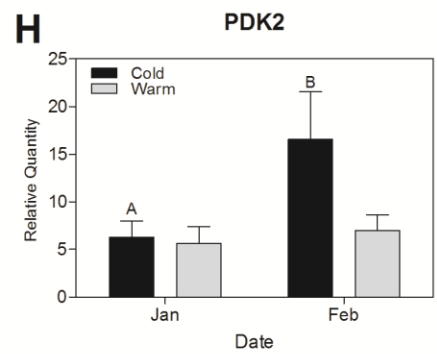
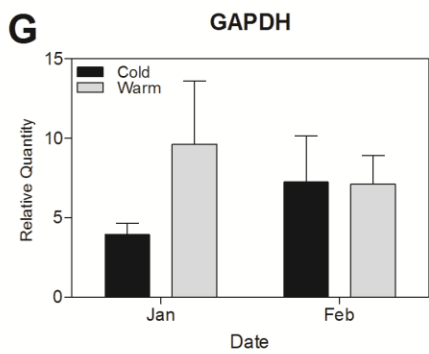
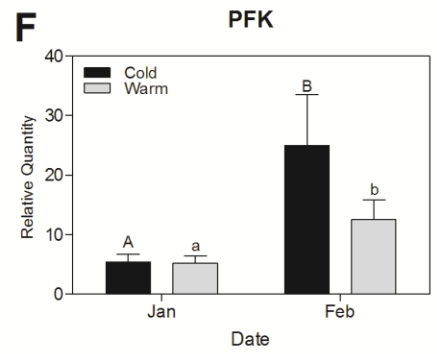
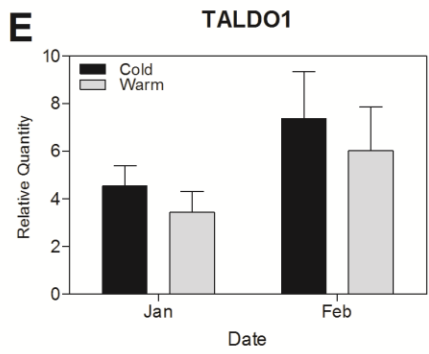
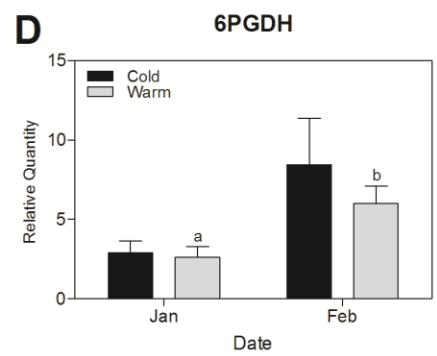
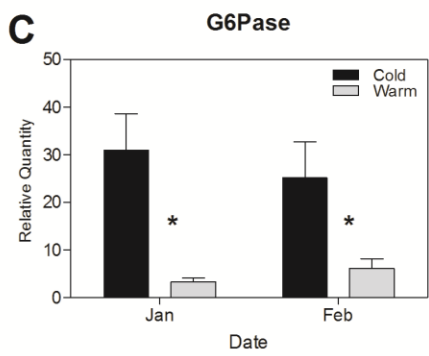
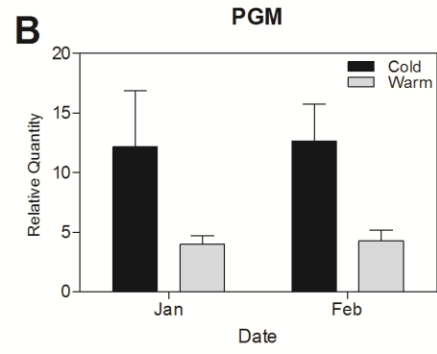
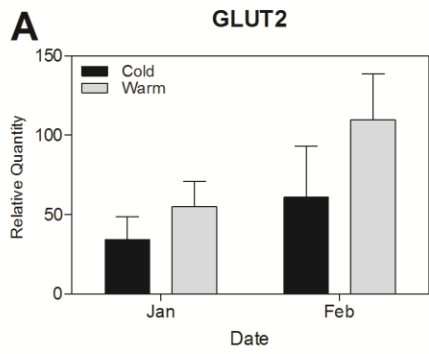
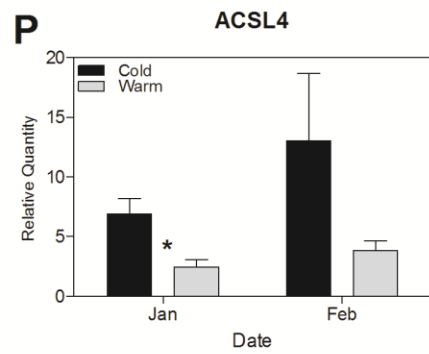
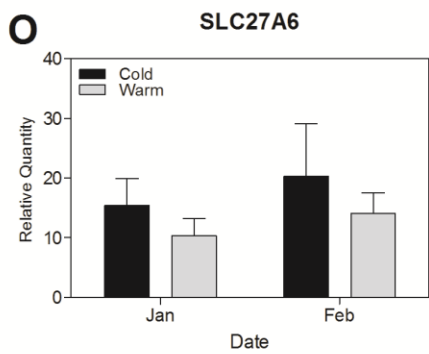
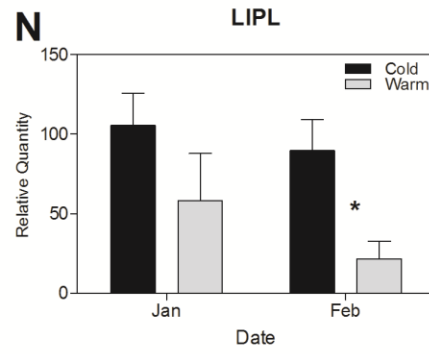
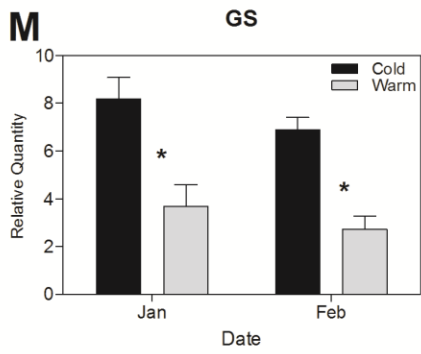
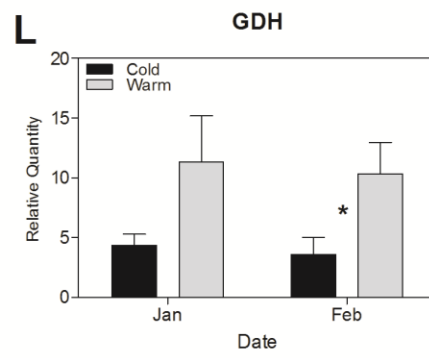
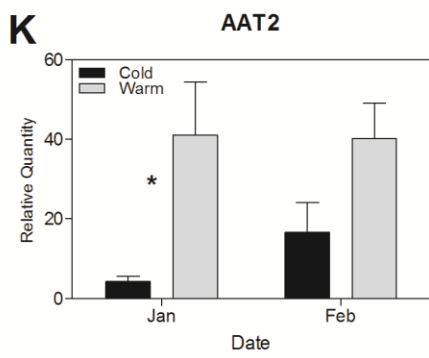
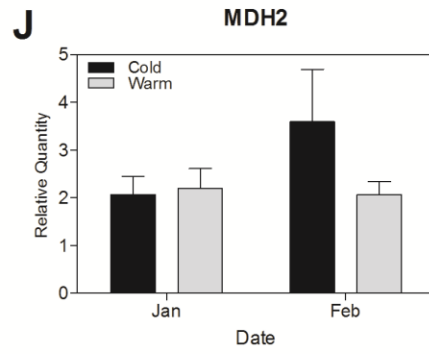
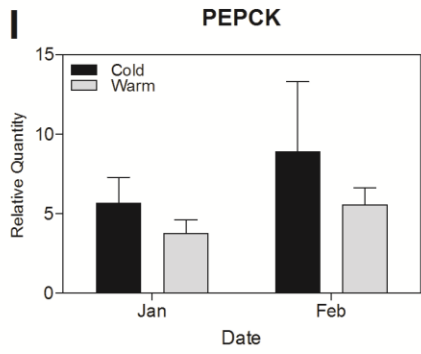
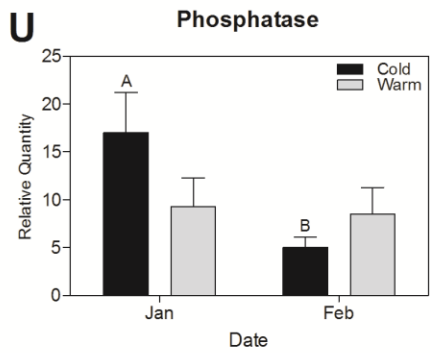
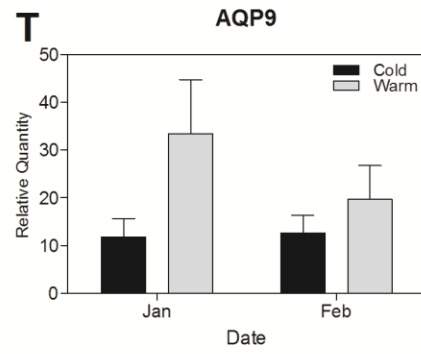
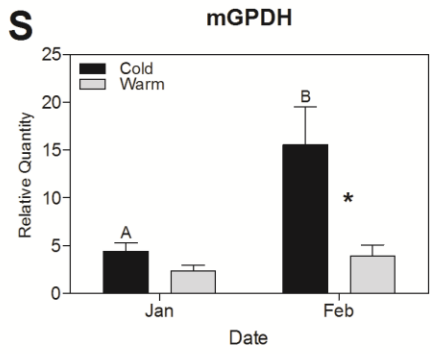
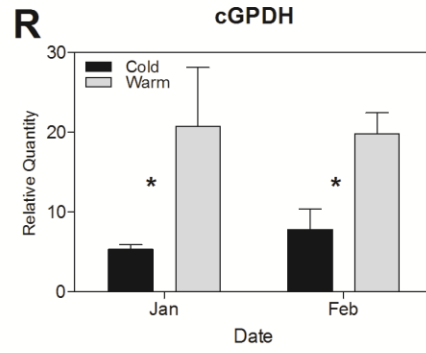
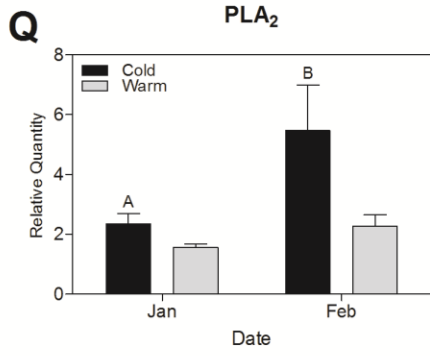


Figure 3.2. QPCR analyses of glycerol metabolism-related liver transcripts in smelt held at high or low temperature. Smelt were either held at 8°C [warm smelt; January (n=8) and February (n=8)] or subjected to a controlled temperature decrease from 8°C to 0°C [cold smelt; January (n=8)] and then held at 0°C to -0.5°C for approximately one month [cold smelt; February (n=7)]. Gene expression data are presented as mean \pm SE relative quantity (RQ) values (i.e. values for the gene of interest were normalized to 18S ribosomal RNA and were calibrated to the individual with the lowest normalized expression of that given gene). Letters (upper case for cold smelt livers and lower case for warm smelt livers) indicate that there were significant differences in transcript levels over time. Asterisks denote significant differences in transcript levels between cold and warm smelt livers at that sampling time point. In all cases, $p < 0.05$ was considered to be statistically significant.







(4.6-fold; Fig. 3.2F), PDK2 (2.6-fold; Fig. 3.2H), PLA₂ (2.3-fold; Fig. 3.2Q) and mGPDH (3.5-fold; Fig. 3.2S)] and one with a significant decrease in levels in February compared to January [phosphatase (3.4-fold; Fig. 3.2U)].

3.4.2.2 Temperature-induced changes

Transcript levels of a number of genes monitored in this study were not significantly influenced by temperature. The following highlights transcripts that changed significantly in level in livers of cold compared to warm smelt.

In contrast to expectation, cGPDH levels were 3.9-fold and 2.5-fold significantly lower in January and February, respectively, in cold compared to warm smelt (Fig. 3.2R); whereas, mGPDH levels were 3.9-fold significantly higher in February (Fig. 3.2S) in cold compared to warm smelt. Two lipid metabolism-related genes showed significantly higher transcript levels in cold compared to warm smelt; LIPL levels were 4.2-fold higher in February (Fig. 3.2N) and ACSL4 levels were 2.8-fold higher in January (Fig. 3.2P). PLA₂ levels tended to be higher (1.5-fold, $p = 0.13$ and 2.4-fold, $p = 0.06$) in January and February, respectively (Fig. 3.2Q), in cold compared to warm smelt.

Transcript levels of the carbohydrate metabolism gene G6Pase were 9.2-fold and 4-fold significantly higher in January and February, respectively (Fig. 3.2C) while PGM (Fig. 3.2B) ($p = 0.06$), PFK (Fig. 3.2F) ($p = 0.18$) and PDK2 (Fig. 3.2H) ($p = 0.11$) tended to be higher at the February time point in cold compared to warm smelt.

Three genes directly associated with amino acid metabolism showed changes in transcript expression as a function of temperature. AAT2 levels were 9.6-fold significantly lower in January and tended to be lower in February (2.4-fold, $p = 0.06$) (Fig. 3.2K) in cold compared to warm smelt. GDH levels were 2.9-fold significantly

lower in February (Fig. 3.2L) in cold compared to warm smelt. Conversely, GS levels were 2.2-fold and 2.5-fold significantly higher in January and February, respectively (Fig. 3.2M), in cold compared to warm smelt.

3.5 DISCUSSION

3.5.1 *Temperature step-down (in vivo) model of glycerol production*

The *in vivo* model of cold-induced glycerol production applied here is based on a direct low temperature-induced response. Two populations of smelt (non-glycerol accumulating and glycerol accumulating) were generated simply by controlling water temperature. After being held at 0°C for approximately one month, plasma glycerol levels had increased to levels that were 20-fold higher than warm smelt.

The main advantage of this model over studies tracking smelt over a natural time course is that non-temperature-related changes should be reduced. Animals sampled over a seasonal time frame are subject to multiple biotic and abiotic changes in addition to a decrease in water temperature. As such, it is impossible to state if the response of a specific transcript is mechanistically due to temperature decrease and/or some other factor. Transcripts involved in the proposed pathway for glycerol synthesis (14, i.e. Chapter 2) could change due to factors unrelated to and/or coincident with glycerol production (e.g. differences in metabolic rate, activity level, nutritional status, immune status, gonad production).

The current model system also differs from studies with isolated cells (14, i.e. Chapter 2). The power of the isolated cell approach is that the same population of hepatocytes can be subjected to different temperature challenges. The *in vitro* approach, though, has its limits in that the time period is restricted to days and the extracellular milieu is minimal; thus the cells lack the richness of a physiological environment including hormonal input.

There is, however, a limitation to the current experimental approach. In these experiments, all smelt were maintained at unnaturally high (i.e. non-glycerol producing) temperature until January, at which point fish were subjected to the controlled temperature decrease. Changes could have occurred in levels of transcripts required for glycerol production in fish maintained at elevated temperature between November and January in anticipation of glycerol synthesis or for coincident reasons. These transcripts would be missed in this analysis. Despite its limitations, the model currently employed is useful in complementing earlier work involving seasonal tracking and isolated cell preparations. Liver transcript levels of genes that are influenced *in vivo* by temperature alone as part of the enhanced glycerol production process are reported herein.

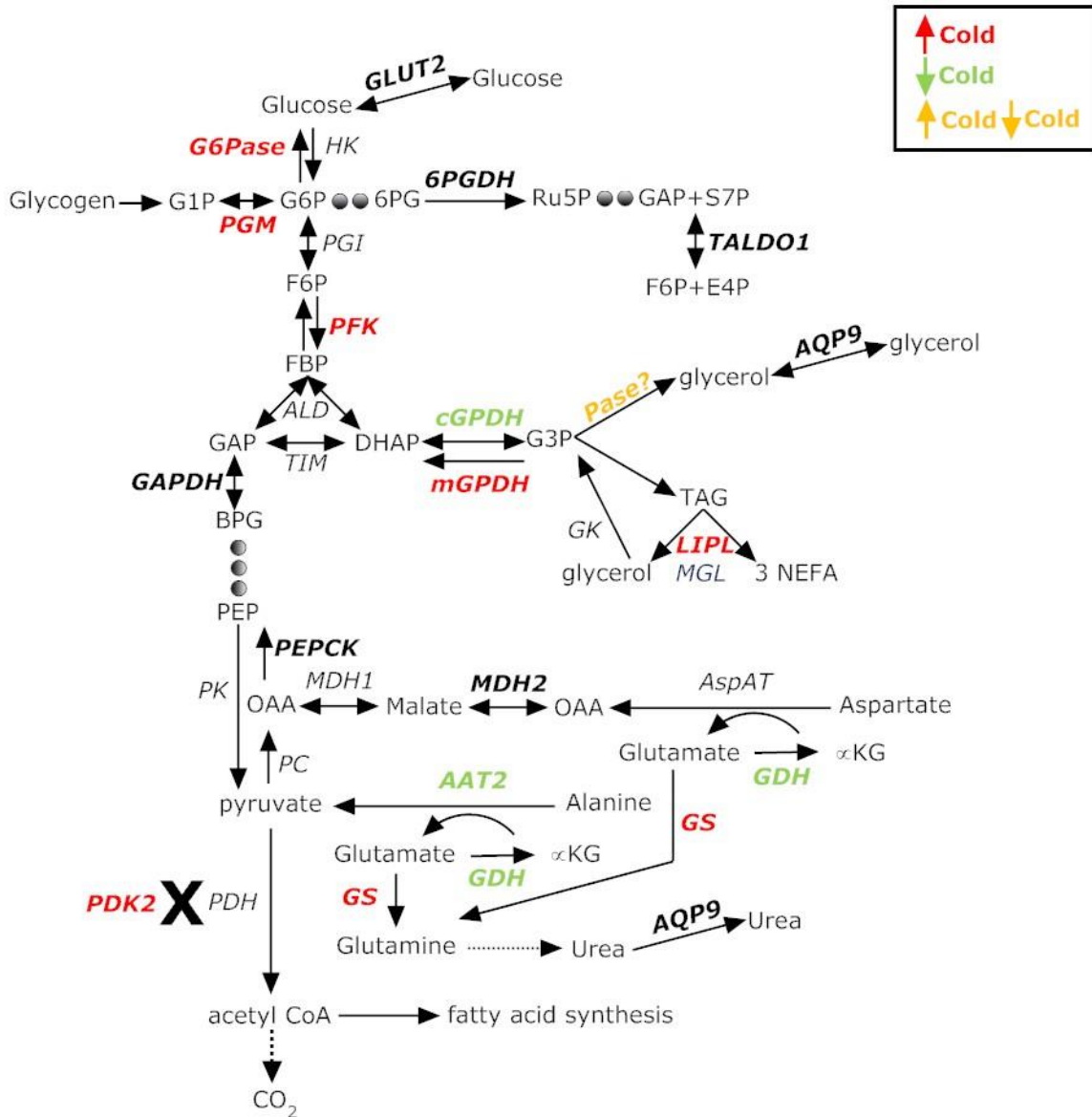
The following discussion focuses on transcripts that are potentially up- or downregulated by a decrease in temperature as one potential mechanism of enhancing glycerol production. Differential gene expression at the transcript level does not necessarily result in increased protein activity levels per se (9); the process of enhanced glycerol production will be under a number of levels of regulation including epigenetics (e.g. microRNAs), immediate enzyme control, post-translational modification (e.g. phosphorylation) and protein quantity (determined by ratio of synthesis to degradation). This study deals with only one aspect of this complex metabolic process. A schematic representation of glycerol synthesis pathway-related transcript levels in livers of glycerol accumulating smelt measured herein is provided in Fig. 3.3.

3.5.2 The branch point pathway to glycerol

In cold smelt livers, there were no significant differences in cGPDH transcript levels with respect to time and cGPDH transcript levels were significantly lower

Figure 3.3. A schematic representation of glycerol synthesis pathway-related transcript levels in liver of glycerol accumulating smelt. The proposed pathway for glycerol synthesis in smelt liver is via a branch point in glycolysis and gluconeogenesis. Genes encoding proteins involved in the conversion of L-amino acids to glyceroneogenic precursors, triglyceride metabolism and the non-glyceroneogenic fates of G6P (glucose synthesis or pentose phosphate pathway) are also included. Gene name abbreviations are in italics and those whose transcripts were analyzed by QPCR are in bold italics. Transcripts expressed at higher levels in cold smelt livers over time or compared to warm smelt livers are coloured red; those expressed at lower levels in cold compared to warm smelt livers are coloured green; those not significantly differentially expressed in cold smelt livers over time or compared to warm smelt livers are shown in black; the phosphatase which was expressed at lower levels in cold smelt livers over time is coloured orange. Gene name abbreviations are: **GLUT2**, glucose transporter 2; **PGM**, phosphoglucomutase; **G6Pase**, glucose-6-phosphatase; **6PGDH**, 6-phosphogluconate dehydrogenase; **TALDO1**, transaldolase; HK, hexokinase; PGI, phosphoglucoisomerase; **PFK**, phosphofructokinase; ALD, aldolase; TIM, triose isomerase; **GAPDH**, glyceraldehyde-3-phosphate dehydrogenase; PK, pyruvate kinase; PDH, pyruvate dehydrogenase; **PDK2**, pyruvate dehydrogenase kinase; PC, pyruvate carboxylase; **PEPCK**, phosphoenolpyruvate carboxykinase; **MDH2**, mitochondrial malate dehydrogenase; MDH1, cytosolic malate dehydrogenase; AspAT, aspartate aminotransferase; **AAT2**, alanine aminotransferase; **GS**, glutamine synthetase; **GDH**, glutamate dehydrogenase; **LIPL**, lipoprotein lipase; MGL, monoacylglycerol lipase; **cGPDH**, cytosolic glycerol-3-phosphate dehydrogenase; **mGPDH**, mitochondrial

glycerol-3-phosphate dehydrogenase; GK, glycerol kinase; **AQP9**, aquaglyceroporin 9. Metabolite abbreviations are: G1P, glucose-1-phosphate; G6P, glucose-6-phosphate; F6P, fructose-6-phosphate; FBP, fructose-1,6-bisphosphate; GAP, glyceraldehyde-3-phosphate; DHAP, dihydroxyacetone phosphate; BPG, 1,3-bisphosphoglycerate; PEP, phosphoenolpyruvate; OAA, oxaloacetate; α KG, alpha-ketoglutarate; 6PG, 6-phosphogluconate; Ru5P, ribulose-5-phosphate; S7P, sedoheptulose-7-phosphate; E4P, erythrose-4-phosphate; G3P, glycerol-3-phosphate; TAG, triglyceride; NEFA, non-esterified free fatty acid. Dots represent pathway intermediates that are not shown.



compared to warm smelt livers in both January and February. These findings are in contrast to smelt tracking a normal seasonal cycle where during the fall-to-winter transition there were significant increases in cGPDH transcript (21, 29) and activity (20) levels associated with a sharp increase in plasma glycerol levels. The different findings may be related to all smelt being held at high temperature prior to the temperature step-down in January. In smelt held at elevated temperature throughout a seasonal cycle, there was a gradual increase in cGPDH activity levels, possibly associated with sexual maturity; by mid-February cGPDH activity levels were actually higher in warm than cold smelt (20). With the current experimental design, cGPDH may have been activated with prolonged exposure to high temperature for reasons not associated with glycerol production per se, and when subsequently exposed to low temperature, transcript levels were sufficient to meet the demands for glycerol production. As well, increased glycerol production in isolated smelt liver cells over 72 h, was associated with an increase in activity of cGPDH (3) with no change in transcript levels (14, i.e. Chapter 2), suggesting other mechanisms of regulation. For example, protein-protein interaction of aldolase with cGPDH resulted in elevated specific activity of cGPDH in rabbit (2). Transcript levels of ALD increase on a seasonal basis such that values in February are about 25-fold higher than in October (28). A similar regulation could be occurring in the present study in smelt liver.

In cold smelt livers, mGPDH transcript levels increased significantly with respect to time and were significantly higher than warm smelt in February. Increased mGPDH expression is likely related to the transfer of the reducing equivalents of cytosolic NADH

to respiratory assemblies in the inner mitochondrial membrane via the G3P shuttle. This point is discussed below with respect to PFK.

Levels of the phosphatase-like (i.e. with significant BLASTx hits against phosphoglycolate phosphatase and pyridoxal phosphate phosphatase) transcript were significantly higher in cold smelt livers in January compared to February. This yet-to-be characterized transcript could potentially be glycerol-3-phosphatase, thereby dephosphorylating G3P directly to glycerol. In a similar temperature step-down experiment (5), crossover analysis of metabolite levels revealed an activation at the G3P to glycerol step.

3.5.3 Lipid metabolism

LIPL is a member of the lipase superfamily which, in mammals, also includes hepatic and pancreatic lipases (23). LIPL transcripts are expressed in adult rainbow trout (*Oncorhynchus mykiss*) (22) and smelt liver, and appear to perform the role of hepatic lipase in mammals. In cold compared to warm smelt livers, LIPL transcript levels were significantly higher in February. The ability to mobilize TAG stores in cold smelt livers could contribute to increased glycerol levels and provide an important energy source since glycolytic sources of energy are being expended for glyceroneogenesis. Consistent with this interpretation is elevated transcript levels of ACSL4 in cold smelt liver that could activate fatty acids to the CoA esters for entry into β -oxidation.

PLA₂ transcript levels were significantly higher in cold smelt livers with respect to time and were borderline significant with respect to temperature. Increased PLA₂ transcript levels with low temperature are likely related to the content of unsaturated fatty acids in membrane lipids as opposed to glycerol production. An inverse correlation

between ambient temperature and the content of unsaturated fatty acids in membrane lipids has been reported for a variety of poikilotherms (16). For instance, rainbow trout exposed to cold temperature undergo a remodeling of membrane lipid composition characterized by an increase in the quantity of polyunsaturated fatty acids and a reduction in the level of saturated fatty acids. In choline and ethanolamine phosphatides, the increase in the content of polyunsaturated fatty acids was confined to the 2-position, a reaction catalyzed by PLA₂ (15).

3.5.4 Glycogen and glucose metabolism

Liver glycogen levels were significantly lower in January and tended to be lower in February in cold compared to warm smelt. It has been previously noted that smelt liver glycogen is utilized in response to a rapid decrease in temperature (6), as well as, during the fall-to-winter transition (35). In accordance with glycogen utilization, liver PGM transcript levels tended to be significantly higher. The ability to mobilize liver glycogen stores is also an important feature of survival in freeze-tolerant frogs (34, 36) and worms (30) that synthesize glucose as a cryoprotectant, and in freeze-tolerant frogs that synthesize glycerol as a cryoprotectant (31).

Plasma glucose levels were significantly higher in cold compared to warm smelt, in both January and February. Consistent with a release of glucose from glycogen, liver G6Pase transcript levels were significantly higher in parallel. Freeze-tolerant frogs (36) and worms (30) mobilize glucose from hepatic stores as a non-anticipatory response to tissue freezing. Furthermore, frogs exposed to cold temperature (7) and to freezing (33) had increased liver G6Pase enzyme activities. In these species, which unlike smelt actually freeze, glucose provides cryoprotection by minimizing the percentage of body

water converted to extracellular ice (32). Increased glucose levels are an important feature of the smelt cold adaptation response, likely to provide additional colligative protection against freezing or perhaps to sustain rates of extrahepatic glucose uptake through an increased diffusion gradient.

PFK is considered to be a key regulatory site in glycolysis. PFK transcript levels were significantly higher in cold smelt livers in February compared to January. Increased PFK transcript levels would suggest increased flux through glycolysis with the production of glycerol and/or pyruvate. An increased glycolysis would result in the generation of cytosolic NADH and could be related to the elevated levels of mGPDH transcripts in cold smelt. In addition, PDK2 transcript levels, in cold smelt livers, were significantly higher in February compared to January. PDK2 is an inhibitor of PDH which would serve to decrease pyruvate oxidation. Pyruvate and amino acid-derived oxaloacetate would be channeled towards glycerol by PDH inhibition. Regardless of the details of the precise metabolic circuitry, the similar profile in PFK, mGPDH and PDK2 levels suggest a connection that may be an important feature of glyceroneogenesis, in cold smelt livers. PFK transcript levels were significantly higher in warm smelt livers in February compared to January, perhaps due to an increased energy demand related to spawning as discussed below.

There were no significant differences in 6PGDH and TALDO1 transcript levels in cold smelt livers with respect to time or temperature. This is in contrast to cold-exposed common carp (*Cyprinus carpio*) livers, in which a microarray-based transcript expression study suggested an activation of the pentose phosphate pathway (13). In warm smelt livers, 6PGDH transcript levels were significantly higher in February compared to

January. The pentose phosphate shunt generates NADPH to support the reductive biosynthesis of lipid; this increase in lipid synthesis may be associated with gonad production as smelt held at high temperature throughout a seasonal cycle underwent spawning earlier (in late February to early March) than those held in ambient water temperatures (20). The timing of this event coincided with the February sampling date.

3.5.5 Amino acid metabolism

There were no significant differences in cold smelt livers with respect to time or temperature in transcript levels of PEPCK and MDH2, two genes required for the mobilization of amino acids for either gluco- or glyceroneogenesis. Furthermore, in cold compared to warm smelt livers, transcript levels of AAT2 and GDH were generally lower in both January and February; however, in cold smelt livers, AAT2 transcript levels were borderline significantly higher ($p = 0.08$) in February than January. Glycerol is synthesized directly from both glucose and amino acids (37). The lower transcript levels reported here in liver of cold compared to warm smelt is surprising given that there are increased GDH transcript levels (28), as well as increased AAT and aspartate aminotransferase enzyme activities, in animals tracking seasonal changes (20). A possible explanation is that smelt maintained at high temperature with access to food have particularly high liver glycogen reserves (35) and when glycolytic sources are readily available, they appear to be the preferred substrate for glycerol synthesis rather than amino acids. The increase in AAT2 transcript levels in cold smelt livers over time may be to supplement glycolytic sources of glycerol so they do not become depleted with prolonged glycerol synthesis.

GS transcript levels were significantly higher in cold than warm smelt livers in both January and February suggesting elevated glutamine levels. Increased glutamine levels were observed in crustaceans (18), worms (30) and insects (10) upon cold exposure. Amino acids that contain positively charged amine groups in their side chain (e.g. glutamine) are thought to minimize membrane disruption by interacting directly with negatively charged phospholipids (1). An alternative explanation is that in cold smelt livers, GS may be upregulated as part of the general stress response and may serve to store nitrogen for biosynthesis (e.g. nucleotides and amino acids) in the spring. GS transcript levels were upregulated in liver of long-jaw mudsucker (*Gillichthys mirabilis*) exposed to hypoxia (12), GS activities and protein levels were upregulated in liver of freshwater Amazonian stingray (*Potamotrygon motoro*) exposed to brackish water (17), and GS transcript and protein levels were upregulated in liver of gulf toadfish (*Opsanus beta*) during confinement stress (19). Two glucocorticoid response elements were identified in the promoter region of the GS gene of gulf toadfish (8), consistent with the contention that an increase in glutamine is a general stress response.

3.5.6 Insights from in vivo compared to in vitro transcript expression levels

There were both substantive differences and important similarities between transcript expression patterns shown here for whole animals subjected to a decrease in temperature over a period of weeks and isolated cells maintained for up to 3 days. In isolated cells, GLUT2 transcript levels plummeted within 24 h (14, i.e. Chapter 2); in intact animals, GLUT2 transcript levels remained quite vigorous (current study). These data suggest that an extracellular signal is required to maintain GLUT2 transcript levels. In the context of glycerol metabolism, it appears that glucose uptake was limited in

isolated cells thus forcing these cells to an amino acid fuelled glycerol production as evidenced by the coordinated response of a suite of related transcripts (PEPCK, MDH2, AAT2, GDH). In contrast, at the whole animal level glucose appears to be more important in supporting glycerol production as based on an increase in PFK transcript levels and either no change or decreases in transcript levels of PEPCK, MDH2, AAT2, and GDH in response to cold temperature.

There were two important cold-responsive changes in transcript levels in common to both the *in vivo* and *in vitro* approaches. PDK2 and GS showed increased transcript levels in both models under a transition to lower temperature associated with an increase in glycerol production. This commonality reveals that these two transcripts are truly activated by a low temperature signal and play a role in the low temperature defense mechanism.

3.5.7 Conclusions

A working scenario for the mechanisms (at the level of transcript expression) involved in glycerol production based on studies in animals tracking seasonal changes, in animals subjected to an abrupt controlled decrease in water temperature, and in isolated cells has now been developed. In smelt living at low temperature, glycerol synthesis can be initiated from both glycolytic and gluconeogenic substrates (27, 37). The first stage in glycerol production during the fall-to-winter transition involves the mobilization of glycogen reserves (6, 35) and is associated with increases in expression of PGM (current study), cGPDH and ALD (21, 28). Elevated cGPDH protein/activity levels would serve to channel DHAP towards glycerol synthesis and increased protein/activity of ALD could serve to enhance the breakdown of fructose 1,6-bisphosphate and also increase the

activity of cGPDH through protein-protein association (2). PFK may be elevated thereafter to maintain flux at the top part of glycolysis at low temperature but activation at this locus does not appear to be a requirement of the initiation of glycerol production. As carbohydrate reserves become limiting, amino acids become increasingly important in supporting glycerol production and a suite of amino acid metabolism-related genes is activated (PEPCK, MDH2, AAT2, GDH). Associated with this is an increase in PDK2 that would inhibit the lower part of glycolysis at the PDH site, thereby ensuring that glyceroneogenesis out-competes glycolysis. Under these conditions lipid reserves may become more important as metabolic fuels to support the energy needs of the liver with LIPL and ASCL4 being activated. In parallel to the above, GS transcript expression is increased perhaps resulting in increased glutamine levels that may serve to protect protein integrity at low temperature, and/or to store nitrogen for biosynthesis (e.g. nucleotides, amino acids) in the spring.

3.6 REFERENCES

1. **Anchordoguy T, Carpenter JF, Loomis SH, Crowe JH.** Mechanisms of interaction of amino acids with phospholipid bilayers during freezing. *Biochim Biophys Acta* 946: 299-306, 1988.
2. **Batke J, Asbóth G, Lakatos S, Schmitt B, Cohen R.** Substrate-induced dissociation of glycerol-3-phosphate dehydrogenase and its complex formation with fructose bisphosphate aldolase. *Eur J Biochem* 107: 389-394, 1980.
3. **Clow KA, Ewart KV, Driedzic WR.** Low temperature directly activates the initial glycerol antifreeze response in isolated rainbow smelt (*Osmerus mordax*) liver cells. *Am J Physiol Regul Integr Comp Physiol* 295: R961-R970, 2008.
4. **Ditlecadet D, Short CE, Driedzic WR.** Glycerol loss to water exceeds glycerol catabolism via glycerol kinase in freeze-resistant rainbow smelt (*Osmerus mordax*). *Am J Physiol Regul Integr Comp Physiol* 300: R674-R684, 2011.
5. **Driedzic WR, Clow KA, Short CE, Ewart KV.** Glycerol production in rainbow smelt (*Osmerus mordax*) may be triggered by low temperature alone and is associated with the activation of glycerol-3-phosphate dehydrogenase and glycerol-3-phosphatase. *J Exp Biol* 209: 1016-1023, 2006.

6. **Driedzic WR, Short CE.** Relationship between food availability, glycerol and glycogen levels in low-temperature challenged rainbow smelt *Osmerus mordax*. *J Exp Biol* 210: 2866-2872, 2007.

7. **Dziewulska-Szwajkowska D, Lozinzka-Gabska M, Dzugaj A.** *Rana esculenta* L. liver Fru-P2ase and G-6-Pase activity and Fru-2,6-P2 concentration after acclimation at 5 and 25°C. *Comp Biochem Physiol A* 118A: 745-751, 1997.

8. **Esbaugh AJ, Walsh PJ.** Identification of two glucocorticoid response elements in the promoter region of the ubiquitous isoform of glutamine synthetase in gulf toadfish, *Opsanus beta*. *Am J Physiol Regul Integr Comp Physiol* 297: R1075-R1081, 2009.

9. **Feder ME, Walser JC.** The biological limitations of transcriptomics in elucidating stress and stress responses. *J Evol Biol* 18: 901-910, 2005.

10. **Fields PG, Fleurat-Lessard F, Lavenseau L, Febvay G, Peypelut L, Bonnot G.** The effect of cold acclimation and deacclimation on cold tolerance, trehalose and free amino acid levels in *Sitophilus granarius* and *Cryptolestes ferrugineus* (Coleoptera). *J Insect Physiol* 44: 955-965, 1998.

11. **Gong H, Croft K, Driedzic WR, Ewart, KV.** Chemical chaperoning action of glycerol on the antifreeze protein of rainbow smelt. *J Thermal Biology* 36: 78-83, 2011.

12. **Gracey AY, Troll JV, Somero GN.** Hypoxia-induced gene expression profiling in the euryoxic fish *Gillichthys mirabilis*. *Proc Natl Acad Sci U S A* 98: 1993-1998, 2001.
13. **Gracey AY, Fraser EJ, Li W, Fang Y, Taylor RR, Rogers J, Brass A, Cossins AR.** Coping with cold: An integrative, multitissue analysis of the transcriptome of a poikilothermic vertebrate. *Proc Natl Acad Sci U S A* 101: 16970-16975, 2004.
14. **Hall JR, Clow KA, Rise ML, Driedzic WR.** Identification and validation of differentially expressed transcripts in a hepatocyte model of cold-induced glycerol production in rainbow smelt (*Osmerus mordax*). *Am J Physiol Regul Integr Comp Physiol* 301: R995-R1010, 2011.
15. **Hazel JR.** Influence of thermal acclimation on membrane lipid composition of rainbow trout liver. *Am J Physiol* 236: R91-R101, 1979.
16. **Hazel JR, Prosser CL.** Molecular mechanisms of temperature compensation in poikilotherms. *Physiol Rev* 54: 620-677, 1974.
17. **Ip YK, Loong AM, Ching B, Tham GH, Wong WP, Chew SF.** The freshwater Amazonian stingray, *Potamotrygon motoro*, up-regulates glutamine synthetase activity and protein abundance, and accumulates glutamine when exposed to brackish (15 per thousand) water. *J Exp Biol* 212: 3828-3836, 2009.

18. **Issartel J, Renault D, Voituron Y, Bouchereau A, Vernon P, Hervant F.** Metabolic responses to cold in subterranean crustaceans. *J Exp Biol* 208: 2923-2929, 2005.
19. **Kong H, Kahatapitiya N, Kingsley K, Salo WL, Anderson PM, Wang YS, Walsh PJ.** Induction of carbamoyl phosphate synthetase III and glutamine synthetase mRNA during confinement stress in gulf toadfish (*Opsanus beta*). *J Exp Biol* 203: 311-320, 2000.
20. **Lewis JM, Ewart KV, Driedzic WR.** Freeze resistance in rainbow smelt (*Osmerus mordax*): seasonal pattern of glycerol and antifreeze protein levels and liver enzyme activity associated with glycerol production. *Physiol Biochem Zool* 77: 415-422, 2004.
21. **Liebscher RS, Richards RC, Lewis JM, Short CE, Muise DM, Driedzic WR, Ewart KV.** Seasonal freeze resistance of rainbow smelt (*Osmerus mordax*) is generated by differential expression of glycerol-3-phosphate dehydrogenase, phosphoenolpyruvate carboxykinase, and antifreeze protein genes. *Physiol Biochem Zool* 79: 411-423, 2006.
22. **Lindberg A, Olivecrona G.** Lipoprotein lipase from rainbow trout differs in several respects from the enzyme in mammals. *Gene* 292: 213-223, 2002.
23. **Mead JR, Irvine SA, Ramji DP.** Lipoprotein lipase: structure, function, regulation, and role in disease. *J Mol Med* 80: 753-769, 2002.

24. **Raymond JA.** Glycerol is a colligative antifreeze in some northern fishes. *J Exp Zool* 262: 347-352, 1992.
25. **Raymond JA.** Glycerol and water balance in a near-isosmotic teleost, winter-acclimated smelt. *Can J Zool* 71: 1849-1854, 1993.
26. **Raymond JA.** Glycerol synthesis in the rainbow smelt *Osmerus mordax*. *J Exp Biol* 198: 2569-2573, 1995.
27. **Raymond JA, Driedzic WR.** Amino acids are a source of glycerol in cold-acclimatized rainbow smelt. *Comp Biochem Phys* 118B: 387-393, 1997.
28. **Richards RC, Short CE, Driedzic WR, Ewart KV.** Seasonal changes in hepatic gene expression reveal modulation of multiple processes in rainbow smelt (*Osmerus mordax*). *Mar Biotechnol* 12: 650-663, 2010.
29. **Robinson J, Hall JR, Charman M, Ewart KV, Driedzic WR.** Molecular analysis, tissue profiles and seasonal patterns of cytosolic and mitochondrial GPDH in freeze resistant rainbow smelt (*Osmerus mordax*). *Physiol Biochem Zool* 84: 363-376, 2011.
30. **Slotsbo S, Maraldo K, Malmendal A, Nielsen NC, Holmstrup M.** Freeze tolerance and accumulation of cryoprotectants in the enchytraeid *Enchytraeus albidus* (Oligochaeta) from Greenland and Europe. *Cryobiology* 57: 286-291, 2008.

31. **Storey JM, Storey KB.** Adaptations of metabolism for freeze tolerance in the gray tree frog, *Hyla versicolor*. *Can. J. Zool* 63: 49-54, 1985.
32. **Storey KB.** Organic solutes in freezing tolerance. *Comp Biochem Physiol A Physiol* 117: 319-326, 1997.
33. **Storey KB, Storey JM.** Biochemical adaptation for freezing tolerance in the wood frog, *Rana sylvatica*. *J Comp Physiol* 155: 29-36, 1984.
34. **Swanson D, Graves BM, Koster KL.** Freezing tolerance/intolerance and cryoprotectant synthesis in terrestrially overwintering anurans in the great plains, USA. *J Comp Physiol [B]* 166: 110-119, 1996.
35. **Treberg JR, Wilson CE, Richards RC, Ewart KV, Driedzic WR.** The freeze-avoidance response of smelt *Osmerus mordax*: initiation and subsequent suppression of glycerol, trimethylamine oxide and urea accumulation. *J Exp Biol* 205: 1419-1427, 2002.
36. **Voituron Y, Joly P, Eugène M, Barré H.** Freezing tolerance of the European water frogs: the good, the bad, and the ugly. *Am J Physiol Regul Integr Comp Physiol* 288: R1563-R1570, 2005.

37. **Walter JA, Ewart KV, Short CE, Burton IW, Driedzic WR.** Accelerated hepatic glycerol synthesis in rainbow smelt (*Osmerus mordax*) is fuelled directly by glucose and alanine: a ^1H and ^{13}C nuclear magnetic resonance study. *J Exp Zool A* 305: 480-488, 2006.

CHAPTER 4

Cloning and characterization of aquaglyceroporin genes from rainbow smelt (*Osmerus mordax*) and transcript expression in response to cold temperature

Preface

The research described in Chapter 4 was published in *Comparative Biochemistry and Physiology - Part B: Biochemistry & Molecular Biology*:

Hall JR, Clow KA, Rise ML, Driedzic WR. Cloning and characterization of aquaglyceroporin genes from rainbow smelt (*Osmerus mordax*) and transcript expression in response to cold temperature. *Comp Biochem Physiol B Biochem Mol Biol* 187: 39-54, 2015.

4.1 ABSTRACT

Aquaglyceroporins (GLPs) are integral membrane proteins that facilitate passive movement of water, glycerol and urea across cellular membranes. In this study, GLP-encoding genes were characterized in rainbow smelt (*Osmerus mordax*), an anadromous teleost that accumulates high glycerol and modest urea levels in plasma and tissues as an adaptive cryoprotectant mechanism in sub-zero temperatures. The gene and promoter sequences for two AQP10b paralogues (AQP10ba, AQP10bb) that are 82% identical at the predicted amino acid level, and AQP9b are reported herein. AQP10bb and AQP9b have the 6 exon structure common to vertebrate GLPs. AQP10ba has 8 exons; there are two additional exons at the 5' end, and the promoter sequence is different from AQP10bb. Molecular phylogenetic analysis suggests that the AQP10b paralogues arose from a gene duplication event specific to the smelt lineage. Smelt GLP transcripts are ubiquitously expressed; however, AQP10ba transcripts were highest in posterior kidney, AQP10bb transcripts were highest in posterior kidney, intestine, pyloric caeca and brain, and AQP9b transcripts were highest in spleen, liver, red blood cells and posterior kidney. In cold-temperature challenge experiments, plasma glycerol and urea levels were significantly higher in cold- compared to warm-acclimated smelt; however, GLP transcript levels were generally either significantly lower or remained constant. The exception was significantly higher AQP10ba transcript levels in posterior kidney. High AQP10ba transcripts in smelt posterior kidney that increase significantly in response to cold temperature in congruence with plasma urea suggest that this gene duplicate may have evolved to allow the reabsorption of urea to concomitantly conserve nitrogen and prevent freezing.

4.2 INTRODUCTION

Rainbow smelt (*Osmerus mordax*, Mitchill, 1814), hereafter referred to as smelt, is an anadromous teleost that survives sub-zero winter water temperatures via the synthesis of type II antifreeze protein, and the accumulation of osmolytes, including glycerol (42), trimethylamine oxide (TMAO) and urea (44) in plasma and tissues. Glycerol level follows a seasonal pattern; for example, plasma values increase from 0.3 mM to levels typically in excess of 200 mM when water temperatures are at their lowest. Glycerol begins to accumulate when water temperature decreases to about 5°C (27, 48). Smelt held at high (8°C) temperature do not accumulate glycerol; however, rapid glycerol production may be triggered artificially with a sharp decrease in water temperature (7, 8, 14, i.e. Chapter 3).

Glycerol is lost across the skin and gills at a rate of about 10% per day in the winter months (6, 43) and must therefore be constantly synthesized to maintain the levels required for its role in freeze prevention. Synthesis primarily occurs in liver (27, 29, 48) directly from both glycolytic and gluconeogenic sources (59). Glycerol production during the fall-to-winter transition involves the mobilization of glycogen reserves (8; 14, i.e. Chapter 3; 55). As carbohydrate reserves become limiting, amino acids become increasingly important in supporting glycerol production. When glycerol synthesis is fuelled by the deamination of amino acids, the resultant ammonia must be excreted or detoxified by the production of urea. Smelt urea levels also follow a seasonal pattern similar to glycerol although levels in plasma increased from 3 mM to only 9 mM in response to cold temperature (55).

The movement of glycerol and urea across cellular membranes is of particular interest in smelt. Aquaporins (AQPs) are a superfamily of integral membrane channel proteins that facilitate passive yet rapid permeation of water molecules across cellular membranes (1, 22). Thirteen AQP subfamilies (AQP0-12) have been identified in mammals (22). The AQP multigene family has been further subdivided into four grades: the classical water-selective subgroup (AQP0, -1, and -4), the water and urea transporter (AQP8), the unorthodox subgroup (AQP11b and -12) and the aquaglyceroporin (GLP) subgroup (AQP3, -7, -9, and -10) (52). GLPs are permeable to glycerol, urea, and ammonia in addition to water (1, 30).

Structurally, functional AQP channels, consisting of a single polypeptide containing a water pore, are assembled in the membrane as tetramers. Each monomer contains six transmembrane α -helices with the amino and carboxyl termini in the cytoplasm, three extracellular loops (A, C, and E), and two intracellular loops (B and D). Loops B and E fold and extend intramembranous hemi-helices that contain a highly conserved Asn-Pro-Ala (NPA) constriction motif and are involved in the formation of the water pore. There are two signature amino acid sequences for GLPs compared to classical AQPs which expand the pore to accept larger molecules such as glycerol and urea. First, there are five (P1-5) amino acids that are conserved in GLPs compared to AQPs; of particular importance is the Asp (D) (P2) in the second NPA box. Second, close to the extracellular exit of the pore, there are four amino acids which form the aromatic residue/arginine (ar/R) constriction. In AQPs, these residues are conserved [Phe (F), His (H), Cys (C) and Arg (R)]; in GLPs, there is no H, and C is replaced by a second

aromatic residue making the ar/R region wider and more hydrophobic (4, 16, 17, 52). These features are depicted in selected piscine AQP10b sequences (Fig. 4.1).

AQP genes, including those encoding GLPs, have been identified in numerous fish species (4). Notably, the zebrafish (*Danio rerio*) genome encodes the largest number of functional vertebrate AQPs reported to date, with 18 putative members present as single copy genes or gene duplicates, or in the case of AQP8, as three copies. The GLP subgroup has 7 putative members (AQP3a, -3b, -7, -9a, -9b, -10a and -10b) (52). The full-length cDNA for smelt AQP9b has been cloned and characterized previously (13, i.e. Chapter 2; 14, i.e. Chapter 3).

The full-length cDNA sequences for two AQP10b-like genes (AQP10ba, AQP10bb), and the gene / promoter sequences for smelt AQP10ba, AQP10bb, and AQP9b are reported herein. Nomenclature was chosen to be consistent with that of the putative zebrafish GLPs (52). Glycerol and urea levels in plasma were measured using biochemical assays, and AQP10b transcript levels in posterior kidney (hereafter referred to as kidney) were measured using quantitative reverse transcription - polymerase chain reaction (QPCR) in two studies. In the first, smelt were either held at ~8°C (warm smelt) or subjected to a controlled decrease (from 8°C to ~0°C) in water temperature and then held at low temperature (cold smelt) (14, i.e. Chapter 3). In the second, smelt were either held at ~8°C (warm smelt) or allowed to follow ambient seawater temperature (ambient smelt) throughout a season (encompassing the glycerol production and termination phases) (48). In a third study, levels of the AQP10ba, AQP10bb, and AQP9b transcripts were measured using QPCR in ten tissues from both warm and cold smelt. This is the

Figure 4.1. Alignment of protein sequences for piscine AQP10b orthologues. Amino acids are displayed using the single letter code. Gaps in the amino acid sequences are indicated with a dash (-). Positions which have a single, fully conserved residue are indicated with an asterisk (*). Conservation among groups with strongly similar properties is indicated with a colon (:). Conservation among groups with weakly similar properties is indicated with a period (.) Non-conserved residues between smelt AQP10ba and AQP10bb are highlighted in black. The six predicted transmembrane α -helices (TMD1-6), and the three extracellular loops (A, C, and E) and two intracellular loops (B and D) are underlined. The two NPA motifs and the GLP-specific residues (P1-5) are highlighted in grey. The four GLP-specific residues that form the (ar/R) constriction are indicated with an arrow. Common names are indicated in Fig. 4.2.


```

: ** ** *****: . * . * : : : . **
A. fimbria VDVFKAGGGWWWVPIVAPCVGALLGTLIYELMVEVHHHP-----SPPELQTSQEAP 277
O. niloticus ADVFKAGSGWWWVPIVAPCVGALLGTLIYELMVEVHHPS-----EQSESQASCPEPT 277
S. aurata VDVFKAGGGWWWVPIVAPCVGALLGTLIYMLMIEVHHHP-----SLSELHTSCQEAT 276
O. dancena VDVFKAGGGWWWVPIVGPCAGALLGTLIYQLMVEVHHHP-----LPSECQASCEEAS 277
P. formosa DDVFRAGRGWWWVPLVAPCIGGLVGTIYELMVEVHHAS-----LSPEDQPSQEQET 277
T. obscurus AEVFTAGGGWWWVPIVAPCVGALLGTLIYELAIEVHHHP-----SAGELRTPSQGAP 277
O. mordax (a) GEVFSAGDGWWWVPLVATNIGALVGTIYELMIEVHHL-----EPGPSSEPPGLDMNA 293
O. mordax (b) GEVFSAGDGWWWVPLVATNIGALVGTIYELMIEVHHL-----EPGPSSEPPGLDMNA 278
O. mykiss DEVFKAGRGWWWVPLVATCAGALVGTIYELLEVHHHP-----EKGLISESSAQGQAT 278
A. mexicanus VEVFRAGGGWWWVPLVATCVGGLVGS LIYELVI AVHHHP-----VPDMTKEVNMDG 275
D. rerio DEVFRAGHGWWWVPIIVTCV GALLGSLLYELLIGVHHHPDSEAVDHEDPTAALQQTVEMEG 285
A. anguilla EQVFWAGGGWWWVPLVAPCVGALVGSVVYVLLIEAHHHP-----ELDLHLEKADQCQTV 278
A. japonica EQVFWAGGGWWWVPLVAPCVGALVGSVVYVLLIEAHHHP-----ELDLHLEKADQCQTV 278

```

P4, 5 TMD6

```

A. fimbria EGKAGLELEG-----VEPDCEKPTK----- 297
O. niloticus NDKMGVELEG-----VEADREKPT----- 296
S. aurata EEKAGVELEG-----VKPHCVKPKSTKM----- 298
O. dancena ESKMELEAEPH-----LKSQC----- 293
P. formosa EAKS-LELKG-----VEPSVGKSA----- 295
T. obscurus GAELELERDG-----KAQ----- 290
O. mordax (a) EGKHVVKLEGEFDLIYYPKELQSGTAM----- 320
O. mordax (b) EGKHV-----QSWRANQT----- 292
O. mykiss ESRQAR-----IKTEK----- 289
A. mexicanus VQEENSEKPKEI-----PTAWQQVAL----- 296
D. rerio AQSFDTIKENKK-----SGIFSITSADVG----- 309
A. anguilla DNKLALELEGVELDLNSPKGCPNEGQEGKKAASGKGEEG----- 317
A. japonica DNKLALELEGVELDLNSPKGCPNEGQEGKKAASGKGEEG----- 317

```

first report in which AQP10b-like transcripts and GLP gene / promoter structure have been assessed in a glycerol accumulating fish.

4.3 MATERIALS AND METHODS

4.3.1 *Study overview and animals*

Experiments were carried out in accordance with Animal Utilization Protocols issued by Memorial University of Newfoundland's Animal Care Committee. For all studies, smelt were collected by seine netting, transported in seawater to the Ocean Sciences Centre, Memorial University of Newfoundland, and were held in indoor free-flowing seawater tanks. Flow-through seawater was run through a polyvinyl chloride (PVC) pipe containing BioBalls (Pentair Aquatic Eco-Systems, Vancouver, BC) to remove excess gas prior to entering the tank. Sweetwater air diffusers (Pentair Aquatic Eco-Systems) were placed in the tank to gradually diffuse air into the seawater. Dissolved oxygen levels were measured daily using the OxyGuard Handy Polaris (Pentair Aquatic Eco-Systems) and were maintained approximately 100%. Smelt were subjected to a natural photoperiod with fluorescent lights set by an outdoor photocell, and were fed a diet of chopped herring twice a week to satiation.

In the first study (temperature decrease challenge), AQP10ba and AQP10bb transcript levels were assessed in kidney, and glycerol and urea levels were determined in plasma of smelt that were either held at 8°C to 11°C (warm smelt) or subjected to a temperature decrease challenge (cold smelt). Smelt were collected in Mount Arlington Heights, Placentia Bay, Newfoundland in late October 2006, and then held in a 3000 l tank maintained at 8°C to 11°C. On January 3, 2007, smelt were removed from this tank and divided into 2 heated (~8°C) (warm smelt) or 2 cold (cold smelt) 350 l tanks. In the cold tanks, the water temperature was gradually decreased from 8°C to 0°C (decreased to 5°C on Jan. 12, to 3°C on Jan. 15, to 1°C on Jan. 17 and to 0°C on Jan. 22) and held at

between 0°C to -0.5°C throughout the duration of the experiment. Smelt (n=7 warm; n=8 cold fish) were sampled from each group on Jan. 26, 2007 and approximately one month later on Feb. 22, 2007 (n=8 warm; n=7 cold fish).

In the second study (seasonal), AQP10ba and AQP10bb transcript levels were assessed in kidney, and glycerol and urea levels were determined in plasma of smelt that were either held at 8°C to 11°C (warm smelt) or allowed to follow ambient seawater temperatures (ambient smelt). Smelt were again collected from Mount Arlington Heights, Placentia Bay, Newfoundland in mid-November 2008 and then placed in either a 3000 l tank that was maintained at 8°C to 11°C or in a 3000 l tank that was allowed to follow ambient seawater temperatures. Smelt [n=8 (Nov., Dec., Jan.); n=7 (thereafter)] were sampled approximately every 30 days. Fish held at ambient temperature were available until May 2009. Fish held at elevated temperature became gravid and could not be maintained past mid-April.

In the third study (tissue distribution), AQP10ba, AQP10bb and AQP9b transcript levels were assessed in 10 tissues, and glycerol levels were determined in plasma from smelt that were either held at ~8°C (warm smelt) or subjected to a temperature decrease challenge (cold smelt). For this study, smelt were collected from First Pond, Horwood, Newfoundland on February 16, 2012 and then divided into two 350 l tanks. Both tanks were maintained at ~8°C until Feb. 25, 2012 to allow the smelt to release any glycerol that was present at collection time. Beginning on Feb. 25, the water temperature in one tank was gradually decreased from 8°C to 0°C (decreased to 5°C on Feb. 25, to 3°C Feb. 29, to 1°C on March 8 and to 0°C on March 13) and held at between 0°C to -0.5°C. Smelt (n=8) were sampled from both the cold and warm tanks on March 23, 2012.

Fish were not anesthetized prior to sampling. Blood was drawn via the caudal vessel using heparinized syringes, placed in a 1.5 ml nuclease-free microcentrifuge tube and centrifuged at 10,000 x g for 10 min at 4°C. Plasma was transferred to another 1.5 ml tube; plasma and red blood cells (RBCs) (study 3) were snap frozen in liquid nitrogen and stored at -80°C. Fish were killed by a sharp blow to the head and the tissues were removed quickly. Tissues were either snap frozen and stored at -80°C (studies 1 and 3) or immediately homogenized in TRIzol Reagent (Life Technologies, Burlington, ON) and then stored at -80°C for a maximum of two weeks before completion of the RNA extraction (study 2).

4.3.2 RNA preparation and cDNA synthesis

In all protocols involving commercial kits cited here and elsewhere in this study, unless otherwise indicated, the manufacturers' instructions were followed. In the first two studies, kidneys were homogenized in TRIzol Reagent using a motorized Kontes RNase-Free Pellet Pestle Grinder (Kimble Chase, Vineland, NJ), and then total RNA was extracted. For the tissue distribution study, for liver and muscle samples, tissues were homogenized using mortars and pestles that had been chilled with liquid nitrogen to generate a homogeneous powder. Individual mortars and pestles were used for each sample, and prior to use, they were washed and baked at 220°C for 5 h to ensure they were RNase-free. Approximately 100 mg tissue was added to TRIzol Reagent and mixed by pipette. All other tissues were homogenized in TRIzol Reagent using a motorized Kontes RNase-Free Pellet Pestle Grinder. However, if the tissue weighed >100 mg, it was divided into ≤100 mg pieces, separate RNA extractions were performed and the RNA was pooled at the end of the procedure. For tissues weighing ≤100 mg, the entire tissue

was used in the RNA extraction. After homogenization, the tissues were further disrupted using QIAshredder spin columns (QIAGEN, Mississauga, ON). The remainder of the protocol was carried out with the manufacturer's instructions.

In the first study, TRIzol extracted total RNA (45 µg) was then treated with 6.8 Kunitz units DNaseI (RNase-Free DNase Set, QIAGEN) at room temperature for 10 min and column-purified using the RNeasy MinElute Cleanup Kit (QIAGEN). In the second and third studies, TRIzol extracted total RNA (10 µg) was then treated with 4 U TURBO DNase (TURBO DNA-free Kit, Ambion/Life Technologies). RNA integrity was verified by 1% agarose gel electrophoresis and purity was assessed by A260/280 (cut-off ratio > 1.9) and A260/230 (cut-off ratio > 1.8) UV NanoDrop spectrophotometry.

First-strand cDNA was synthesized from 1 µg of DNaseI-treated total RNA in a 20 µl reaction using random primers [250 ng (Life Technologies)] and M-MLV reverse transcriptase [200 U (Life Technologies)] with the manufacturer's first strand buffer (1X final concentration) and DTT (10 mM final concentration) at 37°C for 50 min. For the third study, a "no reverse transcriptase" control cDNA synthesis was also performed for each sample.

4.3.3 cDNA cloning

The sequences of all primers used in cDNA cloning and their applications are presented in Table 4.1. In all cases, primers were designed in areas that had a minimum of 3 bp difference between AQP10ba and AQP10bb. Partial sequences for two AQP10b-like cDNAs were available [GenBank accession numbers EL538980 (AQP10ba) and EL537770 (AQP10bb)] (58). The 5' and 3' ends of both AQP10b-like cDNAs were obtained using a commercial kit for RNA ligase-mediated rapid amplification of 5' and 3'

Table 4.1. Sequences of oligonucleotides used in cDNA cloning.

cDNA	Nucleotide sequence (5'-3')	Direction*	Application	Position of 5'-end in cDNA
AQP10ba	AGGTATTGGCCTGCCTTGCCTT	R	5' RACE	217
AQP10ba	TGCCTTGCCTTTGAGGTTACTAC	R	5' RACE (nested)	206
AQP10ba	AATCGTGTTTGGATGTGGATCGGT	F	3' RACE	152
AQP10ba	GTAACCTCAAAGGACAAGGCAGG	F	3' RACE (nested)	186
AQP10ba	ACACACCAGCAATCCATACAGTC	F	sequence verification	1
AQP10ba	CTTTATCCAAAGCGACTTCCAAGA	R	sequence verification	1251
AQP10bb	GAAATACATGTCTGAAAGTGAACATG	R	5' RACE	1103
AQP10bb	AGCACCTGGGAGAACACATAGAA	R	5' RACE (nested)	322
AQP10bb	AATTCTGTTTGGATGTGGATCCGT	F	3' RACE	98
AQP10bb	AACAACCTCAGAGAACAAGAACGG	F	3' RACE (nested)	131
AQP10bb	ATTGTACTTTAGGTATGGACAGACT	F	sequence verification	1
AQP10bb	GTTGTGGTCTGCTTGATGAAAATG	R	sequence verification	1150
AQP10ba	ATGGACAGACTGTTGAAGAAATGT	F	QPCR standard curve	69
AQP10ba	TTAGTGGCCACCAGCGGCACC	R	QPCR standard curve	799
AQP10bb	ATGGACAGACTGTTGAAGAAATGT	F	QPCR standard curve	15
AQP10bb	TTAGTGGCCACCAGCGGCACC	R	QPCR standard curve	745
AQP9b	ATGGAAGAAGAAAGCAAGAGAAAA	F	QPCR standard curve	56
AQP9b	TTAACTCATGGTGATCATCTCAT	R	QPCR standard curve	922

*F is forward and R is reverse direction.

cDNA ends (RLM-RACE) [GeneRacer Kit (Life Technologies)] and DNaseI-treated total RNA (1 µg) extracted from kidney (heated fish 1, study 3). PCR amplification was performed using DyNAzyme EXT DNA polymerase (Thermo Fisher Scientific, Ottawa, ON). Briefly, 50 µl reactions were prepared containing DyNAzyme EXT DNA polymerase (1 U), the manufacturer's Optimized DyNAzyme EXT Buffer (1X final concentration), 0.2 mM dNTPs, 0.2 µM each of forward and of reverse primer, and either one-twentieth of the GeneRacer cDNA synthesis reaction (first PCR) or one-fiftieth of the first PCR reaction (nested PCR). PCR cycling conditions were 40 cycles of [94°C for 30 sec, 70°C decreasing by 0.3°C per cycle (to 58.3°C at cycle 40) for 30 sec and 72°C for 1-2 min].

All PCR products were sequenced using the following protocol. PCR products were electrophoretically separated on a 1% agarose gel, excised and purified using the QIAquick Gel Extraction Kit (QIAGEN). They were then subcloned into pGEM-T Easy (Thermo Fisher Scientific), and transformations were performed using Subcloning Efficiency DH5α chemically competent cells (Life Technologies) and standard molecular biology techniques. Plasmid DNA was isolated from individual clones using the QIAprep Spin Miniprep Kit (QIAGEN) and clone restriction fragments screened for inserts by visual comparison with a DNA size marker (1 kb Plus DNA Ladder; Life Technologies) using 1.0% agarose gel electrophoresis. Triplicate subclones were sequenced in both directions using BigDye Terminator reagents (Applied Biosystems/Life Technologies) and the 3730xl DNA Analyzer (Applied Biosystems/Life Technologies) at the Genomics and Proteomics Facility, CREAT Network, Memorial University. Sequence data was

extracted using Sequence Scanner v1.0 (Life Technologies), and compiled and analyzed using Vector NTI and AlignX (Vector NTI Advance 11, Life Technologies).

Assembled full-length sequences for the two AQP10b-like cDNAs were verified using reverse transcription – polymerase chain reaction (RT-PCR), with primers designed in the untranslated regions (UTRs). Sequences were verified in kidney of two fish from Horwood, NL (heated and cold fish 1) and two from Placentia, NL (study 2, February sampling, heated and cold fish 1). PCR amplifications were performed using DyNAzyme EXT DNA polymerase and cDNA representing 100 ng of input total RNA, with core reaction components as described previously. PCR cycling conditions were 40 cycles of [94°C for 30 sec, 65°C decreasing by 0.5°C per cycle (to 45.5°C at cycle 40) for 30 sec and 72°C for 1.5 min]. The amplicons were then sequenced as described previously.

Partial cDNAs for the two AQP10b-like sequences and AQP9b (GenBank accession number DQ533629) were amplified using RT-PCR and subcloned into a TA cloning vector for use as template to generate standard curves for QPCR assays (see below). For the two AQP10b-like sequences, cDNA was synthesized from kidney (heated fish 1, study 3), and for AQP9b cDNA was synthesized from liver (heated fish 1, study 3). PCR amplifications were performed using DyNAzyme EXT DNA polymerase as described for sequence verification.

4.3.4 Phylogenetic and structural analysis of predicted smelt AQP10b-like protein sequences

Multiple sequence alignments were performed using AlignX (Vector NTI Advance 11, Life Technologies) which uses the ClustalW algorithm (51). These alignments were imported in MSF format into *MEGA* version 6 (50). An unrooted

phylogenetic tree was then constructed using the maximum likelihood statistical method and the Jones-Taylor-Thornton substitution model; the bootstrap test of phylogeny was performed with 1000 replicates. Transmembrane helices and loops were predicted using the TMHMM Server v. 2.0 (25).

4.3.5 Isolation of genomic and promoter sequences of smelt GLP-encoding genes

The genomic and promoter region sequences for AQP10ba, AQP10bb and AQP9b were cloned using a combination of genomic PCR and genome walking. The sequences of all primers used in gene cloning are presented in Table 4.2.

Genomic DNA was extracted from the fresh liver of a warm smelt (study 3) using the Wizard Genomic DNA Purification Kit (Promega, Madison, WI). DNA integrity was verified by 0.5% agarose gel electrophoresis, and purity was assessed by A260/280 and A260/230 (cut-off ratios > 1.8 for both) UV NanoDrop spectrophotometry.

Genome-walking libraries were constructed using the Universal GenomeWalker Kit (Clontech, Mountain View, CA). Briefly, four 2.5 µg aliquots of genomic DNA were restriction digested to completion by either *EcoRV*, *DraI*, *PvuII*, or *StuI*, followed by ligation with GenomeWalker adaptors (provided with the kit), to generate four GenomeWalker libraries.

PCR amplification was performed using DyNAzyme EXT DNA polymerase (Thermo Fisher Scientific, Ottawa, ON) and either 100 ng of genomic DNA (genomic PCR), one-eightieth of the applicable GenomeWalker library (primary GenomeWalker PCR) or one-fiftieth of the primary GenomeWalker PCR (nested GenomeWalker PCR) as template. PCR core reaction component concentrations were as described for cDNA cloning. Cycling conditions for both genomic and genome-walking PCRs were 40 cycles

Table 4.2. Sequences of oligonucleotides used in gene cloning.

*Primer Name	Nucleotide sequence (5'-3')	Position of 5'-end of primer in gene	**Library / position of 3'end of amplicon in gene
AQP10ba_GW1_F1	GACTTTTATGGCTACCCTTGCAGC	301	<i>StuI</i> / 1330
AQP10ba_GW1_F2	TGCAGCTCTACGCTTGAGTGGTA	319	<i>EcoRV</i> / 1834 <i>PvuII</i> / 1905
AQP10ba_GW2_R1	TGACTGTGCTGTTGTCCATATTG	390	<i>EcoRV</i> / - 418
AQP10ba_GW2_R2	ACTCAAGCGTAGAGCTGCAAGG	337	<i>PvuII</i> / -733 <i>StuI</i> / - 880
AQP10ba_GW3_R1	GACGCTGTTGACCGGCATTG	-524	<i>EcoRV</i> / -1120
AQP10ba_GW3_R2	CAGCTGTTTGCACCAGTGGCTGT	-731	
AQP10ba_GW4_F1	GTACAGCATCTTGATCAAGTCTTGAC	1787	<i>DraI</i> / 2718
AQP10ba_GW4_F2	TCAAGGTGCCCGCTGAGTTGTT	1836	<i>StuI</i> / 3153
AQP10ba_GP1_F	TTCGGCAGCGTGACACAACG	2879	N/A
AQP10ba_GP1_R	CGAGACACTCCGCCAGGCACT	4090	
AQP10ba_GP2_F	GGTCAAGAAGTGCCTGGCGGAGT	4070	N/A
AQP10ba_GP2_R	TGCCTTGTCTTTGAGGTTACTAC	5305	
AQP10ba_GW5_F1	GTGGATCGGTGCGCCAGGTAGT	5265	<i>DraI</i> / 6336
AQP10ba_GW5_F2	TCGCCAGGTAGTAACCTCAAAGG	5274	
AQP10ba_GW6_F1	TGCACCAGCGCGAGTTGGAA	6016	<i>PvuII</i> / 6652
AQP10ba_GW6_F2	GATCCCCGGCCGTGCCAAAT	6155	<i>StuI</i> / 7749
AQP10bb_GW1_R1	GAGACACTCCGCCAGGCACTT	83	<i>EcoRV</i> / -767
AQP10bb_GW1_R2	CTTGACCAGGCTGCTTCTGATGC	62	
AQP10bb_GW2_R1	TGAGGGTGAAGGCGAGCATGG	-619	<i>PvuII</i> / -2527
AQP10bb_GW2_R2	GCACTCCAATGCAGCCGGTGT	-651	<i>DraI</i> / -2706
AQP10bb_GW3_F1	TAGAGAACACGTGAGTAGGAAGAGT	-247	<i>DraI</i> / 1081
AQP10bb_GW3_F2	AGGTCAGTGACCCATTAGACTTAG	-37	
AQP10bb_GP1_F	TGGGTCAATGAGTGC GGCAAC	490	N/A
AQP10bb_GP1_R	CCCGCCATGTTTTGCGCTTT	1423	
AQP10bb_GW4_R1	AGCACCTGGGAGAACACATAGAA	2172	<i>DraI</i> / 1081
AQP10bb_GW4_R2	AGGTATTGGCCGTTCTTGTC	1869	
AQP10bb_GW5_F1	GTGGATCCGTCGCCAGGTAAC	1818	<i>PvuII</i> / 2637
AQP10bb_GW5_F2	CGCCAGGTAACAACCTCAGAGA	1828	<i>StuI</i> / 3495
AQP9b_GW1_R1	CGCCAAGAACTCTTTGATGATATC	130	<i>DraI</i> / -589
AQP9b_GW1_R2	CAGGGCGCATCGCTCCCTTAAT	100	<i>StuI</i> / -1634
AQP9b_GW2_F1	AGCAACGCGTGCCTCATAGCA	- 407	<i>PvuII</i> / 881
AQP9b_GW2_F2	CCATGCCAAGGCGCACATGA	- 83	
AQP9b_GW3_F1	GACCAGCATTACAGACAACAAGAG	723	<i>DraI</i> / 2135
AQP9b_GW3_F2	GCCATGCTGTTGGCCATGCTG	814	
AQP9b_GW4_F1	CGTGGCTGGGGGAGTGTGTCAG	1599	<i>StuI</i> / 2811
AQP9b_GW4_F2	GACTGCAGAGGGAGTGGGGAGGT	1918	
AQP9b_GW5_F1	GTCTGGCCAGCCATGGACA	2219	<i>PvuII</i> / 4000
AQP9b_GW5_F2	CTGCCCGGCTGCTTCTCCAC	2550	
AQP9b_GW6_F1	GGCAGGCTGCTTCAGCCGTTT	3607	<i>StuI</i> / 5450
AQP9b_GW6_F2	GGAAGCCGATACCCCCAGCAG	3650	
AQP9b_GP1_F	GCTTAGTTACCCTGCTATAACCAGC	5109	N/A
AQP9b_GP1_R	TCCAGCGAAGGCTCCAGAA	6342	
AQP9b_GP2_F	GCCCATGTCAACCCTGCTGTCTC	6235	N/A
AQP9b_GP2_R	TGCCAACAACACACATGTTCACTGG	7671	

AQP9b_GW7_F1	ATGCTCTCATGGTCTACACGGGT	7316	<i>PvuII</i> / 9504
AQP9b_GW7_F2	GAGTTCTGTCAGTTACTGGGCCA	7340	
AQP9b_GW8_F1	CGTTTGCCAGACCCTGCCTTTC	9023	<i>DraI</i> / 9932 <i>EcoRV</i> / 10081 <i>StuI</i> / 10393
AQP9b_GW8_F2	TGTCCAGGGGAGGTGGCTAGG	9114	
AQP9b_GW9_F1	CGAGTGGGCGGAGACGGAGA	9963	<i>DraI</i> / 11239
AQP9b_GW9_F2	CGTGCCACGCACAATTATCCA	10120	
AP1	GTAATACGACTCACTATAGGGC	N/A	N/A
AP2	ACTATAGGGCACGCGTGGT	N/A	N/A

*GW indicates the primer was used for genome walking; GP indicates the primer was used for genomic PCR. F is forward and R is reverse direction. For a given genome walk, the first primer was used in the primary PCR with the kit adaptor primer AP1; the second primer was used in the nested PCR with the kit adaptor nested primer AP2.

**Only restriction fragments that were sequenced are indicated (i.e. although other libraries may have generated amplicons, they were not sequenced either because of small size or similar amplicon size to that generated by other libraries).

of [94°C for 10 sec, 70°C decreasing by 0.2°C per cycle (to 62.2°C at cycle 40) for 30 sec and 72°C for 3 min].

4.3.6 Analysis of smelt GLP promoter sequences

Putative transcription factor recognition sites were identified in the promoter regions of the 3 GLP-encoding genes using the TRANSFAC (33) module of the BIOBASE Knowledge Library (TRANSFAC Suite, BIOBASE Corporation / QIAGEN, Beverly, MA). Briefly, the MATCH (20) program, which uses positional weight matrices to search DNA sequences for potential transcription factor binding sites, was used with both the vertebrate non-redundant MFP (Minimize False Positives) and the vertebrate non-redundant MSUM [MFP and MFN (Minimize False Negatives)] group of matrices, data version 2014.2, and default parameters. Putative binding sites identified in other vertebrate GLP-encoding genes were based on the MSUM search results, and had a core score > 0.9. The promoter regions were manually searched using Vector NTI (Vector NTI Advance 11, Life Technologies) for the presence of the core negative insulin response element (IRE), T(G/A)TTTT(G/T) (37, 38).

4.3.7 QPCR analysis of GLP transcript levels

mRNA levels of the GLP-encoding genes were quantified by QPCR, using SYBR Green I dye chemistry with normalization to 18S ribosomal RNA using a commercially available TaqMan assay and the 7300 Real Time PCR system (Life Technologies).

The sequences of the primer pairs used for QPCR are presented in Table 4.3. These primers were quality tested to ensure that a single product was amplified (dissociation curve analysis) and that there was no primer-dimer present in the no-template control. Amplicons were electrophoretically separated on 2% agarose gels and

Table 4.3. Primers used in QPCR studies.

Gene Name	Direction*	Nucleotide Sequence (5'-3')**	Position of 5'-end of primer in cDNA	Efficiency (%)***	Amplicon Size (bp)
AQP10ba	F	GCCCAGGTAG TAACCTCAAAGGA	177	93	101
	R	ACCCACGAGAAACAT GGATT	277		
AQP10bb	F	GCCCAGGTAA CAACCTCAGAGA	123	92	102
	R	CACCCACGAGAAACAT AGATCC	224		
AQP9b	F	GGGAGTGATGATGGCTGTCT	244	91	145
	R	GAAGGCTCC CAGAAACTGTG	388		

*F is forward and R is reverse direction.

**Nucleotides highlighted in bold are different between the AQP10b paralogues.

***See Materials and methods for information on the standard curves used to determine amplification efficiency.

compared with the 1 kb Plus DNA Ladder (Life Technologies) to ensure the correct size fragment was being amplified. Amplification efficiencies (41) were calculated and were required to be between 90-110%. Briefly, amplification efficiencies were calculated for both a warm and a cold smelt [AQP10ba and AQP10bb – kidney (February sampling, study 1); AQP9b – liver (study 3)]. A 5-point 1:5 dilution series starting with cDNA representing 10 ng of input total RNA was analyzed for both the warm and the cold smelt. The reported efficiencies are an average of the two values. Finally, to confirm that the AQP10ba and AQP10bb primers were specific to their individual transcripts, amplicons were sequenced. Briefly, PCR amplification was performed using DyNAzyme EXT DNA polymerase and cDNA (representing 100 ng of input total RNA) synthesized from DNaseI-treated total RNA (1 µg) extracted from kidney (cold fish 2, study 3). PCR core reaction component concentrations were as described for cDNA cloning. PCR cycling conditions were 40 cycles of (94°C for 30 sec, 60°C for 30 sec and 72°C for 30 sec). The amplicons were sequenced as described for cDNA cloning except 12 subclones were sequenced for each. Both the AQP10ba and AQP10bb amplicon sequences matched their corresponding sequence in the full-length cDNA sequence submitted to GenBank.

PCR amplification of the target genes (GLPs) was performed in a 25 µl reaction using 1X Power SYBR Green PCR Master Mix (Life Technologies), 50 nM each of each forward and reverse primer and cDNA representing 10 ng of input total RNA. For study 3, a standard curve PCR for the GLP transcript of interest was also included on the plate. It consisted of a 5-point 1:10 dilution series starting with 1 ng of plasmid DNA for the GLP transcript of interest and a no-template control. Expression levels of the target genes were normalized to 18S ribosomal RNA, using the Eukaryotic 18S rRNA Endogenous

Control (VIC / MGB Probe, Primer Limited) (Life Technologies). PCR amplification of 18S was performed in a separate 25 μ l reaction using 1X TaqMan Universal PCR Master Mix, with AmpErase UNG (Life Technologies), 1X probe/primer mix and cDNA representing 0.4 ng of input total RNA. Since fluorescence threshold cycle (C_T) values for 18S rRNA for all samples in a given study were less than 1 cycle apart, it was deemed to be an acceptable normalizer. For study 3, a standard curve PCR for 18S ribosomal RNA was also included on the plate. It consisted of a 7-point 1:5 dilution series starting with cDNA representing 10 ng of input total RNA (using DNaseI-treated total RNA from the kidney of heated fish 1 as template) and a no-template control. For the target genes and normalizer assays, each sample was tested in duplicate. For study 3, a “no reverse transcriptase” control for each sample was also included; the standard curve reactions were tested in duplicate. For all PCR reactions, the real-time analysis program consisted of 1 cycle of 50°C for 2 min, 1 cycle of 95°C for 10 min and 40 cycles of 95°C for 15 sec and 60°C for 1 min, with a dissociation stage included for the target gene analysis.

In the first two studies, AQP10b mRNA levels were measured using the Relative Quantification method. The C_T values were determined using the 7300 PCR Detection System SDS Software Relative Quantification Study Application (Version 1.2.3) (Life Technologies). The relative quantity (RQ) of each transcript was determined with this software using the $2^{-\Delta\Delta C_T}$ relative quantification method and assuming 100% amplification efficiencies (31). For each target gene, the individual with the lowest normalized expression (mRNA) level was set as the calibrator sample (assigned an RQ value = 1). Gene expression data are presented as RQ values [mean \pm standard error (SE)] relative to the calibrator.

In the third study, to directly compare mRNA levels of the three GLP-encoding genes in a given tissue, transcript levels were measured using the Relative Standard Curve Method for Quantification (13). For each experimental sample, the absolute quantity of the target gene (GLP of interest) and endogenous control (18S) was determined by comparing the C_T value for an experimental sample to the appropriate standard curve using the 7300 PCR Detection System SDS Software Absolute Quantification (Standard Curve) Application (Version 1.2.3) (Life Technologies). The relative absolute quantity (RAQ) of each GLP transcript was then determined by dividing the target absolute quantity by the endogenous control absolute quantity to obtain a normalized target absolute quantity. In the first comparison, in which the mRNA levels of a given GLP across different tissues were assessed, the sample with the lowest detectable normalized absolute quantity of that particular GLP transcript was set as the calibrator (assigned an RAQ value = 1). In the second comparison, in which the mRNA levels of each GLP in a given tissue were assessed, the sample with lowest detectable normalized absolute quantity of any GLP transcript was set as the calibrator. Gene expression data are presented as RAQ values (mean \pm SE) relative to the calibrator.

4.3.8 Plasma glycerol and urea

Plasma glycerol was measured as previously described (8). For plasma urea measurements, plasma was deproteinized in 5% TCA and neutralized with 5M KHCO_3 . Urea was then measured as previously described (12).

4.3.9 Statistical analysis

The Mann-Whitney test was used to assess if there were any significant differences in transcript, glycerol and urea levels in cold/ambient compared to warm

smelt (i.e. a temperature response) in all three studies, and to identify if there were any significant differences in levels in cold or warm smelt in February compared to January (i.e. a temporal response) in the first study. In the second and third studies, data were \log_{10} transformed and one-way ANOVA followed by Tukey's B post-hoc test was used to assess if there were any significant differences in all other comparisons. In all cases, $p < 0.05$ was considered to be statistically significant. All data are expressed as mean \pm SE.

4.4 RESULTS

4.4.1 *AQP10ba and AQP10bb cDNA and predicted protein sequences*

Full-length cDNA sequences were deposited in GenBank under accession numbers KM455588 (AQP10ba) and KM455589 (AQP10bb). The AQP10ba mRNA contains a 45 bp sequence immediately 5' of the consensus start codon that could encode a 15 aa sequence (MGTFMATLAALRLSG) that is not present in smelt AQP10bb or in AQP10b orthologues from other fish species (Fig. 4.1). Although there is no direct evidence that this sequence is translated into protein, for descriptive/comparative purposes, this sequence is considered to be part of the open reading frame (ORF) as opposed to the 5'UTR. AQP10ba is a 1295 bp cDNA that contains a 23 bp 5'UTR, a 963 bp ORF and a 309 bp 3'UTR; it encodes a 320 aa protein which has a predicted molecular mass of 33.7 kDa and an isoelectric point of 6.07. AQP10bb is an 1176 bp cDNA that contains a 14 bp 5'UTR, an 879 bp ORF and a 283 bp 3'UTR; it encodes a 292 aa protein which has a predicted molecular mass of 30.9 kDa and an isoelectric point of 6.64. AQP10ba and AQP10bb coding sequences are 87% identical at the nucleotide level; they are 96% identical over the 879 bp overlapping region, however, the 5' and 3' ends are quite different. Predicted amino acid sequences are 82% identical (93% over the 283 aa overlapping region).

The predicted protein sequences for smelt AQP10ba and AQP10bb have the hallmark features of a functional AQP. Structurally, using a hidden Markov model (25), both smelt AQP10b paralogues are predicted to form six transmembrane α -helices with three extracellular loops and two intracellular loops. They also have the two NPA constriction motifs. More specifically, both have the signature amino acid sequences that

distinguish a GLP from a classical AQP, namely, the five conserved amino acids (Y, D, R, P, L) and the ar/R constriction motif (F, G, Y, R) (Fig. 4.1). A summary of the smelt GLP cDNA and predicted protein characteristics is provided in Table 4.4.

Both smelt AQP10b-like sequences were classified as such using direct sequence comparisons and phylogenetic analyses. First, a BLASTx 2.2.29+ search of the non-redundant (nr) protein sequence database of NCBI (August 28, 2014) indicated that the best hit for AQP10ba was against an AQP10 from rainbow trout (*Oncorhynchus mykiss*) (CDQ56658) [74% identity (242/288 amino acids), E-value = 1E-150]; the best hit for AQP10bb was also against this GLP [81% identity (222/282 amino acids), E-value = 2E-159].

Second, an expansive screening of the zebrafish genome identified two AQP10-like paralogues [AQP10a (BC075911) and AQP10b (EU341836)] whose coding sequences are 53% identical at the nucleotide level; both are present in other teleost fish (52). To determine if the smelt AQP10-like sequences were AQP10a or AQP10b orthologues, sequence comparisons were made between the smelt and zebrafish AQP10-like sequences. At the nucleotide level, smelt AQP10ba coding sequences share 51% and 63% identity with zebrafish AQP10a and AQP10b, respectively; smelt AQP10bb coding sequences share 55% and 66% identity with zebrafish AQP10a and AQP10b, respectively.

Third, phylogenetic analyses of selected vertebrate GLP protein sequences were performed. An expansive Bayesian majority rule consensus tree for the codon alignment of piscine and human (*Homo sapiens*) GLPs had been generated previously (52). However, this tree was constructed using only partial sequences for the two smelt

Table 4.4. Smelt GLP cDNA, predicted protein and gene characteristics.

	Feature	AQP10ba	AQP10bb	¹AQP9b
cDNA	GenBank acc. no.	KM455588	KM455589	DQ533629
	² Total length (bp)	1295	1176	1047
	5'UTR (bp)	23	14	55
	³ 3'UTR (bp)	309	283	125
	⁴ ORF (bp)	963	879	867
	STOP codon	TAA	TAA	TAA
	Polyadenylation signal	AATAAA	ATTAAA	AATAAA
protein	No. aa encoded	320	292	288
	Molecular mass (kDa)	33.7	30.9	30.7
	pI	6.07	6.64	5.74
	NPA (C-terminal)	NPA	NPA	NPA
	NPA (N-terminal)	NPA	NPA	NPA
	P1-5	Y, D, R, P, L	Y, D, R, P, L	Y, D, R, P, V
	ar/R constriction	F, G, Y, R	F, G, Y, R	F, G, Y, R
gene	GenBank acc. no.	KM598780	KM598781	KM598782
	⁵ Total length (bp)	7505	3425	10630
	⁶ Exon I (bp)	21	/	/
	⁶ Intron I (bp)	272	/	/
	⁷ Phase	N/A	/	/
	⁶ Exon II (bp)	45	/	/
	⁶ Intron II (bp)	3680	/	/
	⁷ Phase	1	/	/
	⁶ Exon III/I (bp)	89	101	157
	⁶ Intron III/I (bp)	1147	1706	1334
	⁷ Phase	0	0	0
	⁶ Exon IV/II (bp)	127	127	127
	⁶ Intron IV/II (bp)	152	144	4614
	⁷ Phase	1	1	1
	⁶ Exon V/III (bp)	138	138	138
	⁶ Intron V/III(bp)	669	109	945
	⁷ Phase	1	1	1
	⁶ Exon VI/IV (bp)	119	119	119
	⁶ Intron VI/IV (bp)	180	180	799
	⁷ Phase	0	0	0
	⁶ Exon VII/V (bp)	218	218	218
	⁶ Intron VII/V (bp)	110	110	1891
	⁷ Phase	2	2	2
	⁶ Exon VIII/VI (bp)	538	473	288

¹cDNA and predicted protein information were described previously (13, i.e. Chapter 2).

²Excludes polyA tail.

³Excludes STOP codon and polyA tail.

⁴Includes STOP codon.

⁵From Transcription start to end; excludes polyA tail.

⁶AQP10ba has two additional exons that precede exon I for AQP10bb and AQP9b. To keep the alignment of the overlapping exons consistent, the first number is for AQP10ba; the second is for AQP10bb and AQP9b.

⁷Phase class refers to the positions of the introns relative to the CDS (40); class 0, intron located between the codons; class 1, intron sequence between the 1st and 2nd bp of a codon; class 2, intron sequence between the 2nd and 3rd bp of a codon.

AQP10-like sequences fully cloned herein. To confirm the previous classification, a smaller scale tree was constructed using the full-length smelt AQP10-like predicted protein sequences. In both trees, the smelt AQP10-like sequences cluster with other vertebrate AQP10b-like sequences and not with other GLPs [AQP3, AQP7, AQP9, and piscine and human AQP10a] (Fig. 4.2). Therefore, based on the direct sequence and phylogenetic analyses, the full-length smelt AQP10-like sequences cloned herein are likely orthologues of AQP10b and as such are named AQP10ba and AQP10bb.

4.4.2 AQP10ba, AQP10bb and AQP9b gene sequences

Gene sequences were deposited in GenBank under accession numbers KM598780 (AQP10ba), KM598781 (AQP10bb) and KM598782 (AQP9b). These sequences are also presented in Supplemental Fig. S4.1A (AQP10ba), S4.1B (AQP10bb) and S4.1C (AQP9b); the location of the primers used for genomic PCR and genome walking, and the location of the 5' and 3'UTRs, exons and predicted amino acid sequences are highlighted. A schematic depicting the organization of the smelt GLP-encoding genes is presented in Fig. 4.3. The AQP10ba gene is comprised of 8 exons and 7 introns; the 5'UTR is located in exon 1, a potential novel START codon is located in exon 2, the consensus START codon for other GLP-encoding genes (including AQP10bb) is located in exon 3 and the STOP codon and polyadenylation signal are located in exon 8 (Fig. 4.3, Supplemental Fig. 4.1A). The AQP10bb and AQP9b genes are both comprised of 6 exons and 5 introns; the 5'UTR and the START codon are located in exon 1 and the STOP codon and polyadenylation signal are located in exon 6 (Fig. 4.3, Supplemental Fig. 4.1B, 4.1C). All splice sites (GT-AG) match the consensus sequence for splice-acceptor and

Figure 4.2. Phylogenetic analysis of full-length smelt GLP predicted protein sequences.

A phylogenetic tree of protein sequences for aquaglyceroporins 3, 7, 9, and 10 from several vertebrates. A more expansive Bayesian majority rule consensus tree for the codon alignment of piscine and human GLPs is also available (52). Protein accession numbers (GenBank, Unigene or Ensembl) are listed in parentheses. The following common names are from the NCBI Taxonomy Browser. *Anguilla anguilla*: European eel. *Anguilla japonica*: Japanese eel. *Anoplopoma fimbria*: sablefish. *Astyanax mexicanus*: Mexican tetra. *Danio rerio*: zebrafish. *Dicentrarchus labrax*: European seabass. *Fundulus heteroclitus*: mummichog. *Gadus morhua*: Atlantic cod. *Gallus gallus*: chicken. *Gasterosteus aculeatus*: threespine stickleback. *Homo sapiens*: human. *Hyla chrysoscelis*: southern gray treefrog. *Mus musculus*: house mouse. *Oncorhynchus mykiss*: rainbow trout. *Osmerus mordax*: rainbow smelt. *Oreochromis mossambicus*: Mozambique tilapia. *Oreochromis niloticus*: Nile tilapia. *Oryzias dancena*: marine medaka. *Oryzias latipes*: Japanese medaka. *Poecilia formosa*: Amazon molly. *Protopterus annectens*: West African lungfish. *Salmo salar*: Atlantic salmon. *Sparus aurata*: gilthead seabream. *Takifugu obscurus*: mefugu. *Takifugu rubripes*: torafugu. *Tetraodon nigroviridis*: spotted green pufferfish. *Tribolodon hakonensis*: big-scaled redbfin. *Xenopus laevis*: African clawed frog. *Xenopus tropicalis*: western clawed frog. *Xiphophorus maculatus*: Southern platyfish. The tree was constructed as described in the materials and methods section. The scale bar represents the number of substitutions per amino acid site. All bootstrap values are shown, however only values ≥ 90 are considered trustworthy.

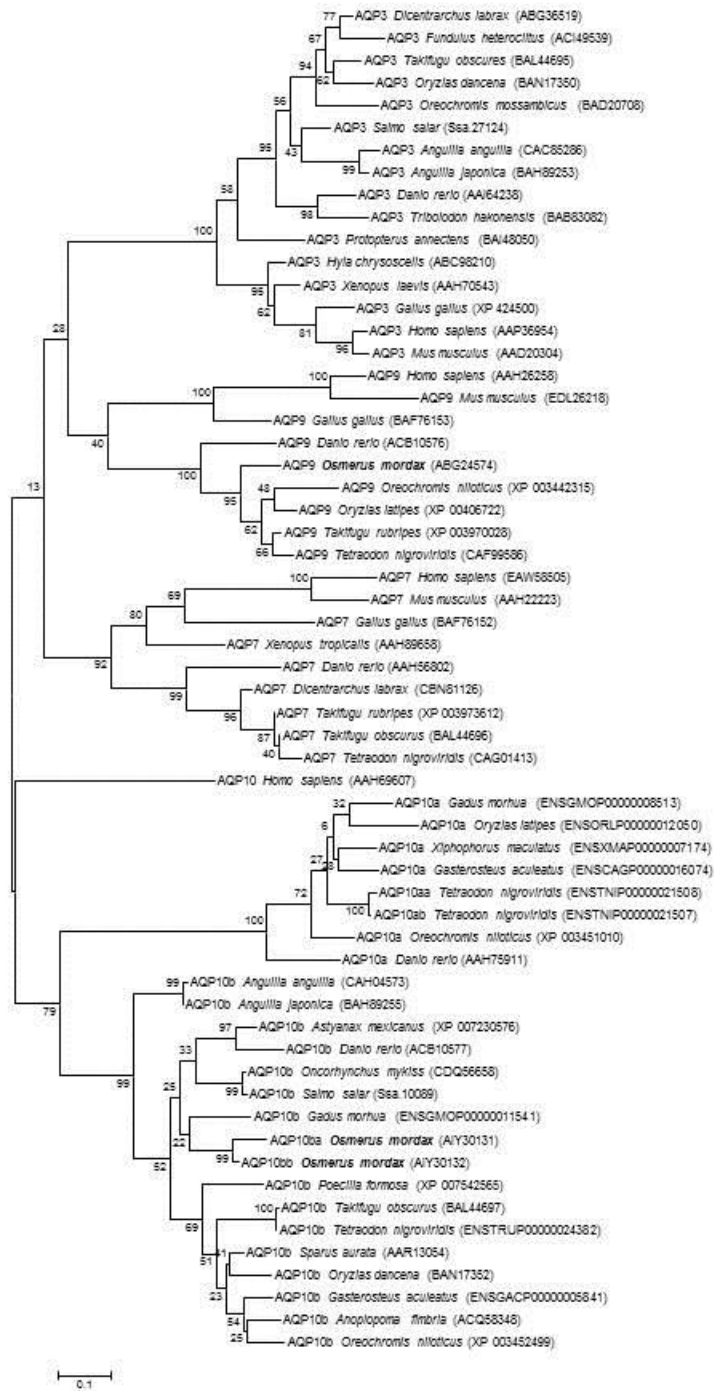
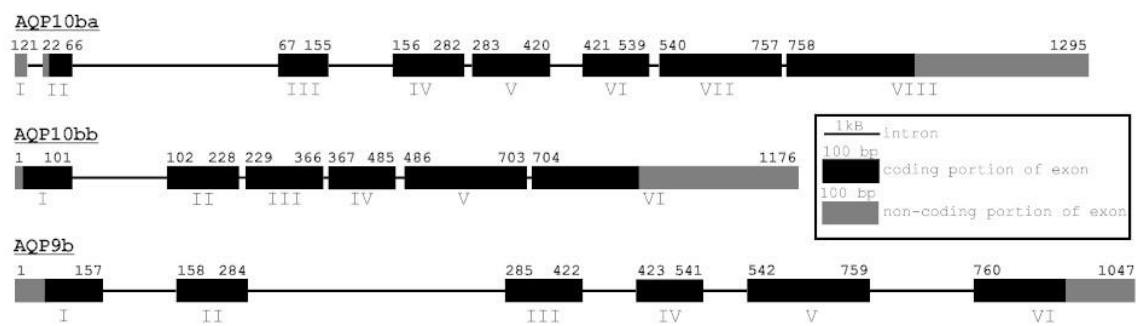


Figure 4.3. A schematic representation of the structure of smelt GLP-encoding genes. The coding and non-coding regions within an exon are shown by solid black and gray boxes, respectively, while horizontal lines represent introns. The numbering at the start and the end of each exon indicates the location with respect to the mRNA, with 1 being the transcription start. GenBank accession numbers for the genomic sequences are KM598780 (AQP10ba), KM598781 (AQP10bb) and KM598782 (AQP9b).



splice-donor sites (35). A summary of the smelt GLP gene characteristics is provided in Table 4.4.

4.4.3 AQP10ba, AQP10bb and AQP9b promoter sequences

As the smelt AQP10b gene paralogues have different promoter sequences and transcript expression profiles (see below), all available sequence data in the 5' flanking regions of these genes and AQP9b (for comparison) was screened for the presence of putative transcription factor recognition sites that could potentially explain these differences in gene expression. Using the vertebrate MFP group of matrices, 45, 88 and 52 sites were identified in the 1120 bp promoter sequences of AQP10ba (Supplemental Table S4.1A), in the 2706 bp promoter sequences of AQP10bb (Supplemental Table S4.1B), and in the 1634 bp promoter sequences of AQP9b (Supplemental Table S4.1C), respectively. Using the less stringent vertebrate MSUM group of matrices, 306, 746 and 428 sites were identified AQP10ba (Supplemental Table S4.1D), AQP10bb (Supplemental Table S4.1E), and AQP9b (Supplemental Table S4.1F), respectively.

The proximal 1 kb of the promoter sequences of the three smelt GLP-encoding genes contained several putative transcription factor binding sites that have been previously reported to be present in the promoter regions of other vertebrate GLP-encoding genes (24, 26, 28, 56). These binding sites were for the core negative insulin response element (4, 1 and 5 sites in AQP10ba, AQP10bb and AQP9b, respectively) (identified manually), and for the glucocorticoid receptor (GR) (7, 5 and 3 sites), CCAAT/enhancer-binding protein alpha (C/EBP alpha) (6, 7 and 10 sites), activator protein-1 (AP-1) (5, 2 and 2 sites), GATA (5, 3 and 4 sites), transcription enhancer factor-1 (TEF-1) (1, 0 and 1 site) and several nuclear factors (NF) [hepatic (H)NF-1,

HNF-6, HNF-3beta, NF-1, NF-Y and NF-AT1] (12, 8 and 7 sites) (MSUM analysis). Furthermore, two putative binding sites for cAMP responsive element binding protein 1 (CREB1) were identified in the proximal promoters of both AQP10ba and AQP10bb; none were present in the AQP9b proximal promoter (Fig. 4.4). Putative binding sites for these transcription factors in all available sequence data in the 5' flanking regions of the three smelt GLP-encoding genes is presented in Supplemental Fig. 4.2.

4.4.4 Biochemical analysis of plasma glycerol and urea levels, and QPCR analysis of kidney AQP10ba and AQP10bb transcript levels

4.4.4.1 Temperature decrease challenge

Plasma glycerol levels were 3.3-fold significantly higher, plasma urea levels were 2.3-fold significantly higher, and kidney AQP10ba transcript levels were 1.3-fold significantly higher in artificially cold-acclimated smelt, in February compared to January. There were no significant differences in AQP10bb transcript levels over time. In warm smelt, in February compared to January, plasma urea levels were 1.6-fold significantly higher; there were no significant differences in plasma glycerol levels, and kidney AQP10ba and AQP10bb transcript levels in warm smelt over time (Fig. 4.5).

Considering temperature-related changes, in cold compared to warm smelt, plasma glycerol levels were 7.3-fold and 20-fold significantly higher in January and February, respectively, plasma urea levels were 3.4-fold and 5.1-fold significantly higher, and kidney AQP10ba transcript levels were 1.3-fold and 2.4-fold significantly higher; there were no significant differences in AQP10bb transcript levels with cold temperature (Fig. 4.5).

Figure 4.4. A schematic comparison of selected putative transcription factor binding motifs in the smelt AQP10ba, AQP10bb and AQP9b proximal (1 kb) promoter sequences. Putative transcription factor recognition sites were identified manually [core negative insulin response element (IRE)] or using TRANSFAC (MSUM analysis; see methods for details). For a complete list, including those present in promoter sequences upstream of this selected 1 kb region, and core and matrix scores, see Supplemental Table S4.1. Some binding sites that have been reported in other vertebrate GLP promoter sequences [core negative IRE, glucocorticoid receptor (GR), CCAAT/enhancer-binding protein (C/EBP) alpha, activator protein-1 (AP-1), GATA, transcription enhancer factor-1 (TEF-1) and several members of the nuclear factor (NF) family] and cAMP responsive element binding protein 1 (CREB1) are shown. Sites identified on the positive (5'–3') and negative (3'–5') strands are indicated with a symbol above or below the line, respectively. For sequence data and specific member of the NF family, see Supplemental Fig. S4.2. Sequences are aligned with respect to the transcription start site (↓).

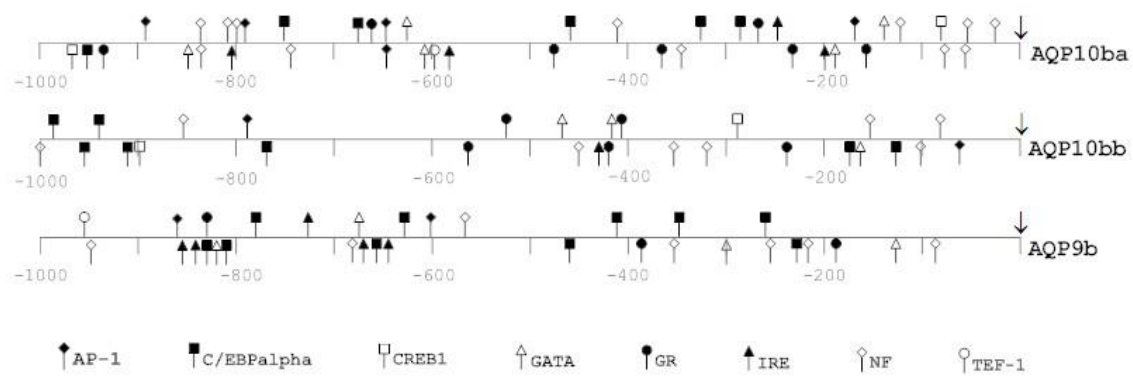
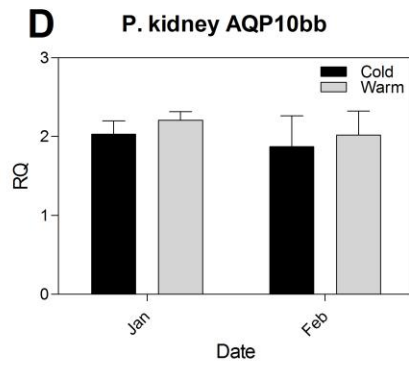
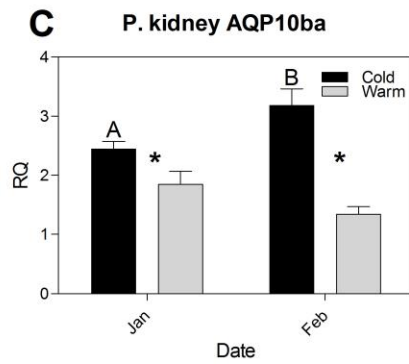
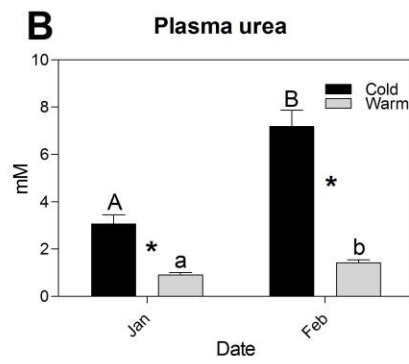
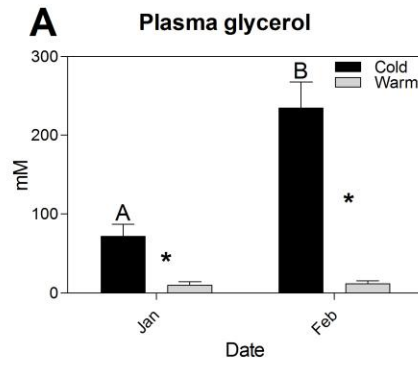


Figure 4.5. (A) plasma glycerol (mM) (B) plasma urea (mM) (C) kidney AQP10ba transcript levels and (D) kidney AQP10bb transcript levels in smelt held at high or low temperature. Smelt were either held at 8°C [warm smelt; January (n=8) and February (n=8)] or subjected to a controlled temperature decrease from 8°C to 0°C [cold smelt; January (n=8)] and then held at 0°C to -0.5°C for approximately one month [cold smelt; February (n=7)]. (A) Plasma glycerol and (B) plasma urea values are presented as mean \pm SE. (C, D) Kidney AQP10ba and AQP10bb transcript levels were measured by QPCR and are presented as mean \pm SE relative quantity (RQ) values (i.e. values for the gene of interest were normalized to 18S ribosomal RNA and were calibrated to the individual with the lowest normalized expression of that given gene). Different letters (upper case for cold smelt and lower case for warm smelt) indicate that there were significant differences in levels over time. Asterisks denote significant differences in levels between cold and warm smelt at that sampling time point. In all cases, $p < 0.05$ was considered to be statistically significant. P. kidney, posterior kidney.



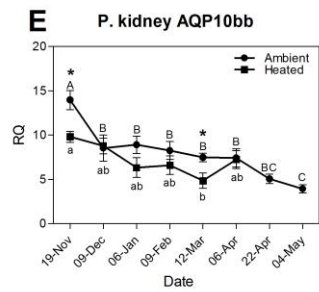
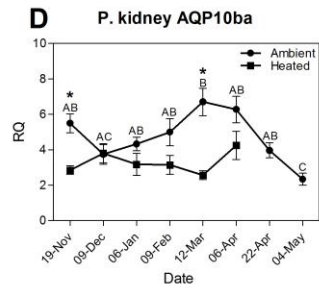
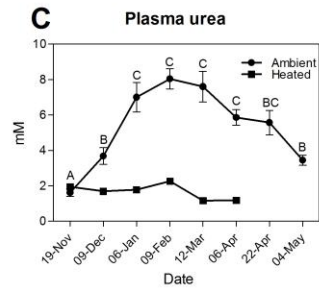
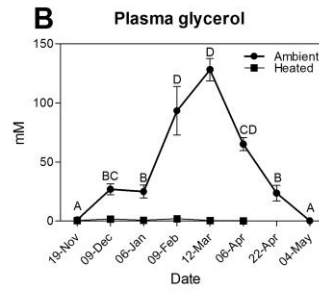
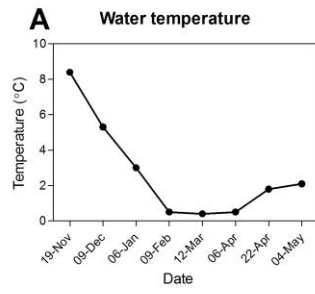
4.4.4.2 Seasonal study

In smelt maintained at ambient water temperature, plasma glycerol levels were significantly higher in December / January than in November; the next significant increase occurred in February (water temperature 0.5°C) to maximal average levels of 128 mM in March (water temperature 0.4°C). Levels dropped significantly by April 6th although water temperature was still at 0.5°C and reached initial levels (0.36 mM) by the final sampling point in May (water temperature 2.1°C). In smelt held at warm temperature, the plasma glycerol level bordered the levels of detection (< 1 mM) throughout the study. In ambient compared to warm smelt, plasma glycerol levels were significantly higher from December 9th to April 6th (no warm smelt were available April 22nd and May 4th) (Fig. 4.6B).

In ambient smelt, plasma urea levels were significantly higher in December than in November; the next significant increase occurred in January (water temperature 3°C) to maximal levels of 8 mM in February (water temperature 0.5°C). The significant increase in plasma urea content between December and January was not observed with glycerol levels. Furthermore, unlike glycerol, average levels did not significantly decrease from maximal levels until water temperature had reached 2.1°C in May. In warm smelt, there were no significant differences in plasma urea level throughout the study; in ambient compared to warm smelt, plasma urea levels were significantly higher from December 9th to April 6th (Fig. 4.6C).

In ambient smelt, there was a gradual increase in AQP10ba transcript levels from December to 1.8-fold significantly higher levels in March when water temperature was at its lowest; March was the only time point in which AQP10ba levels were significantly

Figure 4.6. A seasonal (November 2008 to May 2009) analysis of (A) ambient water temperature (B) plasma glycerol (mM) (C) plasma urea (mM) (D) kidney AQP10ba transcript levels and (E) kidney AQP10bb transcript levels in smelt held at high or ambient seawater temperature. (A) Seasonal ambient seawater temperatures ($^{\circ}\text{C}$); warm temperature was maintained at 8°C to 11°C . (B) Plasma glycerol and (C) plasma urea values are presented as mean \pm SE. (D, E) Kidney AQP10ba and AQP10bb transcript levels were measured by QPCR and are presented as mean \pm SE relative quantity (RQ) values (i.e. values for the gene of interest were normalized to 18S ribosomal RNA and were calibrated to the individual with the lowest normalized expression of that given gene). In all cases, for November 19th to February 9th (n=8); all other sampling points (n=7). Warm smelt were not available on April 22nd and May 4th. Letters (upper case for cold smelt and lower case for warm smelt) indicate Tukey's HSD groupings; there were no significant differences in plasma glycerol and urea, and kidney AQP10ba levels in warm smelt over time. Asterisks denote significant differences in kidney AQP10ba and AQP10bb levels between cold and warm smelt at a given time point; from December 9th to April 6th, plasma glycerol and urea levels were significantly higher in cold compared to warm smelt. In all cases, $p < 0.05$ was considered to be statistically significant. P. kidney, posterior kidney.



higher (2.6-fold) in ambient compared to warm smelt. AQP10ba levels returned to December levels by May (Fig. 4.6D).

In ambient smelt, there were no significant differences in AQP10bb transcript levels from December to April; however, levels were 2.2-fold significantly lower in May than in December. AQP10bb levels were significantly higher (1.5-fold) in ambient compared to warm smelt in March; however, this was due to lower levels in warm smelt (Fig. 4.6E).

4.4.5 Tissue distribution of AQP10ba, AQP10bb and AQP9b transcripts in cold- and warm-acclimated smelt

Plasma glycerol levels were measured to confirm that the controlled decrease in water temperature resulted in glycerol accumulation. In cold smelt, average plasma glycerol levels (97 mM) were 49-fold significantly higher than in warm smelt (< 2 mM).

4.4.5.1 Transcript levels of AQP10ba, AQP10bb and AQP9b across tissues

Transcript levels of each GLP-encoding gene were assessed separately. AQP10ba transcripts were ubiquitously expressed in both cold and warm smelt, and were significantly higher in kidney than in all other tissues. In cold smelt, kidney AQP10ba levels were approximately 28- and 45-fold higher than levels in brain and pyloric caeca, respectively. In warm smelt, kidney AQP10ba levels were approximately 19- and 13-fold higher than levels in brain and pyloric caeca, respectively. At both temperatures, all of the remaining tissues had detectable but substantially lower AQP10ba levels. In cold compared to warm smelt, kidney was the only tissue that had significantly higher (1.7-fold) AQP10ba levels. AQP10ba transcript expression was significantly lower in cold

compared to warm smelt in heart and RBCs (3.9-fold), muscle (3-fold), spleen (1.8-fold) and gill (1.6-fold) (Fig. 4.7A).

AQP10bb transcripts were ubiquitously expressed in both cold and warm smelt. In both cold and warm smelt, highest levels were in kidney, intestine, pyloric caeca and brain, at levels ~20-fold higher than spleen, heart and muscle. The remaining tissues had detectable but substantially lower AQP10bb levels. In cold compared to warm smelt, AQP10bb levels were significantly lower in RBCs (2.4-fold), spleen (2-fold), gill (1.8-fold), and muscle and intestine (1.6-fold) (Fig. 4.7B).

AQP9b transcripts were ubiquitously expressed in both cold and warm smelt. In cold smelt, highest levels were in spleen, liver, RBCs and kidney. In warm smelt, highest levels were in RBCs, spleen and liver followed by kidney; levels in RBCs were 16-fold significantly higher than in kidney. At both temperatures, all of the remaining tissues had detectable but substantially lower AQP9b levels. In cold compared to warm smelt, AQP9b levels were significantly lower in RBCs (9.4-fold), gill (4.4-fold), intestine (2.6-fold), spleen (2.2-fold) and brain (1.6-fold) (Fig. 4.7C).

4.4.5.2 Transcript levels of AQP10ba, AQP10bb and AQP9b in specific tissues

Fig. 4.8 shows the relative actual quantity (RAQ) of each GLP mRNA within specific tissues in both cold and warm smelt. A comparison of transcript levels of the three GLP-encoding genes in ten tissues from cold- and warm-acclimated smelt, indicated that AQP10ba transcripts in cold kidney were expressed at the highest level of all, and kidney was the only tissue in which AQP10ba was a dominant transcript.

AQP10bb was the most abundant transcript in brain, intestine, heart, muscle, and pyloric

Figure 4.7. QPCR analysis of transcript levels of (A) AQP10ba (B) AQP10bb and (C) AQP9b in various tissues from smelt held at high or low temperature. Smelt were either held at 8°C (warm smelt) or subjected to a controlled temperature decrease from 8°C to 0°C and then held at 0°C to -0.5°C for 10 days (cold smelt). Gene expression data are presented as relative absolute quantity (RAQ) values (mean \pm SE) for the GLP transcript of interest normalized to 18S ribosomal RNA and are calibrated to the sample with the lowest normalized transcript level of that particular GLP (assigned a value = 1). P. kidney, posterior kidney; PC, pyloric caeca; RBC, red blood cell. In all cases, (n=8). Letters (upper case for cold smelt and lower case for warm smelt) indicate Tukey's HSD groupings. Asterisks denote significant differences in transcript levels between cold and warm smelt in a given tissue. In all cases, $p < 0.05$ was considered to be statistically significant.

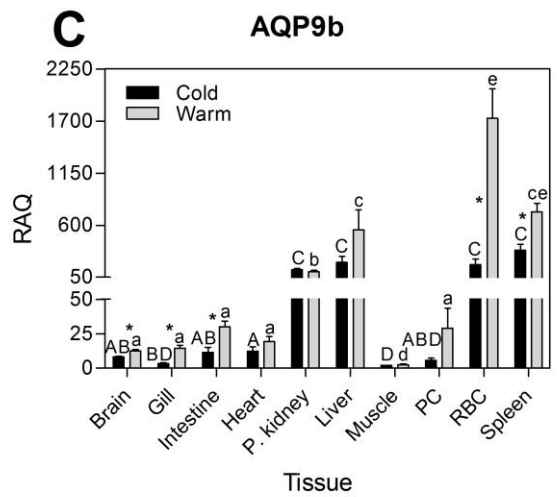
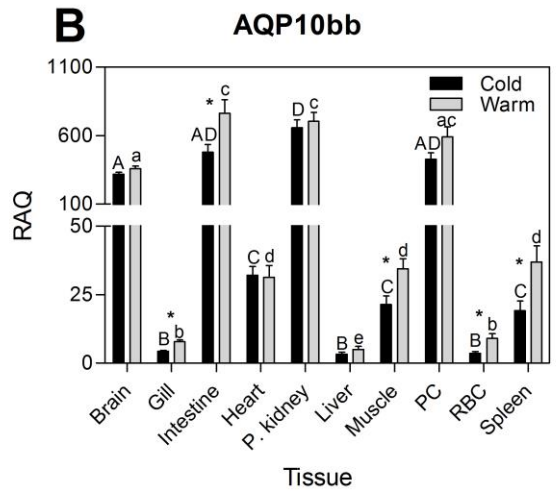
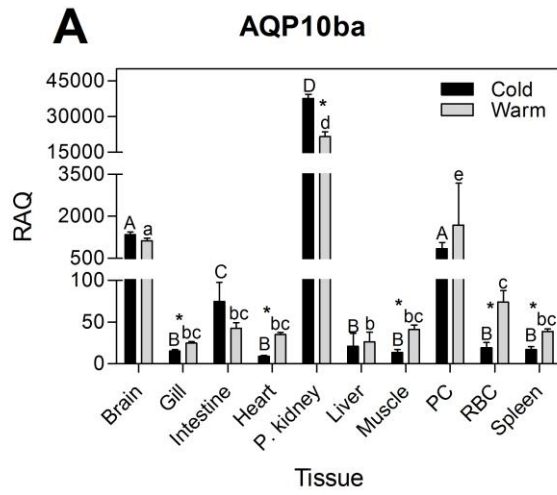
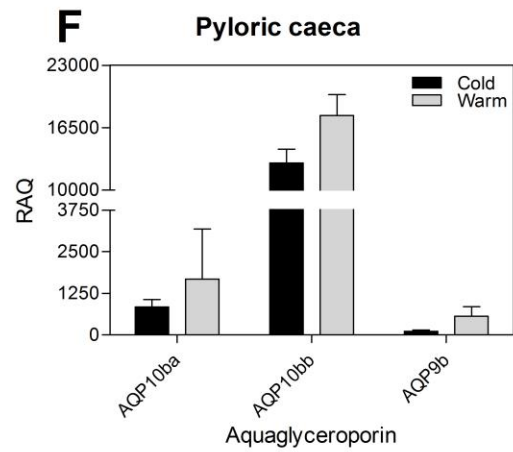
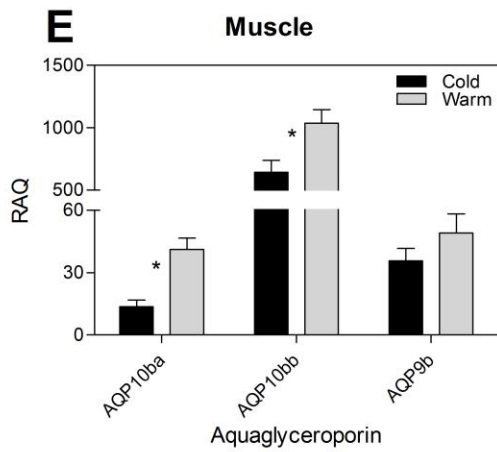
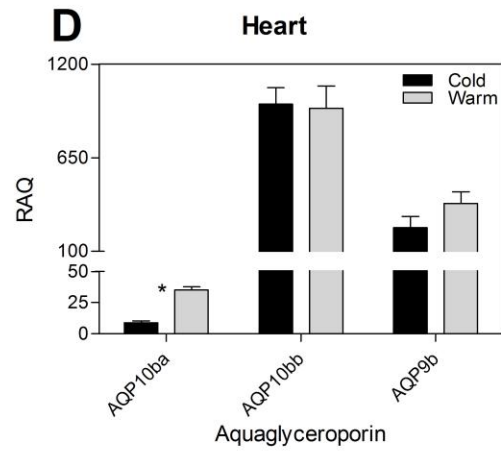
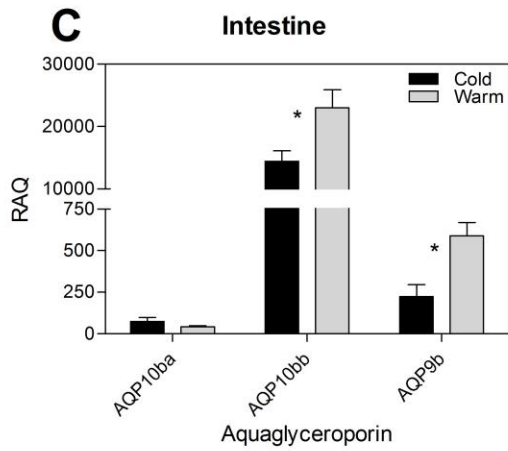
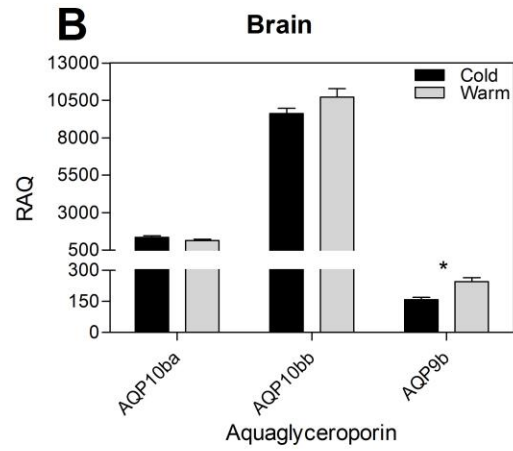
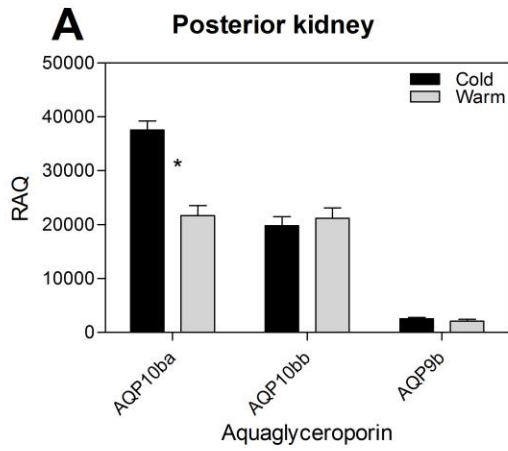
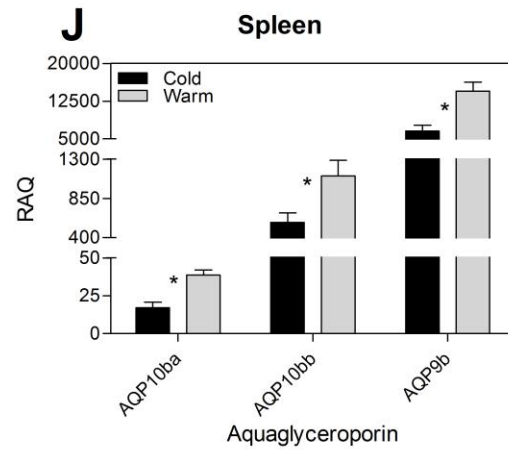
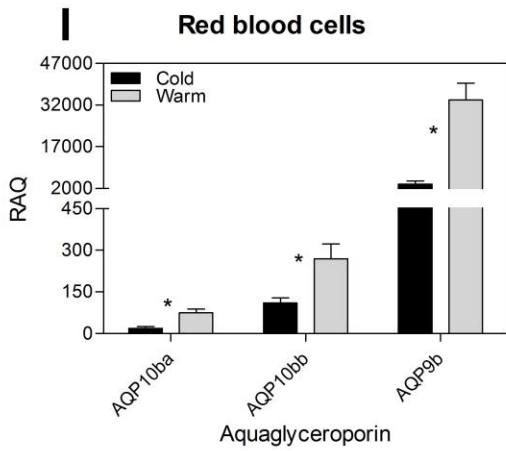
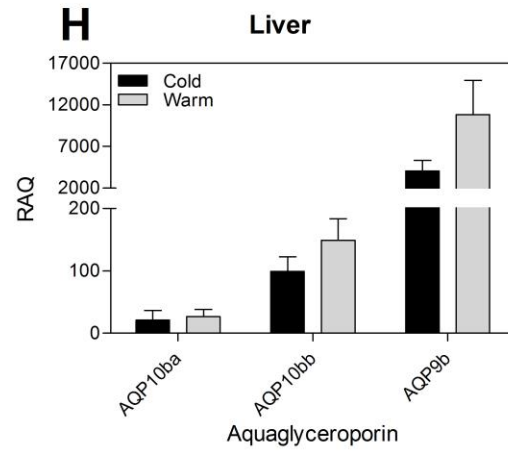
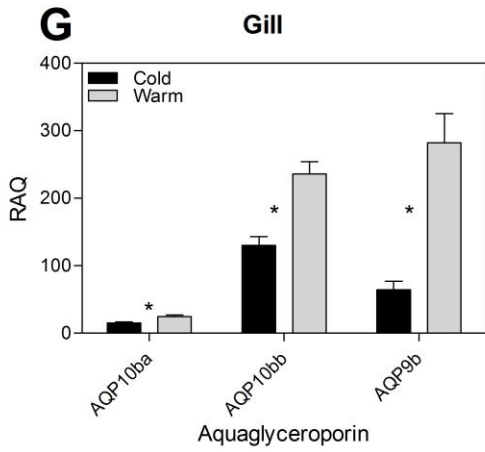


Figure 4.8. Transcript levels of AQP10ba, AQP10bb and AQP9b in various smelt tissues. Gene expression data are presented as RAQ values (mean \pm SE) for the GLP transcript of interest normalized to 18S ribosomal RNA and are calibrated to the sample with the lowest normalized transcript level of any of the three GLPs (assigned a value = 1). In all cases, (n=8). Asterisks denote significant differences in transcript levels between cold and warm smelt. In all cases, $p < 0.05$ was considered to be statistically significant.





caeca at both temperatures and gill at cold temperature. AQP9b was the most abundant transcript in liver, RBCs, and spleen at both temperatures and gill at warm temperature.

4.5 DISCUSSION

4.5.1 Sequence analysis

4.5.1.1 Smelt GLP gene and promoter sequences

The structure of two AQP10b-like genes (AQP10ba and AQP10bb) and an AQP9b-like gene from smelt are reported herein. Their transcribed exon sequences match the cDNA sequences cloned and characterized herein (AQP10ba, AQP10bb) and previously (AQP9b) (13, i.e. Chapter 2). Smelt AQP-like genes are generally similar in structure; however, there are marked differences at the 5' end of the AQP10ba gene in that there are two additional exons that are not present in the AQP10bb and AQP9b genes. The 6 exon structure of the smelt AQP10bb and AQP9b genes has been reported in other GLP-encoding genes in the vertebrate lineage, including those from zebrafish (AQP3b, -7, -9b, -10a and -10b) (52), marine medaka (*Oryzias dancena*) (AQP3b and AQP10b) (21) and human [AQP3 and AQP9 (57), AQP7 (19), and AQP10 (18)]. It is the 8 exon structure of the smelt AQP10ba gene that is atypical. An alignment of the gene sequences for AQP10ba from position 3409 to 4020 (position 4021 is located in exon 3 and corresponds to the START codon for AQP10bb) and for AQP10bb from position -570 to the START codon shows that there is relative homology (~76% identity) in this region. In AQP10ba, the sequence from -1120 to 3408 is novel compared to AQP10bb; AQP10ba has a novel promoter, exon 1, intron 1, exon 2, and an intron 2 that is novel up to the aforementioned region that aligns with the proximal promoter of AQP10bb. The novel 45 bp sequence located at the 5' end of the AQP10ba mRNA that could potentially encode a novel 15 aa sequence at the N-terminus of the AQP10ba putative protein is located in exon 2.

The promoter regions of the smelt AQP10b-like genes and the AQP9b-like gene contain putative transcription factor recognition sites that have also been identified in the promoter regions of other vertebrate GLP-encoding genes. These include sites for the core negative IRE, GR, C/EBP alpha, AP-1 and members of the NF family that were also identified in the promoter regions of the AQP9 genes from human (57) and pig (*Sus scrofa*) (28) and for GATA and TEF-1 (AQP10ba, AQP9b) that were also identified in the human AQP9 promoter. Putative binding sites for the core negative IRE were also identified in the promoter regions of the AQP7 (23, 24) and AQP9 (26) genes from mouse (*Mus musculus*) where they were shown to be regulatory. In fasted rodents, glycerol is released from adipocytes via AQP7 and enters liver via AQP9 where it is an important substrate for hepatic gluconeogenesis (26). In cultured cells from mouse, insulin down-regulated transcript levels of AQP7 in adipocytes (23) and AQP9 in hepatocytes (26), reflective of the fed state. In smelt, the proximal (1 kb) promoter sequences of AQP9b contained 5 putative binding sites for the core negative IRE (Fig. 4.4); and in liver, AQP9b transcripts were expressed at high levels (Fig. 4.7) which is consistent with the traditional role that AQP9b plays in hepatic gluconeogenesis. The proximal (1 kb) promoter sequences of the smelt AQP10b paralogues have more putative binding sites for some transcription factors involved in the stress response than AQP9b (Fig. 4.4). For example, 7 and 5 putative binding sites for GR were identified in AQP10ba and AQP10bb, respectively, compared to 3 for AQP9b. Two putative binding sites for CREB1 were identified in both AQP10b paralogues but none were present in the AQP9b promoter. Glycerol is synthesized in part from liver glycogen stores (59) the breakdown of which can be activated by cAMP. CREB1 binding sites in the AQP10ba

and AQP10bb promoters, similarly activated through a common signal, may help coordinate glycerol synthesis and subsequent entry into cells for its role as a cryoprotectant in smelt.

4.5.1.2 Smelt AQP10b gene duplicates

Sequence comparisons and phylogenetic analyses of the predicted proteins encoded by the smelt AQP10b-like genes suggest that the paralogues did not arise from the whole genome duplication (WGD) event at the root of the crown clade of Teleostei ~350 mya (2) but from a gene duplication event in the smelt lineage that occurred more recently.

There are two AQP10 gene paralogues (AQP10a and AQP10b) in zebrafish that arose through the fish-specific WGD event (52). They encode predicted proteins that are 44% identical; whereas the smelt AQP10b-like genes encode predicted proteins that are 82% identical. Phylogenetic analyses of the predicted proteins encoded by the smelt AQP10b gene paralogues with those from vertebrate GLPs (AQP3, -7, -9, and -10) show that the two putative proteins cluster together (with AQP10bb having a shorter branch length) and with AQP10b-like sequences from zebrafish and other vertebrates, and not with piscine and human AQP10a-like sequences. The high percent identity between the smelt AQP10b-like sequences and their clustering with putative orthologous AQP10b sequences suggest that the smelt AQP10b-like genes are duplicates that arose from a duplication event in the smelt lineage that occurred more recently than the fish-specific WGD event. Osmerids, such as smelt, are diploid and have less than half the amount of genomic DNA of the pseudotetraploid salmonids (58). Therefore, the smelt AQP10b paralogues likely arose from a gene and not a whole genome duplication event. AQP10bb

is likely more similar to the ancestral gene that gave rise to both smelt AQP10b paralogues as it has a conserved gene structure and shorter branch on the phylogenetic tree.

4.5.2 Tissue distribution

QPCR analysis of smelt GLP transcript levels indicated that the smelt AQP10b paralogues and AQP9b were ubiquitously distributed in the ten tissues examined in this study; however, their expression profiles were different. AQP10ba transcripts were most abundant in kidney, brain and pyloric caeca, AQP10bb transcripts were most abundant in kidney, intestine, pyloric caeca and brain, and AQP9b transcripts were most abundant in spleen, liver, RBCs and kidney.

The transcript expression profiles of smelt GLP-encoding genes are consistent with those of orthologous sequences in some tissues but not others. Piscine AQP10b transcript levels have been assessed in zebrafish (52), European eel (*Anguilla anguilla*) (32), gilthead seabream (*Sparus aurata*) (49) and Atlantic salmon (*Salmo salar*) (53). Like smelt, these fish also express AQP10b transcripts at high levels in gastrointestinal tissues and kidney; however, the high AQP10b transcript level in smelt brain is different. AQP10b transcripts were expressed at low levels in eel brain and were not detectable in zebrafish and salmon brains. Low AQP10b levels were detected in smelt and seabream gill but they were not detectable in zebrafish, eel and salmon gill. High AQP10b levels were detected in reproductive tissues from zebrafish and seabream but levels were not assessed in these tissues from smelt, eel or salmon.

Piscine AQP9b transcript levels have been assessed in zebrafish tissues. AQP9b transcripts were detected in brain, gill, liver, eye and ovary but were not detectable in

gastrointestinal tissues, kidney and muscle (15, 52). In humans, AQP9b transcripts were detected in liver and spleen but not in kidney, testis and brain (57). In mouse, AQP9b transcripts were detected in liver, testis and brain but were absent in kidney, colon, heart, and skeletal muscle (56).

The presence of smelt AQP10b and AQP9b transcripts in tissues that have not been shown to express orthologous transcripts in other species may relate to smelt being a glycerol accumulating species (discussed below).

4.5.3 General impact of cold temperature on GLP transcript expression and glycerol transport

Although smelt accumulate high glycerol levels in plasma and tissues to prevent freezing, smelt held at cold temperature generally exhibit lower rates of glycerol transport (5) and lower expression levels of GLP transcripts in all three studies described herein. The exception to this is AQP10ba transcript levels in kidney which increased in response to cold temperature (discussed below). There are, however, physiological correlates that support the concept that GLPs are related to glycerol trafficking in smelt. This was quite pronounced in the case of AQP9b levels and glycerol uptake measurements (5) in smelt RBCs. AQP9b levels were ~9-fold lower in smelt maintained under cold than warm conditions. Glycerol uptake rate by RBCs from smelt acclimated to 8°C and incubated at 8°C was 8 $\mu\text{mol/ g min}$ in comparison to 2 $\mu\text{mol/ g min}$ for RBCs from fish held at 1.2°C and incubated at 1°C. AQP9b transcript levels are substantially higher in smelt RBCs than heart. Glycerol uptake by RBCs is inhibited by phloretin indicating a facilitated transport mechanism; whereas, glycerol uptake rate by hearts from smelt is about 1/10 the

rate of that of RBCs under similar conditions and appears not to involve facilitated transport (5).

There is also evidence that smelt may naturally have a high capacity for glycerol synthesis and transport. Although this contention is yet-to-be assessed, smelt exhibit an increased capacity for metabolic flux (increased enzyme activities) through pathways to glycerol synthesis compared to non-glycerol accumulating species such as capelin (*Mallotus villosus*), Atlantic tomcod (*Microgadus tomcod*) and smooth flounder (*Liopsetta putmani*) including glycolysis (phosphofructokinase, aldolase), amino acid metabolism [aspartate aminotransferase (AspAT), alanine aminotransferase (AAT), and glutamate dehydrogenase (GDH)], gluconeogenesis (phosphoenolpyruvate carboxykinase) and glyceroneogenesis [cytosolic glycerol-3-phosphate dehydrogenase (cGPDH)] (9, 48, 54). Smelt express GLP transcripts in tissues that have not been shown to express orthologous transcripts in other species. As smelt accumulate glycerol in these tissues (8, 42), the ubiquitous expression of smelt GLP transcripts may be an evolutionary response to facilitate glycerol entry into the cell, at least initially. Interestingly, the tissue with the highest glycerol level ($236 \mu\text{mol g}^{-1}$) was kidney and the tissue with the lowest glycerol level ($125 \mu\text{mol g}^{-1}$) was gill (8). Although it does not take into consideration transcript levels of other GLP-encoding genes potentially expressed in these tissues, transcript levels of the three GLP-encoding genes measured in the current study were substantially higher in kidney than in gill. Finally, although glycerol uptake rates are lower in smelt RBCs and hearts at cold than at warm temperatures, they are both higher than in the non-glycerol accumulating Atlantic salmon (5).

Glycerol uptake, and GLP transcript and protein expression have been examined in RBCs from cold- and warm-acclimated Cope's gray treefrogs (*Hyla chrysoscelis*), an anuran that accumulates high glycerol level (> 100 mM) in extracellular fluid in winter (11, 36). Glycerol uptake in frog is consistent with that seen in smelt. Glycerol permeation assessed by osmotic lysis was also lower (~10-fold) at 5°C than at 20°C for both warm- and cold-acclimated frogs. Greater glycerol permeability was observed in northern compared to southern populations. Uptake of radio-labeled glycerol and osmotic lysis was inhibited by 0.3 mM HgCl₂, indicating a facilitated transport mechanism. A GLP cDNA was cloned from Cope's gray treefrog (60) and its putative protein clusters with AQP3s (Fig. 4.2). However, unlike AQP9b and AQP10b transcripts in smelt RBCs, AQP3 transcript and protein levels were cold-upregulated in frog RBCs although this did not enhance glycerol permeability (11, 36).

4.5.4 Plasma urea and kidney AQP10ba transcript levels in response to cold temperature

In both the temperature step-down experiment and the seasonal study, plasma urea levels in cold smelt increased significantly over time in parallel with glycerol build-up, and were significantly higher than warm smelt. Increased urea levels could be attributed to *de novo* synthesis and / or urea retention in kidney.

In terms of urea synthesis, initial glycerol accumulation is fuelled through the mobilization of glycogen (8) resulting in significantly lower liver glycogen levels in cold compared to warm smelt over time (14, i.e. Chapter 3). To sustain the carbon demand for glycerol production, smelt feed constantly on a high-protein invertebrate diet (8, 45) and synthesize glycerol directly from both glucose and amino acids (59). Levels of liver

AspAT, AAT, and GDH were all higher in smelt than in non-glycerol/urea accumulating species (9, 54) and in smelt, increased during the seasonal transition from October through to March (29). The transcript level of GDH increased from October through to January (47) as did transcript levels of both GDH and AAT in cells isolated from 8°C-acclimated fish and incubated at 0.4°C for 24 hr (13, i.e. Chapter 2).

When glycerol synthesis is fuelled by the deamination of amino acids, the resultant ammonia must be excreted or detoxified. In cultured smelt hepatocytes (13, i.e. Chapter 2) and liver (14, i.e. Chapter 3), glutamine synthetase (GS) transcripts were significantly higher at cold compared to warm temperature suggesting that ammonia is converted to glutamine. In adult smelt liver, the ornithine urea cycle appears to be nonfunctional (46), however glutamine could be converted to urea via purine synthesis / uricolysis. Catabolism of arginine (argininolysis) derived from the high-protein diet consumed by smelt is another pathway for urea synthesis. Smelt have high uricase and especially arginase enzyme activities compared to ocean pout (*Macrozoarces americanus*), starry flounder (*Platichthys stellatus*) and saffron cod (*Eleginus gracilis*) suggesting an increased capacity for urea synthesis; however, there was no relation found between urea and activity levels of these enzymes in fall and winter caught smelt (46). In smelt, renal urea conservation may be an important contributor to high urea levels in winter.

The most striking finding of the current study is that AQP10ba transcript levels in kidney always increase at cold temperatures. It is the only GLP transcript that responds in this fashion. The proximal promoter sequences of AQP10ba and AQP10bb are different in terms of numbers of putative transcription factor binding sites (e.g. core negative IRE),

which is consistent with different expression patterns. The AQP10b paralogues encode putative proteins with N- and C-termini that are quite different; whether these differences affect solute permeability warrants further investigation. The physiological consequences of increased AQP10ba transcript levels and presumably increased levels of the resultant protein in kidney could relate to renal urea conservation.

At cold temperatures, smelt have elevated plasma levels of glycerol, urea, and Na^+ relative to animals at summer temperatures (44). In winter-acclimated smelt, glycerol level in urine was similar to that of plasma (43); however, urea levels in urine (6 mM) were lower than in plasma (18 mM) (44). Such a difference requires active mechanisms for the movement of urea against a concentration gradient.

For unknown reasons, urea levels are also lower in urine (1.1 mM) than in plasma (1.9 mM) of rainbow trout. The fractional rate of reabsorption of urea is greater than that of water so the process is not due to solvent drag. Furthermore, the rate of urea reabsorption correlates with Na^+ reabsorption. These findings imply an active mechanism of urea transport that may directly or secondarily be associated with Na^+ retention (3, 34).

Osmerus mordax dentex has a glomerular kidney. The tubular portion of the nephron includes a ciliated neck segment and two proximal segments before entering the collecting tubule. There is no distal segment. Structural integrity of the kidney is maintained between 13°C and 0.4°C (39). Functional integrity is presumably also maintained at low temperatures although urine flow is greatly reduced (43).

Atlantic salmon kidney expresses AQP10b transcripts with the protein being localized to the apical membrane of cells in the proximal tubule (10). If a similar situation occurs in smelt, AQP10ba could serve as a conduit for the passive movement of urea

from the glomerular filtrate into the epithelial cells of the proximal tubule. This would require maintaining low levels of urea within these cells in order to create a concentration gradient and an active mechanism of pumping urea into the plasma.

Taken together, at low winter temperatures, the increased AQP10ba transcript level in smelt kidney could result in elevated levels of protein that would allow the passive diffusion of urea from the glomerular filtrate into the epithelial cells of the proximal tubule. An active urea transport mechanism that may be Na⁺ dependent would move urea against a concentration gradient into the plasma. The challenge is to design experiments to test this hypothesis. Regardless, the repeated finding of increased expression of AQP10ba transcripts in kidney under different challenges at low temperature, in contrast to the expression of AQP10bb and AQP9b in kidney and all three transcripts in all other tissues, is unequivocal and novel and warrants further investigation.

4.5.5 Conclusions

Full-length cDNA sequences for two AQP10b paralogous genes (AQP10ba, AQP10bb), and the gene / promoter sequences for them and AQP9b, were cloned and characterized from smelt. Direct sequence comparisons at the gene structure / promoter, mRNA and predicted protein level, and phylogenetic analyses, suggest that the AQP10b paralogues arose from a gene duplication event specific to the smelt lineage, with AQP10bb retaining ancestral gene structure. QPCR was used to measure transcript levels of the GLP-encoding genes in smelt maintained at warm and cold temperatures. Smelt held at cold temperature generally exhibited lower GLP transcript expression; however, AQP10ba transcripts were consistently cold temperature up-regulated in kidney. As there

is a concomitant increase in plasma urea levels with cold temperature, the differential regulation of AQP10ba expression in kidney may be an evolutionary response to aid in the reabsorption of urea generated as a byproduct of glycerol synthesis-related protein catabolism, thereby conserving nitrogen in a non-toxic form that also serves as a cryoprotectant. The generally lower GLP transcript levels in smelt maintained at cold compared to warm temperature was consistent with lower rates of glycerol transport in smelt RBCs and heart.

4.6 REFERENCES

1. **Agre P, King LS, Yasui M, Guggino WB, Ottersen OP, Fujiyoshi Y, Engel A, Nielsen S.** Aquaporin water channels - from atomic structure to clinical medicine. *J Physiol* 542: 3-16, 2002.
2. **Amores A, Force A, Yan YL, Joly L, Amemiya C, Fritz A, Ho RK, Langeland J, Prince V, Wang YL, Westerfield M, Ekker M, Postlethwait JH.** Zebrafish hox clusters and vertebrate genome evolution. *Science* 282: 1711-1714, 1998.
3. **Bucking C, Wood CM.** Does urea reabsorption occur via the glucose pathway in the kidney of the freshwater rainbow trout? *Fish Physiol Biochem* 30: 1-12, 2004.
4. **Cerdà J, Finn RN.** Piscine aquaporins: an overview of recent advances. *J Exp Zool A Ecol Genet Physiol* 313: 623-650, 2010.
5. **Clow KA, Driedzic WR.** Glycerol uptake is by passive diffusion in the heart but by facilitated transport in RBCs at high glycerol levels in cold acclimated rainbow smelt (*Osmerus mordax*). *Am J Physiol Regul Integr Comp Physiol* 302: R1012-R1021, 2012.
6. **Ditlecadet D, Short CE, Driedzic WR.** Glycerol loss to water exceeds glycerol catabolism via glycerol kinase in freeze-resistant rainbow smelt (*Osmerus mordax*). *Am J Physiol Regul Integr Comp Physiol* 300: R674-R684, 2011.

7. **Driedzic WR, Clow KA, Short CE, Ewart KV.** Glycerol production in rainbow smelt (*Osmerus mordax*) may be triggered by low temperature alone and is associated with the activation of glycerol-3-phosphate dehydrogenase and glycerol-3-phosphatase. *J Exp Biol* 209: 1016-1023, 2006.

8. **Driedzic WR, Short CE.** Relationship between food availability, glycerol and glycogen levels in low-temperature challenged rainbow smelt *Osmerus mordax*. *J Exp Biol* 210: 2866-2872, 2007.

9. **Driedzic WR, West JL, Sephton DH, Raymond JA.** Enzyme activity levels associated with the production of glycerol as an antifreeze in liver of rainbow smelt (*Osmerus mordax*). *Fish Physiol Biochem* 18: 125-134, 1998.

10. **Engelund MB, Madsen SS.** Tubular localization and expressional dynamics of aquaporins in the kidney of seawater-challenged Atlantic salmon. *J Comp Physiol B* 185: 207-223, 2015.

11. **Goldstein DL, Frisbie J, Diller A, Pandey RN, Krane CM.** Glycerol uptake by erythrocytes from warm- and cold-acclimated Cope's gray treefrogs. *J Comp Physiol B* 180: 1257-1265, 2010.

12. **Gutmann I, Bergmeyer HU.** Enzymes as biochemical reagents. In: *Methods of Enzymatic Analysis*, edited by Bergmeyer HU. New York: Academic Press, 1974, vol. 4, p. 1794-1798.
13. **Hall JR, Clow KA, Rise ML, Driedzic WR.** Identification and validation of differentially expressed transcripts in a hepatocyte model of cold-induced glycerol production in rainbow smelt (*Osmerus mordax*). *Am J Physiol Regul Integr Comp Physiol* 301: R995-R1010, 2011.
14. **Hall JR, Short CE, Rise ML, Driedzic WR.** Expression analysis of glycerol synthesis-related liver transcripts in rainbow smelt (*Osmerus mordax*) exposed to a controlled decrease in temperature. *Physiol Biochem Zool* 85: 74-84, 2012.
15. **Hamdi M, Sanchez MA, Beene LC, Liu Q, Landfear SM, Rosen BP, Liu Z.** Arsenic transport by zebrafish aquaglyceroporins. *BMC Mol Biol.* 10: 104, 2009.
16. **Hub JS, de Groot BL.** Mechanism of selectivity in aquaporins and aquaglyceroporins. *Proc Natl Acad Sci U S A* 105: 1198-1203, 2008.
17. **Ishibashi K, Kondo S, Hara S, Morishita Y.** The evolutionary aspects of aquaporin family. *Am J Physiol Regul Integr Comp Physiol* 300: R566-R576, 2011.

18. **Ishibashi K, Morinaga T, Kuwahara M, Sasaki S, Imai M.** Cloning and identification of a new member of water channel (AQP10) as an aquaglyceroporin. *Biochim Biophys Acta* 1576: 335-340, 2002.
19. **Ishibashi K, Yamauchi K, Kageyama Y, Saito-Ohara F, Ikeuchi T, Marumo F, Sasaki S.** Molecular characterization of human Aquaporin-7 gene and its chromosomal mapping. *Biochim Biophys Acta* 1399: 62-66, 1998.
20. **Kel AE, Gößling E, Reuter I, Cheremushkin E, Kel-Margoulis OV, Wingender E.** MATCH: A tool for searching transcription factor binding sites in DNA sequences. *Nucleic Acids Res* 31: 3576-3579, 2003.
21. **Kim YK, Lee SY, Kim BS, Kim DS, Nam YK.** Isolation and mRNA expression analysis of aquaporin isoforms in marine medaka *Oryzias dancena*, a euryhaline teleost. *Comp Biochem Physiol A Mol Integr Physiol* 171: 1-8, 2014.
22. **King LS, Kozono D, Agre P.** From structure to disease: the evolving tale of aquaporin biology. *Nat Rev Mol Cell Biol* 5: 687-698, 2004.
23. **Kishida K, Shimomura I, Kondo H, Kuriyama H, Makino Y, Nishizawa H, Maeda N, Matsuda M, Ouchi N, Kihara S, Kurachi Y, Funahashi T, Matsuzawa Y.** Genomic structure and insulin-mediated repression of the aquaporin adipose (AQPap), adipose-specific glycerol channel. *J Biol Chem* 276: 36251-36260, 2001.

24. **Kondo H, Shimomura I, Kishida K, Kuriyama H, Makino Y, Nishizawa H, Matsuda M, Maeda N, Nagaretani H, Kihara S, Kurachi Y, Nakamura T, Funahashi T, Matsuzawa Y.** Human aquaporin adipose (AQPap) gene. Genomic structure, promoter analysis and functional mutation. *Eur J Biochem* 269: 1814-1826, 2002.
25. **Krogh A, Larsson B, von Heijne G, Sonnhammer EL.** Predicting transmembrane protein topology with a hidden Markov model: application to complete genomes. *J Mol Biol* 305: 567-580, 2001.
26. **Kuriyama H, Shimomura I, Kishida K, Kondo H, Furuyama N, Nishizawa H, Maeda N, Matsuda M, Nagaretani H, Kihara S, Nakamura T, Tochino Y, Funahashi T, Matsuzawa Y.** Coordinated regulation of fat-specific and liver specific glycerol channels, aquaporin adipose and aquaporin 9. *Diabetes* 51: 2915-2921, 2002.
27. **Lewis JM, Ewart KV, Driedzic WR.** Freeze resistance in rainbow smelt (*Osmerus mordax*): seasonal pattern of glycerol and antifreeze protein levels and liver enzyme activity associated with glycerol production. *Physiol Biochem Zool* 77: 415-422, 2004.
28. **Li X, Lei T, Xia T, Chen X, Feng S, Chen H, Chen Z, Peng Y, Yang Z.** Molecular characterization, chromosomal and expression patterns of three aquaglyceroporins (AQP3, 7, 9) from pig. *Comp Biochem Physiol B Biochem Mol Biol* 149: 468-476, 2008.

29. **Liebscher RS, Richards RC, Lewis JM, Short CE, Muise DM, Driedzic WR, Ewart KV.** Seasonal freeze resistance of rainbow smelt (*Osmerus mordax*) is generated by differential expression of glycerol-3-phosphate dehydrogenase, phosphoenolpyruvate carboxykinase, and antifreeze protein genes. *Physiol Biochem Zool* 79: 411-423, 2006.
30. **Litman T, Søgaard R, Zeuthen T.** Ammonia and urea permeability of mammalian aquaporins. In: *Handb Exp Pharmacol*, edited by Beitz E. Berlin: Springer, 2009, p. 327-358.
31. **Livak KJ, Schmittgen TD.** Analysis of relative gene expression data using real-time quantitative PCR and the $2^{-\Delta\Delta CT}$ method. *Methods* 25: 402-408, 2001.
32. **Martinez AS, Cutler CP, Wilson GD, Phillips C, Hazon N, Cramb G.** Cloning and expression of three aquaporin homologues from the European eel (*Anguilla anguilla*): effects of seawater acclimation and cortisol treatment on renal expression. *Biol Cell* 97: 615-627, 2005.
33. **Matys V, Kel-Margoulis OV, Fricke E, Liebich I, Land S, Barre-Dirrie A, Reuter I, Chekmenev D, Krull M, Hornischer K, Voss N, Stegmaier P, Lewicki-Potapov B, Saxel H, Kel AE, Wingender E.** TRANSFAC and its module TRANSCompel: transcriptional gene regulation in eukaryotes. *Nucleic Acids Res* 34: D108-D110, 2006.

34. **McDonald MD, Wood CM.** Reabsorption of urea by the kidney of the freshwater rainbow trout. *Fish Physiol Biochem* 18: 375-386, 1998.
35. **Mount SM.** A catalogue of splice junction sequences. *Nucleic Acids Res* 10: 459-472, 1982.
36. **Mutyam V, Puccetti MV, Frisbie J, Goldstein DL, Krane CM.** Dynamic regulation of aquaglyceroporin expression in erythrocyte cultures from cold- and warm-acclimated Cope's gray treefrog, *Hyla chrysoscelis*. *J Exp Zool A Ecol Genet Physiol* 315: 424-437, 2011.
37. **O'Brien RM, Granner DK.** Regulation of gene expression by insulin. *Physiol Rev* 76: 1109-1161, 1996.
38. **O'Brien RM, Streeper RS, Ayala JE, Stadelmaier BT, Hornbuckle LA.** Insulin-regulated gene expression. *Biochem Soc Trans* 29: 552-558, 2001.
39. **Ogawa M, Fukuda M, Hayashida A, Fukuchi M.** On the kidney and the adrenocortical tissue of toothed smelt, *Osmerus mordax dentex* and surf smelt, *Hypomesus pretiosus japonicas* and their cold adaptation. *Proc NIPR Symp Polar Biol* 4: 30-35, 1991.

40. **Patthy L.** Intron-dependent evolution: preferred types of exons and introns. *FEBS Lett* 214: 1-7, 1987.
41. **Pfaffl MW.** A new mathematical model for relative quantification in real-time RT-PCR. *Nucleic Acids Res* 29: e45, 2001.
42. **Raymond JA.** Glycerol is a colligative antifreeze in some northern fishes. *J Exp Zool* 262: 347-352, 1992.
43. **Raymond JA.** Glycerol and water balance in a near-isosmotic teleost, winter-acclimated smelt. *Can J Zool* 71: 1849-1854, 1993.
44. **Raymond JA.** Seasonal variations of trimethylamine oxide and urea in the blood of a cold-adapted marine teleost, the rainbow smelt. *Fish Physiol Biochem* 13: 13-22, 1994.
45. **Raymond JA.** Glycerol synthesis in the rainbow smelt *Osmerus mordax*. *J Exp Biol* 198: 2569-2573, 1995.
46. **Raymond JA.** Trimethylamine oxide and urea synthesis in rainbow smelt and some other northern fishes. *Physiol Zool* 71: 515-523, 1998.

47. **Richards RC, Short CE, Driedzic WR, Ewart KV.** Seasonal changes in hepatic gene expression reveal modulation of multiple processes in rainbow smelt (*Osmerus mordax*). *Mar Biotechnol* 12: 650-663, 2010.
48. **Robinson J, Hall JR, Charman M, Ewart KV, Driedzic WR.** Molecular analysis, tissue profiles and seasonal patterns of cytosolic and mitochondrial GPDH in freeze resistant rainbow smelt (*Osmerus mordax*). *Physiol Biochem Zool* 84: 363-376, 2011.
49. **Santos CR, Estêvão MD, Fuentes J, Cardoso JC, Fabra M, Passos AL, Detmers FJ, Deen PM, Cerdà J, Power DM.** Isolation of a novel aquaglyceroporin from a marine teleost (*Sparus auratus*): function and tissue distribution. *J Exp Biol* 207: 1217-1227, 2004.
50. **Tamura K, Stecher G, Peterson D, Filipinski A, Kumar S.** MEGA6: Molecular Evolutionary Genetics Analysis version 6.0. *Mol Biol Evol* 30: 2725-2729, 2013.
51. **Thompson JD, Higgins DG, Gibson TJ.** CLUSTAL W: improving the sensitivity of progressive multiple sequence alignment through sequence weighting, position-specific gap penalties and weight matrix choice. *Nucleic Acids Res* 22: 4673-4680, 1994.

52. **Tingaud-Sequeira A, Calusinska M, Finn RN, Chauvigné F, Lozano J, Cerdà J.** The zebrafish genome encodes the largest vertebrate repertoire of functional aquaporins with dual paralogy and substrate specificities similar to mammals. *BMC Evol Biol* 10: 38, 2010.
53. **Tipsmark CK, Sørensen KJ, Madsen SS.** Aquaporin expression dynamics in osmoregulatory tissues of Atlantic salmon during smoltification and seawater acclimation. *J Exp Biol* 213: 368-379, 2010.
54. **Treberg JR, Lewis JM, Driedzic WR.** Comparison of liver enzymes in osmerid fishes: key differences between a glycerol accumulating species, rainbow smelt (*Osmerus mordax*), and a species that does not accumulate glycerol, capelin (*Mallotus villosus*). *Comp Biochem Physiol A Mol Integr Physiol* 132: 433-438, 2002.
55. **Treberg JR, Wilson CE, Richards RC, Ewart KV, Driedzic WR.** The freeze-avoidance response of smelt *Osmerus mordax*: initiation and subsequent suppression of glycerol, trimethylamine oxide and urea accumulation. *J Exp Biol* 205: 1419-1427, 2002.
56. **Tsukaguchi H, Shayakul C, Berger UV, Mackenzie B, Devidas S, Guggino WB, van Hoek AN, Hediger MA.** Molecular characterization of a broad selectivity neutral solute channel. *J Biol Chem* 273: 24737-24743, 1998.

57. **Tsukaguchi H, Weremowicz S, Morton CC, Hediger MA.** Functional and molecular characterization of the human neutral solute channel aquaporin-9. *Am J Physiol* 277: F685-696, 1999.
58. **von Schalburg KR, Leong J, Cooper GA, Robb A, Beetz-Sargent MR, Lieph R, Holt RA, Moore R, Ewart KV, Driedzic WR, ten Hallers BF, Zhu B, de Jong PJ, Davidson WS, Koop BF.** Rainbow smelt (*Osmerus mordax*) genomic library and EST resources. *Mar Biotechnol (NY)* 10: 487-491, 2008.
59. **Walter JA, Ewart KV, Short CE, Burton IW, Driedzic WR.** Accelerated hepatic glycerol synthesis in rainbow smelt (*Osmerus mordax*) is fuelled directly by glucose and alanine: a ^1H and ^{13}C nuclear magnetic resonance study. *J Exp Zool A* 305: 480-488, 2006.
60. **Zimmerman SL, Frisbie J, Goldstein DL, West J, Rivera K, Krane CM.** Excretion and conservation of glycerol, and expression of aquaporins and glyceroporins, during cold acclimation in Cope's gray tree frog *Hyla chrysoscelis*. *Am J Physiol Regul Integr Comp Physiol* 292: R544-R555, 2007.

CHAPTER 5: SUMMARY

5.1 SUMMARY OF THESIS FINDINGS

5.1.1 *Glycerol synthesis*

The first objective of this thesis was to identify informative transcripts in the initiation and early stages of cold adaptation and more specifically glyceroneogenesis by using functional genomic techniques and QPCR to compare the transcript expression profiles of livers from non-glycerol and from glycerol accumulating smelt generated using cold temperature-induced models of glycerol synthesis. As hypothesized and as described below, these analyses made significant contributions towards elucidating the molecular underpinnings of glycerol synthesis and identifying novel aspects of the cold temperature response in smelt liver. The results of the QPCR analyses from the *in vitro* and *in vivo* studies are summarized in sections 5.1.1.1 and 5.1.1.2, respectively. An interpretation of these results is provided in section 5.1.1.3.

5.1.1.1 *Hepatocyte model of cold temperature-induced glycerol synthesis*

In Chapter 2, the transcript expression profiles of cultured hepatocytes incubated at warm (8°C; non-glycerol accumulating) or cold (0.4°C; glycerol accumulating) temperature (5) were compared over a 72 h time course. Reciprocal SSH cDNA libraries, enriched for cold-responsive transcripts, generated 581 ESTs from the forward SSH library (enriched for transcripts that were expressed at higher levels in cold than warm cells at 72 h) and 179 ESTs from the reverse SSH library (enriched for transcripts that were expressed at higher levels in warm than cold cells at 72 h). Microarray analyses using a cGRASP 16K salmonid cDNA array (49) identified 112 reproducibly informative transcripts (25 higher expressed in cold cells, 87 higher expressed in warm cells) for the

24 h, 48 h and 72 h time points. Expression of type II AFP and 21 glycerol synthesis pathway-related transcripts were validated using QPCR. These analyses confirmed at the cellular level that increases in type II AFP transcript levels were not significantly influenced by temperature. However, cold temperature-induced glycerol synthesis had a profound effect on the metabolism of cold compared to warm cells. Highlights of the glyceroneogenesis-related QPCR analyses are described below.

In terms of carbohydrate metabolism, it should be noted that in both warm and cold cells, there were significant decreases in transcript levels of the glucose transporter, GLUT2, at all three incubation times compared to pre-incubation. This may have impaired glucose transport into the cells, even in the presence of the exogenous glucose supplement. Therefore, to provide G6P, transcript levels of PGM (glycogen catabolism) were higher in cells incubated at both warm and cold temperatures compared to pre-incubation.

In warm cells, the G6P that was available was readily oxidized with levels of glucose oxidation-related transcripts significantly higher than pre-incubation levels. Considering glucose oxidation to drive ATP synthesis, transcript levels of PFK (glycolysis) and mGPDH (transfer of glycolysis-derived cytosolic NADH to the mitochondrion via the glycerol-3-phosphate shuttle) were significantly higher at all 3 time points, and PDK2 (inhibits PDH, and hence the oxidation of pyruvate to acetyl CoA) were significantly lower by 48 h. Considering glucose oxidation via the pentose phosphate shunt (generates NADPH for the reductive biosynthesis of lipids), transcript levels of 6PGDH and TALDO1 were significantly higher at all 3 time points. Transcript

levels of G6Pase (glucose synthesis) were not significantly different from pre-incubation levels.

In cold cells, however, transcript levels of PFK, mGPDH, 6PGDH and TALDO1 were not significantly different from pre-incubation levels and were significantly lower than warm cells throughout the incubation. Although PFK levels in cold cells were not significantly different from pre-incubation and were only 2- to 3-fold significantly lower than warm cells, levels of PDK2 in cold cells were approximately 3-fold significantly higher than pre-incubation and 20-fold significantly higher than warm cells by 72 h. PDH inhibition would serve to inhibit the lower portion of glycolysis and thereby channel G6P-derived DHAP towards glycerol as opposed to oxidation to drive ATP and / or lipid synthesis. G6Pase transcript levels, at least transiently, were significantly higher compared to pre-incubation levels and marginally higher ($p=0.08$) than warm cells at 24 h.

In terms of amino acid metabolism, in warm cells, transcript levels of AAT2 (alanine to pyruvate) and GS (glutamate to glutamine), were significantly lower at all 3 time points compared to pre-incubation. This is likely related to warm cells being heavily reliant on glucose oxidation to drive ATP synthesis.

In cold cells, however, a number of transcripts (PEPCK, MDH2, AAT2, GDH, GS and AQP9) associated with mobilization of amino acids were all transiently higher during the early stage of the temperature transition, with AAT2 and GS levels significantly higher in cold compared to warm cells at all time points. With high levels of PDH inhibition in cold cells, amino acid-derived pyruvate or oxaloacetate would be channeled towards glyceroneogenesis as opposed to oxidation to acetyl CoA / CO₂.

In terms of lipid metabolism, in warm cells, there were higher levels of lipid synthesis-related transcripts (6PGDH and TALDO1) and lower levels of lipid catabolism-related transcripts (LIPL) compared to pre-incubation.

In cold cells, where amino acids (e.g. alanine) and / or carbohydrates are channeled to glycerol as opposed to oxidation (PDH inhibition), fatty acid oxidation was an important pathway for generating reducing equivalents to drive ATP synthesis. As such, levels of most lipid metabolism genes remained at pre-incubation levels, with significantly higher levels of lipid catabolism-related transcripts and significantly lower levels of lipid synthesis-related transcripts in cold compared to warm cells. For example, transcripts levels of LIPL were significantly higher in cold compared to warm cells at all three time points. As LIPL catalyzes the rate limiting step in the hydrolysis of triglyceride to generate 2-monoacylglycerol and non-esterified fatty acids, in cold cells, triglyceride breakdown could be a transient source of glycerol while supplying fatty acids as a metabolic fuel. Levels of transcripts involved in the activation of fatty acids to CoA esters for entry into β -oxidation were higher in cold compared to warm cells at 48 and 72 h [SLC27A6 (activates very long chain fatty acids)] or increased over time in cold cells [ACSL4 (preferentially utilizes arachidonate)]. The first step in the β oxidation of fatty acids is catalyzed by acyl-CoA dehydrogenase, with electrons transferred to FAD; FADH₂ donates its electrons to an electron carrier of the mitochondrial respiratory chain, electron-transferring flavoprotein (ETF). The second step is catalyzed by enoyl-CoA hydratase. Although not verified by QPCR, ETF subunit beta (GenBank accession numbers GR556955, GR556956) and enoyl-CoA hydratase (GR557174) transcripts were

identified in the forward (genes expressed at higher levels in the cold than warm cells at 72 hours) hepatocyte SSH library (Supplemental Table S2.1).

In terms of glyceroneogenesis-related genes, increased glycerol production by isolated hepatocytes was not associated with increased transcript levels of cGPDH. Finally, in cold cells, transcript levels of a phosphatase that is potentially G3Pase were significantly higher than pre-incubation at 24 h, and were significantly higher than warm cells at all three incubation times.

In conclusion, metabolism in warm cells was characterized by glucose oxidation driving ATP synthesis, and lipid synthesis. However, metabolism in cold, glycerol accumulating cells was characterized by PDH inhibition channeling G6P-derived DHAP and amino acid-derived pyruvate and oxaloacetate towards glycerol as opposed to oxidation to CO₂, with fatty acid oxidation driving ATP synthesis. In cultured cells, where glucose was potentially limiting, amino acid-derived metabolites were an important source of glycerol. Increased glycerol production was not associated with increased transcript levels of cGPDH.

5.1.1.2 Whole animal temperature “step-down” model of cold temperature-induced glycerol synthesis

In Chapter 3, the whole animal temperature “step-down” model of cold temperature-induced glycerol production (7) was used to determine if the transcript expression profiles of the genes measured by QPCR in Chapter 2 held true *in vivo*, where livers were exposed to a physiological extracellular environment. In warm smelt livers, transcript levels of only two genes, PFK and 6PGDH, were significantly higher in February compared to January. These increases were likely related to increased energy

demand and lipid synthesis associated with gonad production. Smelt held at warm temperatures underwent spawning earlier (in late February) than those following ambient water temperatures. Therefore, this section will describe transcript expression levels in cold smelt livers over time and in comparison to warm smelt livers.

In terms of carbohydrate metabolism, there were no significant differences in GLUT2 transcript levels in cold smelt livers with respect to time or temperature. In cold compared to warm smelt, liver glycogen levels were significantly lower in January and tended to be lower in February. In accordance with glycogen utilization, liver PGM transcript levels tended to be significantly higher. PFK (4.6-fold) and mGPDH (3.5-fold) transcript levels were significantly higher in cold smelt livers in February compared to January, suggesting increased flux through glycolysis. However, PDK2 (2.6-fold) transcript levels were also significantly higher in cold smelt livers in February compared to January, likely to channel some of the G6P-derived DHAP towards glycerol; thereby regulating glucose oxidation and G6P-derived glycerol synthesis. Plasma glucose levels were significantly higher in cold compared to warm smelt, in both January and February; consistent with a release of glucose from glycogen, liver G6Pase transcript levels were significantly higher in parallel.

In terms of amino acid metabolism, there were no significant differences in cold smelt livers with respect to time or temperature in transcript levels of PEPCK and MDH2. Furthermore, in cold compared to warm smelt livers, transcript levels of AAT2 and GDH were generally lower in both January and February; however, in cold smelt livers, AAT2 transcript levels were borderline significantly higher ($p = 0.08$) in February than January. GS transcript levels were significantly higher in cold than warm smelt livers in both

January and February; however, there were no significant differences in cold smelt livers with respect to time or temperature in transcript levels of AQP9.

In terms of lipid metabolism, in cold compared to warm smelt livers, transcript levels of LIPL were significantly higher in February and transcript levels of ACSL4 were significantly higher in January, suggesting fatty acid oxidation as a metabolic fuel.

In terms of glyceroneogenesis-related transcripts, in cold smelt livers, there were no significant differences in cGPDH transcript levels with respect to time and cGPDH transcript levels were significantly lower compared to warm smelt livers in both January and February. Levels of a phosphatase that is potentially G3Pase were significantly higher in cold smelt livers in January compared to February.

In conclusion, metabolism in cold smelt livers was characterized by glucose and fatty acid oxidation driving ATP synthesis, with PDH inhibition channeling a portion of the G6P-derived DHAP towards glycerol. With glucose readily available, it was likely the main source of glycerol; however, as liver glycogen decreased over time, amino acid-derived substrates may have become more important as AAT2 levels tended to be higher in February than January. Increased glycerol production was not associated with increased transcript levels of cGPDH.

5.1.1.3 Insights from in vitro compared to in vivo transcript levels in liver

There were both substantive differences and important similarities between the transcript expression profiles of isolated hepatocytes that were maintained at 0.4°C for up to 3 days, and of livers from whole animals that were subjected to a decrease in temperature (from 8°C to 0°C) over a period of weeks and then held at between 0°C to -0.5°C for ~1 month. In isolated cells, GLUT2 transcript levels plummeted within 24 h; in

intact animals, GLUT2 transcript levels remained quite vigorous. These data suggest that an extracellular signal is required to maintain GLUT2 transcript levels. In the context of glycerol metabolism, it appears that glucose uptake was limited in isolated cells thus forcing these cells to an amino acid fuelled glycerol production that was not associated with increased PFK transcript levels. Although PFK is a key regulatory enzyme in glycolysis, increased PFK expression was not a requirement for the initial increase in glycerol production. In isolated cells, glyceroneogenesis was associated with the coordinated increase in transcript levels of a suite of genes associated with the mobilization of amino acids (PEPCK, MDH2, AAT2, GDH, GS and AQP9) at 24 h, which is consistent with previous studies that have identified amino acid-derived metabolites as important sources of glycerol (35, 50). In contrast, at the whole animal level, glucose appears to be more important in supporting glycerol production as based on an increase in PFK transcript levels and either no change or decreases in transcript levels of PEPCK, MDH2, AAT2, GDH and AQP9 in response to cold temperature. These findings reveal that although smelt liver glycogen is utilized in response to a rapid decrease in temperature *in vivo* (7; 16, i.e. Chapter 3), as well as, during the fall-to-winter transition (45), the initiation of glycerol synthesis can also be supported by amino acids. Furthermore, although carbohydrate and amino acids are both important sources of glycerol, carbohydrate is the preferred source when it is readily available.

There were several important cold-responsive changes in transcript levels in common to both the *in vitro* and *in vivo* approaches. The first and perhaps the most important discovery in this thesis was increased levels of PDK2, an inhibitor of PDH, in association with cold temperature-induced glyceroneogenesis. An inhibition of PDH

would serve to inhibit the lower portion of glycolysis and thereby channel any glucose-derived DHAP towards glycerol. In addition, PDH inhibition would serve to direct pyruvate and oxaloacetate derived from amino acids to glycerol as opposed to oxidation to acetyl CoA / CO₂. These are the first studies identifying the regulation of PDH expression as a key locus in the switch from glycolysis / gluconeogenesis to glyceroneogenesis.

The second key discovery of this thesis was an increase in levels of a phosphatase-like transcript in association with the initiation and early stages of cold temperature-induced glyceroneogenesis which levels off during the glycerol maintenance stage. Interestingly, this transcript expression pattern is consistent with G3Pase enzyme activity which in a seasonal study reached peak levels during the glycerol accumulation phase (Dec / Jan) and thereafter began to decline (6). If the protein encoded by the phosphatase analyzed herein does indeed have the ability to dephosphorylate G3P, this is potentially an extremely important finding as the gene encoding this enzyme has yet to be identified in any vertebrate species.

The third key discovery of this thesis was significantly higher GS transcript levels in cold compared to warm smelt livers suggesting higher glutamine levels. Although increased glutamine levels have been observed as part of the cold adaptation response in crustaceans (20), worms (40) and insects (10), this was the first study suggesting increased glutamine levels as part of the cold adaptation response in smelt. Increased glutamine levels may minimize membrane disruption by interacting directly with negatively charged phospholipids (2) while concomitantly storing ammonia / nitrogen, generated when glyceroneogenesis is supported by amino acid catabolism, in a non-toxic

form. Alternatively, glutamine may be used to support urea synthesis. Plasma urea levels in smelt from the *in vivo* study were 2.3-fold significantly higher in February compared to January, and were 3.4- and 5.1-fold significantly higher in cold compared to warm smelt in January and February, respectively (15, i.e. Chapter 4). They were also shown to follow a seasonal pattern similar to glycerol with levels in plasma increasing from 2-3 mM to 8-9 mM in response to cold temperature (15, i.e. Chapter 4; 45). In adult smelt liver, the ornithine urea cycle appears to be nonfunctional; however urea can be synthesized via argininolysis and via purine synthesis (glutamine donates amino groups) - uricolysis (33). Although not verified by QPCR, urate oxidase (alias uricase; uric acid to allantoin) (GenBank accession number GR557289) was identified in the forward (transcripts expressed at higher levels in cold than warm cells at 72 hours) hepatocyte SSH library (Supplemental Table S2.1) (14, i.e. Chapter 2), suggesting that at least transiently glutamine could contribute to increased urea levels. However, in the long term, although liver was shown to have high uricase enzyme activities, there was no relation found between urea and activity levels in fall and winter caught smelt (33), suggesting that renal urea conservation in addition to *de novo* synthesis may be an important contributor to high urea levels in winter (15, i.e. Chapter 4; 33)

The fourth key discovery of this thesis was increased G6Pase transcript levels in congruence with increased plasma glucose levels. Increases in glucose in association with elevated G6Pase transcript levels may, in addition to glycerol, be another component of the cold temperature defense mechanism in smelt, just as increases in glucose in association with elevated G6Pase enzyme activity are part of the defense strategy in freeze-tolerant frogs (8, 47). Increased glucose levels could provide additional colligative

protection against freezing or help to sustain rates of extrahepatic glucose uptake through an increased diffusion gradient.

Finally, transcript levels of cGPDH, a key locus in glycerol synthesis, did not increase in isolated cells and were significantly lower in cold- than warm-acclimated liver. These results suggest that regulation of cGPDH is more likely by post-translational modification. In rabbit, protein-protein interaction of ALD with cGPDH resulted in elevated specific activity of cGPDH (3). Transcript levels of ALD increased on a seasonal basis such that values in February were about 25-fold higher than in October (36). A similar regulation could be occurring in smelt liver.

5.1.2 Glycerol trafficking

The second objective of this thesis was to clone GLP-encoding genes from smelt and assess their transcript expression profiles in tissues from non-glycerol and from glycerol accumulating smelt. The hypothesis was that transcript levels of GLP-encoding genes would increase in response to cold temperature to facilitate the movement of glycerol across cellular membranes. The research reported herein does not support this hypothesis. However, as described below, it led to the discovery of an AQP10b gene duplicate whose transcript levels increase in posterior kidney only with cold temperature. A new hypothesis arising from this research is that this AQP10b gene duplicate may have evolved to aid in the reabsorption not of glycerol but of urea from the proximal tubule of the posterior kidney.

In Chapter 4, full-length cDNA sequences for two AQP10b-like genes (AQP10ba, AQP10bb), and the gene / promoter sequences for them and AQP9b were cloned and characterized. Transcript levels of the three GLP-encoding genes were measured using

QPCR in ten tissues from both non-glycerol and glycerol accumulating smelt. Plasma glycerol, plasma urea and posterior kidney AQP10b transcript (by QPCR) levels were measured in two studies. In the first, smelt were subjected to the whole animal temperature “step-down” model of cold temperature-induced glycerol production (16, i.e. Chapter 3). In the second, smelt were either held at ~8°C (warm smelt) or allowed to follow ambient seawater temperature (ambient smelt) throughout a season (encompassing the glycerol production and termination phases) (37).

5.1.2.1 Smelt GLP gene and promoter sequences

Smelt AQP-like genes are generally similar in structure; however, there are marked differences at the 5' end of the AQP10ba gene. AQP10bb and AQP9b have 6 exons, whereas AQP10ba has 8 exons. AQP10ba has two additional exons at the 5' end, and the promoter sequence is different from AQP10bb. Their transcribed exon sequences matched their cDNA sequences cloned and characterized in Chapter 4 (AQP10ba, AQP10bb) (15) and in Chapters 2 and 3 (AQP9b) (14, 16). Their putative proteins have structural features characteristic of vertebrate GLPs including the six putative membrane spanning domains with five intertransmembrane loops and the two NPA constriction motifs common to all aquaporins, as well as the five conserved amino acids (Y, D, R, P, L/V) and the ar/R constriction motif amino acids (F, G, Y, R) specific to GLPs. The proximal promoter regions of the smelt GLPs contain putative transcription factor recognition sites that have also been identified in the promoter regions of other vertebrate GLP-encoding genes. These include sites for the core negative IRE, GR, C/EBP alpha, AP-1, members of the NF family, GATA and TEF-1.

5.1.2.2 *Smelt AQP10b gene duplicates*

Direct sequence comparisons at the gene structure / promoter, mRNA and predicted protein levels, and phylogenetic analyses, suggest that both smelt AQP10b-like gene sequences cloned herein are AQP10b orthologues. Furthermore, the high sequence identity between the AQP10b paralogues and phylogenetic clustering pattern suggest that they arose from a gene duplication event in the smelt lineage that occurred more recently than the fish-specific WGD event at the root of the crown clade of Teleostei (1). As smelt are diploid (i.e. their genome did not duplicate after the fish-specific WGD), these AQP10b paralogues likely arose from a gene and not a WGD event. AQP10bb is likely more similar to the ancestral gene that gave rise to both smelt AQP10b paralogues as it has a conserved gene structure and shorter branch on the phylogenetic tree.

At the gene level, the 6 exon structure of the smelt AQP10bb and AQP9b genes has been reported in other GLP-encoding genes in the vertebrate lineage; it is the 8 exon structure of the smelt AQP10ba gene that is atypical. Exon 2 of AQP10ba encodes a novel 45 bp sequence located at the 5' end of the AQP10ba mRNA that could potentially encode a novel 15 aa sequence at the N-terminus of the AQP10ba putative protein that is not present in smelt AQP10bb or in AQP10b orthologues in other species.

At the predicted protein level, the AQP10ba and AQP10bb genes encode proteins with predicted amino acid sequences that are 82% identical. They are 93% identical over the 283 aa overlapping central region; however, the N- and C-termini are quite different between the two putative proteins. By comparison, there are two AQP10 gene paralogue-encoded putative proteins (AQP10a and AQP10b) in zebrafish that arose through the fish-specific WGD event that are 44% identical (43). Phylogenetic analyses of the

predicted proteins encoded by the smelt AQP10b gene paralogues with those from vertebrate GLPs (AQP3, -7, -9, and -10) show that the two putative proteins cluster together (with AQP10bb having a shorter branch length) and with AQP10b-like sequences from zebrafish and other vertebrates, and not with piscine and human AQP10a-like sequences.

5.1.2.3 Transcript tissue expression profiles

QPCR analysis of smelt GLP transcript levels indicated that the smelt AQP10b paralogues and AQP9b were ubiquitously distributed in the ten tissues examined in this study; however, their expression profiles were different. AQP10ba transcripts were most abundant in kidney, brain and pyloric caeca, AQP10bb transcripts were most abundant in kidney, intestine, pyloric caeca and brain, and AQP9b transcripts were most abundant in spleen, liver, RBCs and kidney. The ubiquitous expression of AQP10b and AQP9b transcripts has not been reported in other fish species (17, 27, 38, 43, 44) and may relate to smelt being a glycerol accumulating species. Abundant AQP10b transcripts in smelt kidney and gastrointestinal tissues is consistent with other fish species; however, high AQP10b levels in brain has not been reported in other fish (27, 38, 43, 44). AQP9b transcripts were detected in brain, gill, liver, eye and ovary but were not detectable in gastrointestinal tissues, kidney and muscle (17, 43).

5.1.2.4 Impact of cold temperature on glycerol and urea levels in plasma and on GLP transcript levels in smelt tissues

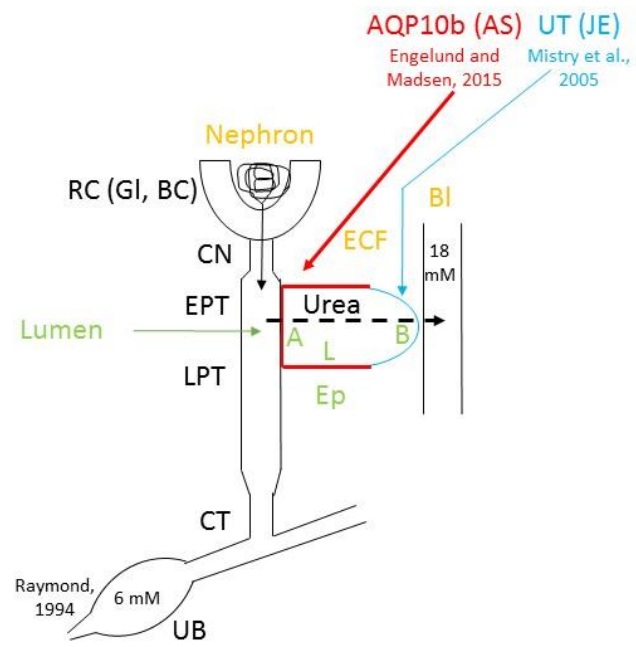
Plasma glycerol and urea, and GLP transcript levels were measured in warm- and cold-acclimated smelt tissues. Consistent with previous studies, cold temperature was associated with high glycerol (24, 25, 37) and modest urea levels (45) in plasma. Smelt

maintained at cold temperature generally exhibited lower GLP levels than smelt maintained at warm temperature. This was consistent with lower rates of glycerol transport in smelt RBCs and heart (4), and in RBCs from Cope's gray treefrogs (11).

The most striking finding of Chapter 4 (15) was that AQP10ba transcript levels in kidney always increased at cold temperatures. It was the only GLP transcript that responded in this fashion. The physiological consequences of increased AQP10ba transcript levels and presumably increased levels of the resultant protein in kidney could relate to renal urea conservation [i.e. urea levels in urine (6 mM) are lower than in plasma (18 mM) (32)]. In smelt, urea can be synthesized from dietary arginine and from glutamine-dependent purine synthesis-uricolysis. GS levels were higher in cold compared to warm smelt liver (14, i.e. Chapter 2; 16, i.e. Chapter 3) and urate oxidase transcripts were identified in an SSH library enriched for cold-responsive transcripts in cultured hepatocytes (14, i.e. Chapter 2), which suggests that *de novo* synthesis could contribute to the increased urea levels at least transiently; however, renal conservation is likely important to maintain the elevated urea levels with cold temperature.

I hypothesize that urea may be reabsorbed from smelt posterior kidney as depicted in Fig. 5.1. The smelt nephron is glomerular. The tubular portion is divided into specialized segments; there is a ciliated neck, an early and a late proximal tubule and a collecting tubule that drains into the urinary bladder. The lumen of the proximal tubule contains epithelial cells on its surface (30). In Atlantic salmon, AQP10b is localized to the apical and lateral membranes of the epithelial cells (9). In Japanese eel (*Anguilla japonica*), there is a facilitative urea transporter that is localized to the basolateral membrane of the epithelial cells and is thought to be involved in the transepithelial

Figure 5.1. Proposed model for urea reabsorption from the proximal tubule of the smelt nephron. The glomerular filtrate enters the lumen of the proximal tubule. The movement of urea from the lumen into the epithelial cells may be facilitated by AQP10ba. The movement of urea from the epithelial cells into the plasma may be facilitated by a urea transporter orthologous to that found in Japanese eel. The urea level in urine is 6 mM; the urea level in plasma is 18 mM. RC, renal corpuscle; Gl, glomerulus; BC, Bowman's capsule; CN, ciliated neck; EPT, early proximal tubule; LPT, late proximal tubule; CT, collecting tubule; UB, urinary bladder; Ep, epithelial cell; A, apical membrane; L, lateral membrane; B, basolateral membrane; ECF, extracellular fluid; Bl, blood; UT, urea transporter; AS, Atlantic salmon; JE, Japanese eel.



reabsorption of urea across the proximal tubule (29). It is unknown if an orthologous urea transporter is present in smelt kidney. What could be happening in the smelt nephron is as follows. The glomerular filtrate enters the lumen of the proximal tubule. At low winter temperatures, the increased AQP10ba transcript levels may have resulted in elevated levels of protein to facilitate the movement of urea from the lumen into the epithelial cells. A urea transporter would then facilitate the movement of urea from the epithelial cells into the plasma.

In conclusion, the AQP10ba gene duplicate may have evolved to aid in the reabsorption of urea, generated as a byproduct of glycerol synthesis-related protein catabolism, to concomitantly conserve nitrogen in a non-toxic form that also serves as a cryoprotectant.

5.1.3 Cold adaptation in smelt compared with other teleosts

Glycerol synthesis is a component of the cold temperature response in smelt that is rare amongst teleost fishes. However, it is but one of a multitude of biological processes that respond to cold temperature. A comparison of the cold temperature responsive transcripts in smelt liver (Supplemental Tables S2.1 to S2.6) with those identified as cold temperature responsive in other teleost fishes (13, 19, 28, 31) has identified several transcripts in common. For example, HMGB1 was identified as expressed at higher levels in response to cold temperature in smelt (14), common carp (13), zebrafish (19), seabream (28) and killifish (31). CIRBP was identified as expressed at higher levels in response to cold temperature in smelt (14), common carp (13) and zebrafish (19). Heat shock protein 70 was identified as expressed at higher levels in response to cold temperature in smelt (14), common carp (13), zebrafish (19) and killifish

(31). The identification of these transcripts in teleosts with different thermal histories (i.e. smelt are subjected to sub-zero temperatures; whereas these other fishes are eurythermal and are not subjected to sub-zero temperatures) provides strong support for their role as putative global regulators of transcription in response to cold temperature in teleost fishes.

A comparison of PDK2 and GS transcript levels in smelt liver with levels in liver of the aforementioned teleost fishes in response to cold temperature revealed that increased transcript levels of PDK2 and GS are unique to the cold temperature response in smelt liver. PDK2 transcript levels were lower in liver of zebrafish (19) and seabream (28), and PDH (which is inhibited by PDK2) transcript levels were higher in common carp (13) in response to cold temperature. GS transcript levels were lower in liver of zebrafish (19) and seabream (28) in response to cold temperature. The differences in transcript levels of these genes in the liver of smelt compared to non-glycerol accumulating teleosts in response to cold temperature provides support for their role in glycerol synthesis in smelt liver that was elucidated herein. The research conducted in this thesis suggests that regulation of PDH expression by PDK2 is key in the switch from glycolysis / gluconeogenesis to glyceroneogenesis. Furthermore, increased glutamine synthesis may serve to store ammonia / nitrogen, generated when glyceroneogenesis is supported by amino acid catabolism, in a non-toxic form. Alternatively, glutamine may be used to support urea synthesis.

5.2 PERSPECTIVES AND SIGNIFICANCE

This thesis marks the culmination of an extensive research program dedicated to an understanding of cold adaptation and more specifically osmolyte (especially glycerol) accumulation in smelt that was conducted in the laboratories of Dr. William Driedzic, Dr. Vanya Ewart, and collaborators, namely Dr. Matthew Rise for the research conducted herein. This thesis, in conjunction with research conducted by my colleagues, has led to the development of a working scenario for the mechanisms involved in cold adaptation in smelt based on studies in animals tracking seasonal changes, in animals subjected to an abrupt controlled decrease in water temperature, and in isolated cells. The initiation of type II AFP production is photoperiod dependent and occurs in early fall when water temperatures are $\sim 11^{\circ}\text{C}$ (14, i.e. Chapter 2; 24; 25). However, high glycerol production is low temperature dependent and follows a seasonal pattern (24, 25, 37).

In smelt living at low temperature, glycerol synthesis occurs in liver and can be initiated from both glycolytic and gluconeogenic substrates (14, i.e. Chapter 2; 16, i.e. Chapter 3; 35; 50). The first stage in glycerol production (i.e. naturally during the fall-to-winter transition or artificially with an abrupt decrease in temperature) involves the mobilization of glycogen reserves (7; 16, i.e. Chapter 3; 45) and is associated with increases in expression of PGM (16, i.e. Chapter 3), cGPDH and ALD (24, 25, 36). Elevated cGPDH protein / activity levels would serve to channel DHAP towards glycerol synthesis and increased protein / activity of ALD could serve to enhance the breakdown of fructose 1,6-bisphosphate and also increase the activity of cGPDH through protein-protein association (3). PFK may be elevated thereafter to maintain flux at the top part of glycolysis at low temperature (16, i.e. Chapter 3) but activation at this locus does not

appear to be a requirement for the initiation of glycerol production (14, i.e. Chapter 2). As carbohydrate reserves become limiting, amino acids become increasingly important in supporting glycerol production and a suite of related genes is activated (PEPCK, MDH2, AAT2, GDH) (14, i.e. Chapter 2; 16, i.e. Chapter 3; 24; 25). Associated with this is an increase in PDK2 that would inhibit the lower part of glycolysis at the PDH site, thereby ensuring that glyceroneogenesis out-competes glycolysis and channels amino acid-derived pyruvate and oxaloacetate towards glyceroneogenesis (14, i.e. Chapter 2; 16, i.e. Chapter 3).

In parallel to high glycerol level, liver G6Pase and plasma glucose levels increased with cold temperature to perhaps provide additional colligative protection against freezing or help to sustain rates of extrahepatic glucose uptake through an increased diffusion gradient (5; 14, i.e. Chapter 2; 16, i.e. Chapter 3). Finally, smelt have developed two strategies to conserve nitrogen when amino acid-derived metabolites are used for glyceroneogenesis. GS transcript expression in liver is increased perhaps resulting in increased glutamine levels that may also serve to protect protein integrity at low temperature (14, i.e. Chapter 2; 16, i.e. Chapter 3). High glutamine levels could also support *de novo* synthesis of urea, an osmolyte which also serves as a cryoprotectant. High urea level could then be maintained through AQP10ba-mediated renal conservation. Kidney AQP10ba transcript levels always increased with cold temperature in congruence with plasma urea levels (15, i.e. Chapter 4).

5.3 FUTURE DIRECTIONS

The research conducted in this thesis was performed with the best available functional genomic and molecular tools and techniques at that time. However, advances in this field have led to the development of additional tools and techniques that could be applied to this research. For example, in terms of microarray platforms, there is now a cGRASP 32K salmonid cDNA array (22) and a cGRASP-designed 44K salmonid oligonucleotide array from Agilent (21) available. This thesis research involved inter-specific (i.e. cross-species) hybridizations, which may be more effectively performed using cDNA compared with oligonucleotide arrays; the probe sequences on cDNA microarray platforms are longer than those on oligonucleotide platforms, thereby increasing the likelihood of a given probe being in a region that is conserved between the two species. The development of novel high-throughput DNA sequencing methods (e.g. Illumina Next Generation Sequencing) would allow deeper sequencing of the SSH cDNA libraries constructed herein. In addition, this technology led to the development of a new method for both mapping and quantifying transcriptomes called RNA sequencing (RNA-Seq). Briefly, a population of RNA is converted to a library of cDNA fragments with adaptors attached to one or both ends. Each molecule is then sequenced to obtain short sequences (i.e. 30–400 bp) from one end (single-end sequencing) or both ends (pair-end sequencing). Following sequencing, to elucidate transcriptional structure and/or transcript expression levels, the resulting reads are either aligned to a reference genome or reference transcripts or assembled *de novo* for non-model species (51). RNA-Seq was used to help elucidate the genetic networks and cis-regulatory elements of the cold response in zebrafish (19). However, one potential limitation of applying this technology

to smelt is that, unlike zebrafish, smelt is a non-model species. As such, there are limited genomic resources available [i.e. BAC library; 36,758 ESTs (48)], and RNA-Seq reads would have to be assembled *de novo* to generate a transcriptome. In terms of QPCR, instruments are now available in 384-well format [e.g. ViiA 7 Real-Time PCR System (Applied Biosystems)] which has increased throughput. The development of software packages such as geNorm (46) has allowed the identification of the most stably expressed candidate normalizer transcripts to more accurately normalize gene of interest transcript expression data, and high-throughput systems such as the ViiA 7 have facilitated the use of multiple normalizers in QPCR experiments.

The research conducted in this thesis has left several aspects of glycerol synthesis and trafficking that need to be further evaluated. One aspect is to determine if cGPDH enzyme activity can be regulated post-translationally by protein-protein interactions with ALD. Common techniques used for protein-protein interaction analysis include yeast two-hybrid assays, pull-down assays and co-immunoprecipitation assays.

A second area of potential future research would be to determine if the phosphatase-like sequence identified and analyzed herein has the ability to dephosphorylate G3P. The four phosphatase-like ESTs cloned herein assembled into a contig (n=3) and a singleton which are 96% (over 162 bp) and 92% (over 190 bp) identical at the nucleotide level, respectively, to another smelt phosphatase-like assembled sequence (based on ESTs generated by von Schalburg et al.; GenBank accession numbers EL545480, EL537488 and EL542406) (48). The predicted amino acid sequences encoded by these seven smelt phosphatase-like ESTs were found to resemble a G3Pase protein sequence (CCP44457) recently identified in the bacterium

Mycobacterium tuberculosis (23, 34). As the smelt phosphatase-like assembled sequence based on ESTs generated herein and the smelt phosphatase-like assembled sequence based on ESTs generated by von Schalburg et al. (48) were incomplete cDNAs, a synthetic hybrid construct (in which the codons were optimized for expression in *Escherichia coli*) was designed (34); this construct encoded the first 53 amino acids from the contig generated herein, and the remaining 253 amino acids from the sequences generated by von Schalburg et al. (48). A recombinant protein was generated and was found to have G3Pase activity on the order of a few $\mu\text{Mol Pi/mg enzyme/min}$ (34).

Although these results are encouraging, in future it would be helpful to design paralogue-specific primers for the contig generated herein so that 3'RACE could be performed to obtain the remaining sequence. This would also determine if the singleton generated herein is from the same transcript as the contig generated herein, or if it represents a third phosphatase-like sequence. In future it would be helpful to design paralogue-specific primers for the smelt phosphatase-like sequence generated by von Schalburg et al. (48) so that 5'RLM-RACE could be performed to obtain the remaining sequence. Recombinant proteins for each of the phosphatase-like sequences could then be generated and assayed for G3Pase activity individually. The importance of treating paralogous sequences individually was exemplified in the case of the AQP10b gene paralogues cloned herein. In addition to the aforementioned smelt phosphatase-like sequences, another phosphatase with sequence identity to a G3Pase from a glycerol-producing alga, *Dunaliella salina* was identified in smelt and was also found to have G3Pase activity (18, 34).

With several candidate genes for the smelt G3Pase having been identified, knock down of gene expression using RNA interference (RNAi) [e.g. small interfering RNAs (siRNAs), small hairpin (shRNAs)] technology or the powerful new precise genome-editing (PGE) technology Clustered Regularly Interspaced Short Palindromic Repeats (CRISPR)-Cas [reviewed in (41)] may help determine if any of these genes encode the true G3Pase. It may be possible to study this *in vitro* using the hepatocyte model of cold temperature-induced glycerol synthesis to compare the ability of smelt hepatocytes isolated from the same liver to synthesize glycerol in the presence or reduced expression / absence of a given candidate G3Pase. Whether or not these techniques can be applied to cultured smelt hepatocytes remains to be elucidated. In primary human hepatocytes, it had been reported that application of RNAi has had some technical hurdles (e.g. conventional transfection techniques by lipophilic agents result in low transfection efficiency), however the use of adenoviral and especially lentiviral vector transduction is promising (42). A set of plasmids and vectors derived from adeno-associated virus (AAV) that allow robust and specific delivery of the two essential CRISPR components - Cas9 and chimeric g(uide)RNA even into hard-to-transfect targets has recently been reported (39).

A third area of potential future research would be to further characterize the GLPs cloned herein. At the functional level, the cloned GLP cDNAs could be expressed in *Xenopus laevis* oocytes. Osmotic water permeability could then be determined using an oocyte-swelling assay, and solute permeability determined using radiolabeled [³H] glycerol and [¹⁴C] urea. These techniques have been used to functionally characterize GLPs from seabream and zebrafish (38, 43). GLP paralogue-specific antibodies could be

developed to measure GLP expression at the protein level, using Western blot methodology, to complement the transcript expression studies conducted herein. *In situ* hybridization could be used to characterize cellular expression of GLP transcripts (38), and immunohistochemistry, using the aforementioned antibodies, could be used to localize expression of GLP proteins to a given segment of the smelt nephron, for example (9).

A fourth area of potential future research would be to determine if smelt express a urea transporter orthologous to that found in Japanese eel (29). Orthologous sequences are present in fugu (*Takifugu rubripes*), rainbow trout and zebrafish (29). These sequences could be aligned and degenerate PCR primers designed based upon consensus sequences from conserved areas. The smelt cDNA sequence could then be cloned using the methodologies described herein. If present, it could be characterized as per the GLPs.

Other areas of potential future research could be to determine if there are any effects of sex on glycerol synthesis. As well, cortisol levels could be measured to determine if cold exposure and glycerol synthesis are stressful for smelt. In addition, given that in smelt, glycerol chaperones type II AFP (12), it could be determined if there is a quantitative relationship between the two. Further to that, marine cartilaginous fishes and the coelacanth use, as osmolytes, a combination of urea and TMAO in a 2:1 molar ratio (26). It could be determined if there is a quantitative relationship between the two in smelt. Finally, levels of glutamine could be measured to determine if increased GS transcript levels result in increased glutamine levels or if glutamine is a biochemical intermediate (i.e. used to support urea synthesis, for example). Overall, the current experiments have revealed many avenues for future endeavours.

5.4 REFERENCES

1. Amores A, Force A, Yan YL, Joly L, Amemiya C, Fritz A, Ho RK, Langeland J, Prince V, Wang YL, Westerfield M, Ekker M, Postlethwait JH. Zebrafish hox clusters and vertebrate genome evolution. *Science* 282: 1711-1714, 1998.
2. Anchordoguy T, Carpenter JF, Loomis SH, Crowe JH. Mechanisms of interaction of amino acids with phospholipid bilayers during freezing. *Biochim Biophys Acta* 946: 299-306, 1988.
3. Batke J, Asbóth G, Lakatos S, Schmitt B, Cohen R. Substrate-induced dissociation of glycerol-3-phosphate dehydrogenase and its complex formation with fructose biphosphate aldolase. *Eur J Biochem* 107: 389-394, 1980.
4. Clow KA, Driedzic WR. Glycerol uptake is by passive diffusion in the heart but by facilitated transport in RBCs at high glycerol levels in cold acclimated rainbow smelt (*Osmerus mordax*). *Am J Physiol Regul Integr Comp Physiol* 302: R1012-R1021, 2012.
5. Clow KA, Ewart KV, Driedzic WR. Low temperature directly activates the initial glycerol antifreeze response in isolated rainbow smelt (*Osmerus mordax*) liver cells. *Am J Physiol Regul Integr Comp Physiol* 295: R961-R970, 2008.

6. **Ditlecadet D, Driedzic WR.** Glycerol-3-phosphatase and not lipid recycling is the primary pathway in the accumulation of high concentrations of glycerol in rainbow smelt (*Osmerus mordax*). *Am J Physiol Regul Integr Comp Physiol* 304: R304-R312, 2013.

7. **Driedzic WR, Short CE.** Relationship between food availability, glycerol and glycogen levels in low-temperature challenged rainbow smelt *Osmerus mordax*. *J Exp Biol* 210: 2866-2872, 2007.

8. **Dziewulska-Szwajkowska D, Lozinzka-Gabska M, Dzugaj A.** *Rana esculenta* L. liver Fru-P2ase and G-6-Pase activity and Fru-2,6-P2 concentration after acclimation at 5 and 25°C. *Comp Biochem Physiol A* 118A: 745-751, 1997.

9. **Engelund MB, Madsen SS.** Tubular localization and expressional dynamics of aquaporins in the kidney of seawater-challenged Atlantic salmon. *J Comp Physiol B* 185: 207-223, 2015.

10. **Fields PG, Fleurat-Lessard F, Lavenseau L, Febvay G, Peypelut L, Bonnot G.** The effect of cold acclimation and deacclimation on cold tolerance, trehalose and free amino acid levels in *Sitophilus granarius* and *Cryptolestes ferrugineus* (Coleoptera). *J Insect Physiol* 44: 955-965, 1998.

11. **Goldstein DL, Frisbie J, Diller A, Pandey RN, Krane CM.** Glycerol uptake by erythrocytes from warm- and cold-acclimated Cope's gray treefrogs. *J Comp Physiol B* 180: 1257-1265, 2010.

12. **Gong H, Croft K, Driedzic WR, Ewart, KV.** Chemical chaperoning action of glycerol on the antifreeze protein of rainbow smelt. *J Thermal Biology* 36: 78-83, 2011.

13. **Gracey AY, Fraser EJ, Li W, Fang Y, Taylor RR, Rogers J, Brass A, Cossins AR.** Coping with cold: An integrative, multitissue analysis of the transcriptome of a poikilothermic vertebrate. *Proc Natl Acad Sci U S A* 101: 16970-16975, 2004.

14. **Hall JR, Clow KA, Rise ML, Driedzic WR.** Identification and validation of differentially expressed transcripts in a hepatocyte model of cold-induced glycerol production in rainbow smelt (*Osmerus mordax*). *Am J Physiol Regul Integr Comp Physiol* 301: R995-R1010, 2011.

15. **Hall JR, Clow KA, Rise ML, Driedzic WR.** Cloning and characterization of aquaglyceroporin genes from rainbow smelt (*Osmerus mordax*) and transcript expression in response to cold temperature. *Comp Biochem Physiol B Biochem Mol Biol* 187: 39-54, 2015.

16. **Hall JR, Short CE, Rise ML, Driedzic WR.** Expression analysis of glycerol synthesis-related liver transcripts in rainbow smelt (*Osmerus mordax*) exposed to a controlled decrease in temperature. *Physiol Biochem Zool* 85: 74-84, 2012.
17. **Hamdi M, Sanchez MA, Beene LC, Liu Q, Landfear SM, Rosen BP, Liu Z.** Arsenic transport by zebrafish aquaglyceroporins. *BMC Mol Biol* 10: 104, 2009.
18. **He Q, Qiao D, Bai L, Zhang Q, Yang W, Li Q, Cao Y.** Cloning and characterization of a plastidic glycerol 3-phosphate dehydrogenase cDNA from *Dunaliella salina*. *J Plant Physiol* 164: 214-220, 2007.
19. **Hu P, Liu M, Zhang D, Wang J, Niu H, Liu Y, Wu Z, Han B, Zhai W, Shen Y, Chen L.** Global identification of the genetic networks and cis-regulatory elements of the cold response in zebrafish. *Nucleic Acids Res* 43: 9198-9213, 2015.
20. **Issartel J, Renault D, Voituron Y, Bouchereau A, Vernon P, Hervant F.** Metabolic responses to cold in subterranean crustaceans. *J Exp Biol* 208: 2923-2929, 2005.
21. **Jantzen SG, Sanderson DS, von Schalburg KR, Yasuike M, Marass F, Koop BF.** A 44K microarray dataset of the changing transcriptome in developing Atlantic salmon (*Salmo salar* L.). *BMC Res Notes* 4: 88, 2011.

22. **Koop BF, von Schalburg KR, Leong J, Walker N, Lieph R, Cooper GA, Robb A, Beetz-Sargent M, Holt RA, Moore R, Brahmhatt S, Rosner J, Rexroad CE 3rd, McGowan CR, Davidson WS.** A salmonid EST genomic study: genes, duplications, phylogeny and microarrays. *BMC Genomics* 9: 545, 2008.
23. **Larrouy-Maumus G, Biswas T, Hunt DM, Kelly G, Tsodikov OV, de Carvalho LPS.** Discovery of a glycerol 3-phosphate phosphatase reveals glycerophospholipid polar head recycling in *Mycobacterium tuberculosis*. *Proc Natl Acad Sci USA* 110: 11320-11325, 2013.
24. **Lewis JM, Ewart KV, Driedzic WR.** Freeze resistance in rainbow smelt (*Osmerus mordax*): seasonal pattern of glycerol and antifreeze protein levels and liver enzyme activity associated with glycerol production. *Physiol Biochem Zool* 77: 415-422, 2004.
25. **Liebscher RS, Richards RC, Lewis JM, Short CE, Muise DM, Driedzic WR, Ewart KV.** Seasonal freeze resistance of rainbow smelt (*Osmerus mordax*) is generated by differential expression of glycerol-3-phosphate dehydrogenase, phosphoenolpyruvate carboxykinase, and antifreeze protein genes. *Physiol Biochem Zool* 79: 411-423, 2006.
26. **Lin TY, Timasheff SN.** Why do some organisms use a urea-methylamine mixture as osmolyte? Thermodynamic compensation of urea and trimethylamine N-oxide interactions with protein. *Biochemistry* 33: 12695-12701, 1994.

27. **Martinez AS, Cutler CP, Wilson GD, Phillips C, Hazon N, Cramb G.** Cloning and expression of three aquaporin homologues from the European eel (*Anguilla anguilla*): effects of seawater acclimation and cortisol treatment on renal expression. *Biol Cell* 97: 615-627, 2005.
28. **Mininni AN, Milan M, Ferraresso S, Petochi T, Di Marco P, Marino G, Livi S, Romualdi C, Bargelloni L, Patarnello T.** Liver transcriptome analysis in gilthead sea bream upon exposure to low temperature. *BMC Genomics* 15: 765, 2014.
29. **Mistry AC, Chen G, Kato A, Nag K, Sands JM, Hirose S.** A novel type of urea transporter, UT-C, is highly expressed in proximal tubule of seawater eel kidney. *Am J Physiol Renal Physiol* 288: F455-F465, 2005.
30. **Ogawa M, Fukuda M, Hayashida A, Fukuchi M.** On the kidney and the adrenocortical tissue of toothed smelt, *Osmerus mordax dentex* and surf smelt, *Hypomesus pretiosus japonicas* and their cold adaptation. *Proc NIPR Symp Polar Biol* 4: 30-35, 1991.
31. **Podrabsky JE, Somero GN.** Changes in gene expression associated with acclimation to constant temperatures and fluctuating daily temperatures in an annual killifish *Austrofundulus limnaeus*. *J Exp Biol* 207: 2237-2254, 2004.

32. **Raymond JA.** Seasonal variations of trimethylamine oxide and urea in the blood of a cold-adapted marine teleost, the rainbow smelt. *Fish Physiol Biochem* 13: 13-22, 1994.
33. **Raymond JA.** Trimethylamine oxide and urea synthesis in rainbow smelt and some other northern fishes. *Physiol Zool* 71: 515-523, 1998.
34. **Raymond JA.** Two potential fish glycerol-3-phosphate phosphatases. *Fish Physiol Biochem* 41: 811-818, 2015.
35. **Raymond JA, Driedzic WR.** Amino acids are a source of glycerol in cold-acclimatized rainbow smelt. *Comp Biochem Phys* 118B: 387-393, 1997.
36. **Richards RC, Short CE, Driedzic WR, Ewart KV.** Seasonal changes in hepatic gene expression reveal modulation of multiple processes in rainbow smelt (*Osmerus mordax*). *Mar Biotechnol* 12: 650-663, 2010.
37. **Robinson J, Hall JR, Charman M, Ewart KV, Driedzic WR.** Molecular analysis, tissue profiles and seasonal patterns of cytosolic and mitochondrial GPDH in freeze resistant rainbow smelt (*Osmerus mordax*). *Physiol Biochem Zool* 84: 363-376, 2011.

38. **Santos CR, Estêvão MD, Fuentes J, Cardoso JC, Fabra M, Passos AL, Detmers FJ, Deen PM, Cerdà J, Power DM.** Isolation of a novel aquaglyceroporin from a marine teleost (*Sparus auratus*): function and tissue distribution. *J Exp Biol* 207: 1217-1227, 2004.
39. **Senís E, Fatouros C, Große S, Wiedtke E, Niopek D, Mueller AK, Börner K, Grimm D.** CRISPR/Cas9-mediated genome engineering: an adeno-associated viral (AAV) vector toolbox. *Biotechnol J* 9: 1402-1412, 2014.
40. **Slotsbo S, Maraldo K, Malmendal A, Nielsen NC, Holmstrup M.** Freeze tolerance and accumulation of cryoprotectants in the enchytraeid *Enchytraeus albidus* (Oligochaeta) from Greenland and Europe. *Cryobiology* 57: 286-291, 2008.
41. **Taylor J, Woodcock S.** A Perspective on the Future of High-Throughput RNAi Screening: Will CRISPR Cut Out the Competition or Can RNAi Help Guide the Way? *J Biomol Screen* 20: 1040-1051, 2015.
42. **Thomas M, Rieger JK, Kandel BA, Klein K, Zanger UM.** Targeting nuclear receptors with lentivirus-delivered small RNAs in primary human hepatocytes. *Cell Physiol Biochem* 33: 2003-2013, 2014.

43. **Tingaud-Sequeira A, Calusinska M, Finn RN, Chauvigné F, Lozano J, Cerdà J.** The zebrafish genome encodes the largest vertebrate repertoire of functional aquaporins with dual paralogy and substrate specificities similar to mammals. *BMC Evol Biol* 10: 38, 2010.
44. **Tipsmark CK, Sørensen KJ, Madsen SS.** Aquaporin expression dynamics in osmoregulatory tissues of Atlantic salmon during smoltification and seawater acclimation. *J Exp Biol* 213: 368-379, 2010.
45. **Treberg JR, Wilson CE, Richards RC, Ewart KV, Driedzic WR.** The freeze-avoidance response of smelt *Osmerus mordax*: initiation and subsequent suppression of glycerol, trimethylamine oxide and urea accumulation. *J Exp Biol* 205: 1419-1427, 2002.
46. **Vandesompele J, De Preter K, Pattyn F, Poppe B, Van Roy N, De Paepe A, Speleman F.** Accurate normalization of real-time quantitative RT-PCR data by geometric averaging of multiple internal control genes. *Genome Biol* 3: RESEARCH0034, 2002.
47. **Voituron Y, Joly P, Eugène M, Barré H.** Freezing tolerance of the European water frogs: the good, the bad, and the ugly. *Am J Physiol Regul Integr Comp Physiol* 288: R1563-R1570, 2005.

48. **von Schalburg KR, Leong J, Cooper GA, Robb A, Beetz-Sargent MR, Lieph R, Holt RA, Moore R, Ewart KV, Driedzic WR, ten Hallers BF, Zhu B, de Jong PJ, Davidson WS, Koop BF.** Rainbow smelt (*Osmerus mordax*) genomic library and EST resources. *Mar Biotechnol (NY)* 10: 487-491, 2008.

49. **von Schalburg KR, Rise ML, Cooper GA, Brown GD, Gibbs AR, Nelson CC, Davidson WS, Koop BF.** Fish and chips: various methodologies demonstrate utility of a 16,006-gene salmonid microarray. *BMC Genomics* 6: 126-144, 2005.

50. **Walter JA, Ewart KV, Short CE, Burton IW, Driedzic WR.** Accelerated hepatic glycerol synthesis in rainbow smelt (*Osmerus mordax*) is fuelled directly by glucose and alanine: a ^1H and ^{13}C nuclear magnetic resonance study. *J Exp Zool A* 305: 480-488, 2006.

51. **Wang Z, Gerstein M, Snyder M.** RNA-Seq: a revolutionary tool for transcriptomics. *Nat Rev Genet* 10: 57-63, 2009.